



Defense Threat Reduction Agency
8725 John J. Kingman Road, MS-6201
Fort Belvoir, VA 22060-6201



DTRA-TR-12-041

TECHNICAL REPORT

Radiation Dose Assessments for Fleet-Based Individuals in Operation Tomodachi

DISTRIBUTION A. Approved for public release: distribution is unlimited

September 2013

Prepared by:

Operation Tomodachi Registry,
Dose Assessment and Recording Working Group

For:

Assistant Secretary of Defense for Health Affairs

This page intentionally left blank.

REPORT DOCUMENTATION PAGE				Form Approved OMB No. 0704-0188	
<small>Public reporting burden for this collection of information is estimated to average 1 hour per response, including the time for reviewing instructions, searching data sources, gathering and maintaining the data needed, and completing and reviewing the collection of information. Send comments regarding this burden estimate or any other aspect of this collection of information, including suggestions for reducing this burden to Washington Headquarters Service, Directorate for Information Operations and Reports, 1215 Jefferson Davis Highway, Suite 1204, Arlington, VA 22202-4302, and to the Office of Management and Budget, Paperwork Reduction Project (0704-0188) Washington, DC 20503.</small> PLEASE DO NOT RETURN YOUR FORM TO THE ABOVE ADDRESS.					
1. REPORT DATE (DD-MM-YYYY) 09-30-2013		2. REPORT TYPE FINAL		3. DATES COVERED (From - To)	
4. TITLE AND SUBTITLE Radiation Dose Assessments for Fleet-Based Individuals in Operation Tomodachi				5a. CONTRACT NUMBER	
				5b. GRANT NUMBER	
				5c. PROGRAM ELEMENT NUMBER	
6. AUTHOR(S) ¹ Marro, Ralph; ² McKenzie-Carter, Michael; ³ Rademacher, Steven; ⁴ Knappmiller, Kevin; ⁴ Ranellone, Richard; ² Case, David; ⁵ Miles, Terry.				5d. PROJECT NUMBER	
				5e. TASK NUMBER	
				5f. WORK UNIT NUMBER	
7. PERFORMING ORGANIZATION NAME(S) AND ADDRESS(ES) ¹ Armed Forces Radiobiology Research Institute, ² Leidos; ³ Air Force Safety Center, ⁴ Engility, Inc., ⁵ Navy and Marine Corps Public Health Center.				8. PERFORMING ORGANIZATION REPORT NUMBER	
9. SPONSORING/MONITORING AGENCY NAME(S) AND ADDRESS(ES) Nuclear Technologies Department, Attn: Dr. Blake Defense Threat Reduction Agency 8725 John J. Kingman Road, Mail Stop 6201 Fort Belvoir, VA 22060-6201				10. SPONSOR/MONITOR'S ACRONYM(S) DTRA J9-NTSN	
				11. SPONSORING/MONITORING AGENCY REPORT NUMBER DTRA-TR-12-041	
12. DISTRIBUTION AVAILABILITY STATEMENT DISTRIBUTION A. Approved for public release: distribution is unlimited.					
13. SUPPLEMENTARY NOTES					
14. ABSTRACT This report provides the radiation dose assessments for the Department of Defense fleet-based population of interest that was potentially exposed to radioactive fallout resulting from the Fukushima Daiichi nuclear power station units' radiological releases that followed the earthquake and tsunami on March 11, 2011. The associated Department of Defense disaster relief operation to the citizens of Japan was entitled, "Operation Tomodachi." Finalized radiation dose assessments for the population of interest should be loaded into an Operation Tomodachi Registry by the end of 2013, which will support public inquiries.					
15. SUBJECT TERMS Operation Tomodachi, Radiation Dose, Department of Defense, Japan, Fukushima, Earthquake, Tsunami					
16. SECURITY CLASSIFICATION OF:			17. LIMITATION OF ABSTRACT U	18. NUMBER OF PAGES 196 Pages	19a. NAME OF RESPONSIBLE PERSON Paul K. Blake, PhD
a. REPORT U	b. ABSTRACT U	c. THIS PAGE U			19b. TELEPHONE NUMBER (Include area code) (703) 767-3433

UNIT CONVERSION TABLE

U.S. customary units to and from international units of measurement*

U.S. Customary Units	<div style="display: flex; justify-content: space-around; align-items: center;"> <div style="text-align: center;"> Multiply by </div> <div style="text-align: center;"> Divide by† </div> </div>	International Units
Length/Area/Volume		
inch (in)	2.54 $\times 10^{-2}$	meter (m)
foot (ft)	3.048 $\times 10^{-1}$	meter (m)
yard (yd)	9.144 $\times 10^{-1}$	meter (m)
mile (mi, international)	1.609 344 $\times 10^3$	meter (m)
mile (nmi, nautical, U.S.)	1.852 $\times 10^3$	meter (m)
barn (b)	1 $\times 10^{-28}$	square meter (m ²)
gallon (gal, U.S. liquid)	3.785 412 $\times 10^{-3}$	cubic meter (m ³)
cubic foot (ft ³)	2.831 685 $\times 10^{-2}$	cubic meter (m ³)
Mass/Density		
pound (lb)	4.535 924 $\times 10^{-1}$	kilogram (kg)
atomic mass unit (AMU)	1.660 539 $\times 10^{-27}$	kilogram (kg)
pound-mass per cubic foot (lb ft ⁻³)	1.601 846 $\times 10^1$	kilogram per cubic meter (kg m ⁻³)
Pound-force (lbf avoirdupois)	4.448 222	Newton (N)
Energy/Work/Power		
electronvolt (eV)	1.602 177 $\times 10^{-19}$	joule (J)
erg	1 $\times 10^{-7}$	joule (J)
kiloton (kT) (TNT equivalent)	4.184 $\times 10^{12}$	joule (J)
British thermal unit (Btu) (thermochemical)	1.054 350 $\times 10^3$	joule (J)
foot-pound-force (ft lbf)	1.355 818	joule (J)
calorie (cal) (thermochemical)	4.184	joule (J)
Pressure		
atmosphere (atm)	1.013 250 $\times 10^5$	pascal (Pa)
pound force per square inch (psi)	6.984 757 $\times 10^3$	pascal (Pa)
Temperature		
degree Fahrenheit (°F)	[T(°F) – 32]/1.8	degree Celsius (°C)
degree Fahrenheit (°F)	[T(°F) + 459.67]/1.8	kelvin (K)
Radiation		
activity of radionuclides [curie (Ci)]	3.7 $\times 10^{10}$	per second (s ^{-1‡})
air exposure [roentgen (R)]	2.579 760 $\times 10^{-4}$	coulomb per kilogram (C kg ⁻¹)
absorbed dose (rad)	1 $\times 10^{-2}$	joule per kilogram (J kg ^{-1§})
equivalent and effective dose (rem)	1 $\times 10^{-2}$	joule per kilogram (J kg ^{-1**})

* Specific details regarding the implementation of SI units may be viewed at <http://www.bipm.org/en/si/>.

† Multiply the U.S. customary unit by the factor to get the international unit. Divide the international unit by the factor to get the U.S. customary unit.

‡ The special name for the SI unit of the activity of a radionuclide is the becquerel (Bq). (1 Bq = 1 s⁻¹).

§ The special name for the SI unit of absorbed dose is the gray (Gy). (1 Gy = 1 J kg⁻¹).

** The special name for the SI unit of equivalent and effective dose is the sievert (Sv). (1 Sv = 1 J kg⁻¹).

Table of Contents

List of Figures	vii
List of Tables	ix
Acknowledgements	xi
Executive Summary	1
Section 1. Introduction	5
1.1 Overview	5
1.2 Summary of the FDNPS Accident and Radioactive Material Releases	6
1.3 DOD Involvement	7
1.4 Affected DOD Resources	8
1.4.1. Affected Area	8
1.4.2. Affected U.S. Ships and Aircraft	8
1.5 Radiological Support for the Fleet	15
1.6 Scope of this Report	16
1.7 Dose Assessment Approach	17
Section 2. Exposed Populations	19
2.1 Population of Interest	19
2.2 Potentially Exposed Populations	19
2.2.1. Ship (PEP A)	20
2.2.2. Air (ship-based/non-flight) (PEP B)	20
2.2.3. Air (ship-based/flight) (PEP C)	20
2.3 Excluded Individuals	20
2.4 Other Population Activities with Potential for Exposure to Radiation	21
2.4.1. Exposure from Decontamination Efforts	21
2.4.2. Exposure during Small-Craft Operations	22
2.4.3. Exposure below Deck on Ships	22
2.4.4. Exposure related to Surface Contamination on Ships	22
2.4.5. Exposure from Skin Contamination	26

2.4.6.	Exposure Related to Salvage Operations	26
2.4.7.	Exposure Related to Dust-Producing Activities	27
2.4.8.	Exposure Related to Incidental Air Operations involving Ships.....	27
Section 3.	Radiological Environment	29
3.1	FDNPS Radiological Conditions	29
3.1.1.	Accident Progression	29
3.1.2.	Core Damage	30
3.1.3.	Source Term	31
3.1.4.	Spent Fuel Pools	32
3.2	Environmental Data.....	32
3.2.1.	External Radiation (Ship).....	32
3.2.2.	Air Monitoring.....	32
3.2.3.	Water Monitoring	37
3.2.4.	Food Monitoring.....	39
3.2.5.	Soil Monitoring.....	39
3.2.6.	USS Ronald Reagan Radiation Survey Data.....	39
3.3	Radiological Environmental Modeling	40
3.3.1.	Hazard Prediction and Assessment Capability.....	41
3.3.2.	Calibration/Fidelity of the Computer Model.....	47
3.3.3.	HPAC Modeling Concepts and Limitations.....	54
3.4	Major Isotopes.....	58
3.5	Discussion/Summary	58
Section 4.	Dose Assessment Methodologies	61
4.1	Overview of the Approach to Dose Assessment.....	61
4.2	Basic Dose Model	61
4.2.1.	Dose while at Sea.....	63
4.2.2.	Dose Coefficients.....	63
4.2.3.	External Dose while at Sea.....	64
4.2.4.	Internal Dose while at Sea.....	66
4.2.5.	Dose while in Port	66
4.2.6.	Dose during Flight Operations	67
4.2.7.	Total Dose	67
4.2.8.	General Discussion	67

Section 5. Results and Discussion	69
5.1 Dose Results.....	69
5.2 Discussion.....	69
Section 6. Conclusions	77
Section 7. References	79
Appendix A. Radiological Quantities and Units	85
A-1. Introduction	85
A-2. Absorbed Dose	85
A-3. Equivalent Dose.....	85
A-4. Effective Dose	85
A-5. Committed Dose.....	86
A-6. Radioactivity and Activity	86
A-7. Doses Calculated in this Report	86
Appendix B. Fleet History.....	87
B-1. Introduction	87
B-2. USS Blue Ridge (LCC 19).....	87
B-3. USS George Washington (CVN 73).....	87
B-4. USS Cowpens (CG 63)	88
B-5. USS Shiloh (CG 67)	88
B-6. USS Curtis Wilbur (DDG 54)	88
B-7. USS John S. McCain (DDG 56).....	89
B-8. USS Fitzgerald (DDG 62).....	89
B-9. USS Stethem (DDG 63).....	89
B-10. USS Lassen (DDG 82).....	90
B-11. USS McCampbell (DDG 85)	90
B-12. USS Mustin (DDG 89).....	90
B-13. USS Ronald Reagan (CVN 76)	91
B-14. USS Chancellorsville (CG 62)	91
B-15. USS Preble (DDG 88).....	91
B-16. USS Essex (LHD 2).....	92
B-17. USS Germantown (LSD 42)	92
B-18. USS Tortuga (LSD 46)	93
B-19. USS Harpers Ferry (LSD 49).....	93
B-20. USNS Richard E. Byrd (T-AKE 4)	94
B-21. USNS Carl Brashear (T-AKE 7)	94
B-22. USNS Matthew Perry (T-AKE 9)	95
B-23. USNS Pecos (T-AO 197).....	95
B-24. USNS Rappahannock (T-AO 204).....	96
B-25. USNS Bridge (T-AOE 10).....	96
B-26. USNS Safeguard (T-ARS 50)	97
Appendix C. Aircraft Information	99
C-1. Introduction	99

C-2.	Aircraft History	99
C-2.1.	Helicopter Anti-Submarine Squadron Light Five One (HSL-51) ..	99
C-2.2.	Helicopter Sea Combat Squadron Two Three (HSC-23)	99
C-2.3.	Helicopter Sea Combat Squadron Two Five (HSC-25)	99
C-2.4.	Helicopter Sea Combat Squadron Four Three (HSC-43)	99
C-3.	Carrier Air Wing Five (CVW-5)	99
C-3.1.	Strike Fighter Squadron Two Seven (VFA-27)	100
C-3.2.	Strike Fighter Squadron One Zero Two (VFA-102)	100
C-3.3.	Strike Fighter Squadron One One Five (VFA-115)	100
C-3.4.	Strike Fighter Squadron One Nine Five (VFA-195)	101
C-3.5.	Carrier Airborne Early Warning Squadron One One Five (VAW-115)	101
C-3.6.	Electronic Attack Squadron One Four One (VAQ-141)	101
C-3.7.	Fleet Logistics Support Squadron Three Zero (VRC-30)	101
C-3.8.	Helicopter Anti-Submarine Squadron One Four (HS-14)	101
C-4.	Carrier Air Wing Eleven (CVW-11)	101
C-4.1.	Strike Fighter Squadron One Four Six (VFA-146)	102
C-4.2.	Strike Fighter Squadron One Four Seven (VFA-147)	102
C-4.3.	Strike Fighter Squadron One Five Four (VFA-154)	102
C-4.4.	Marine Fighter Attack Squadron Three Two Three (VMFA-323)	103
C-5.	Carrier Air Wing Fourteen (CVW-14)	103
C-5.1.	Carrier Airborne Early Warning One One Three (VAW-113) ..	103
C-5.2.	Electronic Attack Squadron One Three Nine (VAQ-139)	104
C-5.3.	Helicopter Sea Combat Squadron 4 (HSC-4)	104
C-5.4.	Aircraft Utilization in OT	104
Appendix D. Potentially Exposed Population Assumptions		107
D-1.	Introduction	107
D-2.	PEP Assumptions	107
D-2.1.	Assumptions for PEP Category A	107
D-2.2.	Assumptions for PEP Category B	109
D-2.3.	Assumptions for PEP Category C	109
D-2.4.	Decontamination	110
D-2.5.	Consumables	110
D-2.6.	Source Term	110
Appendix E. Internal Dose from Ingestion of Contamination by Hand-to-Mouth Transfer		113
E-1.	Introduction	113
E-2.	Formulation for Determining Doses from Hand-to-Mouth Transfer	113
E-3.	Parameters for Operation Tomodachi	114
E-4.	Results	115
Appendix F. Dose from Skin Contamination		117
Appendix G. Shipboard Water Analysis		121
G-1.	Potable Water Analysis	121
G-2.	MEXT Surveys of Water Activity Concentrations	124

Appendix H. External and Internal Monitoring of Personnel	129
H-1. Dosimeter Data.....	129
H-2. External Dosimetry.....	129
H-3. Other Individual Dosimetry Data	133
H-4. Internal Monitoring.....	133
H-5. USS Ronald Reagan Air Monitoring Data.....	137
H-6. USS Ronald Reagan Contamination Data	148
Appendix I. HPAC Modeling and Uncertainties	151
I-1. HPAC Modeling Process	151
I-2. Source Term	151
I-2.1. Physical Form of Released Material	152
I-2.2. Isotopic Fractions in Releases	152
I-2.3. Comparison of HPAC-generated Results with Measured Data...	154
I-2.4. Iodine Gas Fraction	155
I-2.5. Calibration of the Isotopic Mix	156
I-3. Weather	159
I-3.1. HPAC Weather Input Source Types	159
I-3.2. HPAC-predicted Deposition Field and the “Northwest plume” ..	159
I-3.3. Terrain and Land Cover Impact on the Wind Field	164
I-4. Ship Location	165
I-5. HPAC Software Component Validation and Maturity	166
I-5.1. NFAC Incident Model.....	167
I-5.2. SCIPUFF Transport and Dispersion Model.....	167
I-6. Estimated Uncertainties	167
I-6.1. Uncertainties Computed and Propagated in the T&D Process	167
I-6.2. Combining Sources of Uncertainty	168
I-7. Outputs during the FDNPS Accident.....	170
Appendix J. Calculated Doses for Crews of All Ships	171
Abbreviations, Acronyms, and Symbols.....	177

This page intentionally left blank.

List of Figures

Figure 1. Map of Japan and surrounding sea area affected including the major U.S. military bases (red stars) and FDNPS (yellow trefoil)	8
Figure 2. Ship survey process flowchart	24
Figure 3. Typical shipboard radiological control sheet.....	24
Figure 4. External dose rate by MEXT at Shinyuku, Tokyo Prefecture.....	34
Figure 5. U.S. Air Force high-volume air sampling, Yokota AB, aerosol-only.....	35
Figure 6. Results of DOE aerosol sampling on aerial monitoring missions near FDNPS	37
Figure 7. HPAC flow diagram.....	42
Figure 8. TEPCO sensor locations at FDNPS	44
Figure 9. Measured exposure rates at FDNPS Main Gate 1 from TEPCO	45
Figure 10. The computational domain relative to FDNPS and Honshu Island	46
Figure 11. Example wind barb plot for Fukushima region	48
Figure 12. Comparison of HPAC-calculated and TEPCO measured exposure rates	49
Figure 13. Air activity concentrations of I-131 in aerosols from HPAC results compared to measurements at Yokota AB.....	51
Figure 14. Locations of the USS Ronald Reagan (R) and the USS John S. McCain (M) at eight times on March 13, 2011	52
Figure 15. Comparison of USS Ronald Reagan measured and HPAC-generated air concentrations.....	53
Figure 16. HPAC Output for USS George Washington.....	55
Figure 17. HPAC air submersion output for USS Ronald Reagan.....	56
Figure 18. HPAC air immersion output for USS Shiloh.....	57
Figure 19. HPAC Output for USS Fitzgerald.....	57
Figure 20. Yokosuka NB air submersion and ground shine exposure rates.....	58
Figure 21. At-sea and in-port time periods and doses for ships involved in OT	71
Figure 22. Thyroid doses and in-port fractions for ships with calculated thyroid equivalent crew doses greater than 1 mSv	72
Figure 23. Annual radiation dose from background in Japan prior to FDNPS releases	75
Figure E-1. Detection efficiency as a function of beta energy for an HP-210 probe	115
Figure G-1. Example of a potable water gamma ray energy spectrum.....	122
Figure G-2. Location of MEXT ocean sampling points.....	125

Figure H-1. Beta particle energy and associated detection efficiency	145
Figure H-2. Comparison of HPAC-predicted results to USS Ronald Reagan PAS data.....	147
Figure H-3. USS Ronald Reagan aircrew survey results	149
Figure H-4. USS Ronald Reagan aircraft contamination survey results.....	150
Figure I-1. Comparison of HPAC results with measured exposure rates at the FDNPS main gate	153
Figure I-2. Release rate groups in version 26	157
Figure I-3. Release rate groups in version 31	158
Figure I-4. “Northwest Plume” Data.....	160
Figure I-5. Demonstration regarding how a wind barb indicates wind direction.....	161
Figure I-6. Demonstration showing how a wind barb indicates wind speed.....	161
Figure I-7. Wind barbs on March 15, 2011, 1200	162
Figure I-8. HPAC Northwest plume result for version 26	164
Figure I-9. Hypothetical route for the USS John S. McCain.....	166

List of Tables

Table ES-1. Range of estimated doses during Operation Tomodachi	5
Table 1. Navy ships, vessels, and air wings that supported Operation Tomodachi.....	10
Table 2. Ship dose periods and locations used in dose calculations	12
Table 3. Summary of PEPs.....	19
Table 4. USS Ronald Reagan radiological survey data	40
Table 5. HPAC modeled and measured isotope air concentrations for Yokota AB.....	51
Table 6. Parameter values used for calculation of in-port doses	67
Table 7. Maximum external, internal, and total effective and thyroid doses for all fleet personnel	69
Table C-1. List of CVW-5 Squadrons.....	100
Table C-2. List of CVW-11 Squadrons.....	102
Table C-3. List of CVW-14 Squadrons.....	103
Table C-4. List of U.S. Navy aircraft used for Operation Tomodachi.....	105
Table D-1. PEP categories considered in this report	107
Table E-1. Parameter values used for example calculation of incidental ingestion of surface contamination	116
Table E-2. Count rate corresponding to a 10 μ Sv (1 mrem) dose to the thyroid from incidental ingestion of surface contamination.....	116
Table F-1. Radionuclide dose conversion factors for skin contamination.....	118
Table G-1. Summary of U.S. Navy water analyses	123
Table G-2. Location of MEXT ocean sampling points.....	124
Table G-3. Sea water activity concentration	126
Table H-1. External individual monitoring data.....	130
Table H-2. Summary of TLD results (USS Ronald Reagan)	131
Table H-3. USS Ronald Reagan TLD results grouped by dates with duplicates removed.....	132
Table H-4. Summary of issued EPD results from USS Ronald Reagan.....	132
Table H-5. Summary of EPD readings from USS Ronald Reagan.....	132
Table H-6. Summary of OT internal monitoring results.....	134
Table H-7. Fleet internal monitoring summary	135
Table H-8. USS Ronald Reagan air monitoring results	138
Table H-9. Locations of USS Ronald Reagan air monitoring equipment.....	143
Table H-10. List of isotopes and associated efficiencies for PAS analysis	146

Table J-1. Effective doses for crews of all OT ships while at sea, in port, and totals	172
Table J-2. Thyroid doses for crews of all OT ships while at sea, in port, and totals	174

Acknowledgements

The authors gratefully acknowledge the support of the following:

- National Council on Radiation Protection and Measurements, Scientific Committee No. 6-8 members (Dr. John Till, Dr. John Boice, Dr. Iulian Apostoaei, and Mr. William Kennedy, Jr.) and Dr. John Mercier, Colonel (ret.), USA, who provided peer review.
- Colonel L. Andrew Huff, USAF, MC, SFS, Director, Armed Forces Radiobiology Research Institute (AFRRI), Captain David Lesser, MSC, USN, Deputy Director, AFRRI, and Mr. Stephen I. Miller, Head, Radiation Sciences Department, AFRRI, who allowed Commander Marro the time to work with the DARWG to prepare this report.
- Mr. Jeffrey Brann of Naval Sea Systems Command, who provided technical consultation and critical review.
- Captain Luis Benevides, MSC, USN of Naval Sea Systems Command, who provided critical access to relevant computer-based fleet radiation and radiological controls data.
- Commander Chad Mitchell, MSC, USN of Bureau of Medicine and Surgery, whose leadership and foresight during Operation Tomodachi efforts resulted in acquisition of critical data.
- Commander Lisa Kennemur, MSC, USN, and Commander Anthony Williams, MSC, USN of Naval Dosimetry Center, who provided critical dosimetry and other information.
- Mr. Brian Sanchez of ARA, Inc., who designed and administered the MS SharePoint website that supported this effort.
- Ms. Hilda Maier, Mr. Hanson Gaugler, and Ms. Debra Gross of L-3 Services, Inc., who provided logistics and computing support for this effort.
- Operation Tomodachi DARWG members, who provided critical information and/or especially useful reviews: Dr. Paul Blake, Defense Threat Reduction Agency, Dr. Gerald Falo, U. S. Army Institute of Public Health, and Dr. Mondher Chehata, Leidos.
- Dr. Craig Postlewaite, Mr. Brad Hutchens, Ms. Cristine Maranville, and Mr. Scott Gordon of the Operation Tomodachi Registry, Oversight Working Group, who provided enthusiastic support and critical guidance.

This page intentionally left blank.

Executive Summary

The Assistant Secretary of Defense for Health Affairs requested establishment of the Dose Assessment Recording and Working Group (DARWG) to provide radiation dose assessments for the Department of Defense (DOD) fleet-based population of interest (POI) during the two-month period from March 12, 2011 to May 11, 2011, following a 9.0 magnitude earthquake and subsequent tsunami that damaged the Fukushima Daiichi Nuclear Power Station (FDNPS) in Japan. This population represents about 17,000 fleet-based individuals who are the remainder of the approximately 70,000 DOD-affiliated individuals described in Cassata et al. (2012), which assessed doses for the corresponding shore-based population of approximately 53,000 individuals.

The intent of this report is to estimate doses that are conservative (i.e., high-sided, likely greater than the doses anyone received) as was done in the shore-based report. The basic dose model for all reported doses calculated the total radiation dose received by an individual (or organ or tissue) by addition of the radiation dose from external sources and the radiation dose from radioactive material taken into the body. The radiological environments to which the fleet individuals were exposed provided input parameters to the dose model.

Calculations were performed based on the periods of time the individual ships were located in port and at sea. When a ship was in port, dose calculations were based on shore-based report methods and assumptions. The shore-based report's methods were used for in-port times because of the potential for crew members to go ashore. The analyses indicated that the magnitude of the reported doses depended heavily on location in time and space, especially early in the event (i.e., March 12 through March 31). For example, ships that spent time in port at Yokosuka Naval Base (NB) early in the event generally received higher doses than ships that were at sea during the same time period.

The analysis associated with estimating fleet-based doses relied heavily on time-dependent functions of: (1) atmospheric releases of radioactive material, (2) the transport and dispersion of those releases in both the land and sea environments, and (3) the locations of the ships. Computer modeling was required to evaluate doses for ships at sea because of the relative lack of empirical data to estimate radiation exposure rates and airborne activity concentrations. Computer-generated activity concentration data, conservative assumptions about breathing rates and exposure times, and dose coefficient factors were utilized to calculate doses. The Defense Threat Reduction Agency's (DTRA) Hazard Prediction and Assessment Capability (HPAC) model was used to generate the radiation exposure rates and air activity concentrations for at-sea crew. Inputs to the HPAC model included data on the isotopes inside the FDNPS reactors that had the potential for release to the environment. Using the isotopic data, weather conditions, and known times of releases, HPAC modeling predicted the transport and dispersion of radioactive material from FDNPS throughout the main islands of Japan and the ocean out to 200 miles from the plant.

The range of total effective doses presented in this report for the 25 participating ships is 0.005–0.33 mSv (0.0005–0.033 rem) and the range for the corresponding total thyroid equivalent doses is 0.07 mSv–3.3 mSv (0.007 rem–0.33 rem). To be conservative in accounting for the

dynamic nature of the work site locations and duties throughout the two-month period, and to provide fleet-based doses that are likely to exceed actual doses any individual could have received, single values for the maximum total effective dose and the maximum thyroid dose applicable to all ships were calculated. The maximum total doses were calculated by summing the highest dose from external exposure and the highest dose from internal exposure from among the doses calculated for individual ships. The resulting maximum total doses are therefore higher than the total doses for any individual ship, and they represent maximum doses (effective and thyroid) that are applicable to all fleet-based individuals. The results are listed in Table ES-1.

Table ES-1. Maximum total effective and thyroid doses

Maximum Total Effective Dose (mSv [rem])	Maximum Total Thyroid Dose (mSv [rem])
0.35 (0.035)	3.4 (0.34)

The DARWG is confident that the reported doses are conservative. In addition to the calculation of a maximum dose for all ships, the steps taken to ensure doses were conservative included:

- Assuming an individual spent the two-month period continuously outdoors, exposed to the weather while aboard ship when at sea or ashore while in port;
- Assuming that shipboard personnel were not shielded from the airborne radioactive material the ships encountered while they worked below decks;
- No dose mitigating actions, e.g., administration of potassium iodide; utilization of time, distance or shielding to reduce exposure; decontamination of ship surfaces, etc., were applied in the dose calculations; and
- Calculations of internal dose from inhalation assumed maximum physical activity levels; i.e., inhalation rates, time spent outdoors, and water and soil ingestion rates.

Scientific Committee 6-8 of the National Council on Radiation Protection and Measurements (NCRP) reviewed this report and stated that the estimated doses to shipboard personnel were very small and radiologically insignificant. In addition, the in-port doses were calculated using the shore-based dose calculation methodology of Cassata et al. (2012), which was reviewed by the same NCRP committee, which concluded that those doses were high-sided.

The results of probabilistic analysis of shore-based doses reported in Chehata et al. (2013) provided further support that doses reported herein are high sided. In that report, probabilistic analyses were performed for four locations including Yokosuka NB to provide a basis for comparison with the doses estimated by deterministic methods reported in Cassata et al. (2012). Those comparisons showed that in all the scenarios evaluated at the four locations, including Yokosuka NB, the total effective doses and total equivalent doses to the thyroid estimated by deterministic methods were much higher than the 95th percentile values determined using the probabilistic method (Chehata et al., 2013). Since the methods of Cassata et al. (2012) were used for the calculation of in-port doses in this report, it is reasonable to conclude that the in-port doses in this report are also conservative.

To put the maximum doses into perspective, they were compared to the doses for several relevant groups. The highest calculated effective dose is significantly less than the average U.S. annual ubiquitous background radiation dose¹ of 3.1 mSv (0.31 rem) as reported in NCRP (2009a). The calculated thyroid dose is significantly less than the U.S. annual occupational organ dose limit of 500 mSv (50 rem). In addition, when compared to doses for shore-based individuals, the maximum total effective dose for ship-based individuals of 0.35 mSv (0.035 rem) is approximately four times lower than the maximum effective dose of 1.2 mSv (0.12 rem) calculated for DOD-affiliated individuals at 13 shore-based locations in Cassata et al. (2012). A comparison of the thyroid doses for ship-based and shore-based individuals shows a similar pattern.

Doses for fleet-based individuals are lower than doses for shore-based individuals because of several factors associated with the modeling of at-sea exposures and factors that tend to increase or decrease actual dose. Model calculations used the specific time and location data about ships' movements, which would tend to produce more realistic dose estimates because:

- Ships spent most of their time at sea sailing outside of airborne radioactive clouds² and contaminated ocean areas, whereas the shore-based population was continuously present in areas of low-level contamination in the air and on the ground.
- Timely and accurate DOD forecasts of plume dispersion and transport allowed U.S. ships to maneuver so as to minimize the time that they were impacted by radiological releases.

Factors that tend to overestimate calculated doses are listed immediately following Table ES-1 above. On the other hand, factors that were judged to be minimal potential dose contributors to individuals on ships and were not included in the dose calculations for this report include:

- There was limited re-suspension of radioactive materials from the surface of contaminated water in contrast to ground-deposited radioactive materials that could more-readily be re-suspended into the air.
- Aircrews who flew through radioactive clouds were generally on missions of short duration, and exposure to airborne radioactive material during passage through the cloud would have been limited by air filtering capabilities of the aircraft, whereas shore-based individuals could have experienced continuous exposure to passing clouds of radioactive materials.

The reported radiation doses to the fleet-based individuals are at least one order of magnitude less than any dose associated with adverse health effects. This conclusion is supported

¹ The term "ubiquitous" refers only to natural radiation sources and does not include other sources such as medical procedures, occupational exposure, consumer products, etc.

² The terms "cloud" and "plume" are used throughout the report. Although both terms are associated with FDNPS releases, the term "cloud" refers to the volume of air that passed overhead as a result of airborne radiological effluent from FDNPS, while "plume" refers to the immediate volume of gas released from FDNPS and subsequently transported and dispersed over time.

by the Health Physics Society official position statement regarding radiation dose and health effects:

There is substantial and convincing scientific evidence for health risks following high-dose exposures. However, below 5–10 rem (which includes occupational and environmental exposures), risks of health effects are either too small to be observed or are nonexistent. (HPS, 2010)

The radiation doses presented in this report will be posted on the [Operation Tomodachi Registry website](#).

Section 1.

Introduction

1.1 Overview

This report presents the results of radiation dose assessments conducted by the Operation Tomodachi Registry's (OTR) Dose Assessment and Recording Working Group (DARWG) for the Department of Defense (DOD) fleet-based population of interest (POI) during the two-month period from March 12, 2011 to May 11, 2011, following a 9.0 magnitude earthquake and subsequent tsunami that damaged the Fukushima Daiichi Nuclear Power Station (FDNPS) in Japan. This population represents more than 17,000 of the approximately 70,000 DOD-affiliated individuals described in Cassata et al. (2012), hereafter referred to as the "shore-based report," which assessed doses for the corresponding shore-based population of approximately 53,000 individuals.

The dose assessment process involved the collection and evaluation of available radiation measurements taken aboard ship, identification of data gaps, use of airborne radioactive material transport models, and external and internal radiation monitoring results, especially for ships and attached units while at sea. In addition, fleet-based doses were derived by prorating doses from the shore-based report for those times when ships were in port. In addition, radiation exposure rate data for ship-based locations and times were not as robust as for shore-based populations. The purpose of this report is to document high-sided radiation doses and to serve as a scoping study (as defined by NAS [1995] and discussed in the shore-based report) or first assessment, which can serve as a guide for future work. The reported doses are intended to inform members of the POI and medical providers, but should not be used for ionizing radiation epidemiological studies.

This report provides the technical basis for doses that will be posted on the Operation Tomodachi Registry (OTR) website³. These doses and information about the possible health effects from them will be accessible to all members of the POI, members of the medical community, and the public at large. This report is part of a series of reports undertaken by the DARWG to assess radiation doses to DOD-affiliated individuals or characterize the radiological environment at J-Village. The series includes the following reports:

- Radiation Dose Assessments for Shore-Based Individuals in Operation Tomodachi, Revision 1 (DTRA-TR-12-001 [R1]).
- Probabilistic Analysis of Radiation Doses for Shore-Based Individuals in Operation Tomodachi (DTRA-TR-12-002).
- Radiation Internal Monitoring by In Vivo Scanning in Operation Tomodachi (DTRA-TR-12-004).

³ <https://registry.csd.disa.mil/registryWeb/Registry/OperationTomodachi/DisplayAbout.do>

- Radiation Dose Assessments for the Embryo, Fetus, and Nursing Infant during Operation Tomodachi (DTRA-TR-12-017).
- Characterization of the Radiological Environment at J-Village during Operation Tomodachi (DTRA-TR-12-045).
- Comparison of Radiation Dose Studies of the 2011 Fukushima Nuclear Accident Prepared by the World Health Organization and the U.S. Department of Defense (DTRA-TR-12-048).
- Standard Methods (SM) and Standard Operating Procedures (SOPs) for Responding to Operation Tomodachi Individual Dose Assessments and Responding to VA Radiogenic Disease Compensation Claims (AIPH SM/SOP).

1.2 Summary of the FDNPS Accident and Radioactive Material Releases

At 1446 Japan Standard Time⁴ on March 11, 2011, a 9.0 magnitude earthquake, the largest ever recorded in Japan, occurred at a depth of approximately 19 miles, 80 miles east of Sendai and 231 miles northeast of Tokyo off the coast of Honshu Island (USGS, 2011). Seismic sensors immediately detected the earthquake and activated the rapid shutdown systems for 11 operating nuclear power plants at four sites along the northeast coast of Japan (Onagawa Units 1, 2 and 3; FDNPS Units 1, 2 and 3; Fukushima Daini Units 1, 2, 3 and 4; and Tokai Unit 2). At the time of the earthquake, FDNPS Units 1, 2 and 3 were operational and producing power, and Units 4, 5 and 6 had been shut down for refueling and maintenance activities. Irradiated reactor fuel in Unit 4 had been offloaded previously to the Unit 4 spent fuel pool. Irradiated fuel assemblies for Units 5 and 6 were still secured in the reactor cores.

The earthquake and tsunami caused the loss of both offsite power and onsite backup power to FDNPS, and this resulted in station blackout conditions (GOJ, 2011). Working under blackout conditions, plant workers focused their attention on maintaining the necessary cooling of the shut-down reactors and spent fuel pools. However, the extended station blackout conditions led to substantial reactor core meltdowns for Units 1, 2 and 3 with subsequent containment leakage and releases of radioactive materials to the environment. No significant releases of radioactivity from spent fuel pools were apparent. Intermittent large releases of radioactive fission products from the damaged reactors were detected during the 10 days following the earthquake. The fission products entered the atmosphere as gases and aerosols. In addition, radioactive fission products entered the ocean when seawater pumped in for emergency cooling of the units became contaminated while inside the units and were released when containment leaked. The radioactive fission product gases and aerosols were transported in air by changing weather patterns across much of Japan's main island of Honshu, as well as out to sea. In addition, deposition of fission products was observed on land, buildings and water bodies in and around Honshu (INPO, 2011).

⁴ Japan Standard Time (JST), 0000-2400, is used throughout this report, unless otherwise noted. JST is 9 hours ahead of Coordinated Universal Time (UTC). DOD's use of UTC is traditionally noted by the "Zulu (Z) designation; e.g., 1630Z."

1.3 DOD Involvement

Shortly after initial news reports of the devastating earthquake and tsunami surfaced, the DOD began responding to the developing situation in Japan in order to protect health and prevent illness. In Japan and Hawaii, the response involved efforts to evaluate the magnitude of the potential health threat by obtaining external radiation dose measurements with portable radiation detection equipment at U.S. installations in Japan, on naval vessels, and in mission areas where DOD Service members were deployed. Special DOD radiation health, environmental health, and emergency response teams from the continental United States and Okinawa were also deployed to Honshu Island, to augment the DOD capabilities within the U.S. Forces Japan (USFJ) region. Department of Energy (DOE) accident response teams were also deployed to the area. DOD took actions to ensure that radioactively contaminated food and bottled water did not reach the DOD-affiliated population.

Military commands within the Pacific/Japan area, including U.S. Pacific Command (USPACOM), USFJ, and the Commander, U.S. Pacific Fleet (COMPACFLT), also took a number of separate actions to protect the health of the DOD population on mainland Japan. These included releasing health protection guidance to control radiation exposure, establishing criteria for entry into hot and warm zones around the FDNPS, and publishing guidance for distribution and consumption of potassium iodide (KI) for protection against inhalation or ingestion of radioactive iodine.

The following list highlights events that are relevant to the fleet-based individuals addressed in this report.

On March 13, 2011, the media first reported possible radiation exposure to U.S. forces after the USS Ronald Reagan carrier strike group encountered a radioactive cloud⁵ released from FDNPS while en route to assist in humanitarian assistance and disaster relief (HADR) operations for Japan. Contamination situations continued to be reported as U.S. aircraft, vessels, and personnel deployed to assist the Government of Japan (GOJ) in HADR operations.

On March 16, 2011, U.S. Pacific Command (USPACOM) released guidance on health protection requirements for radiation exposure and established criteria for USFJ for hot and warm zone entries (USFJ, 2011a).

On March 16, 2011, the first internal monitoring scans were performed at Puget Sound Naval Shipyard on DOD personnel returning from Japan.

On March 26, 2011, the Commander, U.S. Pacific Fleet (COMPACFLT) issued medical and radiological limit guidance (COMPACFLT, 2011).

On April 14, 2011, an internal monitoring scan program for DOD-affiliated personnel was initiated in Japan.

On September 1, 2011, the internal monitoring scan program was completed.

⁵ “Cloud” refers to the volume of air that passed overhead as a result of airborne radiological effluent from FDNPS.

1.4 Affected DOD Resources

1.4.1. Affected Area

At the time of the FDNPS accident, some fleet-based individuals were on board ships that were already in Japan (e.g., USS George Washington (CVN 73) was undergoing planned regular maintenance at the Yokosuka Naval Base [NB]), while others were far away from Japan and responded (transited from other locations) to provide HADR support during Operation Tomodachi (OT). Figure 1 provides a map of the affected area including the main islands of Japan and surrounding sea waters, with major U.S. military bases identified.



Figure 1. Map of Japan and surrounding sea area affected including the major U.S. military bases (red stars) and FDNPS (yellow trefoil)

1.4.2. Affected U.S. Ships and Aircraft

The Seventh Fleet, home ported at Yokosuka NB, has an area of responsibility that includes Japan, encompasses over 48 million square miles (133.33 million square kilometers), and extends from the Kuril Islands in the north, to the Antarctic in the south, and from the International Date Line to the 68th meridian in the east (C7F, 2012a). Although Japan is within the Seventh Fleet's area of responsibility, ships from other numbered fleets responded because of their close proximity at the time of the earthquake and their capabilities to support HADR efforts. In addition, not all ships officially assigned as part of a carrier strike group (CSG) took

part in HADR efforts and those ships were not included in this report. In other cases, some ships were included despite being located outside the 200 nautical-mile (nmi) radius from the FDNPS because the OTR contained individual crew member's names. For example, USS Stethem, which was assigned to the USS George Washington CSG, was included although it was well outside the 200 nmi radius from FDNPS during the two-month time period.

The Seventh Fleet comprises 60–70 ships, 200–300 aircraft, and 40,000 Navy and Marine Corps personnel, including those located at bases in Japan and Guam, who are rotationally deployed back to the U. S. mainland (C7F, 2012a). Commander, U.S. Seventh Fleet (C7F), was embarked aboard USS Blue Ridge (LCC 19) which was forward deployed at Yokosuka NB (C7F, 2012a).

This report applies to the ships and the approximately 17,000 DOD-affiliated individuals (to include civilian Military Sealift Command [MSC] individuals) that supported OT under the U.S. Pacific Command, specifically the Third and Seventh Fleets, and the Military Sealift Command (MSC). The Third Fleet Carrier Strike Group Seven (CSG-7) comprised the USS Ronald Reagan (CVN 76), other assigned ships that provided support and protection, and attached air wings (CNSF, 2012).

The Seventh Fleet Carrier Strike Group Five (CSG-5), consisted of the USS George Washington (CVN-73), other ships that provided support and protection, and attached air wings, which included Carrier Air Wing Five (CVW 5) (the U.S. Navy's only forward deployed air wing) based at Naval Air Facility (NAF), Atsugi (NAFA, 2012). Several MSC ships provided fleet logistical and support functions such as fuel handling, delivery of supplies, and rescue/salvage operations. The USS Essex Amphibious Ready Group (ESX ARG) included several amphibious type ships and over 2,200 U.S. Marines of the forward-deployed 31st Marine Expeditionary Unit (MEU) that provided ground support and conducted amphibious type operations (C7F, 2012b).

Amphibious assault ships embark Landing Craft Air Cushion (LCAC) and Landing Craft Utility (LCU)-type vessels that can operate independently. In addition, surface ships can utilize rigid-hull inflatable boats to quickly transport personnel and supplies.

Table 1 lists individual ships, attached vessels and air wings, and the numbers of individuals for each group included in this POI. Appendices B and C provide details of the locations, missions, and activities of the individual ships and aircraft units.

Table 1. Navy ships, vessels, and air wings that supported Operation Tomodachi

Ship	Hull No.	Attached Air Wings	Vessels Attached*	Number of Individuals (Ships)
Commander, U.S. Seventh Fleet (C7F)				
USS Blue Ridge	LCC 19	N/A	N/A	926 (1)
Seventh Fleet Carrier Strike Group Five (CSG-5)				
USS George Washington	CVN 73	VAQ-141, VAW-115, VFA-102, VFA-195, VFA-27, VRC-30, Det. 5 and HS-14	N/A	8,298 (10)
USS Cowpens	CG 63	N/A	N/A	
USS Shiloh	CG 67	N/A	N/A	
USS Curtis Wilbur	DDG 54	N/A	N/A	
USS John S. McCain	DDG 56	N/A	N/A	
USS Fitzgerald	DDG 62	N/A	N/A	
USS Stethem	DDG 63	N/A	N/A	
USS Lassen	DDG 82	N/A	N/A	
USS McCampbell	DDG 85	N/A	N/A	
USS Mustin	DDG 89	N/A	N/A	
Third Fleet Carrier Strike Group Seven (CSG-7)				
USS Ronald Reagan	CVN 76	CVW-14, VFA-154, VFA-147, VFA-146, VMFA-323, VAW-113 VAQ-139, VRC-30, and HS-4	N/A	4,701 (3)
sUSS Chancellorsville	CG 62	N/A	N/A	
USS Preble	DDG 88	N/A	N/A	

Table 1. Navy ships, vessels, and air wings that supported Operation Tomodachi (cont.)

Ship	Hull No.	Attached Air Wings	Vessels Attached*	Number of Individuals (Ships)
USS Essex Amphibious Ready Group (ESX ARG)				
USS Essex	LHD 2	N/A	LCU 1631, 1634, 1651	1,960 (4)
USS Germantown†	LSD 42	N/A	LCAC 9, 29	
USS Tortuga†	LSD 46	N/A	N/A	
USS Harpers Ferry	LSD 49	N/A	LCAC 10, 81	
Military Sealift Command (MSC)				
USNS Richard E. Byrd	T-AKE 4	N/A	N/A	1,084 (7)
USNS Carl Brashear	T-AKE 7	N/A	N/A	
USNS Matthew Perry	T-AKE 9	N/A	N/A	
USNS Pecos	T-AO 197	N/A	N/A	
USNS Rappahannock	T-AO 204	N/A	N/A	
USNS Bridge	T-AOE 10	N/A	N/A	
USNS Safeguard	T-ARS 50	N/A	N/A	
TOTAL				16,969 (25)

* Only hull numbers are assigned for these vessel types. Other vessels could have been assigned to various ships and performed HADR operations.

[†] Not officially assigned to ESX ARG; forward-deployed and performed similarly as ESX ARG.

Table 2 provides a summary of the time periods and locations used for the dose calculations for each ship (typically based on actual latitude/longitude positioning). The time a ship spent in port or at sea greatly affected the calculated dose values largely because of the associated shore-based dose for in-port times, ability to maneuver at sea, and other factors. Effective doses and thyroid doses were determined for those periods discussed in Section 4. For example, shore-based doses for the time in port were generated for times when the ship was in port at a naval base, such as Sasebo NB or Yokosuka NB. Computer modeling results were used to calculate external doses for times when ships were at sea. To calculate the total doses, the modeling results for dispersion of FDNPS effluents due to wind direction and speed and release times were combined with each ship location based on latitude/longitude coordinates, and associated date/time periods for each ship.

Table 2. Ship dose periods and locations used in dose calculations

Ship	Dose Period (2011)	Location[*]
USS Blue Ridge (LCC 19)	Mar 12–Apr 10 Apr 11–May 11	At Sea Yokosuka NB
USS George Washington (CVN 73)	Mar 12–21 Mar 22–Apr 5 Apr 6 Apr 7–12 Apr 13–14 Apr 15–20 Apr 21–May 11	Yokosuka NB At Sea Sasebo NB At Sea Sasebo NB At Sea Yokosuka NB
USS Cowpens (CG 63)	Mar 12–14 Mar 15–Apr 5 Apr 6–May 11	Yokosuka NB At Sea Yokosuka NB
USS Shiloh (CG 67)	Mar 12–18 Mar 19–Apr 5 Apr 6–May 9 May 10–11	Yokosuka NB At Sea Yokosuka NB At Sea
USS Curtis Wilbur (DDG 54)	Mar 12–25 Mar 26–Mar 29 Mar 30–Apr 6 Apr 7–May 11	At Sea Yokosuka NB At Sea Yokosuka NB
USS John S. McCain (DDG 56)	Mar 12 Mar 13–22 Mar 23 Mar 24–28 Mar 29–Apr 1 Apr 2–5 Apr 6–10 Apr 11–12 Apr 13–May 11	Yokosuka NB At Sea Sasebo NB At Sea Yokosuka NB At Sea In port, Chinae, ROK [†] At Sea Yokosuka NB
USS Fitzgerald (DDG 62)	Mar 12 Mar 13–28 Mar 29–Apr 11 Apr 12–13 Apr 14–May 11	Yokosuka NB At Sea Yokosuka NB At Sea Yokosuka NB
USS Stethem (DDG 63)	Mar 12–16 Mar 17 Mar 18–20 Mar 21–28 Mar 29–31 Apr 1–10 Apr 11–May 11	At Sea Sasebo NB Donghae Harbor, ROK At Sea Sasebo NB At Sea Yokosuka NB

Table 2. Ship dose periods and locations used in dose calculations (cont.)

Ship	Dose Periods (2011)	Locations
USS Lassen (DDG 82)	Mar 12–21 Mar 22–25 Mar 26–May 11	Yokosuka NB At Sea Sasebo NB
USS McCampbell (DDG 85)	Mar 12–Apr 1 Apr 2–7 Apr 8–9 Apr 10 Apr 11–25 Apr 26–May 6 May 7–11	At Sea Yokosuka NB At Sea Yokosuka NB At Sea Yokosuka NB At Sea
USS Mustin (DDG 89)	Mar 12 Mar 13–31 Apr 1–8 Apr 9–10 Apr 11–14 Apr 15–May 11	Yokosuka NB At Sea Yokosuka NB At Sea Sasebo NB At Sea
USS Ronald Reagan (CVN 76)	Mar 12–Apr 18 Apr 19–22 Apr 23–May 11	At Sea Sasebo NB At Sea
USS Chancellorsville (CG 62)	Mar 12–Apr 18 Apr 19–22 Apr 23–May 11	At Sea Sasebo NB At Sea
USS Preble (DDG 88)	Mar 12–Apr 18 Apr 19–22 Apr 23–May 11	At Sea Sasebo NB At Sea
USS Essex (LHD 2)	Mar 12–Apr 13 Apr 14–May 11	At Sea Sasebo NB
USS Germantown (LSD 42)	Mar 12–Apr 10 Apr 11–May 11	At Sea Sasebo NB
USS Tortuga (LSD 46)	Mar 12 Mar 13–Apr 10 Apr 11 Apr 12–14 Apr 15–27 Apr 28–May 11	Sasebo NB At Sea Yokosuka NB At Sea Sasebo NB At Sea
USS Harpers Ferry (LSD 49)	Mar 12–Apr 6 Apr 7–May 4 May 5 May 6–May 10 May 11	At Sea Sasebo NB At Sea Sasebo NB At Sea

Table 2. Ship dose periods and locations used in dose calculations (cont.)

Ship	Dose Periods (2011)	Locations
USNS Richard E. Byrd (T-AKE 4)	Mar 12–25 Mar 26–27 Mar 28–Apr 4 Apr 5–7 Apr 8–11 Apr 12–13 Apr 14–22 Apr 23–25 Apr 26–May 11	At Sea Sasebo NB At Sea Sasebo NB At Sea Yokosuka NB At Sea Sasebo NB At Sea
USNS Carl Brashear (T-AKE 7)	Mar 12–18 Mar 19–21 Mar 22–29 Mar 30–Apr 4 Apr 5–15 Apr 16–19 Apr 20–29 Apr 30–May 4 May 5–11	At Sea Sasebo NB At Sea Sasebo NB At Sea Yokosuka NB At Sea Sasebo NB At Sea
USNS Matthew Perry (T-AKE 9)	Mar 12–16 Mar 17–18 Mar 19–27 Mar 28–31 Apr 1–7 Apr 8–11 Apr 12–May 11	At Sea Sasebo NB At Sea Sasebo NB At Sea Sasebo NB At Sea
USNS Pecos (T-AO 197)	Mar 12–19 Mar 20–21 Mar 22–28 Mar 29–31 Apr 1–3 Apr 4–6 Apr 7–12 Apr 13 Apr 14–May 11	At Sea Akasaki POL [‡] Depot At Sea Yokosuka NB At Sea Sasebo NB At Sea Akasaki POL Depot At Sea

Table 2. Ship dose periods and locations used in dose calculations (cont.)

Ship	Dose Periods (2011)	Locations
USNS Rappahannock (T-AO 204)	Mar 12–24 Mar 25–27 Mar 28–29 Mar 30–31 Apr 1–Apr 7 Apr 8–13 Apr 14 Apr 15–22 Apr 23–25 Apr 26–May 2 May 3–8 May 9–11	At Sea Sasebo NB At Sea Yokosuka NB At Sea Sasebo NB At Sea Sasebo NB At Sea Sasebo NB At Sea Sasebo NB
USNS Bridge (T-AOE 10)	Mar 12–20 Mar 21–24 Mar 25–Apr 3 Apr 4–May 1 May 2–11	At Sea Sasebo NB At Sea Sasebo NB At Sea
USNS Safeguard (T-ARS 50)	Mar 12–15 Mar 16–21 Mar 22–Apr 9 Apr 10–15 Apr 16–May 11	At Sea Yokosuka NB At Sea Yokosuka NB At Sea

* “At Sea” may also indicate an in-port location that is outside of mainland Japan such as White Beach Naval Facility on the island of Okinawa, or a port location with no U.S. military facilities such as Hachinohe. See Appendix B for details of these locations.

† “ROK” means Republic of Korea.

‡ “POL” means petroleum, oil, and lubricants.

1.5 Radiological Support for the Fleet

Only the nuclear-powered aircraft carriers USS Ronald Reagan and USS George Washington had the trained personnel, equipment and supplies necessary to detect and analyze radioactive contamination and perform decontamination activities on a large scale. Soon after release of radioactive material from FDNPS, USPACOM requested assistance to fill this gap, and all services provided health physics support. For example, the U.S. Navy Bureau of Medicine and Surgery (BUMED) coordinated the deployment of 34 active Navy radiation health officers (RHOs), shore-based radiological control technicians (RCTs) and one retired RHO to various ships and shore facilities to provide radiological support for the HADR and force health protection efforts. However, logistical challenges prevented their full deployment until several days after the first known FDNPS release. The RHO and RCT duties included:

- Assistance in:
 - Establishing an internal monitoring program;
 - Coordinating decontamination efforts;

- Gathering radiological data;
- Radiological risk communication to the fleet;
- Orderly acquisition and distribution of personnel dosimetry; and
- Liaison with USPACOM, USFJ, Naval Sea Systems Command (NAVSEA), BUMED, and other organizations.

1.6 Scope of this Report

This report provides the approach, methods, and results of a study to estimate conservative radiation doses that may be assigned to individuals who were part of a potentially exposed population (PEP). The PEPs defined in Section 2 include personnel who served on the ships and aircraft shown in Table 1 and performed HADR efforts during the two-month period from March 12, 2011 to May 11, 2011. The radiation exposure circumstances and resulting doses for these individuals were not addressed in the dose assessment performed for shore-based DOD-affiliated individuals (Cassata et al., 2012).

Fleet-based individuals experienced unique environments that involved ship movements or aircraft missions through changing concentrations of airborne radioactivity at different times and locations. In addition, individuals would have been restricted to the confines of a particular ship and possibly exposed to radioactive contamination on deck and below deck.

For the shore-based report, environmental sampling data were used to determine external exposure rates, activity concentrations of airborne radionuclides, water and soil for exposed populations and then input parameters were determined to calculate external and internal radiation doses. In this report, external and internal radiation doses for PEPs that apply to ships at sea were estimated using computer modeling of the activity concentrations of airborne radioactive materials to calculate external radiation dose rates and committed doses to internal organs and tissues when ships were at sea. For ships in port, the dose for each in-port period was calculated as a time-dependent dose for the specific port location (Yokosuka NB or Sasebo NB) using methods of Cassata et al. (2012) and this prorated dose was assigned to the ship's crew. Personal dosimetry data from thermoluminescent dosimeters (TLDs), electronic personal dosimeters (EPDs), posted TLDs, and surface contamination surveys were used to assess the validity of modeled doses. Internal radiation doses were also compared to internal monitoring (IM) results for shipboard and air-crew personnel who were monitored relatively soon after exposure.

Radiation dose calculations accounted for external radiation levels, airborne radioactive material concentrations, physical activity levels and breathing rates of personnel, particle size distributions, and other factors as was done in Cassata et al. (2012). From the ranges of parameter values used in Cassata et al. (2012), which were chosen to be reasonably conservative estimates for a range of daily physical activities, the highest values were selected for fleet-based individuals. Reported doses for fleet-based individuals were calculated assuming maximum values for breathing rate, physical activity, and time outdoors.

1.7 Dose Assessment Approach

The quantities calculated in this report are the effective dose and the equivalent dose to the thyroid (herein called thyroid dose) as described in ICRP Publication 60 (ICRP, 1991) and used in the ICRP databases of dose coefficients (DCs) (ICRP, 2001). The effective dose is commonly associated with a whole-body dose. Cassata et al. (2012) subscribed to conclusions that effective doses “are intended for use in radiation protection, including the assessment of risk in general terms” (ICRP, 1991).

DARWG considers the doses in this report to be conservative estimates that can be expected to be greater than the dose any individual actually received. Additional investigation is required if an individualized dose assessment is requested. To estimate radiation doses in this report, the DARWG assumed that:

- The potentially exposed populations were exposed to the radiological conditions described by:
 - The computer modeled external dose rates and airborne activity concentrations described in Section 4 for ships at sea and aircraft, and
 - The environmental data reported in Cassata et al. (2012) for ships in port at appropriate DARWG locations.
- The human behavior or habit data⁶ are “upper percentile” values from EPA (2011), and
- The ICRP databases of dose coefficients for inhalation and ingestion released on compact disc read-only memory (CD-ROM) (ICRP, 2001) apply assuming 1 μm activity median aerodynamic diameter (AMAD) aerosols.

The basic exposure model assumes that a hypothetical person representative of a much larger population:

- Was exposed to photons⁷ from a passing plume and deposits of radioactive material;
- Breathed contaminated air from the passing plume(s) and resuspended material; and
- Ingested negligible amounts of radioactive material from contaminated surfaces of ships or aircraft or in water, food, or soil and dust each day while on shore.

These doses were calculated for exposures to both external and internal radiation sources. As discussed later in this report, the DARWG believes that the total effective doses and thyroid equivalent doses estimated using the approach described above are conservative indicators of potential health effects for the DOD-affiliated POI.

⁶ “Habit data” is a broad term used to describe those conditions that bring members of the public in contact with radiation or radioactive material. Commonly used habit data are ingestion and inhalation rates, time spent indoors and time spent outdoors. See, for example, *Radiological Conditions in Areas of Kuwait with Residues of Depleted Uranium* (IAEA, 2003) and *Generalised Habit Data for Radiological Assessments* (Smith and Jones, 2003).

⁷ Photons are the radiation type typically responsible for external exposures and commonly include x rays and gamma rays.

This page intentionally left blank.

Section 2.

Exposed Populations

2.1 Population of Interest

The fleet-based POI is the population of DOD-affiliated individuals (Service members, civilian employees, and contractor employees) aboard ships or involved in aircraft operations from ships anywhere within or around the four main islands of Japan (Hokkaido, Honshu, Shikoku, and Kyushu). For this report, an individual in this population is called a fleet-based individual. The radiation doses estimated in this study are based on human behavior characteristics for “person(s) of reasonably high-end behavior” (Cassata et al., 2012; EPA, 2011), and are therefore intended to be conservative.

2.2 Potentially Exposed Populations

A potentially exposed population (PEP) is a subpopulation of the POI that is defined by a particular set of characteristics, common locations, exposure scenarios, and habit data within the larger POI associated with OT. Members of a PEP were likely to be exposed to the same radiation sources; however, the environmental radiation data are not part of the definition of a PEP. It is acknowledged that within a PEP actual radiation doses to real individuals varied widely; however, the dose assessment process is intended to produce a credible (NCRP, 2009b) radiation dose for a PEP (Cassata et al., 2012). The preparation of estimated doses for specific PEPs involves assumptions about the values for the numerous parameters required for calculations. In this report, estimates of doses involve the selection of conservative parameter values that are reasonable overestimates of the actual values or ranges of values.

Individual PEPs were developed for three groups based on work location, job function, and other factors. Those three groups are (1) ship-based, (2) aircrew (ship-based/non-flight), and (3) aircrew (ship-based/ flight) as listed in Table 3. The PEPs serve to allow easy identification of a Service member’s category of exposure. For example, aircrew members who served on board USS Ronald Reagan (CVN 76) (or any other ship) but did not participate in flight operations could read this report and quickly determine that PEP B characteristics closely matched their activities.

Table 3. Summary of PEPs

PEP	Description
A	Ship’s crew
B	Aircrew (ship-based/non-flight)
C	Aircrew (ship-based/flight)

2.2.1. Ship (PEP A)

This PEP includes personnel who were assigned shipboard duties and who were onboard and deployed with a ship identified in this report. Personnel in this PEP were officially assigned as members of the ship's crew and performed general shipboard duties according to their military rating (e.g., medical duties, navigation, damage control, etc.). These duties do not include those associated with additional potential for radiation exposure such as conducting flight operations.

2.2.2. Air (ship-based/non-flight) (PEP B)

PEP B includes individuals assigned as part of a ship-based aircrew who did not perform any flight operations. It consists of individuals administratively assigned to an aircrew, who lived and worked aboard the ship, and were potentially exposed to the same radiological environments as those of PEP A. This PEP category was created to assure fleet individuals that the DARWG understood that some individuals were administratively assigned to a flight crew but did not actually fly in air operations.

2.2.3. Air (ship-based/flight) (PEP C)

PEP C includes individuals assigned as part of a ship-based (operates from the ship instead of from a land-based air strip) aircrew that performed flight operations.⁸ In addition to the flight environment, these individuals lived and worked aboard ship and were potentially exposed to the same radiological environments as those of PEP A.

2.3 Excluded Individuals

Some individuals who could have been considered for inclusion in these PEP categories were not included in the dose calculations. These include pregnant females and those who were not ship-based (i.e., individuals who participated in land-based flight operations).

This report provides dose assessments for fleet-based personnel including personnel temporarily assigned to the ships (i.e., aircrew who embarked when the ship left homeport and went to sea). Although individuals who participated in land-based flight operations had the potential to fly back and forth to the ships, they are not included in this report because:

- Their associated exposure conditions would more appropriately fall within the scope of Cassata et al. (2012) because they spent the majority of their time on shore; and
- The specialized nature of their duties and potential exposure scenarios are more appropriately addressed via an individualized dose assessment.

Falo et al. (2013) reported effective and committed radiation doses to embryos/fetuses associated with pregnant females⁹ and nursing infants based on external dose and radioactive material intakes; to be conservative and calculate maximum values, all of the intake was assumed to have occurred on March 11, 2011. The potential doses to an embryo/fetus were not

⁸ Flight operations are defined as flying in an aircraft in support of OT; this does not include personnel who were assigned to an aircrew but did not actually fly.

⁹ This includes females who are either pregnant at the time of exposure or those who conceive post exposure and potential internal contamination provides a radiation source to the embryo/fetus.

included in this report. Rather, these doses are more appropriately generated using Falo et al. (2013) procedures based on the mother's exposure level. The reasons for this are:

- The U.S. Navy generally prohibits pregnant Service members from deployment on ship. In addition, they can be shipboard for 20 weeks post-conception restricted to shipboard in-port movements. (USN, 2007)
- Detailed estimates were provided in Falo et al. (2013), and
- Individual dose assessments should be performed that more accurately account for specific environmental factors for the pregnant female.

2.4 Other Population Activities with Potential for Exposure to Radiation

2.4.1. Exposure from Decontamination Efforts

Although personnel did participate in decontamination efforts¹⁰, assignment of PEP categories did not include potential exposure while performing decontamination efforts because:

- On many occasions, individuals wore dosimetry and personal protective equipment (PPE) while performing the work according to radiological control requirements (Benevides, 2012);
- The use of a ship's water wash-down system and heavy use of soap and water significantly reduced potential re-suspension of radioactive contamination during decontamination efforts; and,
- Actual radiation exposure and subsequent inhalation or ingestion associated with decontamination efforts would almost certainly be less than the assessed dose based on the assumption used that the individual was standing topside while exposed to a radioactive plume for reasons discussed below.

DARWG assumed that the dose from inhalation or ingestion associated with decontamination would be less than the conservatively calculated dose an individual would receive by standing topside continuously for a two-month period of time while being exposed to passing radioactive clouds because:

- Topside dose was calculated assuming no exposure reducing factors (e.g., wearing of PPE, water washdown, etc.) whereas many decontamination efforts involved extensive PPE (including a mask to cover the mouth and nose).
- Individuals who performed decontamination efforts were typically exposed to relatively low contamination levels after a radioactive cloud had passed compared to those exposed directly to the passing cloud while topside.
- The water washdown system would effectively minimize resuspension of surface contamination and subsequent inhalation of particles.

¹⁰ Decontamination efforts include the decontamination of ships, aircraft, and personnel.

2.4.2. Exposure during Small-Craft Operations

Although the structural features of small-craft vessels such as the Landing Craft Air Cushion (LCAC), Landing Craft Units (LCU), and rigid-hull inflatable boats are substantially different from the larger surface ships, the conservative assumption that an individual was exposed while continuously topside over the two-month period is also relevant for small craft operators. The LCACs, LCUs, and inflatable boats typically operated in the same vicinity as the larger ships and did not perform a significant amount of independent operations. For instance, LCACs 10 and 81, assigned to the USS Harpers Ferry (LSD 49), only operated during one day on April 1, 2011 (NSWC, 2012a).

2.4.3. Exposure below Deck on Ships

Exposures to personnel working and living below deck on ship were limited compared to topside exposures because:

- The inherent shielding of the ship's structure reduced external radiation doses to crew while below deck relative to when they were topside. Although many system concentrators¹¹ were located below deck, these concentrators were not readily accessible to crew, and the associated contamination was fixed (i.e., not easily removable), therefore exposure from these sources was limited.
- On many ships, outside air was generally filtered prior to entering below deck spaces via a Collective Protection System¹² (CPS).
- Steps were taken aboard ship to identify and limit access to known contaminated spaces. Many areas on the ship and aircraft where radioactive material was primarily concentrated were not readily accessed by the crew. Personnel with access to these contaminated spaces were either trained radiation workers or those with specialized training to properly perform duties associated with potentially contaminated equipment. These personnel were required to wear dosimetry and PPE (e.g., anti-contamination clothing and gloves), and to follow detailed radiological control procedures (COMNAVSURFPAC, 2011).

2.4.4. Exposure related to Surface Contamination on Ships

Ships and aircraft exposed to radioactive fallout or re-suspended surface contaminants (e.g., wind from aircraft rotors can re-suspend contaminants onto or into the aircraft) created a source of radiation to which personnel could be exposed. The contamination was considered either loose (removable or transferable under normal working conditions) or fixed. Both forms of

¹¹ System concentrators have the potential to accumulate contaminated material due to the nature of their operation. For example, a filter would naturally concentrate air particulates and over time build up a quantity of radioactive material. Shipboard examples include air compressors, boilers, heat exchangers, ventilation registers, ducts, cooling coils, precipitators, laundry systems, sea strainers, grease/oily waste, deck drains, trash incinerators, plumbing p-traps, catapult troughs, and gas turbine generators (COMNAVSURFPAC, 2011).

¹² "The Collective Protection System (CPS) is a full-time air filtration system seamlessly integrated into a ship's Heating, Ventilation, and Air Conditioning (HVAC) system. The CPS provides protection against chemical, biological, and radiological (CBR) agents by filtering all supply air and over-pressurizing (relative to atmospheric pressure) selected ship zones". (Liska et al., 2011)

contamination were sources of external radiation exposure to individuals in proximity of a contaminated surface. Loose contamination was a potential source of internal exposure, such as through inhalation of air-suspended contamination, or inadvertent ingestion after direct contact with contaminated surfaces. Because of this, measures were taken to identify those ships and specific areas onboard ship that had potential contamination. By quantifying and decontaminating known contaminated areas, this provided data regarding the magnitude and extent of contaminated areas and prevented further spread of contamination. Because wide-spread radiation detection equipment, supplies, and qualified radiological-trained personnel were not immediately available after the early releases from FDNPS, steps to limit the potential spread of contamination were particularly important.

Commander, Naval Surface Force, U.S. Pacific Fleet (COMNAVSURFPAC), generated a detailed, mandatory ship survey process outlined in COMNAVSURFPAC Note 3441.1 (CNSF, 2012). This directive required all ships that came within 125 nautical miles of FDNPS from March 11, 2011 to April 12, 2011, to monitor for contamination utilizing trained contamination technicians and identify surface areas with greater than 100 corrected counts per minute (CCPM)¹³ in the following locations:

- High traffic areas;
- System concentrators;
- Frequently handled surfaces (i.e., door knobs, light switches, faucets, etc.); and
- Passageways/decks and bulkhead vertical surfaces (walls).

Areas identified as greater than 100 CCPM were mapped and decontaminated. Naval Sea Systems Command closely monitored the decontamination effort. Although many of these efforts occurred after the two-month time period of this report, it indicates the importance of identifying and decontaminating known contaminated areas. In addition, survey results support the conclusion that affected ships were not contaminated to levels associated with adverse health effects. Figure 2 provides a copy of the survey process flowchart contained in COMNAVSURFPAC Note 3441.1. Figure 3 provides a sample of a typical shipboard radiological survey sheet. Table 4 provides a summary of shipboard contamination survey results (NSWC, 2013).

¹³ CCPM stands for “corrected counts per minute” and represents the net survey count rate defined as the observed gross count rate (which includes background count rate) minus background count rate.

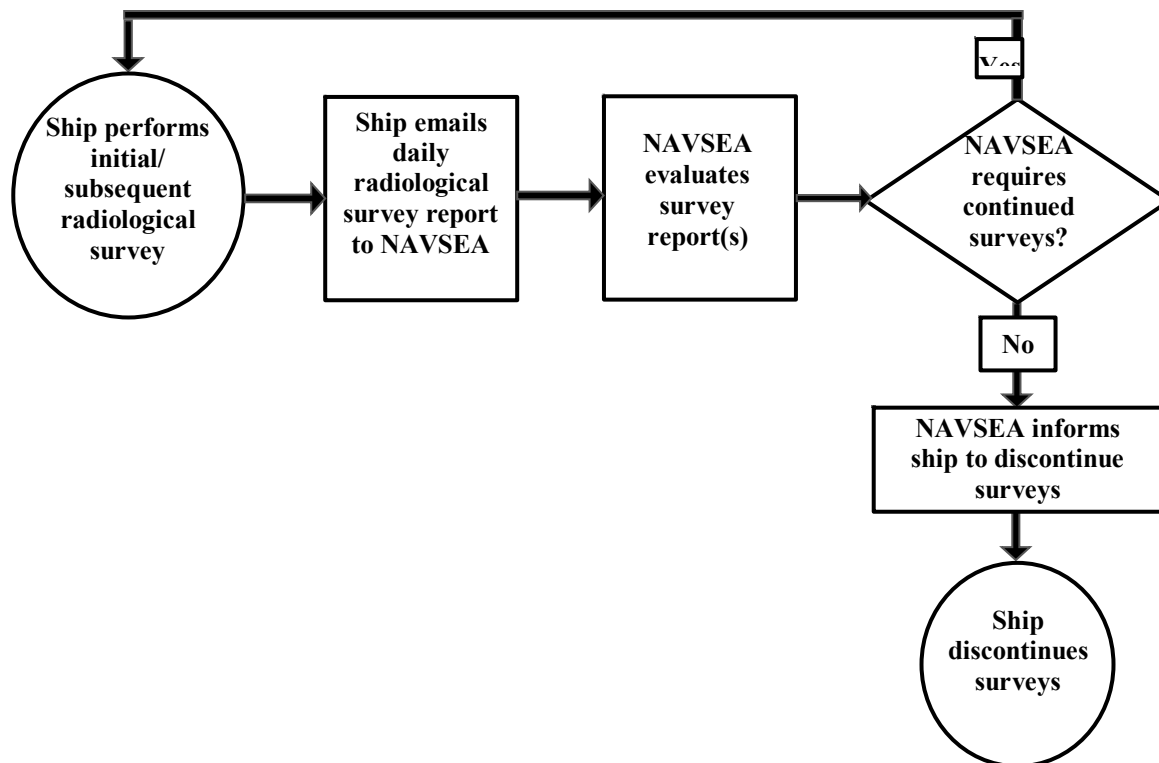


Figure 2. Ship survey process flowchart

UNCLASSIFIED

RADIOLOGICAL SURVEY DATA SHEET

SHIP/BLDG/AREA	ITEM/LOCATION	DATE/TIME	INSTRUMENT	SERIAL NO.	CAL DATE	CAL DUE DATE
DDG-54 USS CURTIS WILBUR	1B Main Engine Intake Filters (Weather Deck Side)	14SEP11	IM-265	A01229	14 APR 11	14 APR 12
		0906	DT-685	A00547	06 APR 11	06 APR 12
			DT-304	B00035	N/A	N/A
			E600	EE11537	06 DEC 10	31 DEC 11

SURVEY NO.	BACKGROUND (cpm)	SURVEY RESULTS (cpm)	REMARKS
2	900	3300	E600 READINGS INDICATE CONTAMINATION LEVELS >100CPM

* All surveys are <100 cpm unless indicated above. ** All E600 readings did not indicate a source of contamination unless indicated above.

"A" TYPE PANEL

"B" TYPE PANEL

◆ - E-600 SURVEY * - GAMMA ON CONTACT ① - SWIPE # - FRISK □ - PAS LAW-1 - LARGE AREA WIPE #A - FRISK WITH CONTAMINATION

SURVEYED BY: [Signature] DATE: 14SEP11 REVIEWED BY: [Signature] DATE: 9/16/11

UNCLASSIFIED

Page 1 of 6

Figure 3. Typical shipboard radiological control sheet

The results in Table 4 demonstrate the low levels of contamination detected overall. The results were compiled from available radiation survey results taken with a Geiger-Mueller (GM) type pancake probe/frisker during the two-month time period for 11 of the ships. All survey locations were located topside or in areas directly exposed to the weather.

Table 4. Summary of shipboard contamination results during March 12–May 11, 2011

Ship	Contamination Survey Range (CCPM)*								Survey Date(s) (>2,000)†
	0–99	100–300	301–500	501–700	701–900	901–1,000	1,001–2,000	>2,000	
USS Chancellorsville	18	16	1	0	0	0	0	0	N/A
USS Cowpens	12	11	3	0	1	0	0	0	N/A
USS Shiloh	5	1	0	0	1	0	0	0	N/A
USS Curtis Wilbur	52	24	5	4	3	2	6	1	3/21/11
USS John S. McCain	21	4	0	1	1	1	0	0	N/A
USS Fitzgerald	38	5	0	0	0	0	2	0	N/A
USS McCampbell	25	11	6	2	1	1	2	2	3/15/11
USS Preble	16	19	3	2	4	3	0	2	3/24/11
USS Mustin	33	0	0	0	0	0	0	1	3/21/11
USS Essex	56	0	0	0	0	1	0	2	3/31/11
USS Tortuga	28	0	0	0	0	0	0	0	N/A
TOTAL	304	91	18	9	11	8	10	8	

* The highest contamination survey result was one measurement of 8,000 CCPM.

† Survey date is provided for the highest measurement(s) on a ship.

The Table 4 results indicate:

- The majority (approximately 86 percent) of the results were less than 300 CCPM;
- The dates associated with the greater than 2,000 CCPM results were spotty and occurred on or relatively soon after dates of known major releases from FDNPS; and
- Ship survey results did not necessarily correspond to dose assessments. For example, although dose calculations for the USS McCain and USS Fitzgerald were relatively higher than most ships, from Table 4, it appears other ships recorded greater than 2,000 CCPM results while the USS McCain and USS Fitzgerald did not. This occurrence is not surprising and does not invalidate the dose assessments. Actual radiation countermeasures and weather effects (which would directly affect contamination survey readings) were not taken into account as part of the dose calculations but did in fact occur. Although individual survey results varied to a large degree, the conservative nature of the dose assessment method ensured that reported doses were not less than actual dose received. Survey results were highly dependent on timing (before or after potential contamination was diminished).

The potential contribution to effective dose from surface contamination was assessed using the methods discussed in Appendix E. Cassata et al. (2012) demonstrated that the thyroid is the organ with the potential to receive the greatest dose primarily because the thyroid concentrates iodine radionuclides following intake. Although radiation surveys were performed to identify, restrict access to, and decontaminate contaminated surfaces as described above, it was possible that an individual was unknowingly exposed to or inadvertently ingested radioactive contamination prior to completion of these actions. Also, although a representative number of fleet-based personnel were internally monitored to determine committed internal dose from ingestion or inhalation of radioactive material, the theoretical calculation accounts for the unmonitored personnel scenario. Although the results from this assessment were not included as part of the reported doses, the method for calculating internal doses from ingestion of contaminated material is available on a case-by-case basis.

2.4.5. Exposure from Skin Contamination

Radioactive contamination on the surface of the outer, dead skin layer may produce a dose to underlying live skin cells. However, a conservative evaluation of the skin dose as discussed in Appendix F indicated that even under very conservative exposure conditions and assumptions, the potential skin dose from contamination was about 2 mSv, which is less than one percent of the annual occupational skin dose limit of 500 mSv (50 rem). In addition, this level of skin contamination is not sufficient to contribute significantly to effective dose. Therefore, unlike effective and thyroid doses, skin doses were not reported or included in the OTR.

2.4.6. Exposure Related to Salvage Operations

The rescue and salvage ship USNS Safeguard (T-ARS 50), along with Explosive Ordnance Disposal Mobile Unit (EODMU) 5 and Underwater Construction Team (UCT) 2, arrived in Hachinohe (Aomori Prefecture¹⁴) to assist Japanese Coast Guard personnel to identify and remove submerged debris from the city's waterway. Both EODMU 5 and UCT 2 operated from Fleet and Industrial Supply Center (FISC) Yokosuka Fuel Terminal-Hachinohe; UCT 2 personnel provided underwater surveillance, and EODMU 5 personnel conducted diving operations to inspect the wreckage to develop plans for debris removal (C7F, 2012c).

Personnel performing salvage operations anywhere in Japan had no significantly increased risk of radiation exposure from the salvage work itself because the tsunami that damaged and sunk the craft occurred prior to any release of radioactive material from FDNPS; therefore, the submerged craft would not have been contaminated. In addition, Hachinohe is located at a significant distance from FDNPS. Hachinohe is about 14 miles south-southeast of Misawa AB, which is 228 miles from FDNPS. Cassata et al. (2012) found the Misawa AB location to have one of the lowest effective and thyroid doses to shore-based DOD personnel. This result was expected because of the low airborne radioactivity concentrations, external radiation dose rates, and surface soil activity concentrations of reactor-based radionuclides there.

¹⁴ Prefecture is subnational jurisdiction, similar to a U.S. state.

2.4.7. Exposure Related to Dust-Producing Activities

Activities that had the potential to produce airborne concentrations of radioactive material were not specifically evaluated and factored into the dose assessment. The potential dose associated with these activities was minimized because:

- Many individuals who performed these tasks routinely wore PPE including respirators or filter masks which effectively reduced or eliminated the potential for inhalation or ingestion of radioactive materials.
- For at least part of the two-month time period, formal guidance was provided that specifically required minimizing dust-producing activities, and prohibited eating, drinking, smoking, or chewing gum to minimize ingestion of radioactive material (COMNAVSURFPAC, 2011).
- Potentially contaminated areas were actively monitored for surface contamination and airborne contamination levels, and known contaminated areas that required dust-producing activities were only performed under strict radiological control procedures including the use of dosimeters and PPE including respirators or filtered masks when necessary (Benevides, 2012).

2.4.8. Exposure Related to Incidental Air Operations involving Ships

Many of the ships included in this report did not have aircraft officially assigned to them but were involved in flight operations, including the USS Germantown whose flight deck was used for offloading supplies or personnel. Inadvertent transfer of aircraft contamination onto the flight deck or individuals from these activities is not expected to significantly contribute to the radiation environment or potential for contamination. This is supported by survey measurements, such as those from the USS Germantown, which determined that only one area of the flight deck had any detectable contamination (200 CCPM), and this area was easily decontaminated to a level indistinguishable from background (NSWC, 2012b). In addition, individual whole-body survey results indicated low frequencies and levels of contamination. Furthermore, the assumption that an individual was exposed topside continuously during the two-month time period is sufficiently conservative to account for any potential exposure from inadvertent transfer of contamination.

This page intentionally left blank.

Section 3.

Radiological Environment

The FDNPS releases created a radiological environment both on shore and at sea. The extent of the contamination, such as the types and amounts of radioisotopes available for release, rates of release, types and levels of containment of radioactive material damage, etc., was greatly affected by weather conditions and nuclear power plant status. Unlike shore installations, the fleet and associated aircraft were able to navigate around suspected areas of radioactive contamination and avoid potential exposure. The ships and aircraft each provided a measure of protection from the radioactive material released from FDNPS, as did buildings and other structures described in the shore-based report. However, the ships contain equipment, such as pumps or filters, which could have collected radioactive material over time (i.e., radioactive material concentrators). Although the PEPs included in this report considered radioactive material from the same sources as those in the shore-based report, the manner and amount in which they were exposed was different. To fully understand the radiological environment, a review of relevant aspects of the radiation sources was required. The following sections provide details regarding (1) radiological conditions at the FDNPS following the earthquake and subsequent tsunami, (2) environmental data, and (3) computer modeling of the radiological environment associated with the releases.

3.1 FDNPS Radiological Conditions

When the earthquake occurred, seismic actuators caused the immediate shutdown of FDNPS Units 1, 2 and 3 by control rod insertion. Unit 4 had been shut down for a refueling outage. FDNPS Units 5 and 6 were in cold shutdown¹⁵ during an outage but were conducting (or about to conduct) pressure testing of the reactor pressure vessel when the tsunamis hit. As a result, heat removal capability was temporarily lost, so the heat from the reactor decay served to pressurize the reactors. That is the reason that a second date was claimed for cold shutdown after the heat removal capability was restored despite the understanding that Units 5 and 6 were technically in cold shutdown before the tsunamis (ANS, 2012).

3.1.1. Accident Progression

The design basis accident for a light water reactor is a loss of core cooling coupled with a loss of offsite alternating current (AC) power (station blackout). When a decrease in core water level is sensed, multiple, emergency core-cooling systems are actuated and powered by emergency diesel generators. These redundant safety systems provide defense-in-depth for loss of core-cooling accidents. However, the height of at least one of the tsunamis exceeded the elevation of the emergency diesel generators, and the flooding rendered the generators inoperable. A few steam-powered emergency cooling systems were operational for a limited time. Some battery power did exist, but this source of power typically provides for no more than

¹⁵Defined as a condition in which the reactor pressure vessel water temperature is <100°C.

eight hours of operation (ANS, 2012). The lack of heat removal capability ultimately led to reactor plant damage. For consistency with time progression of the accident, computer modeling was based on the actual shutdown time of the reactors—March 11, 2011, at 1446.

3.1.2. Core Damage

In a loss-of-coolant accident, core temperatures are dependent on decay heat coupled with loss of coolant in the core. As the fuel rod temperatures increase, pressure builds inside the rods as a result of the expanding fill gas (usually helium), and the small amounts of fission gases that are released to the gap (cladding/pellet) during normal operation and heat-up. This internal pressure causes swelling of the cladding that tends to restrict steam flow resulting in rupture of the cladding. Eventually, the Zircaloy™ (zirconium alloy) fuel cladding reaches a temperature that results in an exothermic reaction that accelerates the rise in core temperature resulting in core damage and fuel melting.

Modeling doses to the fleet requires knowledge of the source terms for the FDNPS reactors, which were the isotopic releases from the plant to the surrounding environment during an event that involved core meltdown. Although a complete core meltdown could release most fission products to the primary containment, it was assumed that only a small fraction of the core inventory was released from the primary containment to the external environment (Yasunari et al., 2011; Stohl et al., 2011). Natural removal processes such as aerosol deposition and the sorption of vapors on equipment and structural surfaces reduce the source term available for release from containment. The noble gases krypton (Kr) and xenon (Xe) were exceptions because it was conservatively assumed for this analysis that 100 percent of the noble gases were released to the surrounding environment (NRC, 1995). However, noble gases were minor contributors to internal doses.

Most other isotopes were susceptible to retention mechanisms within the primary containment or did not form compounds or gases that were easily transported to the external environment. According to the shore-based report, the primary contributors to offsite doses were I-131, Te-132, Cs-134, and Cs-137. Other isotopes such as Sr-90, which has a high fission yield, were measured external to FDNPS at activity levels about three orders of magnitude below Cs-137 as described in the shore-based report. Release fractions—the amount of core inventory released to the environment for these isotopes—are typically in the 1–3 percent range for light water reactors (Yasunari et al., 2011; Stohl et al., 2011). Although each of the three damaged reactors lost core cooling at different times, it was assumed that all reactors experienced a complete core meltdown. The release fractions were based on the combined core inventories of the three units. The quantity of each isotope in the three reactor cores depended on several parameters including fuel irradiation history, power level, and enrichment level. Core inventories of all isotopes in FDNPS Units 1, 2, and 3 at shutdown were obtained from Oak Ridge National Laboratory, which used the Oak Ridge Isotope Generation (ORIGEN) code to produce the inventories. ORIGEN is widely used in the nuclear industry to determine core isotopic inventories at reactor shutdown and at specific times in the fuel cycle. The core inventory, as well as assumptions and empirical data after radiological release, can be used to determine the source term.

3.1.3. Source Term

In this report, source term is defined as the radiological release from primary containment of a reactor to the external environment. As the core melts down, fission products are released to the primary containment. In the radioactive material transport process, much of the radioactive material will plate out (deposit) on the extensive inner surfaces of containment walls, compartments and equipment (NRC, 1995). This slowing of the isotopic mass transfer rate coupled with retention of the radioactive materials within the plant enables decay of short-lived isotopes and a significant reduction in total radiological releases from the plant. In loss of coolant accidents involving fuel failure in boiling water reactors, fission product transport in the primary containment is through the pressure suppression pool where scrubbing (partial removal) of fission products occurs. This is a particularly significant retention mechanism for cesium and certain compounds of iodine that are water soluble. For noble gases such as xenon and krypton in a loss of coolant accident, releases from the primary containment can be through drywell venting or leaks in containment caused by overpressure (NRC, 1995).

The Tokyo Electric Power Company (TEPCO) estimated the total releases of Cs-137 and I-131 from three FDNPS units were 1.5×10^{17} Bq (3.24×10^5 Ci) and 1.2×10^{16} Bq (4.05×10^6 Ci) (GOJ, 2011). The estimate for Cs-137 was within a factor of three compared with estimates in Kobayashi et al. (2013) and Stohl et al. (2011); the estimate for I-131 was within 25 percent of the estimate by Kobayashi et al. (2013). Using these releases and the reactor inventories at shutdown provided by ORNL, changes in release fraction rates over time (the ratio of activity released to activity at shutdown) were calculated. ORNL's fission product inventory accounted for each reactor's fuel loading and irradiation history including burn-up. These calculations involved a complex iterative process accounting for reactor power levels, the timeline of the response to events for each reactor (e.g., the time that coolant make-up was lost following shutdown), the radiation level data acquired by on-site detectors, the isotopic air concentrations measured at Yokota AB, and from USS Ronald Reagan.

When I-131 is released from the core it usually builds up in the primary containment as an aerosol, typically in the form of CsI. However, on March 12, 2011, TEPCO began injecting boric acid (H_3BO_4) into the sea water used to cool the reactor cores because there was concern that nuclear criticality could be re-established in the damaged reactors. Boron has a very high neutron absorption cross-section, and its presence in the cooling water would eliminate or greatly reduce the probability of re-criticality as a result of neutron interactions with the boron. Boron preferentially combined with aerosols and thereby increased the gaseous I-131 release fraction in the plant effluent. Secondly, boric acid reduced the pH of the containment water and steam, another factor that increased the iodine gas-to-aerosol ratio, particularly when the cooling water became acidic (pH <7). These two factors were likely causes of the higher-than-anticipated gaseous iodine fraction detected at Yokota AB.

It was assumed that nearly all (more than about 98 percent) of the noble gases were released from the primary containment; much of those releases occurring during the controlled venting early in the accident sequence. As fuel rods lost integrity during core meltdown, noble gases that accumulated between fuel pellets and fuel rod cladding migrated rapidly from the core to the primary containment. A controlled venting at the upper level of the primary containment was dominated by noble gases (Stohl et al., 2011; NRC, 1995).

These release fractions were used in the Hazard Prediction and Assessment Capability (HPAC) model to produce radiological plumes. Appendix I, Section I-2 provides details of the approach for modeling isotopic releases.

3.1.4. Spent Fuel Pools

Spent fuel pools were considered as an additional source term. However, given the long cooling time of most spent fuel bundles prior to the accident, and the use of water cannons to cool the pools after the earthquake, it was unlikely that spent fuel failures contributed significantly to the offsite radiological hazards.

It has not been determined that the tops of the spent fuel pools were uncovered at any time during the event. Debris from hydrogen-induced explosions in the secondary containments of FDNPS Units 1 and 3 may have damaged a small inventory of spent fuel, but any resulting releases would have been negligible compared to the isotopic releases from the Unit 1, 2 and 3 reactors.

The last batch of spent fuel was placed in the common spent fuel pool in December 2010; before the earthquake and tsunami (ANS, 2012). After more than 90 days of decay from December to March, I-131, with its 8.1 day half-life, would be below minimum detectable levels or present only in trace quantities. The high solubility of cesium in water was a factor in the high retention of most of the Cs-134 and Cs-137 in the spent fuel pools. Therefore, spent fuel releases were not considered in this analysis of fleet doses.

3.2 Environmental Data

3.2.1. External Radiation (Ship)

Fleet-based individuals were potentially exposed to external radiation in the environment in which they operated. The most accurate method to assess the amount of radiation an individual received from external sources was by monitoring with a personal TLD or EPD during the entire exposure period; however, when personal monitoring was not conducted or results were not available, as was the case for many fleet-based individuals, other approaches to assessing the radiological characteristics of the potential exposures must be used. For fleet-based individuals, limited radiological survey and air activity concentration data were available. In addition, aerial monitoring of external dose rates and monitoring of external dose rates and air activity concentrations inside airborne platforms were performed and results reported.

3.2.2. Air Monitoring

Flights from the fleet to shore locations could result in submersion of the aircraft in a radioactive cloud and inhalation doses that vary more than for flights in the vicinity of the fleet, which were calculated in this report. Initial portions of flights from fleet locations to Honshu Island were in the general geographical location of the fleet, and were expected to have comparable doses from submersion and inhalation. Similarly, when nearing the flight termination point, the potential doses from submersion and inhalation would be comparable to those at the termination point. The shore-based report contains estimates of airborne concentrations of radioactive materials and dose rates for USFJ installations at temporary deployment areas on Honshu Island. Geographical areas along the flight routes that were not near the geographical areas of flight take-off or landing were not estimated in this or the shore-

based report. Although atmospheric effects had considerable temporal variability during and after the periods of time when the reactors released radioactive materials, in general, airborne concentrations of radioactive materials and submersion doses were higher for locations closer to the reactors than those located at greater distances. Only a limited number of DOD flights purposefully flew in close proximity to the FDNPS. These include a few distinguished visitor flights between Yokota AB and J-Village, which is located 20 km (12 mi) from the FDNPS, and multiple Air Force missions in support of DOE aerial monitoring of deposited contamination in proximity to and above the FDNPS and surrounding areas. Although initial portions of some flights may have encountered higher airborne concentrations of radioactive materials and submersion doses than those estimated for the geographical areas in the vicinity of take-off and termination points, the total time an aircrew spent in these areas was assumed to be a small fraction of the total flight time.

The magnitude of committed doses from inhalation of airborne radioactive materials depends on a number of factors including breathing rate, exposure duration, airborne concentrations of radioactive materials, chemical form of the radioactive material, particle size, and others. For aircraft, airborne activity concentrations outside the aircraft were expected to differ from those in the interior occupied spaces. For example, the WC-135 aircraft, which is specially designed for aerial radiological sampling operations, has an environmental control unit (ECU) containing high efficiency particulate air (HEPA)-activated charcoal filters that provided a high degree of protection from airborne radiological materials, except noble gases. The WC-135 aircraft has a continuous radiological monitoring system for the interior air. A review of monitoring data from this system revealed that radiological contaminants were not detected in the cabin of the WC-135 during OT sampling missions.

Other military aircraft, however, did not have the same type of protective equipment. Aircraft designed to operate at high altitudes are pressurized; including most fixed wing military aircraft. Fresh air for pressurized areas of these aircraft is typically brought into the aircraft's ECU from bleed ports in the engine(s). Depending on the aircraft model, return air from aircraft's cabin can be mixed with fresh air prior to venting in the aircraft. In high-performance aircraft, oxygen from onboard sources is mixed with outside air in a closed breathing system. Pilots have the option of switching to 100 percent oxygen, which would be completely free of contamination, but this is not routinely done. With the exception of special applications, such as in the WC-135, the fresh air intake on other aircraft was not purposely filtered for particulate matter, although fresh air could deposit particles as the air passes through the compressor stages of the engine, ECU, moisture removal systems, and ducting. Therefore, it is reasonable to expect that a large fraction of the aerosol would be removed from fresh air before entry into the occupied spaces of an aircraft. Radioactive contamination found on various engine components during post-flight radiation surveys confirmed such removal mechanisms. Helicopters, on the other hand, generally afford little, if any, filtration of airborne particulates; these aircraft have the ability to fly with some windows and doors open.

In general, (1) flights that remained in the same geographical area as the fleet were expected to encounter concentrations of airborne radiological contaminants similar to those predicted for exterior locations on surface ships, and (2) concentrations of airborne contaminants inside the aircraft cabin were expected to be lower than outside because the outside air brought into the aircraft undergoes some filtration. As discussed above, pressurized aircraft were expected to have a greater filtration than unpressurized ones, such as helicopters which would be

expected provide only minor filtration. External radiation dose rates at flight altitudes from terrestrial sources were expected to be substantially lower than those estimated for exterior locations on the surface of ships, while submersion doses from the radioactive plumes would be expected to be higher than those on the surface of a ship for the same external exposure rates. The reason for this is that an aircraft would be exposed from all directions (i.e., 4π solid angle geometry), rather than only from above and the side (i.e., 2π solid angle geometry), which was the case for individuals at ground level below a cloud of radioactive material. External dose rates inside the aircraft would be lower than outside because of the radiation attenuation provided by the aircraft. Overall, at similar geographical locations, differences between the submersion doses to aircrew during flight were not expected to be different than aircrew on the deck of a ship.

3.2.2.1 Air Survey

Relative submersion and inhalation dose potential at given locations was highly time dependent. To illustrate this point, Figure 4 contains a plot of external dose rates at the MEXT monitoring station in the Tokyo Prefecture.

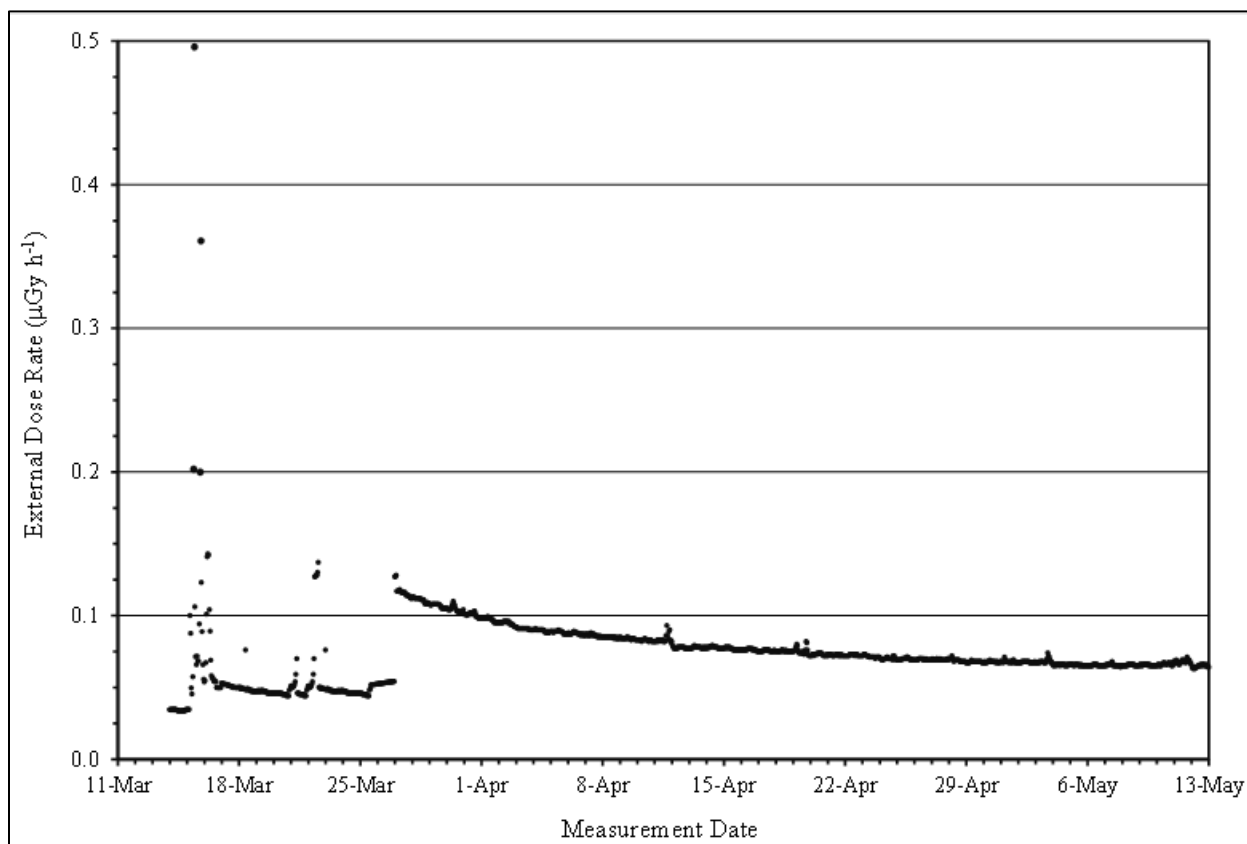


Figure 4. External dose rate by MEXT at Shinyuku, Tokyo Prefecture

External dose rate, as measured by these systems, consisted of contributions from natural terrestrial sources, submersion in radioactive plumes, and fallout deposited on ground surfaces. As discussed in the shore-based report, the MEXT systems did not quantify most of the cosmic radiation dose. Although these detection systems respond to the combined influence of all

sources listed above, from the plots some characteristics for each source were able to be described. Prior to the accident, dose rates were predominantly from natural terrestrial sources, with a mean of about $0.044 \mu\text{Gy h}^{-1}$. The large spike on March 15, 2011, was largely due to noble gases released from FDNPS, which were short-lived and influenced dose rates for a small fraction of a day. Other spikes of lower magnitude were observed on March 21–22, 2011. After the passage of the noble gases and the associated large spike in dose rate receded, the residual dose rates above natural terrestrial background were primarily from ground-deposited fallout emissions. The contribution of submersion dose to total external dose received by individuals was very small compared to the external dose from ground-deposited fallout, with the most significant exposure periods being during passage of clouds containing noble gases. It was generally recognized that the vast majority of noble gases contained in the core inventories were released during controlled venting on March 15–16 and 21–22, 2011 (NRC, 1995; Stohl et al., 2011). The greatest airborne concentrations of radioactive materials subject to intake and internal dose existed for a few weeks after reactor venting actions. Figure 5 contains a plot of Cs-137 and I-131 concentrations as measured at Yokota AB, a location west of metropolitan Tokyo. For this location, most of the committed internal dose from inhalation was received over about a nine-day period from March 15–23, 2011, temporally near the initial release times from the FDNPS. For the latter period of time, a pervasive lingering of airborne radioactivity existed, but at concentrations substantially lower than those shortly after the release. One notable characteristic of airborne contamination during these latter periods was the similar temporal pattern of Cs-137 and I-131 air activity, with Cs-137 activity being slightly greater than I-131 activity, which was different from the variability seen in the earlier time period.

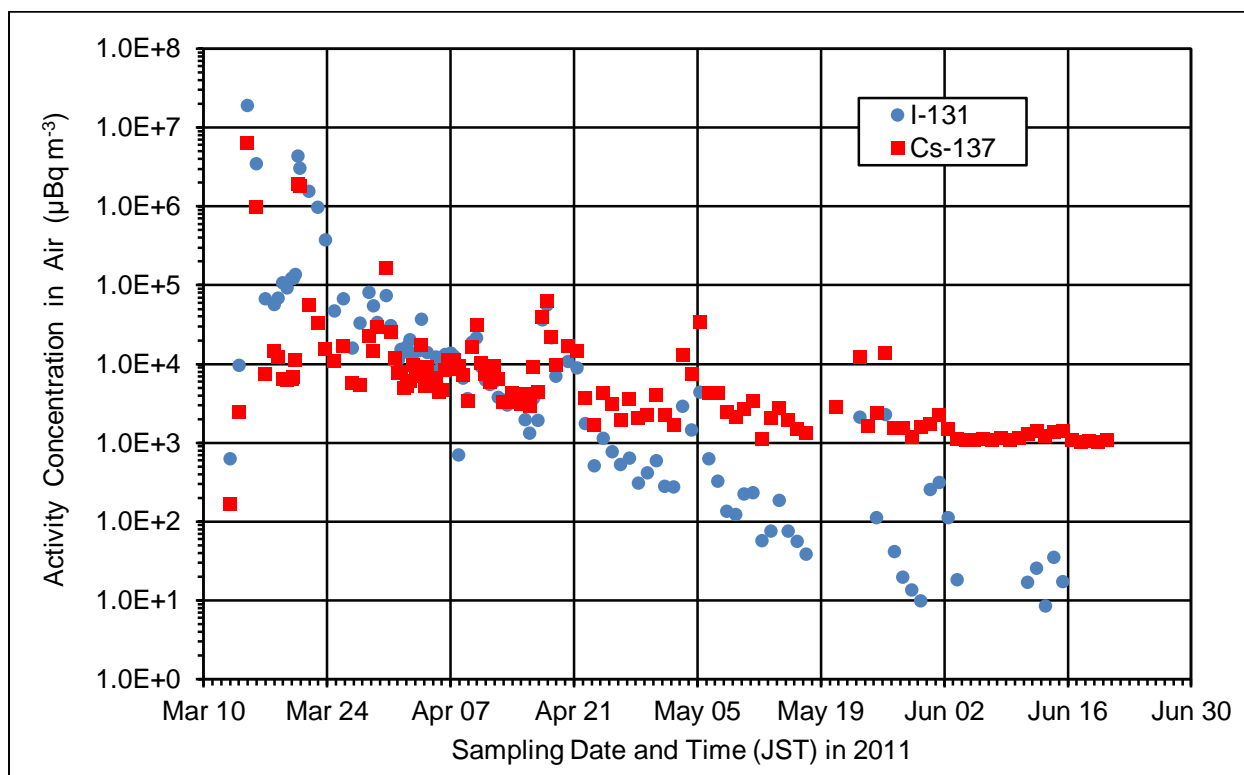


Figure 5. U.S. Air Force high-volume air sampling, Yokota AB, aerosol-only.

3.2.2.2 Measurements during Flight

Personnel dosimetry monitoring or aircraft cabin air sampling occurred during flight operations above Honshu Island and WC-135 flights. General observations from these measurements were used to draw conclusions about the exposure potential for flights conducted between fleet locations off the eastern and northern coasts of Japan and land areas on Honshu Island. As noted previously, WC-135 missions had continuous interior cabin air sampling during their missions, but as expected, detectable concentrations of radionuclides were not observed because of the filtering of air brought into the cabin.

The U.S. Air Force provided EPDs for flight crews and passengers on monitoring missions. Passengers and crew were permanently or temporarily assigned to air bases on Honshu Island. Dosimetry results were unremarkable for aircrew members compared to personnel with other duties and well within DARWG dose estimates for individuals assigned to these locations. Air Force aircrews operated aircraft for DOE's aerial monitoring missions over contaminated land areas surrounding FDNPS. The missions were conducted on UH-1 and UH-60 helicopters and on C-12 fixed-wing aircraft. The DOE conducted air sampling of aircraft interiors during these missions with low-flow rate systems that were fitted with in-line aerosol and charcoal canister filters. Compared to other flights conducted during these periods of time, these flights were purposely flown over some of the most heavily contaminated areas and into areas with higher expected airborne concentrations than USFJ installations and temporary HADR support duty locations. In addition, some of the flights were of long duration (several hours) compared to the relatively short duration flights (less than one hour) conducted between ship locations and Honshu Island destinations. Continuous air sampling was conducted during these air monitoring missions with sampling times that varied between 1.3 and 15.4 hours. Results of the sampling are provided in Figure 6 for Cs-134, Cs-137, and I-131.

In contrast to the air sampling conducted at Yokota AB shown in Figure 5, and which included only the aerosol fraction, the I-131 data shown in Figure 6 represent the sum of the activity concentrations measured on aerosol filters and on charcoal canisters. For practical purposes, this is important for I-131 because the fraction of gaseous forms were typically about two times higher than the fraction of aerosol forms. The data points in Figure 6 are not connected by lines because the activities were not from air sampling conducted at a single location, but are the daily average concentrations obtained from daily monitoring missions that covered hundreds of acres of land. In addition, some days include results of sampling from different platforms. The maximum number of samples per day was three. Similar to the general trend observed for activity concentrations from the high-volume air sampling system at Yokota AB, activity concentrations were greatly reduced for dates later in March and April. The results from air sampling during aerial monitoring missions sampling are about an order of magnitude higher than the results reported for Yokota AB. The highest I-131 results were observed in this dataset for sampling on March 20–22, 2011, and were consistent with the expected total I-131 for air samples collected on Yokota AB on March 15, 2011. Another important consideration regarding these missions was that aircrew may have supported a number of these missions, but there were intentional crew rotations to spread flight hours across personnel in the squadron to maintain proficiency. The DOE also rotated its personnel who supported these missions, although not in the same manner as the U.S. Air Force. The DOE, in general, assigned two-member teams to an aerial platform for two to three weeks, although each crew did not fly every day. The DOE teams were based from Yokota AB.

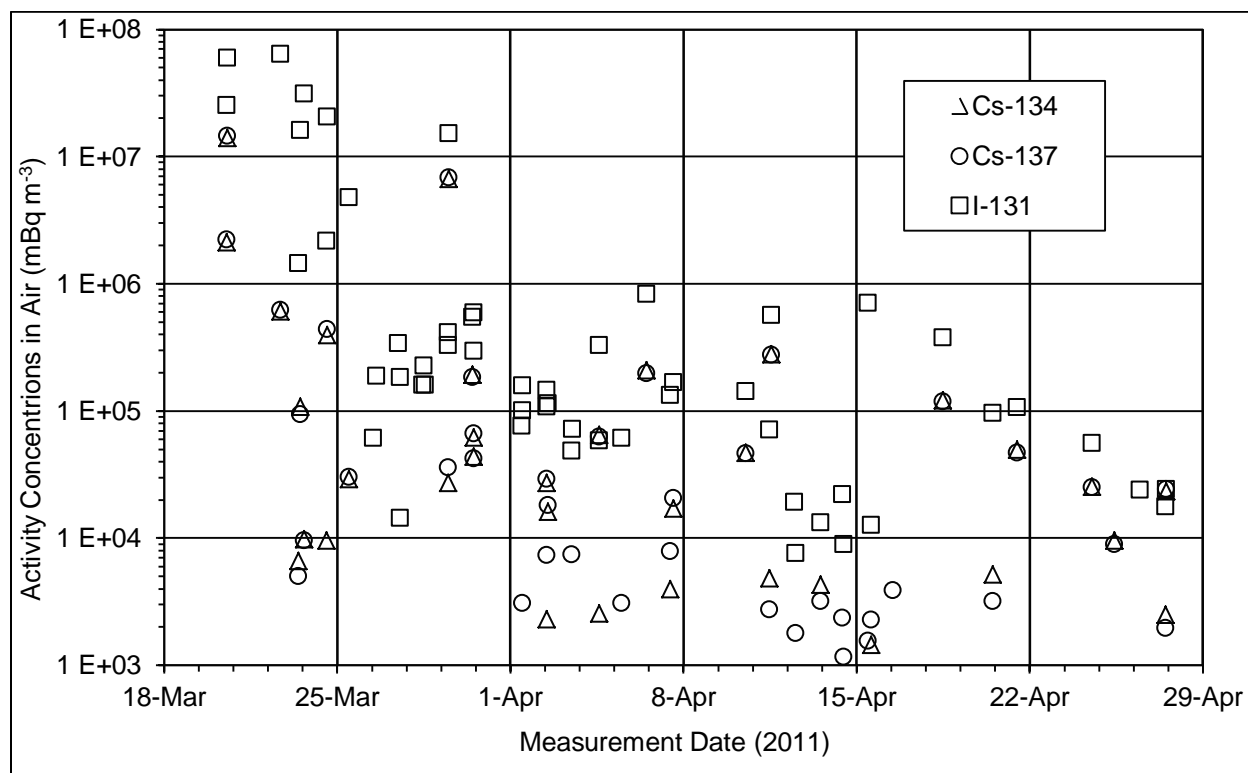


Figure 6. Results of DOE aerosol sampling on aerial monitoring missions near FDNPS

3.2.2.3 Discussion/Summary

Aircrews conducting flight operations from fleet locations off the eastern coast of Honshu Island had similar radiation exposure potential as ships' crewmembers on deck. Some differences may have existed in the partitioning of dose. For example, during flight, aircrews had negligible dose from fallout, which was assumed to be deposited on the surfaces of ships. Some minor differences may have existed in the submersion doses received by aircrew versus doses estimated for the decks of ships; however, submersion doses were not a significant contributor to external dose, which was dominated by exposure to deposited fallout. Although aircrews may have flown in areas that had higher concentrations of airborne activity compared to those on the decks of ships, aerosol concentrations were reduced somewhat by the aircraft's air supply systems and the limited durations of occupancy in these areas compared to the total exposure time during the OT response from March 12 to May 11, 2011.

3.2.3. Water Monitoring

3.2.3.1 Potable Water

Shipboard potable water¹⁶ primarily came from approved shore-based sources and/or shipboard water production plants, which included distillation and reverse osmosis plants. These

¹⁶Potable water is used for drinking, galley and scullery activities, personal hygiene, and laundry.

processes significantly reduced or effectively removed a large portion of any potential contamination in the source water. Appendix G provides U.S. Navy water analysis results for various sources of water. Deliberate release of contaminated water ($\sim 1.5 \times 10^{11}$ Bq) at the FDNPS site, as well as leakage of highly contaminated water originating from FDNPS Units 2 and 3 ($\sim 4.7 \times 10^{15}$ Bq and $\sim 2.0 \times 10^{13}$ Bq, respectively), resulted in transfer of radioactive materials offsite. The contaminated water released to the sea was not considered to be a significant source of radiation exposure for individuals on ships and in the air because of the significant distance from FDNPS (typically more than 100 kilometers) when these events occurred, the ship's physical structure and engineering systems that provided barriers between the contaminated sea water and shipboard individuals, and the use of radioactive material dispersion forecasts to avoid potentially contaminated areas (see Section 3.3 for details).

Extensive radiological analyses of sea systems of the USS McCampbell and USS Preble, while in dry dock, consisted of sampling all 15 valves downstream of the sea chests¹⁷. All results were indistinguishable from that associated with a non-contaminated sample. Similar results were obtained from other ships (NSWC, 2012c). This analysis strongly suggested that shipboard drinking water was not contaminated with radioactive material, thereby eliminating a potential exposure source for the crew. This analysis is discussed further in Appendix G.

3.2.3.2 Seawater

Seawater was used aboard ships in the fire mains, for decontamination, and for marine sanitation. Since conservation of potable water was a constant requirement, it was impractical to provide potable water for all purposes. The shipboard sea water systems consisted of components used to process seawater for its various uses on ships, such as piping, valves, pumps, strainers, and sea chests. Examples of these systems include:

- **Fire-main system (primary water supply system for fighting fires)** is used primarily to supply the fireplug and the sprinkling system; other uses of the system are secondary. Naval ships have three basic types of fire-main systems: the single-main system, the horizontal-loop system, and the vertical-loop system.
- **Seawater cooling** systems on surface ships and submarines provide cooling water for heat exchangers, removing heat from the propulsion plant and mechanical auxiliary systems.
- **Wash down countermeasures (WDCM)** provide a continuous spray of water to reduce the level of contaminants on the deck or surface of a ship. The wash down system has been designed to protect crew against chemical, biological, and radiological (CBR) attacks by washing any contaminant from the ship's skin (e.g., flight deck or hangar bay) before it can enter the ship.

¹⁷ The term "sea chest" refers to areas of the ship where intake of sea water occurs.

3.2.4. Food Monitoring

Fleet-based personnel received virtually all of their food from DOD-affiliated sources, which did not include sources on the Japanese mainland. Additionally, fleet-based individuals spent less time on the Japanese mainland compared to shore-based individuals, which further reduced their opportunity to ingest contaminated foodstuffs. The shore-based report explained in detail that shore-based, DOD-affiliated individuals had low potential for ingesting contaminated foodstuffs and any radiation dose associated with this exposure route was insignificant compared to possible doses from other pathways. Therefore, as in the shore-based report, doses from ingestion of radiation-contaminated foodstuffs or water, while on shore, was not considered for this report.

3.2.5. Soil Monitoring

It was possible to inhale or ingest soil via re-suspended dust. The shore-based report demonstrated that the radiation dose contribution from soil ingestion was not significant compared to the external dose—even less so for the exposure scenarios associated with PEPs in this report. Furthermore, unlike on shore where radioactive fallout could be re-suspended from the ground and subsequently inhaled or ingested, fallout deposited on the ocean was rapidly dispersed in the water and not available for re-suspension. Therefore, it was assumed that ingestion of soil did not contribute to significant internal dose.

3.2.6. USS Ronald Reagan Radiation Survey Data

Some empirical data were taken on board USS Ronald Reagan on March 13 and 14, 2011, when the ship passed through a radioactive cloud from FDNPS. The data consist of exposure rate readings and airborne activity concentration measurements. Table 4 provides a summary of these data.

Table 4. USS Ronald Reagan radiological survey data

Date (2011)	Time (JST)	Location	Exposure Rate (mR h⁻¹)	Surface Activity*	Air Concentration ($\mu\text{Ci mL}^{-1}$)
March 13	1200	Helo 614		1.5×10^4 pCi/100 cm ²	
March 13	1300	Flight Deck (section 1)			7.50×10^{-9}
March 13	1430	Flight Deck (section 2)			3.00×10^{-9}
March 13	1630	Flight Deck (section unknown)			1.20×10^{-8}
March 13	1700	Flight Deck (section 3)	0.3		
March 13	1745	Flight Deck (section 4)	0.9		
March 13	1800	Helo 46		6.8×10^4 CCPM/LAW [†]	
March 13	1830	Flight Deck (section 2)			2.0×10^{-9}
March 13	1845	Flight Deck (section 5)	0.7		
March 13	1900	Flight Deck (section 6)	0.6		
March 13	1900	Flight Deck (section 6)	2		
March 13	2000	APD 1-4 [‡]			7.20×10^{-9}
March 14	0023	Main Machinery Room		<450 pCi/probe	
March 14	0100	APD 1-4 [‡]			3.0×10^{-10}

* Surface activity was measured using a pancake-type G-M detector probe and rate meter.

[†] LAW: Large Area Wipe; swipe survey area consisting of 1 square meter.

[‡] APD 1-4 represents the permanently installed #4 Air Particulate Detector in the #1 Main Machinery Room.

3.3 Radiological Environmental Modeling

The FDNPS incident began with simultaneous shutdown of all three reactors upon input from seismic sensors detecting the earthquake. DTRA scientists and engineers provided the fleet with forecasts of radiological plumes based on best-estimate source terms and numerical weather predictions up to two days in advance. These forecasts enabled the fleet to avoid projected radiological hazards by changing direction and/or distance from the FDNPS. Because of these avoidance techniques, the resulting radiological impact to the ships was minor after the first few days following shutdown of the reactors.

This report contains retrospective analyses based on actual ship locations and observed weather data to estimate doses to fleet-based personnel during the period from March 12 to May 11, 2011. Because many of the calculated doses were dependent on the computer modeling results, it is essential to discuss computer modeling concepts and limitations and to demonstrate the validity of the modeling techniques and assumptions to provide credibility to the dose estimates in this report.

Computer modeling in conjunction with empirical data was needed to characterize the fleet radiological environment because of limited ship-board external radiation monitoring and airborne activity concentration data. Modeling was used to bridge data gaps in dosimeter and detector readings taken following the reactor accident. Based on ship locations (in time and space) and real weather conditions (observed and ship reported), appropriate source terms were determined to model radiological releases from the FDNPS.

Modeling was not used to calculate doses associated with flight operations because the necessary meteorological data to properly model isotopic air concentration levels associated with air operations, including wind speed/direction, air temperature, and humidity associated with the flight time/flight path of each mission were not available and because at altitudes above the boundary layer¹⁸, surface observations of weather are not applicable. However, empirical data characterizing the radiological environment associated with flight operations is available to use in assessing individualized doses upon request.

3.3.1. Hazard Prediction and Assessment Capability

The DOD performs radiological environmental modeling at DTRA, which provides decision support capability for planning, operations, and post-event analysis to all DOD groups, other Government agencies, and first responders (upon request). The Hazard Prediction and Assessment Capability (HPAC) software (described in Appendix I) is DTRA's primary computational tool for modeling the atmospheric transport and dispersion of radiological materials. Figure 7 provides a flowchart outlining key components of the HPAC-modeling process.

¹⁸ Boundary layer is defined as "the part of the troposphere that is directly influenced by the presence of the earth's surface, and responds to surface forcings with a time scale of about an hour or less." (Stull, 1988)

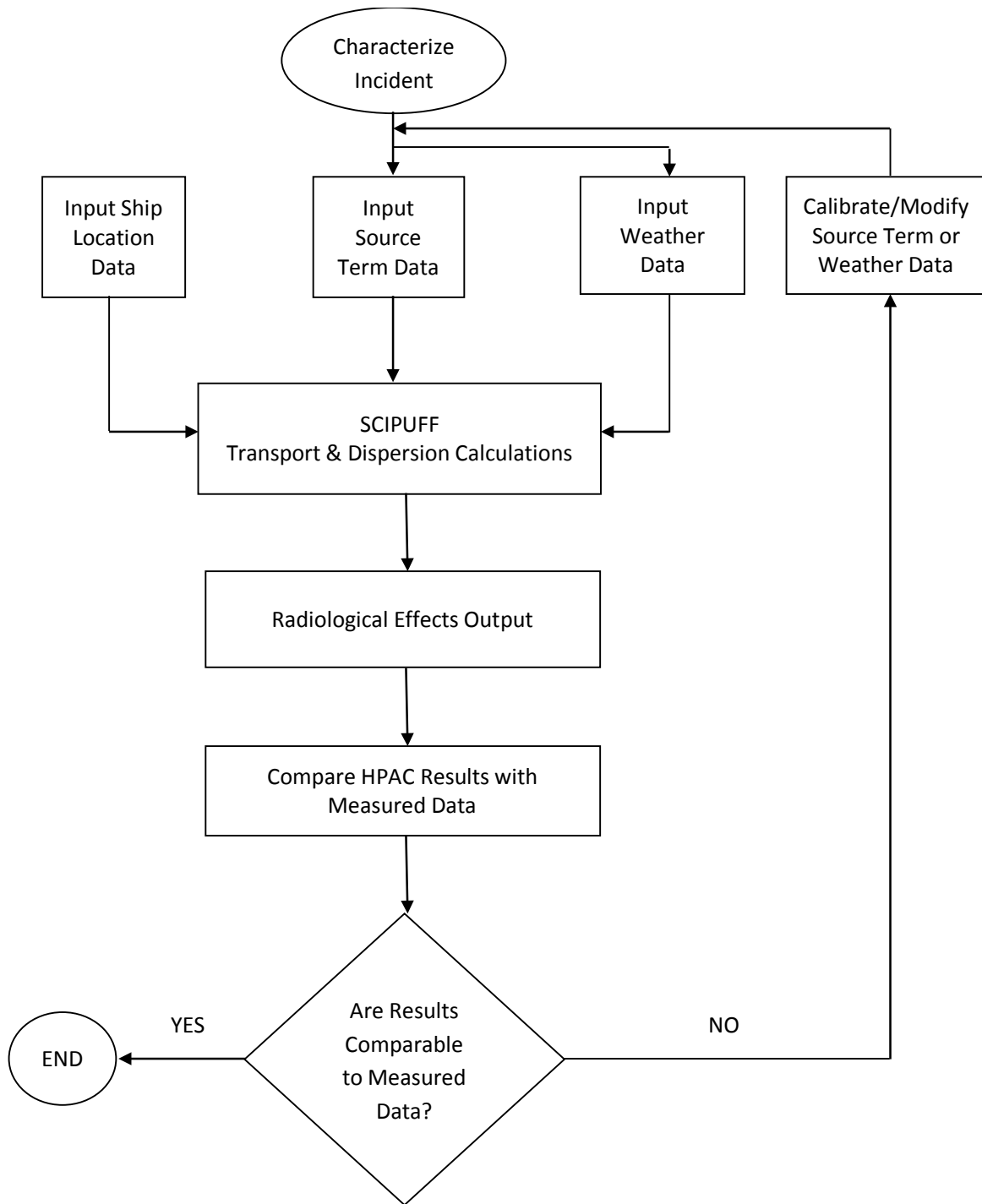


Figure 7. HPAC flow diagram

As shown in Figure 7, the HPAC modeling process used in this report required the following three major inputs to calculate radiation doses:

- Source Term: radionuclides in the FDNPS plants that were released to the environment on a time-dependent basis.
- Ship Locations: latitude and longitude, typically recorded at six-hour intervals over the time period from March 12 to May 11, 2011, were obtained for each ship. The inputs included not only routes traveled by the ships when at sea, but also the times and locations when in port.
- Weather Data: time-dependent wind speed and direction based on surface observations from land-based weather stations and ship-board observations.

3.3.1.1 Source Term Development

Development of the source term input involved the following:

- Reactor core isotopic inventories at time of shutdown.
ORNL-generated isotopic inventories for each reactor using the ORIGEN computer code, which is a widely used tool in the commercial nuclear power industry to determine core inventories of nuclides at the end of a fuel cycle or at intermediate times.
- TEPCO estimates of total releases of I-131 and Cs-137.
TEPCO estimated total I-131 and Cs-137 releases of 4.05×10^6 Ci and 3.24×10^5 Ci, respectively. Using these estimates along with knowledge of the accident progression for each reactor, the fractions of core isotopic inventory released from each plant's primary containment to the external environment were calculated.
- TEPCO exposure rate measurements acquired at FDNPS Main Gate 1.
The combined exposure rate from effluent releases was compared with measured exposure rate data (TEPCO) at FDNPS Main Gate 1. Figure 8 provides a diagram showing the relationship between FDNPS and TEPCO Na(I) scintillation-type sensor locations. Figure 9 provides a graphical representation of the TEPCO exposure rate data at FDNPS Main Gate 1.
- General knowledge of radiation transport of radionuclides that comprised the core inventories of FDNPS-type boiling water reactors.

Radionuclides were divided into groups with similar chemical properties including:

- Noble gases (Xe, Kr)
- Alkali metals (Cs)
- Halogens (I)
- Chalcogens (Te)

Elements in parentheses in the preceding list were the major isotopes of radiological concern in each group. Other nuclide groups (e.g., alkaline earths [Sr-90]) were released from a melting core, but most were retained through plate-out and scrubbing in the primary containment of the plant and were detected in concentrations typically three or more orders of magnitude lower than the four isotopic groups listed above.

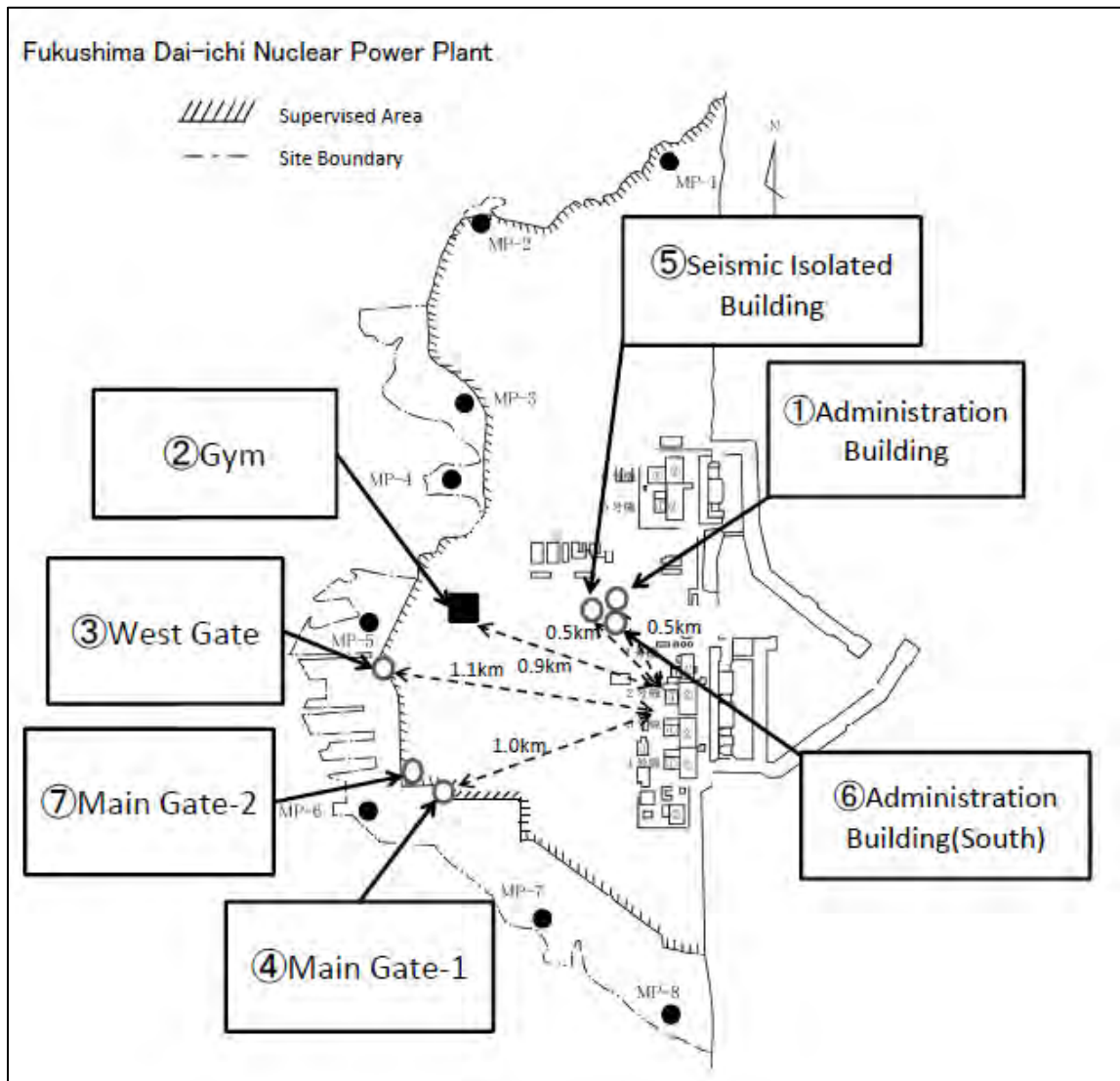


Figure 8. TEPCO sensor locations at FDNPS

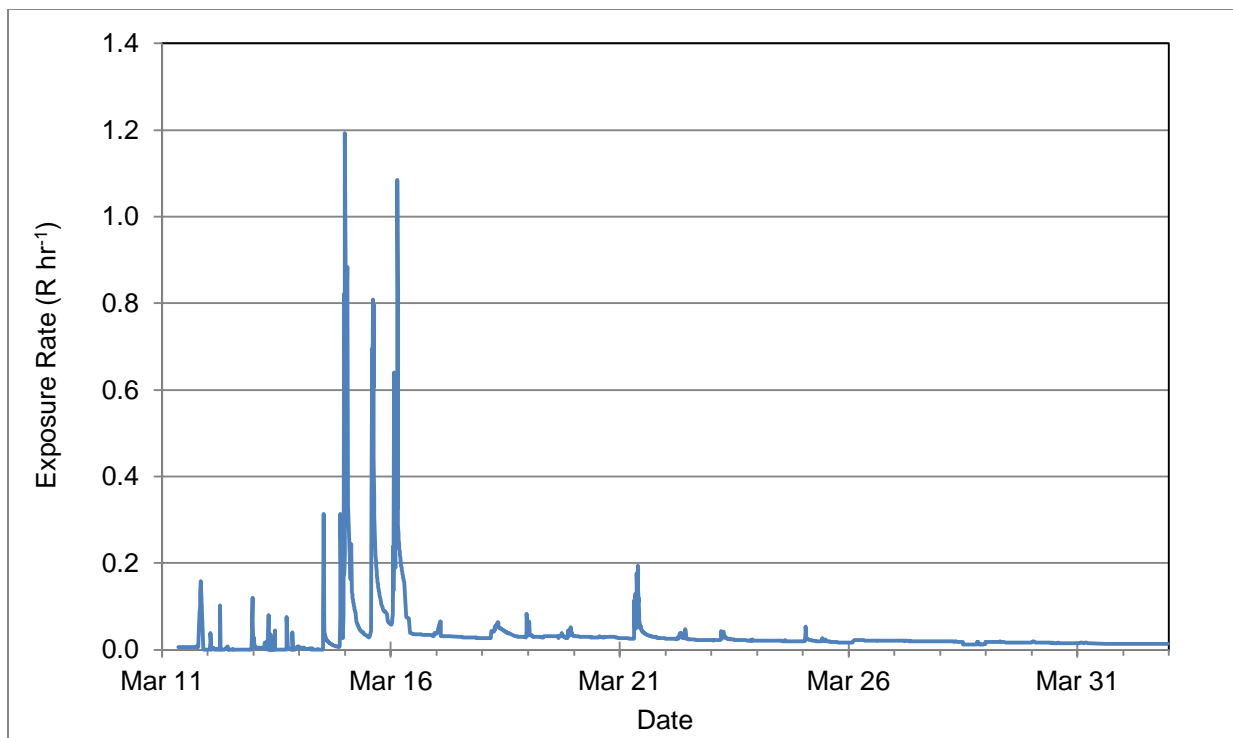


Figure 9. Measured exposure rates at FDNPS Main Gate 1 from TEPCO

As shown in Figure 9, many major peaks in the curves were followed by a distinctive tail resulting from ground deposition of radioactive material in the vicinity of the radiation detectors. Ground deposition included particulates in the form of aerosols and condensates. Peaks with prominent decay tails indicated reactor releases of fission products from primary containment without having been scrubbed by the wet well¹⁹. These releases can result from dry well²⁰ venting or primary containment leaks or cracks. The sharp peaks without a subsequent increase in the baseline dose rate indicated an absence of ground deposition. These occurred from the release of gases (such as noble gases and some chemical forms of iodine) and/or from releases in which strong, steady winds transported particulates away from radiation detector locations.

3.3.1.2 Ship Locations and the Computational Domain

Latitude/longitude, typically reported at six-hour intervals for each ship, was obtained from the Naval Surface Warfare Center Dahlgren. The location data were critical inputs to the HPAC modeling process because when combined with the weather and transport and FDNPS effluent cloud-dispersion results, they allowed for calculation of radiation exposure and subsequent dose.

¹⁹ The wet well is the toroid-shaped pressure suppression pool used to condense steam coming from the reactor pressure vessel.

²⁰ The dry well is the area above the pressure suppression pool between the reactor pressure vessel and primary containment which provides surfaces for fission product accumulation in an accident situation.

The locations of the ships were also used to determine the size of the spatial computational domain. Other factors affecting this domain were the locations of the measured data used for calibration and validation. The computational spatial domain superimposed on the island of Honshu is shown in Figure 10 and is defined by the rectangular area with latitudes at 34.5907 N and 41.1328 N, and longitudes at 139.0532 E and 144.2481 E. This domain encompasses an area of approximately 330,000 square kilometers (130,000 square miles) and extends slightly further south than Yokosuka NB, from the Yokosuka NB out to sea, north past Misawa AB, and west past Yamagata and Yokota AB. To determine the eastern limit of the domain, ships' locations were plotted and the eastern edge of the domain established to include the locations for ships positioned near Japan. The ships left this computational domain when they traveled south to Sasebo NB, and some of the ships were east of this domain at the time of the FDNPS releases but entered it as they approached Japan. The airborne concentrations and at-sea dose calculations only included the time and dose when the ships were inside this spatial domain.

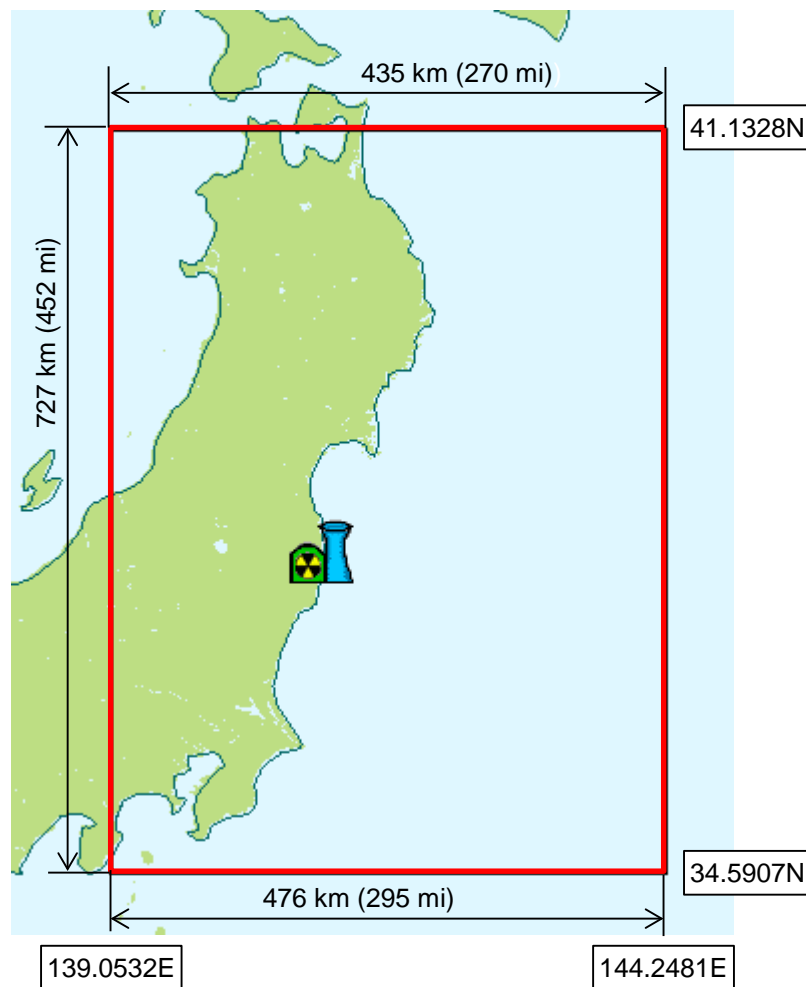


Figure 10. The computational domain relative to FDNPS and Honshu Island

3.3.1.3 Weather Data

Extensive surface observations of wind speed, direction, and other atmospheric conditions were input to HPAC, and these significantly affected the transport and dispersion (T&D) component model. The T&D component describes the magnitude and direction of the effluent cloud as a result of the release of radioactive material from FDNPS into the environment. Figure 11 shows a wind barb plot (weather symbol providing wind speed and wind direction information) indicating wind speed and direction for the Fukushima region. Appendix I provides details regarding specific weather data used in this report.

3.3.1.4 Isotopic Transport and Dispersion

The HPAC's atmospheric T&D model is called SCIPUFF (Second-order Closure Integrated Puff). SCIPUFF is an advanced Lagrangian, Gaussian puff model that uses second-order turbulence closure techniques. The T&D model is based on a three dimensional (3-D) puff methodology that enables computation of airborne concentrations. SCIPUFF uses an adaptive time-stepping scheme in which each puff determines its own step. Step length is determined by the turbulence timescale, horizontal transfer (advection, defined as the horizontal flow of air) velocity, shear distortion rates, and other physical processes, so that the step length increases as puffs grow larger and time scales increase.

3.3.2. Calibration/Fidelity of the Computer Model

As shown in Figure 12 and discussed below, HPAC results were compared with measured data to determine model fidelity. If the model produced results inconsistent with measured data, model inputs were re-evaluated. Therefore, calibration of the HPAC model was an iterative process by which inputs were adjusted to provide outputs that were in reasonable agreement with measurements. Inputs related to the source term and weather usually had a range of uncertainty associated with the database. For example, the initial source term was based on a constant release fraction of I-131 and Cs-137 for all three reactors. As the modeling process progressed, release fractions were tailored to time segments at which each reactor lost emergency cooling. Results were compared to FDNPS Main Gate 1 measured exposure rates (Figure 9) as well as to Yokota AB and Yokosuka NB air concentration data. Source term adjustments were made to achieve approximate agreement between these measurements and the HPAC results. Details of the source term development process and the uncertainties associated with the HPAC modeling process are addressed in Appendix I.

In this report, HPAC model fidelity (defined as its capability to replicate radiological measurements) was demonstrated by several comparative analysis processes. These processes also served to calibrate the HPAC model for specific aspects of the accident including plant conditions, observed weather, and measured radiological quantities, such as dose and airborne activity concentrations. Ensuring model fidelity served to validate the HPAC modeling process because outputs were calibrated based on measurements

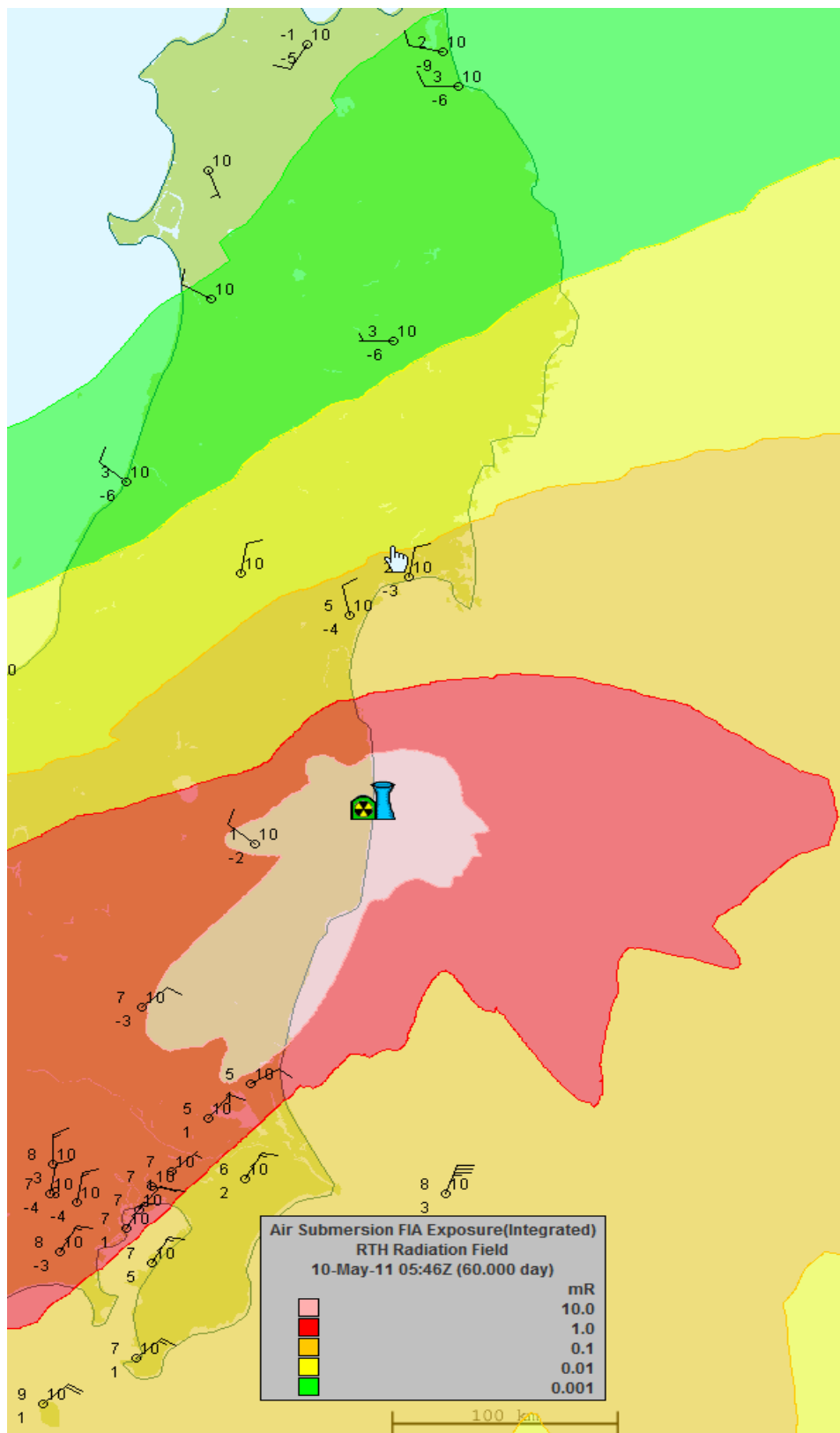


Figure 11. Example wind barb plot for Fukushima region

As was done in the shore-based report, fidelity of the HPAC modeling process was based on the degree to which the model results compared to relevant measurements to ensure calculated doses were conservative (higher than actual doses received). Calibration of HPAC results with (1) FDNPS effluent and subsequent radiological impact on (2) shore-based locations and (3) the fleet were based on the following data sets which were discussed earlier:

- FDNPS Main Gate 1 exposure rate data;
- Yokota AB measured air concentrations; and
- USS Ronald Reagan measured air concentrations.

3.3.2.1 HPAC Result Comparison with FDNPS Main Gate 1 Data

Figure 12 shows the TEPCO measured exposure rates and the HPAC results for the FDNPS Main Gate 1.

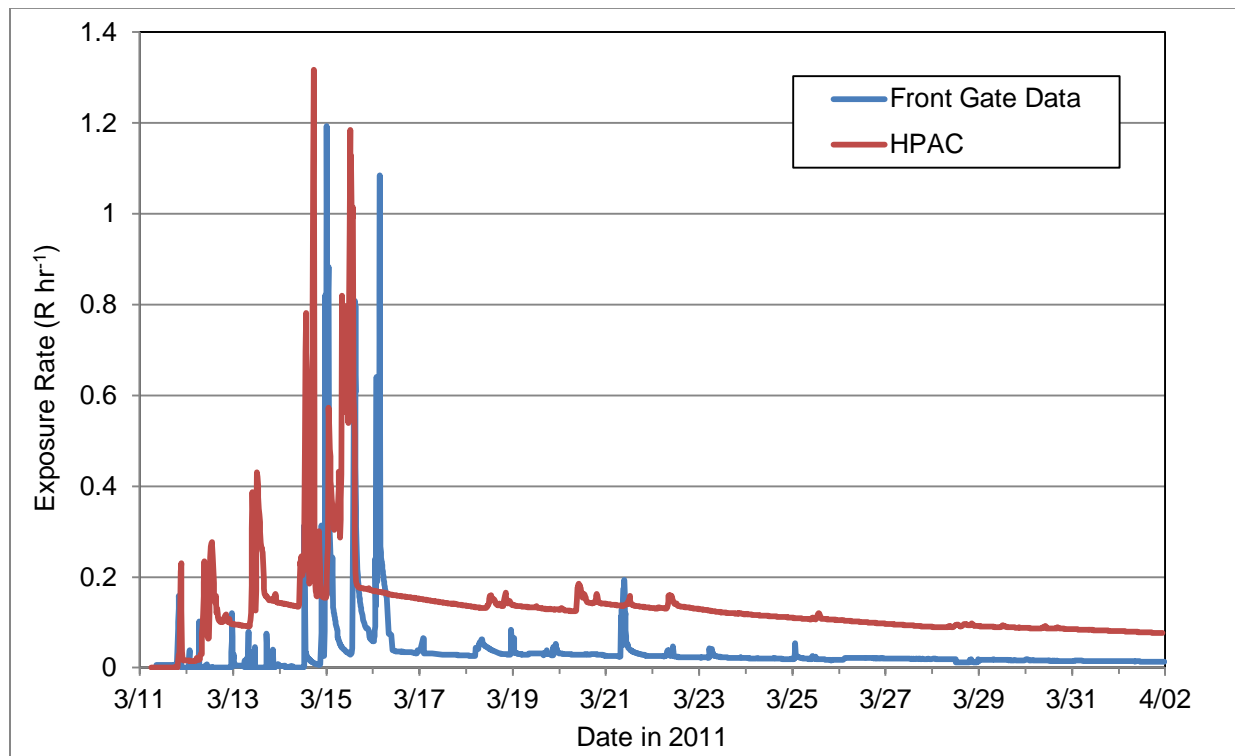


Figure 12. Comparison of HPAC-calculated and TEPCO measured exposure rates

Figure 12 allows a comparison between computer modeling and TEPCO exposure rate data that indicate:

- Measured and predicted exposure rate values were generally within an order of magnitude during the first few days after the initial release and within one-half order of magnitude after March 15, 2011.

- Computer modeling results did not generally replicate the fluctuations in the TEPCO data after approximately March 15, 2011. Prior to March 15, 2011, there were clearly documented events that could be correlated to data measured both at the FDNPS Main Gate 1 and at Yokota AB. After this date, when the core melt-downs, explosions, and deliberate venting occurred, there was not enough information available to try to model the smaller events that were indicated by the smaller peaks in the measured data shown in Figure 12. Average release rates were calculated and modeled. The fact that these were significant and approximately correct was demonstrated by the peaks of the HPAC results (red curve) at about the same height or higher than the peaks in the measured data (blue curve) during this period. Since both curves contained the ground shine component (as a result of radiation emitted from the radioactive material deposited on the ground or surface), it was difficult to evaluate the effect of the air submersion only from this graph. Yokota AB measurements taken at later times and over longer terms were a better metric of the comparison of the air concentrations after this date.
- HPAC results were usually higher than measured results. The HPAC average exposure rate during the period shown, which represents the major portion of potential exposure, was 277 percent higher than the average TEPCO measured exposure rate.
- Comparison between the modeling and Main Gate 1 exposure rate data (1) helped quantify the source term, (2) demonstrated replication of many of the major FDNPS releases, and (3) showed that the integrated exposure was comparable to but higher than the TEPCO empirical data.

3.3.2.2 HPAC Comparison with Yokota AB Air Concentration Data

Air activity concentration data obtained from Yokota AB (located approximately 140 miles southwest of FDNPS) were used to determine the general accuracy of HPAC-calculated air concentrations. Land-based data were used for calibration purposes because there was relatively little radiological data at sea compared to shore-based data. The Yokota AB site was chosen because the measured data on-site compared closely with data from the fixed international monitoring station (IMS) of the Comprehensive Test Ban Treaty Organization (CTBTO) located approximately 41 miles northwest of Yokota AB in Gunma Prefecture. Therefore, comparisons of calculated modeling results to these data provided an indicator of computer modeling fidelity. Table 5 provides a comparison of HPAC-modeled to measured average isotope air concentrations over a 24-hour period (starting at 2322 JST) from March 14–15, 2011, at Yokota AB. As part of the calibration of the HPAC model, total activity concentrations for iodine and cesium radionuclides were adjusted to be slightly higher than the measured values for this 24-hour period.

Figure 13 compares the daily average air concentrations of I-131 aerosols measured at Yokota AB with HPAC-generated results. The HPAC model predicted air concentrations trend similarly to the measured results. However, on certain days the HPAC results are much lower than the measured values. This can be explained by possible residual contamination on the measuring equipment and on the fact that HPAC does not account for re-suspension of deposited particles.

Table 5. HPAC modeled and measured isotope air concentrations for Yokota AB

Isotope	Measured Average Air Activity Concentration ($\mu\text{Bq m}^{-3}$)	HPAC Average Air Activity Concentration ($\mu\text{Bq m}^{-3}$)
Cs-134	6.59×10^6	6.03×10^6
Cs-136	1.46×10^6	1.87×10^6
Cs-137	6.34×10^6	7.23×10^6
I-131	1.92×10^7	3.99×10^7
I-132	4.45×10^7	3.35×10^7
I-133	1.38×10^6	5.58×10^6

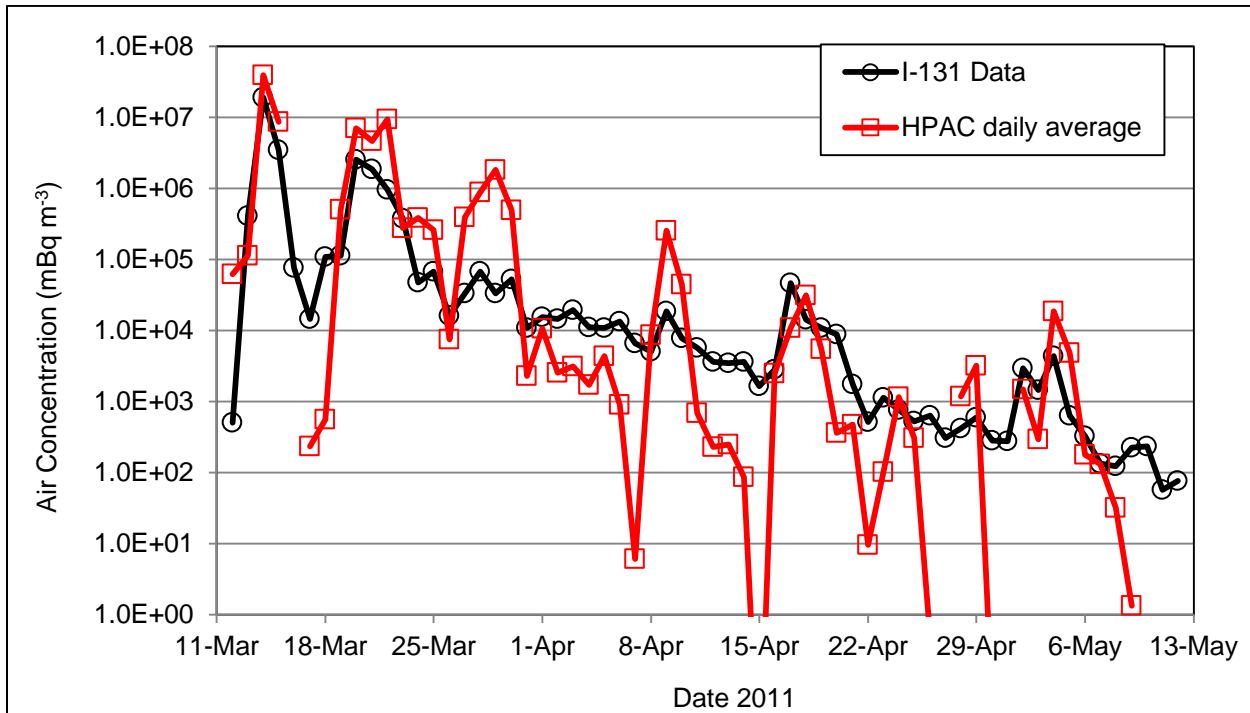


Figure 13. Air activity concentrations of I-131 in aerosols from HPAC results compared to measurements at Yokota AB

3.3.2.3 USS Ronald Reagan Air Monitoring Data

Calibrating the HPAC model involved comparing calculated airborne activity concentration data to empirical shipboard data taken on the flight deck of USS Ronald Reagan. HPAC predicted radioactive cloud concentrations were compared with the activity concentration measurements taken with a portable air sampler (PAS) on the flight deck of the USS Ronald Reagan at the same time and location in the early stages of the accident. Figure 15 contains eight separate plots that superimpose the locations of the USS Ronald Reagan (denoted by the letter “R”) and the USS John S. McCain (denoted by the letter “M”) between 0900 and 1600 on March 13, 2011, on HPAC-predicted air concentration contours.

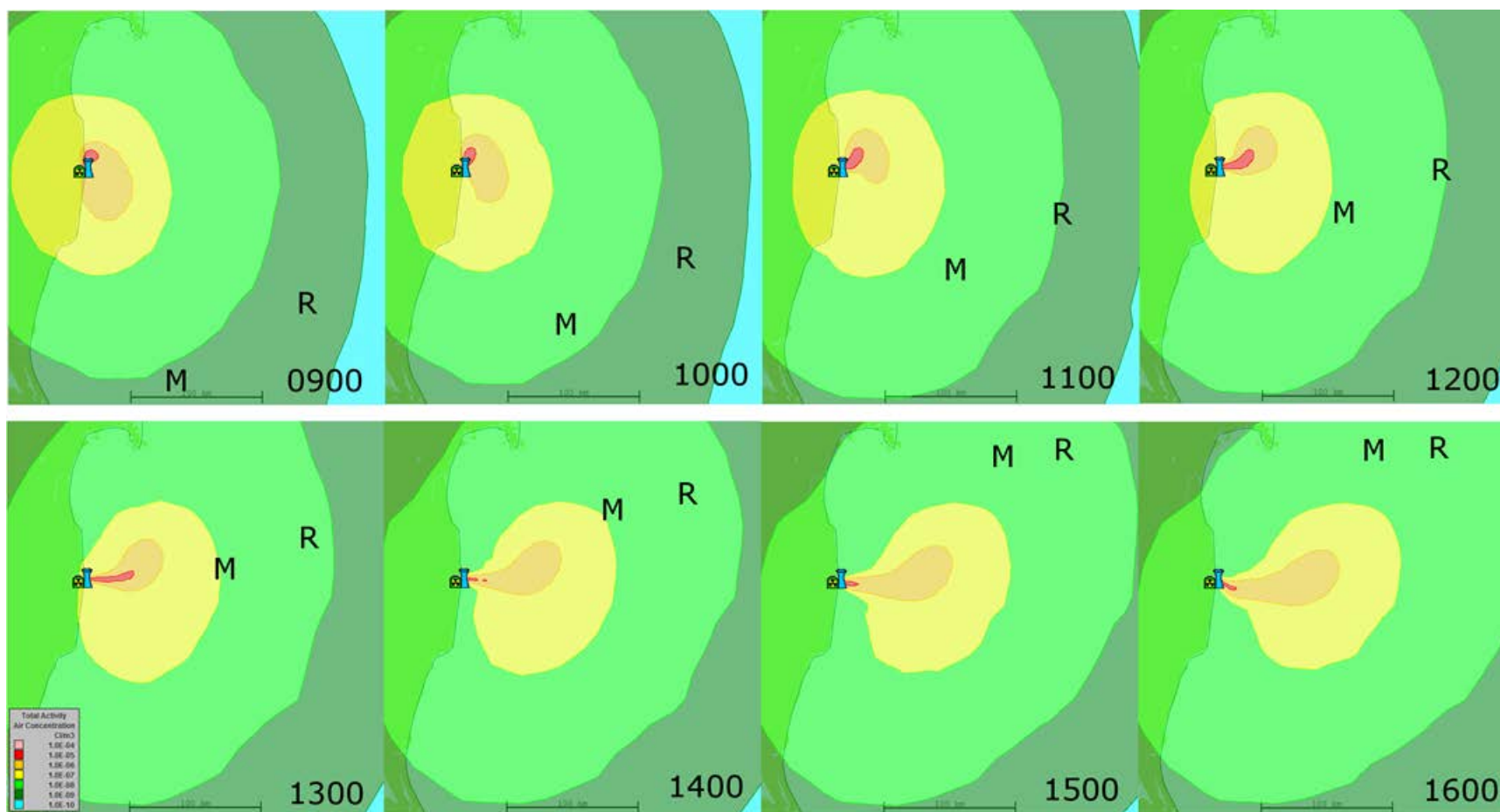


Figure 14. Locations of the USS Ronald Reagan (R) and the USS John S. McCain (M) at eight times on March 13, 2011

The shipboard activity concentrations measured on the USS Ronald Reagan and the HPAC-generated outputs are plotted in Figure 15. Appendix I provides a detailed discussion of the analyses conducted to properly compare the PAS and HPAC-generated air concentration data as well as an expanded comparative analysis of the PAS and HPAC data.

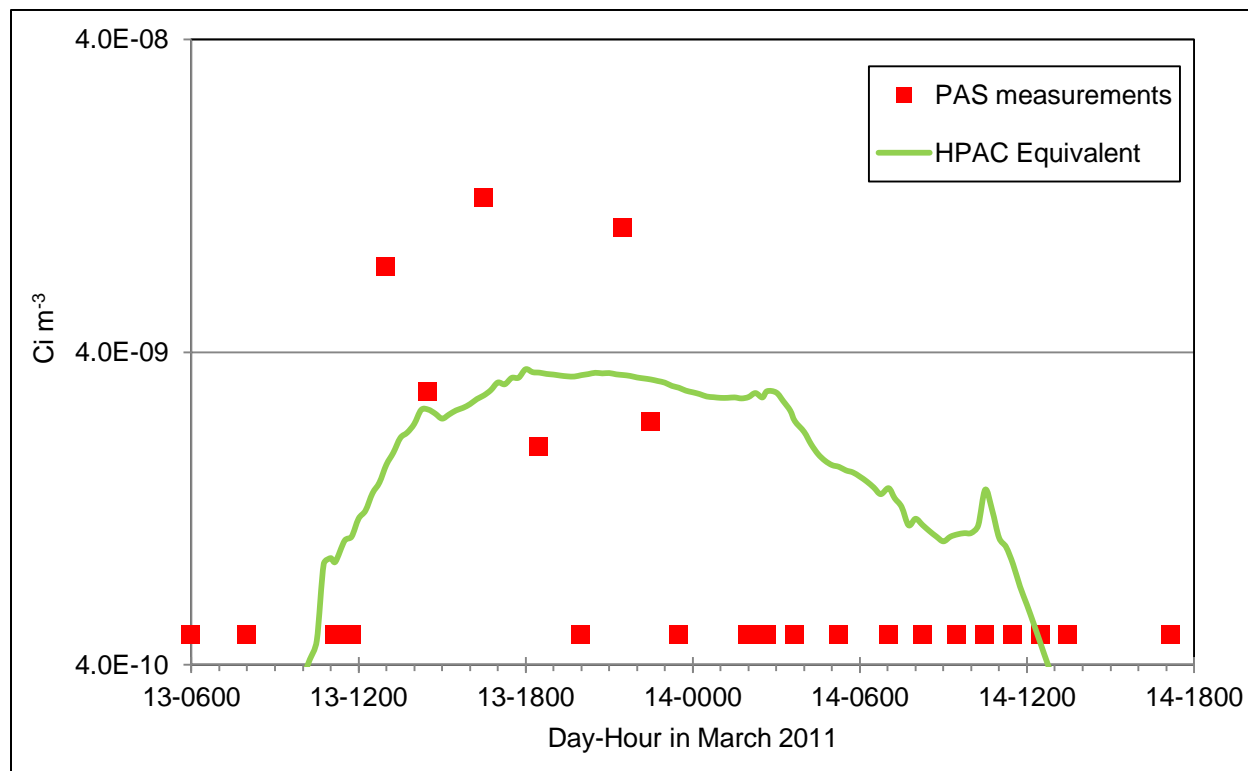


Figure 15. Comparison of USS Ronald Reagan measured and HPAC-generated air concentrations

As shown in Figure 15, HPAC results were generally within an order of magnitude of radiation measurements on the USS Ronald Reagan with a temporal variation of 3 hours. Typically, HPAC comparative results that are within one order of magnitude of the empirical data are considered an acceptable approximation as is the case here, particularly considering the significant distance (over 100 miles) between FDNPS and the USS Ronald Reagan at the time of the measurements. It should be noted that the calibration was performed using the maximum values in the plot shown in Figure 15. The average of the HPAC results was very close to the average of the USS Ronald Reagan PAS measurements. The HPAC inputs were then adjusted to make the predicted values match the measured data which is an integral part of the calibration process. The rest of the data points and the degree to which they temporally or quantitatively match validated the HPAC model.

The most significant encounter between any of the ships at sea and a relatively high concentration of airborne contamination was on March 13, 2011, and data collected on that day on the USS Ronald Reagan were used to calibrate the HPAC model. Any later encounters were much less significant. From Figure 14, the fact that the later peaks at Yokota AB were replicated

by the HPAC model with slightly high-sided results when using a constant release rate from the FDNPS, supported the assumption that any later encounters at sea would have a similar degree of agreement between the model and any actual measured results.

3.3.3. HPAC Modeling Concepts and Limitations

Typically, HPAC modeling simulates radiological conditions to which an individual standing on an extended surface (ground or ocean) is exposed relative to a radioactive plume or cloud passing overhead and subsequent deposition of radioactive material from the cloud onto the ground.

To model fleet doses in this report, fleet-based individuals were assumed to be exposed to both an air submersion component (as a result of being surrounded by the cloud) and a ground shine component. Radiation deposited on the deck of a ship in port is referred to as “ground shine” while radiation deposited on the deck of a ship at sea is referred to as “ship shine.”

The HPAC model calculated the isotopic air concentration from which the air submersion component of the radiation exposure was calculated. HPAC also computed the isotopic surface deposition and from this deposition, calculated the ground shine component in a static environment. When the ships were stationary, such as when they were in port, the HPAC model directly calculated the ground shine component at a location over time. In the case of a moving ship, radioactive material was deposited on the ship and surrounding ocean. The deposition accumulated on the ship and moved with the ship (unlike the scenario for which deposition was on land and not “transported”). Exposures were to an individual standing on the deck to radiations from deposition on the deck as the ship moved along, rather than from deposition on the ocean surrounding the ship.

This situation created a challenge because HPAC does not currently have the capability to model the deposition on the deck of a moving ship and to compute the “ship shine”-related dose component in this dynamic situation. The exposure rates over time were determined by the air submersion and ground shine components in a dynamic environment. For example, the USS George Washington was in port at Yokosuka NB at the time of the FDNPS accident and subsequently went to sea. Therefore, individuals on the ship were potentially exposed to air submersion and ground shine (while in port) and subsequent ship shine (deposition on the deck of the ship traveling with the ship, assuming there was no removal because of decontamination or other removal mechanism such as wind, rain, etc.) after leaving port and going to sea. Figure 16 provides a graphical representation of the exposure rates over time for the USS George Washington.

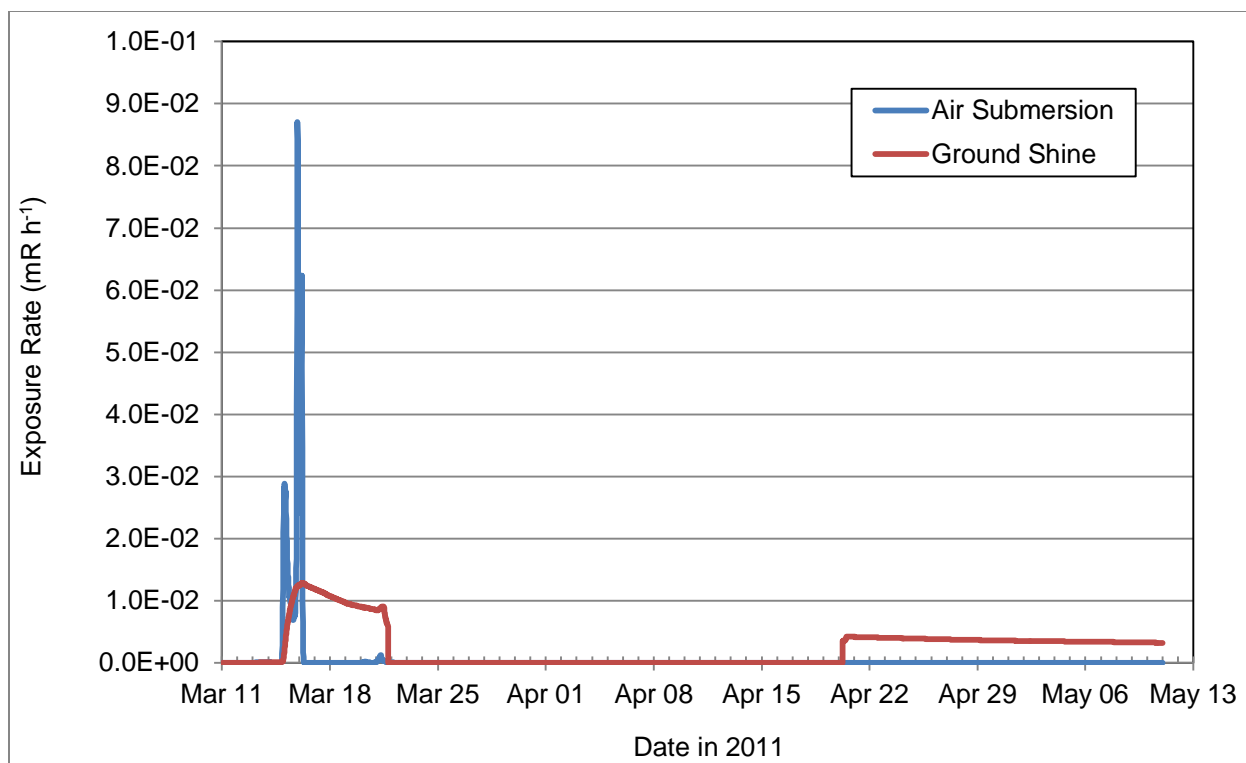


Figure 16. HPAC Output for USS George Washington

From Figure 16, the air submersion component (blue area) shows the relatively short duration of the plume followed by the ground shine component (red area). The shape of the graph demonstrates that deposition on the ground (or deck of the ship) accumulated rapidly during the period that the effluent cloud passed over, from which the ground shine exposure was incurred over a much longer period of time (the slope of the line indicates acquisition and radiological decay of the isotopic deposition) but then abruptly dropped off to zero when the ship left port. The line falls to zero because the ship no longer experienced the ground shine component, which had moved out to sea either to an area where much less deposition had occurred or was outside of the computational domain. However, the ship had potential contamination deposited on the surfaces of the ship and the potential for exposure to ship shine that could have contributed to additional dose. When the ship returned to port on or about April 20, 2011, the ground shine component on the graph, which had become much smaller because of subsequent decay over time, was again greater than zero because upon return to port the ship was subjected to ground shine from previous deposition on land. The blue (air submersion) component was absent at this time because there was no passing effluent cloud to contribute to exposure associated with air submersion. The red line (the HPAC output of ground shine exposure) was shown in this figure to compare the relative strengths of the two components, but it was not used in the values reported as explained in Section 4.2.3. Unlike the USS George Washington that was at Yokosuka NB in the first few days following the start of the reactor accident, the USS Ronald Reagan was at sea for most of the two-month temporal domain for OT; it was in port at Sasebo NB (over 700 miles from FDNPS) from April 19-22, 2011. Figure 17, provides the HPAC air submersion exposure rate results for the USS Ronald Reagan.

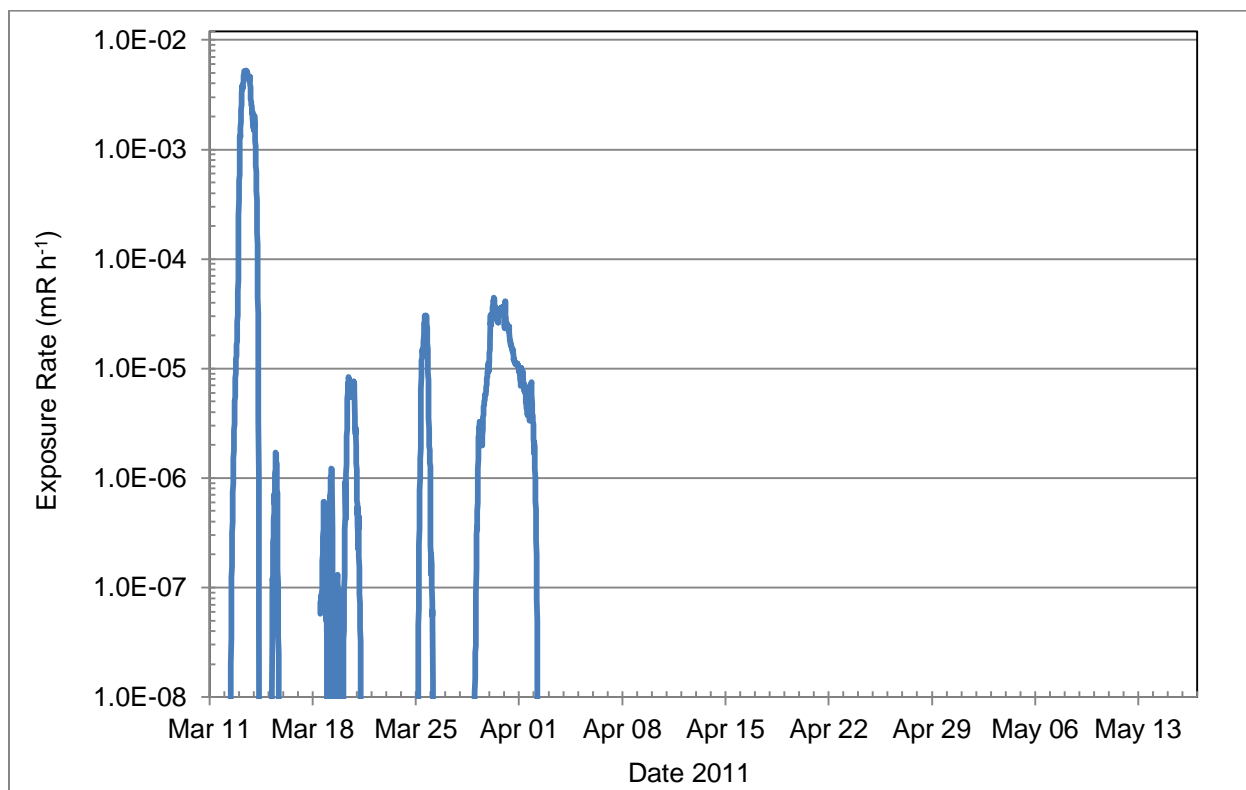


Figure 17. HPAC air submersion output for USS Ronald Reagan

The first peak the USS Ronald Reagan encountered dominated the integrated exposure.

Figure 18 and Figure 19 show the air submersion exposure rate for the USS Shiloh and the USS Fitzgerald, respectively. As shown, from April 7 through early May, 2011, both ships were in port at Yokosuka NB and were subjected to nearly identical exposure rates due to air submersion. Before this time they were at different locations and their exposure rates differed.

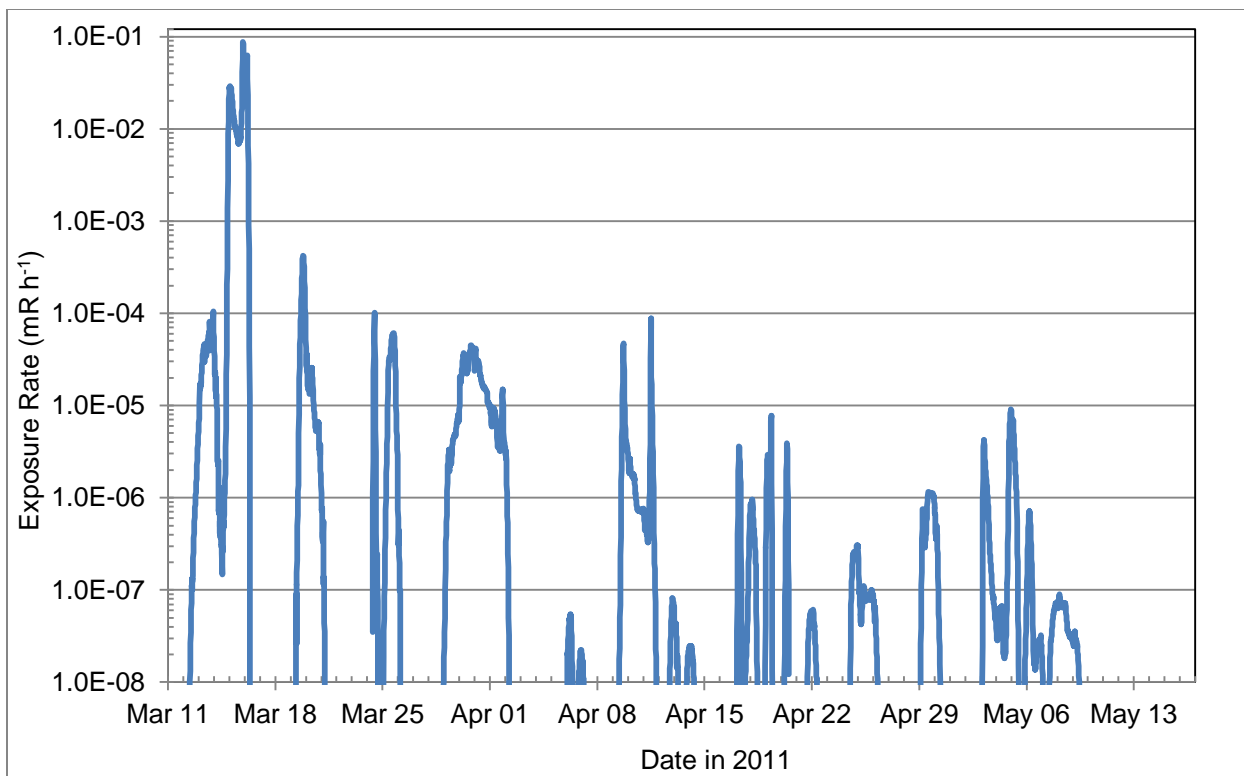


Figure 18. HPAC air immersion output for USS Shiloh

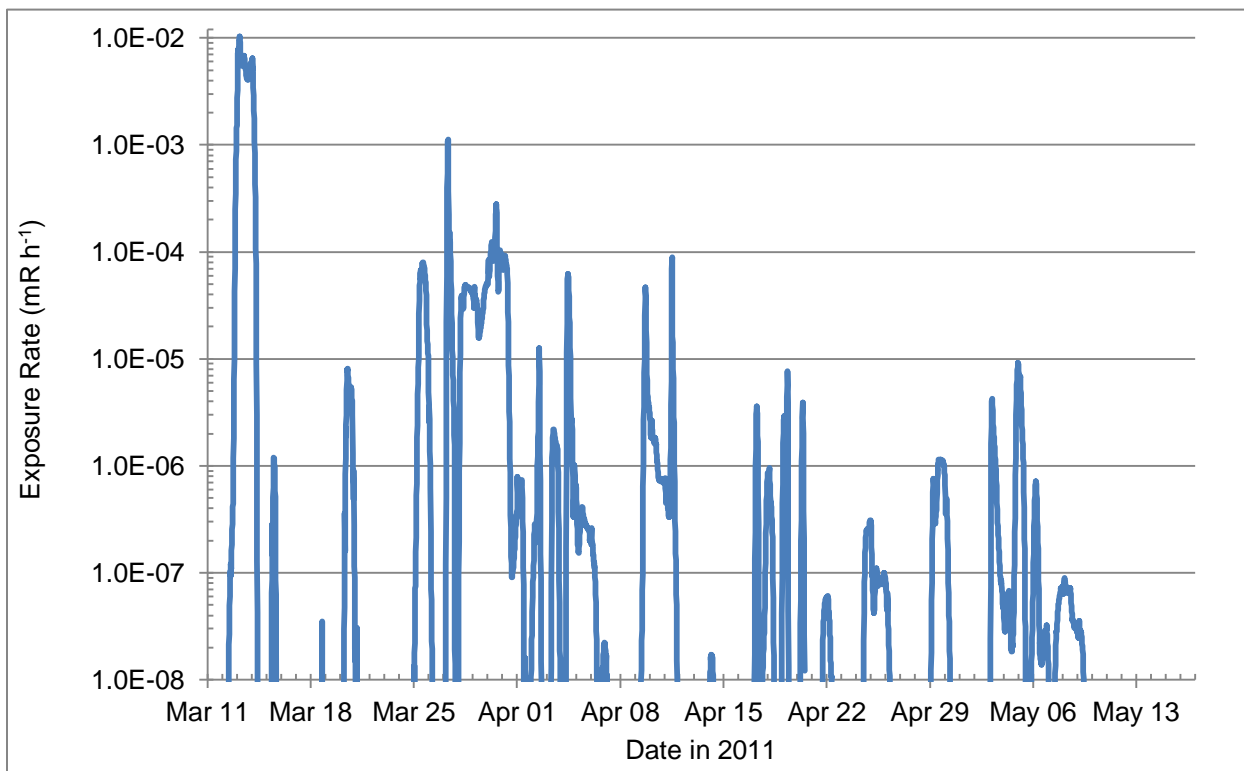


Figure 19. HPAC Output for USS Fitzgerald

Figure 20 shows a comparison of Yokosuka NB external exposure rates (air submersion + ground shine) for shore-based report doses and HPAC calculated doses. The Yokosuka NB external dose was considered to be good quality data and enabled calculation of the air submersion-to-total external dose conversion factor. This approach provided a method to account for limitations in HPAC's modeling of ground shine on a moving ship.

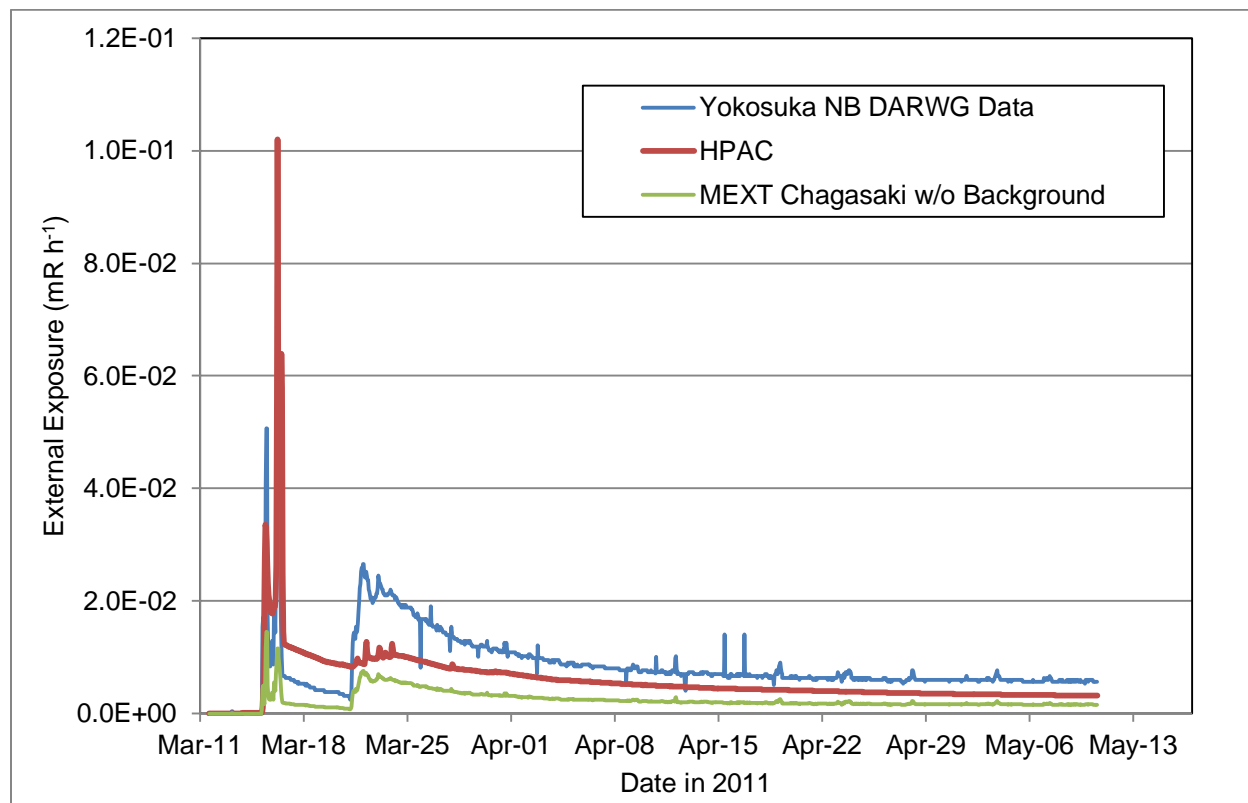


Figure 20. Yokosuka NB air submersion and ground shine exposure rates

3.4 Major Isotopes

Although HPAC's output included over 1,100 isotopes, it was determined that the major contributors to inhalation doses were the following 10 isotopes: I-131, I-132, I-133, Cs-134, Cs-136, Cs-137, Te-129, Te-129m, Te-131m and Te-132. The air concentrations of these 10 isotopes were output at 15-minute intervals for all ships during the two-month OT temporal domain, and these values were used to calculate the inhalation doses for ship's crew while at sea presented in Section 4.

3.5 Discussion/Summary

Calibration of HPAC over a spatial domain from Main Gate 1 to greater than 150 miles from FDNPS was performed using a combination of exposure rates at the Main Gate and air concentrations at Yokota AB and the USS Ronald Reagan. The 150-mile spatial domain encompasses distances from FDNPS to Yokota AB as well as most ship locations except for cases where ships may have been enroute to and ported at Sasebo NB (over 700 miles from

FDNPS) where doses were negligible. Fidelity of the model to replicate radiological measurements was demonstrated by several comparative analysis processes, including:

- FDNPS Main Gate 1 exposure rate data;
- Yokota AB measured air concentration data; and
- USS Ronald Reagan measured air concentration data.

Yokosuka NB data enabled calculation of a scaling factor to account for ground shine on a ship at sea.

The HPAC model used in this report was considered acceptable for modeling radiological conditions at sea to bridge data gaps in personal dosimetry and detector measurements. Doses for each ship are presented in Appendix J.

This page intentionally left blank.

Section 4.

Dose Assessment Methodologies

4.1 Overview of the Approach to Dose Assessment

The fleet dose assessment was accomplished using a two-component methodology—an at-sea component and an in-port component. The at-sea component used HPAC computer-generated isotopic air activity concentrations to calculate external and internal doses for the times ships were at sea. The in-port component used shore-based calculations for those times ships were in port. Because the HPAC-generated external doses cannot be easily separated into at-sea and in-port periods (see Section 4.2.5) the reported external doses consist of the sum of the HPAC and shore-based external dose results.

To calculate an individual's total effective dose²¹ and total equivalent dose to the thyroid, or thyroid dose²² using conservative parameters, the DARWG assumed that:

- While on shore, the PEPs were subjected to the radiological conditions described by the environmental data presented in the shore-based report,
- Human behavior parameters (habit data such as breathing rates, time spent outdoors, etc.) were defined using “upper percentile” values (90th–99.9th percentile) from the parameter distributions in EPA (2011) as discussed in Cassata et al. (2012), and
- The radiological conditions predicted via computer modeling were considered conservative based on the assumption that exposures occurred 24 hours per day for the two-month period.

Evaluations were also done to determine if individuals performing duties that did not involve activities topside on a ship, such as flight operations, were subject to significantly different radiation exposure environments; however, the doses for these individuals were not significantly different and therefore did not require a separate dose assessment.

4.2 Basic Dose Model

The basic dose model uses a hypothetical person representative of a much larger population who:

- Was exposed to photons from a passing cloud and from deposits of radioactive material;
- Breathed contaminated air from the passing cloud(s); and
- Ingested negligible amounts of radioactive material from water, food, and soil and dust.

²¹ The total effective dose includes both the external and internal dose components.

²² Thyroid dose includes both external dose and internal committed equivalent dose to the thyroid from inhalation or ingestion of radioactive materials.

The total radiation dose received by an individual (or organ or tissue) is represented by the sum of the radiation dose from external sources and the radiation dose from radioactive material taken into the body. The total effective dose E and the thyroid dose H_{thy} are modeled as:

$$E = \sum_{i,j} \left\{ \left[(\dot{E}_\gamma)_j + (\dot{E}(\tau)_{inh})_{i,j} + (\dot{E}(\tau)_w)_{i,j} + (\dot{E}(\tau)_s)_{i,j} \right] \times \Delta t_j \right\} \quad (1)$$

$$H_{thy} = \sum_{i,j} \left\{ \left[(\dot{X}_\gamma)_j + (\dot{H}(\tau)_{thy,inh})_{i,j} + (\dot{H}(\tau)_{thy,w})_{i,j} + (\dot{H}(\tau)_{thy,s})_{i,j} \right] \times \Delta t_j \right\} \quad (2)$$

where:

E	=	total effective dose (Sv)
$(\dot{E}_\gamma)_j$	=	effective dose rate from external radiation for time duration j (Sv h ⁻¹)
$(\dot{E}(\tau)_{inh})_{i,j}$	=	committed effective dose rate from inhalation for radionuclide i and time duration j (Sv h ⁻¹)
$(\dot{E}(\tau)_w)_{i,j}$	=	committed effective dose rate from water ingestion for radionuclide i and time duration j (Sv h ⁻¹)
$(\dot{E}(\tau)_s)_{i,j}$	=	committed effective dose rate from soil ingestion for radionuclide i and time duration j (Sv h ⁻¹)
Δt_j	=	increment of duration over which a radiation dose is estimated, and j represents the j^{th} interval (h)
H_{thy}	=	total thyroid dose (Sv)
$(\dot{X}_\gamma)_j$	=	dose rate from external radiation for time duration j (Sv h ⁻¹)
$(\dot{H}(\tau)_{thy,inh})_{i,j}$	=	thyroid committed equivalent dose rate from inhalation for radionuclide i and time duration j (Sv h ⁻¹)
$(\dot{H}(\tau)_{thy,w})_{i,j}$	=	thyroid committed equivalent dose rate from water ingestion for radionuclide i and time duration j (Sv h ⁻¹)
$(\dot{H}(\tau)_{thy,s})_{i,j}$	=	thyroid committed equivalent dose rate from soil ingestion for radionuclide i and time duration j (Sv h ⁻¹).

The three PEPs considered in this report include individuals who were exposed to external radiation sources and internalized radioactive material while the individual was aboard ship at sea and while the ship was in port. Because the availability of environmental measurements of radiation dose rates and air activity concentrations for ships at sea were limited, HPAC modeling was used to generate exposure rates and air activity concentrations for individuals at sea. When ships were in port, shore-based report methods and environmental

monitoring results were used for dose calculations. Total doses for the two-month OT exposure period were then obtained by summing the doses calculated for the times at sea and the times in port.

4.2.1. Dose while at Sea

The dose model for individuals at sea involves exposures to external and internal sources for ship-based individuals (PEPs A and B). In addition to sources of exposure described for the basic dose model, this dose model assumes the individual:

- Was exposed to x-ray and gamma-ray photons while submerged in a radioactive cloud(s) and from radioactive material subsequently deposited on the upper deck of the ship;
- Was located topside of the ship for the entire time the ship was at sea (24 hours per day);
- Received no radiation exposure from isotopes deposited on the ocean surface. Although it was possible that ocean spray might cause some water-borne isotopes to be deposited on the deck of moving ships, this would be a negligible contribution to the total ship ground shine component and was likely to have a decontaminating effect on existing deck deposition due to run-off. This is based on:
 - The high water solubility of the isotopes of concern such as Cs-134, Cs-136, Cs-137, and I-131.
 - Ground shine from fallout deposited on the ocean surface would be rapidly absorbed into the ocean and any radiation from residual surface contamination would be attenuated by distance as well as the ship's hull and structure before reaching a person standing topside.

Dose calculations for PEPs A and B included HPAC modeling to generate ship shine to calculate doses from external sources and air activity concentrations for calculations of dose from internalized radioactive materials.

4.2.2. Dose Coefficients

For external doses calculated for periods of time ships were at sea, dose coefficients were used to convert HPAC isotopic air activity concentrations to external doses. Effective dose coefficients from Leggett and Eckerman [undated] were converted to exposure coefficients using data in ICRP Report 51 (ICRP, 1987) and were used to relate submersion in a semi-infinite cloud containing uniformly distributed radioisotopes to external exposure. Exposure values were converted to dose using the DARWG assumption that one rem is equal to one roentgen. For external doses while in port, exposure rates ($R \text{ h}^{-1}$) were taken as equivalent dose rates (rem h^{-1}) and used for both effective and thyroid equivalent dose calculations.

The dose coefficients used in calculations of committed effective dose and committed equivalent dose for at-sea and in-port periods were taken from the ICRP database of dose coefficients found on ICRP CD-ROM 1, workers and members of the public (ICRP, 2001). Inhalation dose coefficients corresponding to a particle size distribution of 1 μm activity median aerodynamic diameter (AMAD) and absorption Type F were used for all radionuclides. For radioiodines, dose coefficients for elemental and organic forms were also used for the portion of those activity concentrations assumed to be in gaseous forms. As in the shore-based report,

internal doses were considered as conservative through the application of an adjustment factor of three to the dose results to account for the uncertainty in dose coefficients.

4.2.3. External Dose while at Sea

The effective dose from external sources received by an individual is directly related to the sum of the air submersion (immersion in the passing cloud) and ground shine (surface deposited material) components. HPAC assumed that the dose point (individual) was within a semi-infinite cloud with the ground (deck) being the lower boundary. The semi-infinite cloud model assumed a uniform air activity concentration from the reference point (location of a ship) outwards and transports FDNPS effluents as a vapor with a deposition velocity of 3 mm per second.

The HPAC semi-infinite cloud model assumed:

- There was no build-up or increase of additional photon energy as a result of Compton scattering of gamma photons and subsequent bremsstrahlung²³ radiation;
- Gamma photons were attenuated in air;
- An individual was standing on the ground plane (i.e., deck of a ship) while submersed in a hemispherical cloud of some airborne radioactive materials whose radius was:
 - Greater than the distance the most energetic beta particle emitted could travel;
 - Longer than the mean free path²⁴ of the most energetic photon emitted; (La Vie, 2009); and
 - Long enough that the beta dose contribution was a negligible fraction of the total effective dose.

The process for calculating fleet doses at sea begins with determining the isotopic air submersion exposure component based on the air activity concentration for a particular area and time (for this report, the individual ship locations). This served as the input for the isotopic activity term in Equation 3:

$$E(\bar{x}, t) = \int_0^t c(\bar{x}, t') \sum_{i=1}^N A_i(t') ECF_i dt' \quad (3)$$

where:

- $E(\bar{x}, t)$ = exposure from submersion in air (R)
- t = duration of exposure (days at sea)
- $c(\bar{x}, t')$ = air concentration of carrier material at location \bar{x} and time t' (kg m^{-3}). This carrier material is what is transported and dispersed by SCIPUFF. See Appendix I,

²³ Bremsstrahlung radiation results when a negatively charged electron passes near to an atom's positively charged nucleus. This slows and alters the electron's trajectory, and the loss of momentum energy is converted into photon energy.

²⁴ Mean free path is the average distance a photon of certain energy will travel in a medium before interacting.

Section I-2.1 for more detailed discussion.

- $A_i(t')$ = isotope activity per mass of carrier material for isotope i (Ci kg⁻¹). This quantity is a time dependent parameter that when multiplied by the carrier material air concentration of the previous term provides the isotope air concentration.
- ECF_i = exposure conversion factor for air submersion for each isotope (R s⁻¹ per Ci m⁻³).

The ground shine²⁵ exposure component is calculated using Equation 4 by summing up the products of the individual isotope concentrations and the other listed factors.

$$E(\bar{x}, t) = \int_0^t c(\bar{x}, t') k_g \sum_{i=1}^N A_i(t') ECF_i dt' \quad (4)$$

where:

- $E(\bar{x}, t)$ = exposure from ground shine (R)
- t = duration of exposure (days at sea)
- $c(\bar{x}, t')$ = ground deposition of carrier material (kg m⁻²)
- k_g = ground correction factor (unitless)
- $A_i(t')$ = activity concentration in carrier material for isotope i (Ci kg⁻¹)
- ECF_i = exposure conversion factor for ground shine for each isotope (R s⁻¹ per Ci m⁻²)

HPAC is capable of computing the ground shine component on land. The land does not move. Computing this exposure component to individuals on a moving ship would require the capability to accumulate radiological material deposition on a ship's surface over time as it is moving and to compute the ground shine exposure component to individuals on that ship from that deposition. HPAC does not currently have this capability, but the dose component from this exposure must be addressed.

The ground shine component scaled with the air submersion component based on the interdependence of the two and the single deposition velocity. The Yokosuka NB external dose calculated in the shore-based report was considered to be good quality, and it enabled calculation of a high-sided ship deposition external dose from the HPAC air submersion dose. This approach provides a method to account for the limitation discussed in the previous paragraph. The total external exposure (two-month period) at Yokosuka NB calculated in the shore-based report was 12 mR, which included exposures from both air submersion and from radioactive material deposited on the ground. This Yokosuka NB exposure was calculated using 100 percent time outdoors and also included an adjustment factor of 3.49 to increase the external doses to address differences between MEXT and DOD/DOE data (Cassata et al., 2012). The two-month Yokosuka NB integrated air submersion output from HPAC was 0.795 mR, also calculated

²⁵ Ground shine is gamma radiation emitted from radioactive material deposited on the ground (Shleien, et al., 1998).

assuming 100 percent of the time outdoors (topside). The ratio of the two exposure values is 15; this ratio served as a factor for converting air submersion exposures to total (air submersion + ship deposition) external exposures. The factor of 15 was applied to the integrated air submersion exposures for each ship to compute high-sided estimates of the total external exposures for the entire two-month period. Because an adjusting factor of 3.49 is incorporated into the conversion factor of 15, and given the other conservative assumptions used, the calculated total external ship doses are considered to be sufficiently conservative.

Because this factor of 15 was applied to the entire two-month period, external doses from HPAC results were not broken out into at-sea and in-port components. Instead, the entire external HPAC dose was used for each ship and was added to the shore external dose to estimate the total external dose for each ship, thereby contributing an additional amount of conservatism.

4.2.4. Internal Dose while at Sea

The committed effective dose and the committed thyroid dose for individuals at sea were calculated using the appropriate assumptions described in Cassata et al. (2012), together with the air activity concentrations from HPAC modeling discussed in Section 4.2.3 above. The human behavior assumptions from the shore-based report used for these dose calculations were time spent indoors (0 min d^{-1}), and inhalation rate ($32 \text{ m}^3 \text{ d}^{-1}$), which were associated with individuals supporting humanitarian relief efforts. The HPAC modeled air activity concentrations were assumed to represent the radioactivity concentrations of aerosol forms of all radionuclides. Therefore, inhalation of the calculated HPAC air activity concentrations resulted in internal doses from particulate forms of all radionuclides. Because radioiodines were likely to also exist in non-particulate forms, assumptions regarding radioiodines were also taken from the shore-based report, to account for non-particulate forms of these radioisotopes. Specifically, the gaseous forms of radioiodines were estimated by multiplying the aerosol activities by 2.507, and then the gaseous activity ($2.507 \times \text{aerosol activity}$) was apportioned into elemental and organic fractions ($1/3$ and $2/3$ of the gaseous activity, respectively). These assumptions for human behavior and radioiodines were consistent with the assumptions made for calculations of in-port doses.

4.2.5. Dose while in Port

When a ship was in port, individuals aboard had the opportunity to go ashore. The potential radiation exposure environment was different while ashore compared to when an individual was on a ship at sea. The total effective dose and thyroid dose were calculated for all PEPs while in port (mainland Japan) using the data and methodology described in the shore-based report. The specific parameter values used for each dose component (external exposure, inhalation, water ingestion, and soil ingestion) are described in Table 6. Equations 4 and 5 from Cassata et al. (2012) were used as well as the relevant assumptions in that report to calculate effective and organ doses for the time period when the ships were in port and individuals had access to the shore. As described in Appendix C of Cassata et al. (2012), an hourly dose value was calculated for each of the dose components from March 12 to May 11, 2011.

The in-port doses for ship personnel were calculated by summing the hourly doses for each dose component over the period(s) that each ship was in port at Yokosuka NB or Sasebo NB as described previously (see Table 2). For the times that the ships were in port, the HPAC and shore-based external doses were summed resulting in added conservatism to the dose

estimates. Because actual in-port arrival times and departure times were not available it was assumed that a ship was in port for the entire 24 hours on any arrival or departure day.

Table 6. Parameter values used for calculation of in-port doses

Parameter	Value	Comment
Time spent indoors	0 min d ⁻¹	Corresponds to None Category (Table B-9 of Cassata et al., 2012)
Inhalation rate	32 m ³ d ⁻¹	Corresponds to Extreme Activity (Table B-10 of Cassata et al., 2012)
Drinking water ingestion rate	6.0 L d ⁻¹	Corresponds to Extreme Activity (Table B-11 of Cassata et al., 2012)
Soil ingestion rate	500 mg d ⁻¹	Corresponds to Extreme Activity (Table B-12 of Cassata et al., 2012)

4.2.6. Dose during Flight Operations

The doses for PEP C individuals were calculated for the following two exposure scenario components: (1) time on ship in port and at sea, and (2) time spent in flight operations. Doses associated with time on the ship while at sea and on shore, were calculated using the methods discussed in Sections 4.2.1, 4.2.3, 4.2.4 and 4.2.5.

The data required for computer modeling of doses during flight operations were not available. These data included take-off and landing times, flight paths, altitudes, and recorded weather (e.g., wind speed/direction, precipitation). However, analyses indicated that for some routes of exposure, such as external doses associated with flight operations were low compared to those calculated for time on board ship, and that flight durations were only a small portion of the total time spent at sea. Therefore, because estimated shipboard doses were assumed to be similar to the potential doses received while performing flight operations, the shipboard doses were used for the entire at-sea periods for PEP C individuals.

4.2.7. Total Dose

The total effective dose and the total thyroid dose for each PEP were calculated by summing the corresponding contributions for times at sea and times in port. As discussed above, doses for times spent in flight operations were considered to be subsumed in the PEP A dose.

4.2.8. General Discussion

The dose assessment methods discussed above used empirical data, relevant fundamental health physics principles, universally accepted dose coefficients, and high-sided assumptions such as 24-hour exposure time topside per day, continuous working level breathing rates, no reduction factor associated with using the semi-infinite model for ships (as discussed in Section 3), and addition of both shore-based and HPAC-generated external doses (effectively double counting because an individual cannot be in two different places at the same time). For shore-based doses associated with times the ship was in port, various fixed and portable field instruments were used to measure external exposure rates, and shore-based report methods were used to calculate doses. General discussions of these instruments and their placement, as well as

details about dose calculations, are provided in the shore-based report, Appendices A and C, respectively.

The assessment that potential doses related to flight operations were equal to or no greater than shipboard doses was justified because:

- Analysis of air samples collected inside aircraft during missions conducted over areas proximal to FDNPS, which were assumed to have the highest potential regarding levels of contamination, did not indicate significant isotopic air activity concentrations that were directly related to external and internal doses;
- Most aircraft did not fly directly over FDNPS or other areas of potentially higher contamination; HPAC-generated forecasts of exposure potential were provided to aircrews to assist them in determining which areas to avoid. However, some aircraft exterior locations were contaminated from flying through airborne contamination of lower exposure potential;
- Although exterior locations on some aircraft accumulated low levels of contamination, potential isotopic airborne concentrations inside pressurized aircraft were minimized by built-in filters (which were not readily accessible to the aircrew) and overall structure of the aircraft. This reduced or eliminated the potential for inhalation or ingestion of radioactive materials and the associated doses to internal organs;
- Flight times were short compared to the 24 hours per day for the two-month period assumed for shipboard exposure times;
- Although flight crews had the potential for total submersion in airborne radioactive clouds, unlike shipboard individuals, the enclosed structure of the aircraft provided some inherent radiation attenuation (note that no reduction factors were assumed in the shipboard-related dose calculations); and
- A review of TLD/EPD data did not indicate any monitored dose higher than calculated external doses.

Section 5.

Results and Discussion

5.1 Dose Results

External, internal, and total effective and thyroid doses were calculated for personnel on all ships and attached aircrews that supported OT using the methodologies described in 0. The total effective doses calculated for the crews of the 25 ships ranged from 0.005 mSv (0.0005 rem) for USNS Matthew Perry to 0.33 mSv (0.033 rem) for USS Shiloh. Over half (16) of the calculated total effective doses were less than 0.1 mSv (0.01 rem). The total thyroid doses for the crews of these ships ranged from 0.07 mSv (0.007 rem) for USS Blue Ridge and USNS Matthew Perry to 3.3 mSv (0.33 rem) for USS Lassen. More than half (20) of the calculated total thyroid doses are less than 2.0 mSv (0.20 rem). The effective and thyroid doses for each ship are listed in Appendix J and are also discussed in the following section.

To help ensure that no individual in the fleet POI is assigned a dose less than the dose for any individual on any OT ship, maximum total effective and thyroid doses were calculated. These doses were determined by adding the highest external dose and the highest internal dose (effective and thyroid) for any ship. This approach helps to account, for example, for the possibility that an individual was on multiple ships during the OT period of interest. The highest external and internal doses calculated for individuals on any OT ship, and the total maximum doses, are shown in Table 7. For the reasons discussed earlier in this report, individuals in PEP A, PEP B, and PEP C were assigned the same doses. Therefore, the same maximum total effective and thyroid equivalent doses are applicable to all fleet-based individuals regardless of PEP classification, rating, or specific work location.

Table 7. Maximum external, internal, and total effective and thyroid doses for all fleet personnel

Dose Component	Effective Dose [mSv (rem)]	Thyroid Doses [mSv (rem)]
Highest external dose	0.17 (0.017)	0.17 (0.017)
Highest internal doses	0.18 (0.018)	3.2 (0.32)
Maximum total doses*	0.35 (0.035)	3.4 (0.34)

* The maximum total doses are applicable to individuals in PEP A, PEP B, and PEP C on all 25 ships participating in OT.

5.2 Discussion

The calculated total effective doses for fleet-based individuals on specific ships ranged from less than 0.01 mSv to 0.33 mSv (<0.001 rem–0.033 rem), and the total thyroid equivalent doses ranged from 0.07 mSv–3.3 mSv (0.007 rem–0.33 rem). The large dose ranges were not surprising considering the timing and locations of at-sea and in-port periods for each ship, at-sea

travel times and routes, and lengths of time spent at sea and in port. The highest total effective and thyroid equivalent doses are approximately four times lower than the highest doses calculated for shore-based DOD-affiliated individuals in Cassata et al. (2012). The lower doses are not unexpected, in large part because ships could be positioned outside of known plumes of radioactive material released from FDNPS. Also, radioactive cloud concentrations at sea were generally less than those associated with in-port locations.

For many of the ships that participated in OT, the timing of the in-port period(s) was an important factor affecting the doses calculated for the crew. This was especially the case for ships in port at Yokosuka NB, the closest naval base to FDNPS. This conclusion was based on the fact that ships in port were not able to avoid passing clouds of radioactive material as they could when at sea. Also, average air, water, and soil activity concentrations at Yokosuka NB were higher than those at Sasebo NB, which may have resulted in higher calculated overall doses at Yokosuka NB than at Sasebo NB. Figure 21 shows a summary of the in-port and at-sea time periods, the fractions of the period March 12–May 11 that was spent in port, and the total calculated effective and thyroid doses for crew members of each ship. As shown in Figure 21, most ships were at sea for a majority of the first half of the period, and most were in port during much of the second half of the overall period. Several ships (e.g., USS Ronald Reagan, USS Chancellorsville, and USS Preble) spent very little time in port during March 12–May 11, 2011.

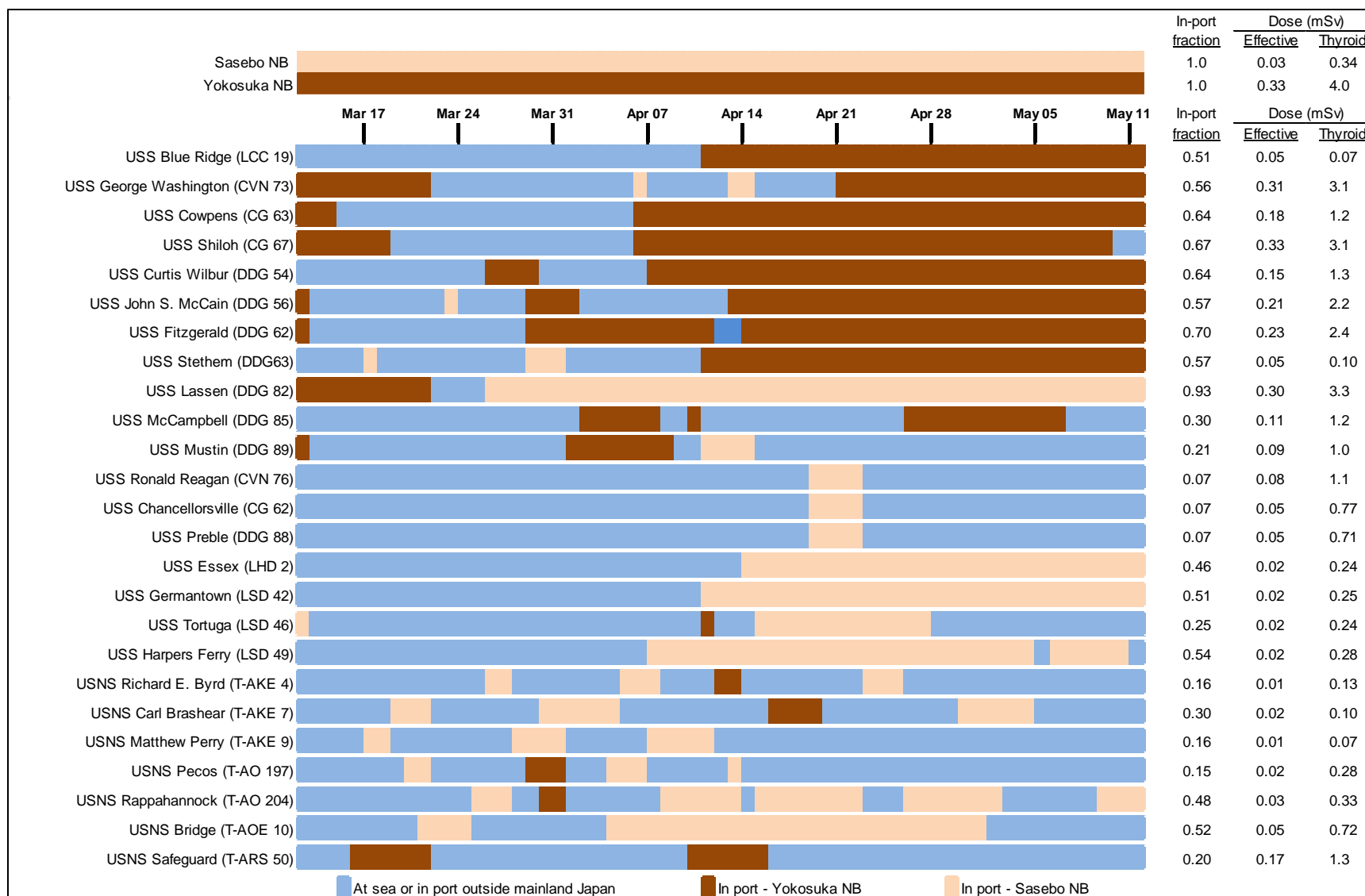


Figure 21. At-sea and in-port time periods and doses for ships involved in OT

In order to better understand the crew doses calculated for individual ships, the relationships of at-sea and in-port thyroid doses were examined for the 11 ships with crew thyroid doses equal to or greater than 1 mSv (0.10 rem). Figure 22 shows the portions of total thyroid dose accrued while at sea and while in port (columns in Figure 22). Also shown in Figure 22 are the fractions of the period of interest spent in port (circles); these fractions are also shown numerically in Figure 21. Together, the information in Figure 21 and Figure 22 illustrates several important points about the calculated doses for individuals on various ships.

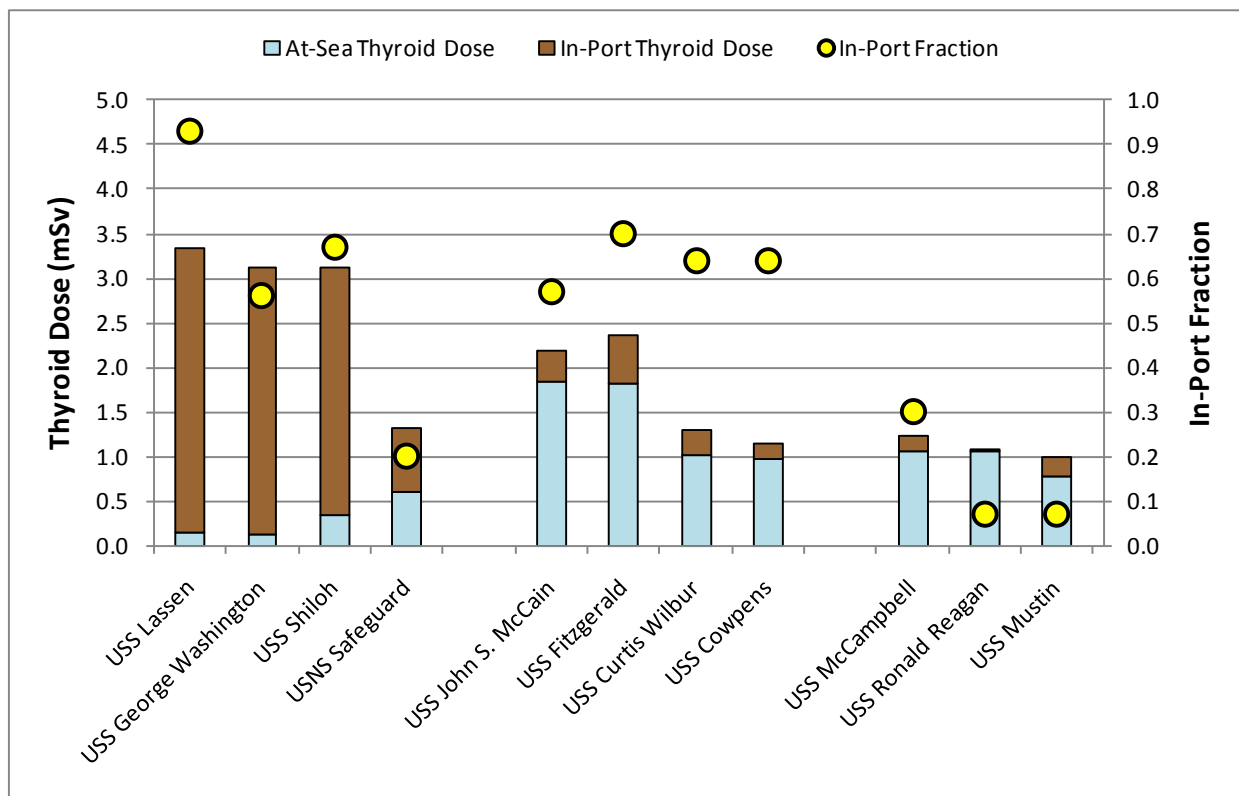


Figure 22. Thyroid doses and in-port fractions for ships with calculated thyroid equivalent crew doses greater than 1 mSv

As shown in Figure 22, the majority of thyroid doses calculated for crews on each of the four ships grouped at the left-hand side of the figure (USS Lassen, USS George Washington, USS Shiloh, and USNS Safeguard) were accrued while the ships were in port. The first three ships spent greater than 50 percent of the time in port at Yokosuka NB, and the doses calculated for the crews of these ships were relatively high. The thyroid dose calculated for the crew of USS Lassen is the highest for all ships involved in OT. The crew doses for these three ships are roughly two and one-half times higher than the doses calculated for the crew of the fourth ship in the group (USNS Safeguard). This difference in the doses was attributed to the timing of the ship's movements: USS Lassen, USS George Washington, and USS Shiloh were in port at Yokosuka NB during passage of a significant cloud of radioactive material released from FDNPS during the period March 14–17, 2011. USNS Safeguard did not arrive at Yokosuka NB until March 16, 2011, and therefore missed a large portion of the dose that resulted from the

March 14–17 cloud. The doses calculated for the first three ships are similar in magnitude to the doses calculated for shore-based individuals at Yokosuka NB (0.33 mSv [0.033 rem] effective dose, 4.0 mSv [0.40 rem] thyroid dose, see Cassata et al., 2012). This is reasonable, because the shore-based individuals at Yokosuka NB accrued more than half of their calculated doses in early and mid-March 2011 (Cassata et al., 2012).

The four ships in the middle grouping in Figure 22 (USS John S. McCain, USS Fitzgerald, USS Curtis Wilbur, and USS Cowpens), all spent greater than 50 percent of the OT temporal period in port at Yokosuka NB (similar to the left-hand grouping of ships). However, the calculated doses for these ships' crews were dominated by the doses accrued while they were at sea. Again, this was due to the timing and locations of the in-port periods, together with the relatively high, modeled air activity concentrations during some of the times at sea. As shown in Figure 21, except during the period March 11–14, the four ships spent essentially all of their in-port time at Yokosuka NB in April and May 2011, when measured external radiation levels and air activity concentrations there were lower than in March 2011. This resulted in lower calculated in-port doses for these ships. Conversely, the HPAC modeled air activity concentrations were relatively high for the area approximately 75–120 km (45–75 miles) off the eastern coast of Japan that the USS John S. McCain, USS Fitzgerald, and USS Curtis Wilbur passed through while traveling north on March 13, 2011. Consequently, the modeled at-sea air activity concentrations were the predominant sources of the calculated doses for these three ships. The fourth ship in this group, USS Cowpens, was in port at Yokosuka NB from March 11–14, 2011, and it subsequently operated off-shore south of Yokosuka NB until March 18, 2011, when it began traveling north. The USS Cowpens was much farther off-shore during this transit than USS John S. McCain, USS Fitzgerald, and USS Curtis Wilbur. Furthermore, USS Cowpens transited north at a later date than the northward travel of the other three ships. These two factors and the timing of FDNPS releases resulted in lower modeled at-sea air activity concentrations for USS Cowpens than those calculated for the other three ships. This resulted in lower (yet still predominant) at-sea doses for individuals on USS Cowpens compared to those for individuals on the USS John S. McCain, USS Fitzgerald, and USS Curtis Wilbur.

The crew thyroid doses for the ships grouped at the right-hand side of Figure 22 (USS McCampbell, USS Ronald Reagan, and USS Mustin) are less than 1.5 mSv (0.15 rem). These ships also had several operational features in common: (1) they spent 30 percent or less of the period in port; (2) they did not spend any significant amount of time at Yokosuka NB in March 2011; and (3) they did not encounter air concentrations while at sea that were as high as those for some of the other ships in the same area that were nearer to the coast. USS Ronald Reagan was in port only at Sasebo NB, while the USS McCampbell and USS Mustin were in port at Yokosuka NB primarily in April and May 2011, during periods of relatively lower in-port dose rates. Consequently, the calculated individual doses for these ships were dominated by doses accrued while at sea.

For ships not discussed above (i.e., those with calculated thyroid doses less than 1 mSv), the dose trends can generally be explained with similar reasoning to that discussed above: in-port timing and location. Exceptions to this are seen for some of the ships that were in port at Sasebo NB in April and/or May, 2011. For example, USS Blue Ridge and USS Germantown were in port during the same dates, yet the USS Blue Ridge thyroid doses do not reflect the higher average dose rates at Yokosuka NB where USS Blue Ridge was in port, as compared to the dose rates at Sasebo NB where USS Germantown was in port. This result is a consequence of the

conservative methodology used for calculation of the shore-based thyroid inhalation doses at Sasebo NB. Air activity concentrations were available and used for Yokosuka NB, but were not available for Sasebo NB. Therefore, inhalation doses for Sasebo NB were calculated by applying a ratio to the Sasebo NB ambient external dose rates as explained in Cassata et al. (2012). This methodology resulted in calculated inhalation doses for Sasebo NB that were more high-sided than those calculated for Yokosuka NB, especially during April and May 2011. Because of this methodology, doses calculated for USS Germantown while in port at Sasebo NB were higher than those calculated for Yokosuka NB during the same period.

If a ship left port shortly before arrival of a passing effluent cloud and the subsequent deposition of radioactive material, the ship would have actually missed immersion in any contaminated air associated with the passing cloud or ground shine from any deposited material. This is also the case for ships that arrived in port after passage of an effluent cloud at the port. However, as a conservative assumption used in the shore-based methodology, the in-port ship dose was calculated assuming the ship was in port for the entire day of departure and arrival (i.e., the full 24 hours in port on the day of departure or arrival). Therefore, a dose was included for some ships that may not have been exposed to the effluent cloud that passed through the port. For example, USNS Safeguard departed Yokosuka NB between 0900 and 1500 on March 21, 2011, but was credited with being in port all of March 21. Consequently, calculated individual doses for the ship were slightly higher than if they had been calculated assuming that the ship departed from Yokosuka NB at 0900 that day. Because external dose rates and air activity concentrations were generally higher at in-port locations than at-sea locations, these calculated doses should be higher than the actual doses received, and would be considered conservative.

Finally, to put the calculated doses into perspective, it is important to note that all of the reported effective doses are small when compared to the average dose from natural background radiation (including radon) for the U.S. population (3.1 mSv [0.31 rem]) as reported in NCRP (2009a). In addition, Figure 23 provides ubiquitous background radiation levels (excluding contributions from radon) for the prefectures in Japan prior to the FDNPS releases (Cassata et al, 2012).

Radiation from space and the earth, and Doses of radiation received by ingestion (those by the inhalation such as radon are excluded.)

- Less than 0.99
- 1.00~1.09
- More than 1.10 (mSV/year)

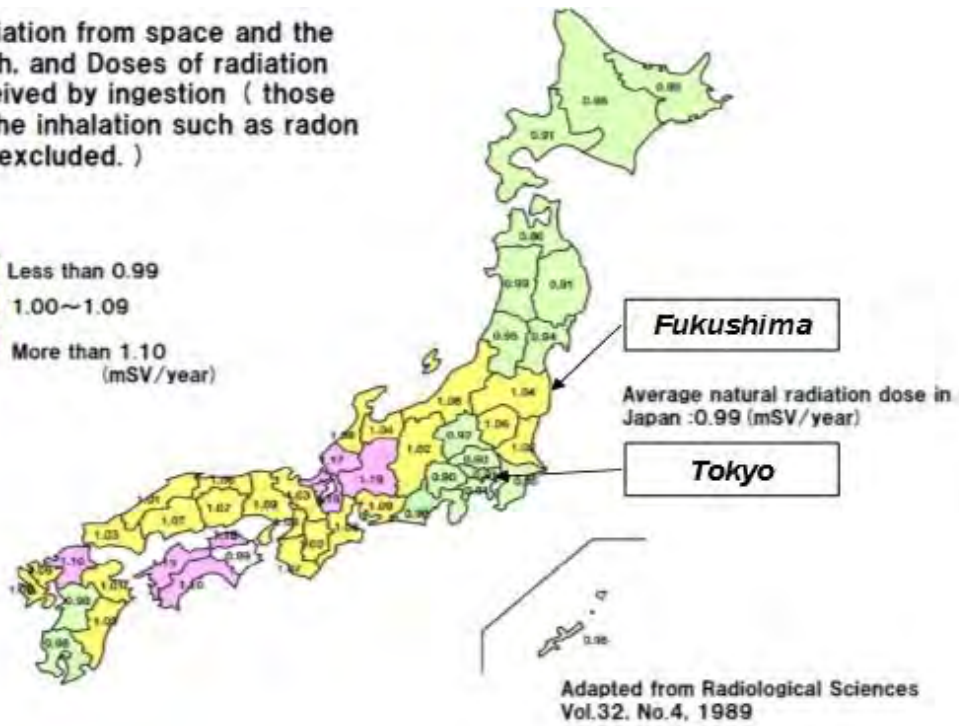


Figure 23. Annual radiation dose from background in Japan prior to FDNPS releases

This page intentionally left blank.

Section 6.

Conclusions

The radiation doses reported for U.S. fleet-based individuals resulted from an assessment of exposures to the radiological conditions in and near Japan during the two months between March 12 and May 11, 2011. Total effective doses calculated for the crews of each of the 25 participating ships ranged from 0.005 to 0.33 mSv; corresponding thyroid doses ranged from 0.07 to 3.3 mSv. These individual doses varied with the amount of time spent in port and the location of the port, with the lower range of doses associated with time spent at Sasebo NB and the higher doses associated with time spent in port at Yokosuka NB, especially soon after the FDNPS accident when external radiation levels increased in the Yokosuka NB area. Doses to ships at sea were generally lower than the doses to ships in port. The reported radiation doses were less than the annual average dose from background in the United States and were largely received during the first few days or weeks after the FDNPS accident.

The radiation doses for fleet-based individuals on each ship were calculated based on conservative assumptions about intake rates, time spent outdoors, and environmental monitoring results; supplemented with modeling where data were lacking. In addition, the following factors supported the conclusion that reported doses were conservative because:

- All calculations assumed an individual was topside when at sea and outdoors when in port;
- No dose mitigating actions, e.g., administration of potassium iodide; utilization of time, distance or shielding to reduce exposure; decontamination of ship surfaces, etc. were applied in the dose calculations; and
- Calculations of internal dose from inhalation assumed maximum physical activity levels (i.e., inhalation rates and water and soil ingestion rates)

It was recognized that there were uncertainties in specific details of ship's locations with respect to air borne radioactive clouds, as well as other uncertainties in locations of individuals aboard ship when at sea and ashore when in port. Therefore, DARWG determined that the calculation of a single dose value for all ships provided additional support for the conclusion about the conservative nature of the reported effective and thyroid doses. Those doses, calculated by summing the highest external dose for any ship and the highest internal dose for any ship result in an effective dose of 0.35 mSv (0.035 rem) and a thyroid dose of 3.4 mSv (0.34 rem).

Calculation of doses for individuals while in port pro-rated the doses reported in Cassata et al. (2012) for the time spent in port. That report had been peer reviewed by the NCRP who concurred the doses were high-sided. In addition, probabilistic analyses of shore-based doses in Chehata et al. (2013) demonstrated that the doses were greater than the 95th percentile doses at four locations studied in the probabilistic analysis, including Yokosuka NB.

The doses to fleet-based individuals associated with flight operations were assumed to be the same as the doses to shipboard/non-flight individuals. The assumption was based on shorter

exposure durations while in flight, partial shielding available in aircraft structures, and several other factors that could have reduced their doses compared to individuals topside aboard ship.

The reported radiation doses to fleet-based individuals were at least one order of magnitude less than any dose associated with adverse health effects. This conclusion is supported by the Health Physics Society official position statement on radiation dose and health effects, which states:

There is substantial and convincing scientific evidence for health risks following high-dose exposures. However, below 5–10 rem (which includes occupational and environmental exposures), risks of health effects are either too small to be observed or are nonexistent. (HPS, 2010)

Section 7.

References

- ACU5 (Assault Craft Unit 5) 2012. E-mail from OIC Assault Craft Unit 5 Det. ALFA to NAVSEA 04 dated March 2, 2012
- AFMSA 2013, E-mail dated March 11, 2013 from Air Force Medical Support Agency, Office of the Surgeon General, to Armed Forces Radiobiology Research Institute
- ANS (American Nuclear Society), 2012. Fukushima Daiichi: American Nuclear Society Committee Report, March 2012
- Benevides, L. 2012. *Radiological Controls Manual for Fukushima Dai-ichi Fallout, Revision 1*. Naval Sea Systems Command, Washington, DC. January 31.
- C7F (Commander, Seventh Fleet) 2011 (<http://www.c7f.navy.mil/news/2011/03-march/053.htm>, accessed on October 18, 2012)
- C7F (Commander, Seventh Fleet), 2012a. (<http://www.c7f.navy.mil/about.htm>, accessed on October 19, 2012)
- C7F (Commander, Seventh Fleet), 2012b. (<http://www.c7f.navy.mil/news/2010/09-september/036.htm>, accessed on October 22, 2012)
- C7F (Commander, Seventh Fleet), 2012c. (<http://www.c7f.navy.mil/news/2011/03-march/067.htm>, accessed on October 22, 2012)
- Cassata, J., Falo, G., Rademacher, S., Alleman, L., Rosser, C., Dunavant, J., Case, D., and Blake, P. 2012. *Radiation Doses for Shore-Based Individuals in Operation Tomodachi, Revision 1*. DTRA-TR-12-001 (R1) Defense Threat Reduction Agency, Fort Belvoir, VA. December 31.
- CNSF (Commander Naval Surface Forces), 2012. (<http://www.public.navy.mil/surfor/cds7/Pages/RonaldReaganCarrierStrikeGroupArrivesin7thFleet.aspx>, accessed October 20, 2012).
- COMNAVSURFPAC Note 3441.
- Delacroix, D., Guerre, J.P., LeBlanc, P., and Hickman, Cl. 2002. *Radionuclide and Radiation Protection Data Handbook*, Nuclear Technology Publishing, Kent, England.
- DTRA (Defense Threat Reduction Agency), 2005. *List of Military and Civil Defense RADIAC Devices*, HQDTRA(AR)-124-3M, Defense Threat Reduction Agency, Alexandria, VA. August.
- EPA (U.S. Environmental Protection Agency), 1998. *National Primary Drinking Water Regulations: Disinfectants and Disinfection Byproducts; Final Rule*. Title 40 Code of Federal Regulations, Part 141. U.S. Environmental Protection Agency, Washington, DC. December 16.

- EPA (U.S. Environmental Protection Agency), 2011. *Exposure Factors Handbook: 2011 Edition*, Report EPA/600/R-09/052F, U.S. Environmental Protection Agency, Washington, DC. September.
- Falo, G., Cassata, J., Rademacher, S., Marro, R., Case, D., Chehata, M., McKenzie-Carter, M., and Blake, P. 2013. *Radiation Dose Assessments for the Embryo, Fetus, and Nursing Infant during Operation Tomodachi*, DTRA-TR-12-017, Defense Threat Reduction Agency, Fort Belvoir, VA. May.
- Floekher, J. 2013. *Swipe Assays*. Application Note ABA-006, Packard Instrument Company, Meriden, CT.
- Gauntt, R., Kalinich, D., Cardoni, J., Phillips, J., Goldmann, A., Pickering, S., Francis, M., Robb, K., Ott, L., Wang, D., Smith, C., St.Germain, S., Schwieder, D., and Phelan, C. 2012. *Fukushima Daiichi Accident Study. Sandia Report*. SAND 2012-6173, Sandia National Laboratory, Albuquerque, NM> July.
- GOJ (Government of Japan). 2011. *Report of the Japanese Government to the IAEA Ministerial Conference on Nuclear Safety, The Accident at TEPCO's Fukushima Nuclear Power Stations*. Nuclear Emergency Response Headquarters, Government of Japan. June.
- HPS (Health Physics Society), 2010. *Radiation Risk in Perspective*. The Health Physics Society, McLean, VA. (http://hps.org/documents/risk_ps010-2.pdf, accessed on April 3, 2013).
- IAEA (International Atomic Energy Agency), 2003. *Radiological Conditions in Areas of Kuwait with Residues of Depleted Uranium*, International Atomic Energy Agency, Vienna.
- ICRP (International Commission on Radiological Protection). 1987. "Data for Use in Protection against External Radiation, ICRP Publication 51". *Annals of the ICRP*, 17(2–3), Elsevier Ltd., Oxford, UK.
- ICRP (International Commission on Radiological Protection). 1991. "1990 Recommendations of the International Commission on Radiological Protection, ICRP Publication 60" *Annals of the ICRP*, 21(1–3), Pergamon Press., Oxford, UK.
- ICRP (International Commission on Radiological Protection), 2001. *ICRP Database of Dose Coefficients: Workers and Members of the Public, Version 2.0.1*, 1998-2001. International Commission on Radiological Protection, Stockholm, Sweden.
- ICRP (International Commission on Radiological Protection). 2007. "The 2007 Recommendations of the International Commission on Radiological Protection, ICRP Publication 103". *Annals of the ICRP*, 37(2–4), Elsevier Ltd., Oxford, UK.
- INPO (Institute of Nuclear Power Operations). 2011. *Special Report on the Nuclear Accident at the Fukushima Daiichi Nuclear Power Station*. INPO 11-005. November. Johnson, T. and Birky, B. 2012. *Health Physics and Radiological Health, 4th Edition*, Lippincott Williams & Wilkins.
- Johnson, W. B., 2011. *Radiac Detector DT-304/PDR, Revision 1*. EE730-AB-MMO-010, and Naval Sea Systems Command, Washington, D.C. July.
- Knoll, G.F., 1989. *Radiation Detection and Measurement 2nd Edition*, John Wiley and Sons, New York, NY.

- Kobayashi, T., Nagai, H., Chino, M., and Kawamura, H. 2013. "Source term estimation of atmospheric release due to the Fukushima Dai-ichi Nuclear Power Plant accident by atmospheric and oceanic dispersion simulations," *Journal of Nuclear Science and Technology*, March 15.
- Leggett, R. and Eckerman, K., undated. *Guide to Tables of Updated Dose Coefficients for HPAC*," unpublished report, Life Sciences Division, Oak Ridge National Laboratory.
- Liska, B., Clark, W., Warder, C., and Wood, S. 2011. "Shipboard Collective Protection System Modernization for Improved Energy Efficiency and Total Ownership Cost Reduction," *Proceedings of the American Society of Naval Engineers (ASNE) Intelligent Ships Symposium (ISS) IX*, ASNE (American Society of of Naval Engineers), Washington, DC. May 25–25.
(<https://www.navalengineers.org/Pages/Login.aspx?ReturnUrl=%2fpublications%2fsymposium%2fPages%2fISSIXProceedings.aspx> , accessed September 10, 2013)
- La Vie, S. 2009. "What's in the Black Box Known as Emergency Dose Assessment?", 2009 National Radiological Emergency Preparedness (NREP) Conference, Norfolk, VA, April 15, 2009. National Radiological Emergency Preparedness (NREP) Conference, Inc., Baton Rouge, LA.
- Marro, R., 2012. "OT-RR Dosimetry Data Analysis," E-mail to Mondher Chehata (SAIC). Armed Forces Radiobiology Research Institute, Bethesda, MD. May 31.
- MEDCOM 2013, E-mail dated March 4, 2013 from Medical Command Radiological Safety Staff Officer, San Antonio, TX to Armed Forces Radiobiology Research Institute.
- NAFA (Naval Air Facility Atsugi), 2012.
(<http://www.cnrc.navy.mil/Atsugi/About/TenantCommands/CVW-5/index.htm>, accessed October 20, 2012).
- NAS (National Academy of Science). 1995. *Radiation Dose Reconstruction for Epidemiologic Uses*, National Research Council, National Academy Press, Washington, DC.
- Navy news service "USS George Washington Departs for Japan" Story Number: NNS080821-05Release Date: 8/21/2008 4:08:00 PM
http://www.navy.mil/submit/display.asp?story_id=39259.
- NCRP (National Council on Radiation Protection and Measurements). 2009a. *Ionizing Radiation Exposure of the Population of the United States (2009)*. NCRP Report No. 160, National Council on Radiation Protection and Measurements, Bethesda, MD.
- NCRP (National Council on Radiation Protection and Measurements). 2009b. *Radiation Dose Reconstruction: Principles and Practice*. NCRP Report No. 163, National Council on Radiation Protection and Measurements, Bethesda, MD.
- NP (Naval Proceedings), 2012. Truver, Scott C., and Holzer, Robert, "U.S. Navy in Review." *Naval Proceedings* Vol. 138/5, 311, May 12.
- NRC (U.S. Nuclear Regulatory Commission), 1995. *Accident Source Term for Light-Water Nuclear Power Plants*, Report NUREG-1465, U.S. Nuclear Regulatory Commission, Washington D.C. February.

- NRC (U.S. Nuclear Regulatory Commission), 2011, Appendix A to Title 10 Code of Federal Regulations Part 20
- NSWC 2011a E-mail dated September 1, 2011 from Naval Surface Warfare Center, Dahlgren, VA to NAVSEA 04.
- NSWC 2011b, E-mail dated March 2, 2012 from Naval Surface Warfare Center Dahlgren Division to NAVSEA 04 (forwarding information from Officer-in-Charge, Assault Craft Unit Five DET Alfa to NAVSEA 04)
- NSWC 2012a, Email dated March 2, 2012 from Naval Surface Warfare Center Dahlgren Division to NAVSEA 04 (forwarding information from Officer-in-Charge, Assault Craft Unit Five DET Alfa to NAVSEA 04)
- NSWC 2012b, Pompeii, M., 2012. "Revision 1: Request for RADCON Release, USS Germantown." E-mail to Benevides, Luis (NAVSEA 04). Naval Surface Warfare Center, Dahlgren, VA, January 13.
- NSWC 2012c, Pompeii, M., 2012. "Revision 1: Request for RADCON Release, Sea Water Systems." E-mail to Benevides, Luis (NAVSEA 04). Naval Surface Warfare Center, Dahlgren, VA, January 31.
- NSWC 2012d, Pompeii, M., 2012. "Recommendation for RADCON Release, R.O./Potable Water Systems." E-mail to Benevides, Luis (NAVSEA 04). Naval Surface Warfare Center, Dahlgren, VA, April 20.
- NSWC (Naval Surface Warfare Center Dahlgren), 2013. *Fleet RAD Survey Results*. Naval Surface Warfare Center Dahlgren, Dahlgren, Virginia.
- Shleien, B., Slaback, L.A., Jr., Birky, B.K., 1998. *Handbook of Health Physics and Radiological Health 3rd Edition*, Williams & Wilkins, Baltimore, MD.
- Smith, K.R., and Jones, A.L. 2003. *Generalised Habit Data for Radiological Assessments*, NRPB-41, National Radiological Protection Board, Chilton, UK. May.
- Steinmeyer, P.R., (2005). "G-M Pancake Detectors: Everything You've Wanted to Know (But Were Afraid to Ask)," RSO Magazine, Volume 10(5), pp. 7-17.
- Stohl, A., Seibert, P., Wotawa, G., Arnold, D., Burkhardt, J., Eckhardt, S., Tapia, C., Vargas, A., and Yasmura, T. 2011. "Xenon-133 and caesium-137 releases into the atmosphere from the Fukushima Dai-ichi nuclear power plant: determination of the source term, atmospheric and dispersion, and deposition," *Atmospheric Chemistry and Physics Discussions*, October 20.
- Tailhook (The Tailhook Association) 2005. "Carrier Air Wing Composition." The Tailhook Association. San Diego, CA. (<http://www.tailhook.net/CVWList1205.pdf>, accessed December 30, 2006).
- USFJ (U.S. Forces, Japan). 2011a. Message 200704Z Mar 2011. March 20.
- USFJ (U.S. Forces, Japan). 2011b. Email from LtCol Cassin, USFJ, J07, OPS/Planner to ENS Alleman, AFRRI, on September 6.

- USN (United States Navy). 2007. "Navy Guidelines Concerning Pregnancy and Parenthood," OPNAV Instruction 6000.1C, Office of the Chief Of Naval Operations, 2000 Navy Pentagon, Washington, D.C. June 14.
- USN (United States Navy) 2008. "USS George Washington Departs for Japan." All Hands Magazine, Navy News Service. Washington, DC. August 21.
(http://www.navy.mil/submit/display.asp?story_id=39259, accessed August 5, 2013).
- USGS (U.S. Geological Survey). 2011. *Magnitude 9.0 Near the East Coast of Honshu, Japan, Earthquake Details*.
(<http://earthquake.usgs.gov/earthquakes/recenteqsww/Quakes/usc0001xgp.php#details>, accessed April 3, 2012). Weitz, R.L. and McKenzie-Carter, M., 2011. *Transfer of Deposited Contaminants from Surfaces to hands and from Hands to Mouth*. NTPR-TM-11-01. Defense Threat Reduction Agency, Fort Belvoir, Va. March 31.
- WHO (World Health Organization). 2012. *Preliminary Dose Estimation from the Nuclear Accident after the 2011 Great East Japan Earthquake and Tsunami*. World Health Organization, Geneva, Switzerland.
- Yasunari, T.J., Stohl, A., Hayano, R.S., Burkhart, J.F., 2011. "Cesium-137 deposition and contamination of Japanese soils due to the Fukushima nuclear accident," *Proceedings of the National Academy of Sciences of the United States of America*, 108(49), December 6.

This page intentionally left blank.

Appendix A.

Radiological Quantities and Units

A-1. Introduction

In this report, radiological quantities are expressed using International System (SI) units along with the value in U.S. customary units (such as rem) in parentheses because the DOD more commonly uses the customary units for reporting doses to Service members, civilian employees and families.

To determine human radiation exposures quantitatively and to provide for radiation protection, radiological quantities and units are needed. The International Commission on Radiological Protection (ICRP) has developed a system of radiation protection (ICRP, 2007a). Within the ICRP system, several radiological quantities are of particular interest for this report: absorbed dose, equivalent dose, effective dose, radioactivity, and activity.

A-2. Absorbed Dose

In radiation protection, the basic quantity of concern is the amount of energy deposited in a particular organ or tissue (e.g., the thyroid). This quantity is called absorbed dose. By definition, the absorbed dose is “the amount of ionizing radiation energy absorbed in matter, including human tissue” (Johnson and Birky, 2012). The SI unit for organ dose is J kg^{-1} and is given the special name gray (Gy). The customary unit for absorbed dose used in the U.S. is the rad; $1 \text{ rad} = 0.01 \text{ Gy}$.

A-3. Equivalent Dose

The sensitivity of specific tissues and organs to radiation exposure depends on the type of radiation, and these types include alpha particle radiation, beta particle radiation, gamma-ray and X-ray photons, and neutrons. To account for this sensitivity, the quantity equivalent dose was developed. The equivalent dose to a tissue or organ is the product of the average absorbed dose to that tissue or organ and a radiation weighting factor, whose value depends on the radiation type (Johnson and Birky, 2012). The SI unit of equivalent dose is the J kg^{-1} and is given the special name sievert (Sv). The customary unit for equivalent dose used in the U.S. is the rem; $1 \text{ rem} = 0.01 \text{ Sv}$. The equivalent dose can also be called an organ dose. For this report, the organ dose of interest is the thyroid dose.

A-4. Effective Dose

Sensitivity is not only based on the type of radiation as described above, but it also depends on the inherent sensitivity of each tissue or organ in the body to the effects of radiation. When considering radiation exposure to the whole body, the concept of effective dose was developed. The effective dose is the sum of the products of equivalent dose to each organ and a tissue weighting factor (WHO, 2012). The SI unit of effective dose is J kg^{-1} and is given the special name sievert (Sv). The customary unit for effective dose used in the U.S. is the rem; $1 \text{ rem} = 0.01 \text{ Sv}$.

In the absence of internal radiation dose, the external radiation dose component (radiation dose from sources outside the body) is equivalent to the effective dose for the external radiation fields from the reactor releases that emit x rays, gamma rays, and beta particles. In practice, the external radiation dose is measured or estimated from personal radiation monitors (dosimeters), by measurements of the external radiation fields (surveys), or calculated based on knowledge of the radiation sources in the area. It is usually assumed that the whole body receives a uniform radiation dose as determined from dosimeters, surveys, or calculations.

A-5. Committed Dose

To describe the radiation dose from intakes of radioactive material, the radiation protection community uses the term “committed doses”. Committed dose results from intakes of radioactive materials are calculated based on the behavior of the radioactive material in a reference person for a period of 50 years after an intake (for adults) or until age 70 (for children). Although the radiation doses are actually delivered over an extended period of time after an intake, this committed dose is “assigned” at the time the intake occurred.

A-6. Radioactivity and Activity

“Radioactivity” is a property of matter and refers to the events associated with nuclear transformations (ICRU, 2011). In contrast, “activity” is the amount of radioactive material at a given time or the rate at which radioactive transformations occur (ICRU, 2011). The SI unit of activity is one transformation per second and is given the name becquerel (Bq). The customary unit for activity used in the U.S. is the curie (Ci); 1 Ci = 37 billion Bq.

A-7. Doses Calculated in this Report

The doses calculated in this report are the effective and organ (thyroid) doses as described in ICRP Publication 60 (ICRP, 1991) and used in the ICRP databases of dose coefficients (DC) (ICRP, 2003 and 2007b). The effective dose replaced the quantity “effective dose equivalent” (EDE)²⁶ in the 1990 recommendations of the ICRP (1991). In addition, absorbed dose to live skin cells (skin dose) from contamination directly on the surface of the outer dead skin layer was calculated.

²⁶ The term EDE is still used in the U. S. Government in its regulations.

Appendix B.

Fleet History

B-1. Introduction

At the time of the earthquake, tsunami, and subsequent radioactive material releases from FDNPS, the U.S. Navy mobilized forward-deployed units, ships from various locations, and embarked personnel to provide HADR services to the affected area and population. The HADR effort eventually involved 25 U.S. ships, more than 240 aircraft, and approximately 17,000 DOD-affiliated individuals.

The radiation dose assessments for fleet-based individuals required knowledge of their locations, duration of exposure, and individual activities. The specific in-port and at-sea periods used for dose estimates in this report are given in Table 2 of the main report. The following sections provide additional details pertinent to ships' histories from March 12 to May 11, 2011, which supplement the dose periods listed in Table 2 of the main report. Some dates listed below may appear inconsistent with the listed references, but this is only an artifact due to the conversion of dates and times to Japan Standard Time.

B-2. USS Blue Ridge (LCC 19)

Ref: <http://www.uscarriers.net/lcc19history.htm> (as of June 4, 2012)

- March 12, ship departed Changi NB in Singapore, after on-loading humanitarian assistance supplies, in support of HADR operations in Japan.
- March 17, ship arrived off Okinawa to fly relief supplies to USNS Tippecanoe and USNS Richard E. Byrd. HSL-51 DET 11 (SH-60F type helicopters: Bureau Numbers [BUNO] 164081 and 164446) flew two air missions into Kadena AB (only flights into Kadena) and performed vertical replenishments²⁷ to USNS Tippecanoe and USNS Richard E. Byrd in and around Okinawa.
- April 9, ship departed Okinawa area and arrived off Honshu on April 10.
- April 11, pulled into Yokosuka NB. Ship contamination survey results of flight deck were indistinguishable from background. (NSWC, 2011)

B-3. USS George Washington (CVN 73)

Ref: <http://www.uscarriers.net/cvn73history.htm> (as of June 4, 2012)

- March 12–21, USS George Washington was in port at Yokosuka NB.
- March 22–April 4, ship was at sea generally greater than 200 nmi from FDNPS.

²⁷ Vertical replenishment is a transfer of cargo between ships using helicopters. The process involves hovering over the flight deck off the ship and unloading supplies without the helicopter itself touching the ship.

- April 6, ship was in port at Sasebo NB to onload supplies and equipment, and to drop off more than 300 Naval shipyard workers who had been working aboard ships in Yokosuka NB.
- April 7–12, ship was at sea operating greater than 200 nmi from FDNPS.
- April 13–14, ship was in port at Sasebo NB to disembark another 150 Naval shipyard workers and to bring aboard 115 Japanese that would continue the ship's routine maintenance at sea.
- April 15–20, ship was at sea operating generally greater than 200 nmi from FDNPS.
- April 21–May 11, ship was in port at Yokosuka NB.

B-4. USS Cowpens (CG 63)

Ref: <http://www.uscarriers.net/cg63history.htm> (as of June 6, 2012)

- March 12–14, USS Cowpens was in port at Yokosuka NB.
- March 15–April 4, ship was at sea in support of OT.
- April 5–May 11, ship was in port at Yokosuka NB.

B-5. USS Shiloh (CG 67)

Ref: <http://www.uscarriers.net/cg67history.htm> (as of June 6, 2012)

- March 12–18, USS Shiloh was in port at Yokosuka NB.
- March 19–April 5, ship was at sea in support of OT.
- April 6–May 9, ship was in port at Yokosuka NB.
- May 10–11, ship was at sea operating greater than 200 nmi from FDNPS.

B-6. USS Curtis Wilbur (DDG 54)

Ref: <http://www.uscarriers.net/ddg54history.htm> (as of June 6, 2012)

- March 12, USS Curtis Wilbur was at sea east of the Boso Peninsula preparing to move into position off Miyagi Prefecture to assist Japanese authorities with providing at-sea search and rescue and recovery operations.
- March 26, ship returned to Yokosuka NB for resupply.
- March 26–29, ship was in port at Yokosuka NB.
- April 7, ship returned to Yokosuka NB after concluding its support of OT.

B-7. USS John S. McCain (DDG 56)

Ref: <http://www.uscarriers.net/ddg56history.htm> (as of June 6, 2012)

- March 12, USS John S. McCain was in port at Yokosuka NB.
- March 13–19, ship was at sea in direct support of OT.
- March 20–22, ship was in transit to Sasebo NB.
- March 23, ship was in port at Sasebo NB.
- March 24–28, ship was at sea greater than 200 nmi from FDNPS.
- March 29–April 1, ship was in port at Yokosuka NB.
- April 2–5, ship operated at sea greater than 200 nmi from FDNPS.
- April 6–10, ship was in port at Chinae, Republic of Korea.
- April 11–12, ship was in transit to Yokosuka NB.
- April 13–May 11, ship was in port at Yokosuka NB.

B-8. USS Fitzgerald (DDG 62)

Ref: <http://www.uscarriers.net/ddg62history.htm> (as of June 6, 2012)

- March 12, USS Fitzgerald was in port at Yokosuka NB.
- March 13–26, ship was at sea in direct support of OT.
- March 27, ship transited to Yokosuka NB.
- March 28–April 11, ship was in port at Yokosuka NB.
- April 12–13, ship was at sea greater than 200 nmi from FDNPS.
- April 14–May 11, ship was in port at Yokosuka NB.

B-9. USS Stethem (DDG 63)

Ref: <http://www.uscarriers.net/ddg63history.htm> (as of April 2, 2013)

- March 18, USS Stethem arrived in Donghae, Republic of Korea, for a scheduled port visit before participating in annual exercise Foal Eagle.
- March 29, ship arrived at Sasebo NB.
- March 31, ship departed Sasebo NB after a brief port call.
- April 3–10, ship participated in exercise Malabar 2011, with the Indian Navy off the coast of Okinawa.
- April 11–May 1, ship in port at Yokosuka NB.
- May 2–11, ship was in port at Yokosuka Naval Shipyard for a selected restricted availability.

B-10. USS Lassen (DDG 82)

Ref: <http://www.uscarriers.net/ddg82history.htm> (as of June 6, 2012)

- March 12–21, USS Lassen was in port at Yokosuka NB.
- March 22–25, ship transited to Sasebo NB.
- March 26–May 11, ship was in port at Sasebo NB.

B-11. USS McCampbell (DDG 85)

Ref: <http://www.uscarriers.net/ddg85history.htm> (as of June 6, 2012)

- March 12–30, USS McCampbell operated off Miyagi and Iwate Prefectures.
- March 31, ship was at sea in direct support of OT.
- April 1, ship was in transit to Yokosuka NB.
- April 2–7, ship was in port at Yokosuka NB.
- April 8–9, ship was at sea greater than 200 nmi from FDNPS.
- April 10, ship was in port at Yokosuka NB.
- April 11–12, ship was in transit to Okinawa.
- April 13–15, ship was in port at Okinawa.
- April 16–19, ship was at sea operating greater than 200 nmi from FDNPS.
- April 20, ship was in vicinity of Nagasaki.
- April 21–22, ship was in transit to Yokosuka NB.
- April 23–25, ship was in vicinity of Sagami Bay, west of Miura Peninsula.
- April 26–May 6, ship was in port at Yokosuka NB.
- May 7–11, ship was at sea greater than 200 nmi from FDNPS.

B-12. USS Mustin (DDG 89)

Ref: <http://www.uscarriers.net/ddg89history.htm> (as of June 6, 2012)

- March 12, USS Mustin was in port at Yokosuka NB.
- March 13–31, ship was at sea in direct support of OT.
- April 1–8, ship was in port at Yokosuka NB.
- April 9–10, ship was in transit to Sasebo NB.
- April 11–14, ship was in port at Sasebo NB.

- April 15–23, ship was at sea in support of OT.
- April 24–May 11, ship was operating greater than 200 nmi from FDNPS.

B-13. USS Ronald Reagan (CVN 76)

Ref: <http://www.uscarriers.net/cvn76history.htm> (as of May 8, 2013)

- March 12, USS Ronald Reagan in transit from Philippine Sea to OT.
- March 13, ship arrives on station off the east coast of Honshu, early Sunday, to serve as an afloat platform for refueling Japan Self Defense Force and other helicopters involved in rescue and recovery efforts ashore.
- March 14–22, ship was operating at sea in support of OT.
- March 23, ship pauses from flight operations to conduct wash down of its flight deck.
- March 24–April 7, ship was operating at sea in support of OT.
- April 8, ship participates in exercise Malabar 2011, with the Indian Navy, in the Philippine Sea.
- April 19–22, ship was in port at Sasebo NB.
- May 1, anchored off the coast of Phuket for a four-day visit to Thailand.

B-14. USS Chancellorsville (CG 62)

Ref: <http://www.uscarriers.net/cg62history.htm> (as of April 3, 2013)

- March 13, The USS Chancellorsville arrived off the coast of Miyagi prefecture to provide humanitarian assistance in support of earthquake and tsunami relief operations in Japan.
- April 19, ship pulled into Sasebo NB for a scheduled port visit.
- May 1, ship anchored off the coast of Phuket for a four-day visit to Thailand.

B-15. USS Preble (DDG 88)

Ref: <http://www.uscarriers.net/ddg88history.htm> (as of June 6, 2012)

- March 12, USS Preble was in transit from Philippine Sea to OT.
- March 13–April 7, ship was at sea operating in direct support of OT.
- April 8–17, ship was at sea operating greater than 200 nmi from FDNPS.
- April 18, ship transited to Sasebo NB.
- April 19–22, ship was in port at Sasebo NB.
- April 23–May 11, ship was operating greater than 200 nmi from FDNPS.

B-16. USS Essex (LHD 2)

Ref: <http://www.uscarriers.net/lhd2history.htm> (as of June 6, 2012)

- March 12, USS Essex departed Malaysia to rendezvous with USS Germantown and USS Harpers Ferry off the coast of Japan.
- March 15, ship took on HADR-related supplies via replenishment at sea.
- March 18, ship arrived off the coast of Akita prefecture.
- March 20–21, ship arrived off eastern shore of Japan mainland and at Hachinohe City. The 31st MEU conducted helicopter HADR operations and aerial surveys of over 200 miles of coastline to identify isolated individuals who required assistance (C7F, 2011).
- March 23, ship is off the coast of Hachinohe conducting HADR operations.
- March 27, ship is off the coast of Kessennuma (approximately 60 miles north of Sendai) supporting OT.
- April 1, 187 Sailors and Marines began Operation "Field Day", a clearing and clean up mission on the remote island of Oshima (approximately 120 miles northwest of Misawa). The ship received Landing Craft Air Cushion (LCAC) 10 and 81 (only LCAC-related operation). (NSWC, 2012c)
- April 7, ship concluded its direct participation in OT.
- April 8–12, ship was transiting to Okinawa.
- April 12, ship offloaded more than 1,200 Marines, 75 vehicles and 300 pieces of cargo at White Beach Naval Facility in Okinawa.
- April 13, ship was in transit to Sasebo NB.
- April 14, ship arrived Sasebo NB.
- April 14–May 11, ship was in port at Sasebo NB.

B-17. USS Germantown (LSD 42)

Ref: <http://www.uscarriers.net/lsd42history.htm> (as of June 6, 2012)

- March 11, USS Germantown was diverted to rendezvous with USS Essex and USS Harpers Ferry, off the coast of Japan.
- March 12–18, ship was at sea operating greater than 200 nmi from FDNPS.
- March 18–April 2, ship operated at sea in direct support of OT. Arrived off the coast of Hachinohe City on March 21 with embarked 31st MEU (C7F, 2011).
- April 3–10, ship was at sea operating greater than 200 nmi from FDNPS (at Okinawa April 7–9).
- April 10, ship was in transit to Sasebo NB.
- April 11–May 11, ship was in port at Sasebo NB.

B-18. USS Tortuga (LSD 46)

Ref: <http://www.uscarriers.net/lsd46history.htm> (as of June 6, 2012)

- March 12, USS Tortuga was in port at Sasebo NB.
- March 12–18, ship operated in the Sea of Japan.
- March 19–April 9, ship operated at sea in direct support of OT.
- April 10, ship was in port at Yokosuka NB.
- April 11–14, ship was in transit to Sasebo NB.
- April 15–27, ship was in port at Sasebo NB.
- April 28–30, ship was at sea operating in the South China Sea.
- May 1–2, ship was in port at Okinawa.
- May 3–11, ship was operating greater than 200 nmi from FDNPS.

B-19. USS Harpers Ferry (LSD 49)

Ref: <http://www.uscarriers.net/lsd49history.htm> (as of June 6, 2012)

- March 12–15, USS Harpers Ferry was operating greater than 200 nmi from FDNPS.
- March 16–19, ship operated in the Sea of Japan.
- March 20–April 2, ship was at sea in direct support of OT.
- April 1, LCAC 10 and 81 were transferred to USS Essex (greater than 200 nmi from FDNPS). (ACU5, 2011)
- April 3–7, ship was at sea greater than 200 nmi from FDNPS.
- April 7–10, ship was in port at Sasebo NB.
- April 10, ship was at sea greater than 200 nmi from FDNPS.
- April 11–May 4, ship was in port at Sasebo NB.
- May 4–5, ship was at sea greater than 200 nmi from FDNPS.
- May 6–10, ship was in port at Sasebo NB.
- May 10–11, ship was at sea greater than 200 nmi from FDNPS.

B-20. USNS Richard E. Byrd (T-AKE 4)

Ref: <http://www.msc.navy.mil/sealift/2011/May/japan.htm> (as of June 6, 2012)

- March 12–24, USNS Richard E. Byrd operated outside of 200 nmi from FDNPS.
- March 26–27, ship was in port at Sasebo NB.
- March 27–29, ship was at sea directly supporting OT while maintaining a distance greater than 200 nmi from FDNPS.
- March 30, the ship (with SA-330J Puma helicopters) arrived off the coast of Sendai and airlifted supplies to USS Preble, USS Harpers Ferry, and USS Tortuga.
- March 31, ship performed vertical replenishment with the Tortuga.
- March 31–April 4, ship was at sea supporting OT greater than 200 nmi from FDNPS.
- April 5–7, ship was in port at Sasebo NB.
- April 7–11, ship in transit and operating off the coast of Okinawa; ship was greater than 200 nmi from FDNPS.
- April 12–13, ship was in port at Yokosuka NB.
- April 13–22, ship transited from Yokosuka NB to Sasebo NB.
- April 23–25, ship was in port at Sasebo NB.
- April 25–May 11, ship in transit and also operated greater than 200 nmi from FDNPS.

B-21. USNS Carl Brashear (T-AKE 7)

Ref: [http://en.wikipedia.org/wiki/USNS_Carl_Brashear_\(T-AKE-7\)](http://en.wikipedia.org/wiki/USNS_Carl_Brashear_(T-AKE-7)) (as of June 4, 2012)

- March 12–18, USNS Carl Brashear was operating greater than 200 nmi from FDNPS and transiting to Sasebo NB.
- March 19–20, ship was in port at Sasebo NB.
- March 22–27, ship was operating within 200 nmi of FDNPS in support of OT.
- March 27–29, ship was in transit to Sasebo NB.
- March 30–April 4, ship was in port at Sasebo NB.
- April 4–15, ship operated greater than 200 nmi from FDNPS.
- April 16–19, ship was in port at Yokosuka NB.
- April 20–29, ship was in transit to Sasebo NB.
- April 30–May 4, ship was in port at Sasebo NB.
- May 5–11, ship was operating greater than 200 nmi from FDNPS.

B-22. USNS Matthew Perry (T-AKE 9)

Ref: <http://www.msc.navy.mil/sealift/2011/May/japan.htm> (as of June 6, 2012)

- March 12–16, USNS Matthew Perry transited from Korea to Okinawa.
- March 17–18, ship was in port at Sasebo NB.
- March 18–20, ship operated in Sea of Japan.
- March 21–24, ship directly supported OT.
- March 25–27, ship operated greater than 200 nmi from FDNPS.
- March 28–31, ship was in port at Sasebo NB.
- March 31–April 2, ship was in transit in the Sea of Japan.
- April 2–7, ship directly supported OT.
- April 8–11, ship was in port at Sasebo NB.
- April 11–May 11, ship was in transit and operated greater than 200 nmi from FDNPS.

B-23. USNS Pecos (T-AO 197)

Ref: <http://www.msc.navy.mil/sealift/2011/May/japan.htm> (as of June 6, 2012)

- March 12–19, USNS Pecos operated greater than 200 nmi from FDNPS.
- March 20–21, Akasaki POL Depot, positioned with USS Blue Ridge on March 21 for transfer of HADR-related supplies.
- March 25–27, ship directly supported OT. Arrived off Sendai to conduct underway replenishment operations.²⁸
- March 28–29, ship in transit to Yokosuka NB.
- March 29–31, ship was in port at Yokosuka NB.
- April 1–3, ship operated greater than 200 nmi from FDNPS.
- April 4–6, ship was in port at Sasebo NB.
- April 7–12, ship operated greater than 200 nmi from FDNPS.
- April 13, Akasaki POL Depot.
- April 14–May 11, ship was at sea.

²⁸ Underway replenishment operations typically involve transfer of supplies from one ship to another by way of secure lines between the two ships.

B-24. USNS Rappahannock (T-AO 204)

Ref: <http://www.msc.navy.mil/sealift/2011/May/japan.htm> (as of June 6, 2012)

- March 12–24, USNS Rappahannock was operating greater than 200 nmi from FDNPS.
- March 25–27, ship was in port at Sasebo NB. The ship loaded diesel and aviation type fuel and sailed to South Korea (arrived March 27, 2011).
- March 27–30, ship was in transit from South Korea to Yokosuka NB.
- March 30–31, ship was in port at Yokosuka NB.
- March 31–April 5, ship was in direct support of OT.
- April 6–7, ship was transiting to Sasebo NB.
- April 8–13, ship was in port at Sasebo NB or in the vicinity of Sasebo NB.
- April 14, ship was at sea.
- April 15–22, ship was in port at Sasebo NB.
- April 23–25, ship was operating south of Japan greater than 200 nmi from FDNPS.
- April 26–May 2, ship was in port at Sasebo NB.
- May 3–9, ship was operating in the China Sea.
- May 9–11, ship was in port at Sasebo NB.

B-25. USNS Bridge (T-AOE 10)

Ref: <http://www.msc.navy.mil/sealift/2011/May/japan.htm> (as of June 6, 2012)

- March 12, USNS Bridge was operating greater than 200 nmi from FDNPS.
- March 13–19, ship was directly supporting OT.
- March 20–21, ship was in transit to Sasebo NB.
- March 21–24, ship was in port at Sasebo NB.
- March 24–30, ship was directly supporting OT.
- March 31–April 3, ship was in transit in the Sea of Japan.
- April 4–May 1, ship was in port at Sasebo NB.
- May 1–11, ship was operating greater than 200 nmi from FDNPS.

B-26. USNS Safeguard (T-ARS 50)

Ref: <http://www.washingtontimes.com/news/2011/mar/27/us-helps-clear-vital-japan-harbor> (as of June 4, 2012)

- March 12–15, USNS Safeguard transited to Yokosuka NB.
- March 16–21, ship was in port at Yokosuka NB.
- March 21–April 9, ship was at sea in direct support of OT; visited port of Hachinohe on March 25 and ports of Miyako and Oshima during March 29–April 6 to clear wreckage.
- April 10–15, ship was in port at Yokosuka NB.
- April 16–May 11, ship was operating greater than 200 nmi from FDNPS.

This page intentionally left blank.

Appendix C.

Aircraft Information

C-1. Introduction

This section contains flight information for all flights conducted by the Department of Defense (DOD) aircraft whose operations were based onboard U.S. Navy (USN) and MSC vessels. These flights included fixed and rotary wing operations conducted by U.S. Navy assets.

Although there were many flights in direct support of Operation Tomodachi, the only missions that would have resulted in radiation exposure from FDNPS releases were accounted for in this report. Specifically, only aircraft that operated from ships included in this report are addressed in this appendix.

C-2. Aircraft History

C-2.1. Helicopter Anti-Submarine Squadron Light Five One (HSL-51)

HSL-51 deployed six aircraft to four Naval ships in support of OT, including two SH-60F helicopters onboard USS Blue Ridge, two SH-60B helicopters onboard USS McCampbell, one SH-60B helicopter onboard USS Cowpens and one SH-60B helicopter onboard USS Mustin.

C-2.2. Helicopter Sea Combat Squadron Two Three (HSC-23)

HSC-23 DET 3 deployed two aircraft onboard USNS Bridge.

C-2.3. Helicopter Sea Combat Squadron Two Five (HSC-25)

HSC-25 DET 6 deployed two aircraft onboard USNS Bridge.









C-2.4. Helicopter Sea Combat Squadron Four Three (HSC-43)

HSC-43 deployed four aircraft to two Naval ships in support of OT. Two SH-60B helicopters from HSC-43 Detachment 5 were deployed onboard USS Chancellorsville and two SH-60B helicopters were deployed onboard USS Preble.

C-3. Carrier Air Wing Five (CVW-5)

Carrier Air Wing Five (CVW-5) was a USN aircraft carrier air wing based at Naval Air Facility (NAF) Atsugi, and attached to the aircraft carrier USS George Washington (USN, 2008). CVW-5 consisted of eight squadrons (Tailhook, 2005). Table C-1 lists all squadrons assigned to CVW-5 during OT.

Table C-1. List of CVW-5 Squadrons

Code	Insignia	Squadron	Nickname	Assigned Aircraft
VFA-27		Strike Fighter Squadron 27	Royal Maces	F/A-18E Super Hornet
VFA-102		Strike Fighter Squadron 102	Diamondbacks	F/A-18F Super Hornet
VFA-115		Strike Fighter Squadron 115	Eagles	F/A-18F Super Hornet
VFA-195		Strike Fighter Squadron 195	Dambusters	F/A-18C Hornet & F/A-18E Super Hornet
VAW-115		Carrier Airborne Early Warning Squadron 115	Liberty Bells	E-2C Hawkeye 2000
VAQ-141		Electronic Attack Squadron 141	Shadowhawks	EA-18G Growler
VRC-30		Fleet Logistics Support Squadron 30 Det. 5	Providers	C-2A Greyhound
HS-14		Helicopter Anti-submarine Squadron 14	Chargers	SH-60F Seahawk and HH-60H Seahawk

C-3.1. Strike Fighter Squadron Two Seven (VFA-27)

VFA-27, known as the "Royal Maces", was a USN strike fighter squadron stationed at NAF, Atsugi. They were a part of Carrier Air Wing 5 and were attached to the USS George Washington. Their tail code is NF. VFA-27 deployed 13 F/A-18E Super Hornets in support of OT.

C-3.2. Strike Fighter Squadron One Zero Two (VFA-102)

VFA-102, known as "Diamondbacks" was a USN Strike Fighter squadron based at NAF, Atsugi. Their tail code is "NF," and they fly the F/A-18F Super Hornet aircraft. The squadron deployed 13 F/A-18F Super Hornets in support of OT.

C-3.3. Strike Fighter Squadron One One Five (VFA-115)

VFA-115, also known as the "Eagles", was a USN strike fighter squadron stationed at NAF, Atsugi. Their tail code is NF. VFA-115 deployed 11 F/A-18F Super Hornets in support of OT.

C-3.4. Strike Fighter Squadron One Nine Five (VFA-195)

VFA-195, also known as the "Dambusters", was a USN strike fighter squadron stationed at NAF, Atsugi. They were part of Carrier Air Wing Five (CVW-5) and their tail code is NF. VFA-195 deployed one F/A-18C Hornet and 11 F/A-18E Super Hornets in support of OT.

C-3.5. Carrier Airborne Early Warning Squadron One One Five (VAW-115)

VAW-115, also known as the "Liberty Bells", was a USN early warning squadron based at NAF, Atsugi that flew the E-2C Hawkeye 2000. The "Liberty Bells" were the Navy's only forward deployed Airborne Early Warning squadron and are the oldest and original squadron in CVW-5. VAW-115 deployed four E-2C Hawkeyes in support of OT.

C-3.6. Electronic Attack Squadron One Four One (VAQ-141)

VAQ-141, also known as the "Shadowhawks", was a USN electronic attack squadron that was based at NAF, Atsugi. VAQ-141 fell under the command of Commander Electronic Attack Wing Pacific (COMVAQWINGPAC) and flew in support of Carrier Air Wing 5 aboard the USS George Washington. VAQ-141 did not deploy any aircraft in support of OT.

C-3.7. Fleet Logistics Support Squadron Three Zero (VRC-30)

VRC-30, also known as the "Providers", was a USN fleet logistics support squadron based at NAF, North Island that consisted of five detachments. VRC-30 deployed two C-2A Greyhounds in support of OT.










C-3.8. Helicopter Anti-Submarine Squadron One Four (HS-14)

HS-14 was a USN helicopter squadron permanently forward-deployed on NAF, Atsugi and aboard the aircraft carrier USS George Washington. They currently fly the Sikorsky SH-60F and HH-60H models of the Seahawk helicopter and fly with the tail code NF. HS-14 deployed 12 rotary aircraft, which included nine SH-60F and three HH-60H helicopters in support of OT.

C-4. Carrier Air Wing Eleven (CVW-11)

CVW-11 was a USN aircraft carrier air wing based at Naval Air Station (NAS), Lemoore, California. The air wing was attached to the USS Nimitz (CVN 68). CVW-11 consisted of nine squadrons and deployed 52 aircraft from the four squadrons discussed in the following subsections in support of OT. Table C-2 lists all squadrons assigned to CVW-11 during OT.

Table C-2. List of CVW-11 Squadrons

Code	Insignia	Squadron	Nickname	Assigned Aircraft
HS-6		Helicopter Anti-submarine Squadron 6	Indians	SH-60F Seahawk and HH-60H Seahawk
HSM-75		Helicopter Maritime Strike Squadron 75	Wolfpack	MH-60R Seahawk
VAQ-142		Electronic Attack Squadron 142	Gray Wolves	EA-6B Prowler
VAW-117		Carrier Airborne Early Warning Squadron 117	The Wallbangers	E-2C Hawkeye
VFA-146		Strike Fighter Squadron 146	Blue Diamonds	F/A-18C/D Hornet
VFA-147		Strike Fighter Squadron 147	Argonauts	F/A-18E/F Super Hornet
VFA-154		Strike Fighter Squadron 154	Black Knights	F/A-18E/F Super Hornet
VMFA-323		Marine Fighter Attack Squadron 323	Death Rattlers	F/A-18C Hornet
VRC-30		Fleet Logistics Support Squadron 30, Detachment 3	Providers	C-2A Greyhound

C-4.1. Strike Fighter Squadron One Four Six (VFA-146)

VFA-146, also known as the "Blue Diamonds" was a USN operational fleet strike fighter squadron based at NAS, Lemoore, California. They flew the F/A-18C Hornet and were attached to CVW 11, deployed aboard USS Nimitz. Their tail code is NH. VFA-146 deployed 14 F/A-18C Hornets in support of OT.

C-4.2. Strike Fighter Squadron One Four Seven (VFA-147)

VFA-147, also known as the "Argonauts", is a USN strike fighter squadron based at NAS, Lemoore, California. VFA-147 flew the F/A-18E Super Hornet as part of CVW 11. Their tail code is NH. VFA-147 deployed 12 F/A-18E Super Hornets in support of OT.

C-4.3. Strike Fighter Squadron One Five Four (VFA-154)

VFA-154, also known as the "Black Knights", was a USN strike fighter squadron stationed at NAS Lemoore, California. The Black Knights were an operational fleet squadron flying the F/A-18F Super Hornet. They were attached to CVW 11 and deployed aboard the aircraft carrier USS Nimitz. This squadron deployed 13 F/A-18F Super Hornets in support of OT.

C-4.4. Marine Fighter Attack Squadron Three Two Three (VMFA-323)

VMFA-323 was a USMC Marine fighter attack squadron. The squadron was based at Marine Corps Air Station (MCAS) Miramar, California and fell under the command of Marine Aircraft Group 11 (MAG-11) and the 3rd Marine Aircraft Wing (3rd MAW) but deployed with CVW 11. VMFA-323 deployed 13 F/A-18C Hornets in support of OT.

C-5. Carrier Air Wing Fourteen (CVW-14)

CVW-14 was an aircraft carrier air wing based at NAS, Lemoore, California. The air wing was attached to the USS Ronald Reagan. CVW-14 consisted of eight squadrons and deployed 15 aircraft from the three squadrons discussed in the following subsections in support of OT. It should be noted that VMFA-323, VFA-154, VFA-147 and VFA-146 were attached to CVW-11 also. Deployments from these squadrons were accounted for in the previous section. Table C-3 lists all Squadrons that were assigned to CVW-14 during OT.

Table C-3. List of CVW-14 Squadrons

Code	Insignia	Squadron	Nickname	Assigned Aircraft
VRC-30		Fleet Logistics Support Squadron 30 Det. 1	Providers	C-2 Greyhound
VMFA-323		Marine Fighter Attack Squadron 323	Death Rattlers	F/A-18C(N) Hornet
VFA-154		Strike Fighter Squadron 154	Black Knights	F/A-18F Super Hornet
VFA-147		Strike Fighter Squadron 147	Argonauts	F/A-18E Super Hornet
VFA-146		Strike Fighter Squadron 146	Blue Diamonds	F/A-18C Hornet
VAW-113		Carrier Airborne Early Warning Squadron 113	Black Eagles	E-2C Hawkeye 2000 NP
VAQ-139		Carrier Tactical Electronic Warfare Squadron 139	Cougars	EA-6B Prowler
HS-4		Helicopter Anti-submarine Squadron 4	Black Knights	SH-60F/HH-60H Seahawk

C-5.1. Carrier Airborne Early Warning One One Three (VAW-113)

VAW-113, known as "Black Eagles", was a carrier airborne early warning squadron stationed at NAS, Point Mugu, at NB Ventura County. VAW-113 was attached to CVW-14 and deployed four E-2C Hawkeyes in support of OT.

C-5.2. Electronic Attack Squadron One Three Nine (VAQ-139)

VAQ-139, also known as the "Cougars", was a USN tactical electronic attack squadron. They specialized in electronic attack and were stationed at NAS, Whidbey Island, Washington. VAQ-139 deployed four E-2C Hawkeyes in support of OT.

C-5.3. Helicopter Sea Combat Squadron 4 (HSC-4)

HSC-4, also known as the "Black Knights", was a USN helicopter squadron established in 1952 as Helicopter Anti-Submarine Squadron 4 (HS-4). On March 29, 2012, HS-4 was re-commissioned as HSC-4. HSC-4 deployed a total of seven rotary aircraft, which included four SH-60F and three HH-60H helicopters in support of OT.

C-5.4. Aircraft Utilization in OT

See Table C-4 for specific aircraft that were utilized in support of OT.

Table C-4. List of U.S. Navy aircraft used for Operation Tomodachi

Command	Squadron/Air Wing/Ship	Type of Aircraft	BUNO
HSL-51	USS Blue Ridge	SH-60F	164081, 164446
	USS McCampbell	SH-60B	164814, 163240
	USS Cowpens	SH-60B	162985
	USS Mustin	SH-60B	163594
HSC-23 Det 3	USNS Bridge	MH-60S	166328, 165754
HSC-25 Det 6	USNS Bridge	MH-60S	167819, 167814
HSC-43	USS Chancellorsville	SH-60B	162987, 164117
	USS Preble	SH-60B	163905, 164461
CVW-5	VFA-27	FA-18E	165791, 165860, 165861, 165862, 165863, 165864, 165865, 165866, 165868, 165869, 165873, 165788, 165790
	VFA-102	FA-18F	166915, 166916, 166917, 166918, 166919, 166920, 166921, 166922, 16688, 166888, 166890, 166891, 166892
	VFA-115	FA-18F	166859, 166860, 166861, 166862, 166863, 166864, 166865, 166866, 166868, 166869, 166870
	VFA-195	FA-18C	164906
		FA-18E	166901, 166902, 166903, 166906, 166907, 166908, 166909, 166910, 166911, 166912, 166913
	VAW-115	E-2C	165817, 165826, 165827, 165828
	VRC-30	C-2A	162166, 162159
	HS-14	SH-60F	164078, 164080, 164101, 164447, 164459, 164460, 164617, 164797, 164798
		HH-60H	163786, 164841, 164842

Table C-4. List of U.S. Navy aircraft used for Operation Tomodachi (cont.)

Command	Squadron/Air Wing/Ship	Type of Aircraft	BUNO
CVW-11	VFA-146	FA-18C	163433, 163462, 163490, 163490, 163502, 163699, 163714, 163716, 163737, 163740, 163742, 163747, 163764, 163766
	VFA-147	FA-18E	166436, 166437, 166438, 166440, 166441, 166442, 166443, 166444, 166445, 166446, 166447, 166448
	VFA-154	FA-18F	165933, 166873, 166874, 166875, 166876, 166877, 166878, 166879, 166880, 166881, 166882, 166883, 166884
	VMFA-323	FA-18C	164698, 164709, 164722, 164724, 164727, 164730, 164733, 164734, 164736, 164873, 164875, 164956, 164975
CVW-14	VAW-113	E-2C	165821, 165822, 165823, 165504
	VAQ-139	E-2C	160434, 161245, 163047, 163887
	HSC-4	SH-60F	164071, 164083, 164084, 164457
		HH-60H	163793, 163798, 165118

Appendix D.

Potentially Exposed Population Assumptions

D-1. Introduction

This appendix contains a detailed discussion of the DARWG-recommended assumptions for the radiation dose assessments and the rationale for the factors selected for each potentially exposed population (PEP) Category listed in Table D-1.

Table D-1. PEP categories considered in this report

Category	Description
A	This PEP includes personnel assigned to shipboard duties who were onboard a ship included in this report anytime during March 12 to May 11, 2011. Personnel in this PEP performed general shipboard duties according to their military rating (e.g., medical duties, damage control, etc.). These duties do not include those associated with flight operations.
B	This PEP includes personnel who were assigned as part of a ship-based aircrew but did not perform any flight operations.
C	This PEP includes personnel assigned as part of a ship-based aircrew (operates from the ship instead of from a land-based air strip) who performed flight operations.

D-2. PEP Assumptions

D-2.1. Assumptions for PEP Category A

The assumptions for PEP Category A are discussed in the following sections. Because of the identical exposure and working conditions, these assumptions apply to PEP B also.

D-2.1.1 Criteria for Ship Contamination Surveys and Decontamination

Ships operating within 125 nmi of FDNPS from March 11–April 12, 2011 required contamination surveys and potential decontamination.

COMNAVSURFPAC established this radius to determine which ships would require radioactive contamination surveys. It was necessary to establish a cut-off point or boundary which would designate where radiological resources would be deployed to address potentially contaminated ships. The radius was established based on HPAC predictions and knowledge at the time of the extent of the spread of radioactive contamination from FDNPS. HPAC modeling and empirical survey data supported the 125 nmi radius.

D-2.1.2 Shipboard Exposure Scenario Characteristics

The assumed location and exposure period for shipboard individuals is topside for 24 hours per day, during the two-month time period.

This parameter was assumed to best account for individuals who routinely worked for long periods of time topside and more easily conformed to the HPAC integrated time-exposure models. For example, certain Sailors routinely worked up to 16 hours or more per day in support of flight operations on board some ships. The HPAC integrated dose model used input parameters and meteorological data to predict radioactive plume concentrations to which individuals could have been exposed. The assumptions that an individual worked topside during the entire two-month time period, under heavy exertion, with no time spent below decks (which would provide significant shielding from most contamination) were adopted as high-sided measures in calculating doses.

The above assumption about time spent outdoors was also applicable if an individual went ashore during times when the ship was in port. In addition, HPAC-generated doses were added to pro-rated shore-based doses reported in Cassata et al., (2012) for additional conservatism. Because this report applied to fleet-based individuals, which included only adults (aged 17 years and above) only adult shore-based doses were used.

All fleet-based individuals were exposed to the same radionuclides as those outlined in Cassata et al. (2012).

Although the methods to assess radiation dose with shore-based and fleet-based individuals was different, the same radiation/contamination source (FDNPS releases) applied to both this report and to Cassata et al. (2012). Therefore, the same radionuclides were used in the exposure scenarios for both the shore- and fleet-based individuals.

Large-scale cohort TLD dose assessment is not valid for shipboard doses.

Although a significant amount of shipboard TLD/EPD data were available for general bounding of assessed doses and provided empirical data to support computer modeling, the variability in type and location of shipboard duties was not conducive to cohort monitoring. For example, a Sailor who worked topside and wore dosimetry and may have been exposed to a radioactive cloud was not representative of an individual working below deck as a cook. Cohort monitoring was not easily accomplished even among individuals who worked topside because they had vastly different work hours and working conditions. In addition, the overall granularity of the empirical TLD/EPD data was not sufficient to separate dosimetry wearers into different groups due to the hectic operational tempo during HADR efforts.

Crews of small craft vessels did not experience significantly different radiation environments from those of the larger ships.

This assumption is reasonable because although small craft such as LCACs were much smaller than the larger ships, placing individuals much closer to the waterline, the same assumptions were still valid for both. The assumption that an individual on a small craft spent all his or her time topside was high-sided because many of these small craft do not have a large topside surface so assigned personnel rarely spend large amounts of time exposed to the elements in contrast to crew on a carrier or helicopter support-type ship with a large flight deck. Also, small craft operations were very limited in time and scope compared to those of the larger ships during OT.

Salvage operations did not create a significant, unique radiation exposure environment.

This was reasonable because the tsunami and resultant sinking of vessels occurred prior to the damage and subsequent release of radioactive material from FDNPS. Therefore, the wreckage had not been contaminated, so salvage operations could not have resulted in additional radiation exposure.

No significant exposure or dose was assumed from dust-producing activities.

Although shipboard individuals routinely performed grinding, chipping, and other activities as part of their duties, COMNAVSURFPAC orders to the fleet restricted these activities. They were either not allowed, or if determined to be operationally necessary, required individuals to wear dosimetry and take actions to minimize or prevent the spread of contamination (i.e., wearing protective clothing, not eating, drinking, or smoking during such activities, etc.). Therefore, methods to assess doses associated with these activities were not necessary.

No significant exposure or dose was assumed from potential spread of contamination from aircraft landing on or taking off from ships.

This assumption was reasonable because of the relatively low levels of contamination detected and the relatively infrequent detection of contamination after the initial major effluent releases. In addition, aircraft contamination detected included fixed contamination, which was not expected to transfer onto individuals or ship surfaces.

D-2.2. Assumptions for PEP Category B

The assumptions used were identical to those of PEP A, because this cohort lived and worked under the same general conditions as non-flight shipboard personnel.

D-2.3. Assumptions for PEP Category C

The specific assumptions for PEP Category C are discussed in the following sections.

Cohort TLD dose assessment was valid for aircrew individuals.

Cohort TLD methods were valid for this PEP because of the nature of the work environment of the aircrews. Individual aircrews spent time in a relatively small area, under relatively similar conditions for almost exactly the same amount of time per flight. Posted TLD data for an aircraft itself can greatly determine the overall dose during flight operations. In this case the representative area dose was comparable to that of the individuals who operate the aircraft.

Air intake systems on pressurized aircraft provide protection from inhaling radioactive, airborne particulate material because incoming air traverses at least one filter prior to entering the aircraft cabin. The filtering process significantly removes contaminants from the air, thereby reducing potential airborne concentrations inside the aircraft. In addition, unlike Sailors on the deck of a ship, the aircraft structure provided aircrews with some shielding from external radiation.

D-2.4. Decontamination

Dose assessment regarding decontamination efforts was not necessary.

Decontamination of ships, aircraft, and personnel was performed during OT. However, doses associated with decontamination were not assessed in this report because:

- Ship's countermeasure wash-down systems to include water spray over ship surfaces greatly reduced the possibility of re-suspension and inhalation or ingestion of radioactive material;
- Individuals performing decontamination procedures were generally required to wear dosimetry to monitor effective radiation dose, follow specific processes to minimize the spread of contamination, and perform internal monitoring (IM) to measure any uptake of radioactive material;
- Decontamination of systems which had relatively high levels of contamination, such as filters, pumps, etc., were not readily accessible to individuals and access often required explicit authorization and strict adherence to radiological procedures to monitor and minimize dose; and
- Assumptions used to calculate effective dose, which included topside exposure for the entire two-month period, more than accounts for any potential incidental exposure and subsequent dose from decontamination activities based on overall dosimetry and measured surface contamination results.

D-2.5. Consumables

No dose was associated with consumption of food, water, or soil while aboard ship.

This assumption was based on the detailed analysis presented in Cassata et al. (2012), which determined the potential dose from occasionally eating off base and consuming water was not significant compared to other exposure pathways. This assumption is considered to be valid because (1) most fleet personnel had even less access to local foodstuffs and potentially contaminated water sources, and (2) all of the food on the ships came from outside Japan. The ingestion and inhalation of re-suspended radioactive material in the soil was also analyzed in Cassata et al. 2012, and not found to be a significant exposure pathway. Again, most fleet individuals had even less access to the Japanese mainland, and the computer modeling accounts for inhalation/ingestion of radioactive material. Because Cassata et al. (2012) included children they had to account for potential dose from ingestion of soil; however, there are no children in the fleet or aircrew. Consequently, doses from ingesting soil or dust while aboard ship were not included in this report.

D-2.6. Source Term

The primary isotopes of concern are I-131, Te-132, Cs-134, and Cs-137.

The results of isotopic analyses in environmental media on land reported in Cassata et al. (2012), TEPCO data, and general knowledge of radiation release and transport following light water reactor accidents supported this assumption.

One-hundred percent of noble gases were assumed to be released from FDNPS but caused negligible dose to individuals.

Because they are chemically inert, noble gases did not react with other elements to form compounds that would cause them to deposit on ground or in water which could result in immersion or ground shine doses to PEP individuals. Noble gases remained airborne and consequently were widely dispersed. As such, the noble gases were negligible contributors to internal radiological dose.

Complete meltdowns of the FDNPS Units 1, 2, and 3 cores were assumed.

Based on reported temperatures inside the reactor pressure vessels and the amount of time core cooling was unavailable for each core, it was conservatively assumed that all three impacted reactor cores melted down.

The principal organ dose (thyroid) contributor is I-131.

This assumption was based on the radiological, chemical, and biological characteristics of I-131, largely because of its effective half-life²⁹, propensity for uptake into the thyroid, and relatively energetic radiation release upon decay.

²⁹ Defined as the time it takes for one-half of the isotope to be removed from the body due to both radiological decay and elimination due to sweating, urination, etc.

This page intentionally left blank.

Appendix E.

Internal Dose from Ingestion of Contamination by Hand-to-Mouth Transfer

E-1. Introduction

Radioactive contamination was detected on various surfaces of several ships that operated off the coast of Japan during Operation Tomodachi. Ship-based personnel performed surveys to determine the presence and level of removable contamination on ship surfaces using portable survey meters and swipes.

The concepts described in Weitz and McKenzie-Carter (2011) were used to determine the possible committed equivalent dose to the thyroid and the committed effective dose to ship personnel from the incidental ingestion of removable radioactive contamination that was transferred from the contaminated surfaces to the hand(s) and then to the mouth.

E-2. Formulation for Determining Doses from Hand-to-Mouth Transfer

Surface contamination was measured directly using a portable survey meter to measure the count rate above the surface (see Cassata et al. [2012] for descriptions of portable survey instruments used). Removable surface contamination was measured on swipes³⁰ and large-area wipes using a portable survey meter to measure the contamination removed from the surface, (Benevides, 2012). The results of the removable surface contamination measurements are typically reported as the count rate corrected for background, or corrected counts per minute (CCPM). The removable activity on a ship surface is calculated using Equations E-1 and E-2 based on Knoll (1989):

$$A = \frac{CR_{corr}}{Det_{Eff} Det_{Area} F_{Swipe} CF 60} \quad (E-1)$$

$$CR_{corr} = CR_{S+B} - CR_B \quad (E-2)$$

where:

- A = removable total activity per unit area on the ship surface (Bq cm⁻²)
- CR_{S+B} = measured count rate on contaminated surface or swipe/wipe (count min⁻¹ (cpm))
- CR_B = measured background count rate (cpm)
- CR_{Corr} = corrected count rate (CCPM)

³⁰ A swipe is a sample of surface contamination obtained by wiping a piece of material over an area of approximately 100 square centimeters.

Det_{Eff}	=	detector efficiency, i.e., number of counts measured by the detector per actual number of disintegrations (count disintegration ⁻¹)
Det_{Area}	=	effective area of the detector or assumed area swiped/wiped (cm ²)
F_{Swipe}	=	transfer factor of radioactive material from the contaminated surface to a swipe or LAW (unitless) (value of 1.0 for an instrument survey)
CF	=	unit conversion factor (1 disintegration second ⁻¹ Bq ⁻¹)
60	=	number of seconds in one minute (seconds min ⁻¹)

The internal dose for an exposure involving the transfer of removable radioactive contamination from surfaces to the hand and then from the hand to the mouth is calculated using Equation E-3 (Weitz and McKenzie-Carter, 2011):

$$D_i = A F_{SH} F_{HM} S_{Palm} DC_i \quad (E-3)$$

where:

D_i	=	committed effective dose or committed equivalent dose to an organ (<i>i</i>) from a specific isotope or known contaminant composition; (Sv)
F_{SH}	=	surface-to-hand transfer factor (unitless)
F_{HM}	=	hand-to-mouth transfer factor (unitless)
S_{Palm}	=	surface area of the palm (palmar surface) of the hand (cm ²)
DC_i	=	dose coefficient for a specific organ or for the effective dose the known isotope or contaminant (Sv Bq ⁻¹)

The measured corrected count rate that would correspond to a specific committed effective dose or committed equivalent dose to a specific organ was calculated by combining Equations E-1 and E-3 above and solving for the corrected count rate as shown in Equation E-4.

$$CR_{corr_i} = \frac{D_i Det_{Eff} Det_{Area} F_{Swipe} 60}{F_{SH} F_{HM} S_{Palm} DC_i} \quad (E-4)$$

where:

CR_{corr_i}	=	Corrected count rate resulting in a dose to organ <i>i</i> from ingestion for the known isotope or contaminant (CCPM)
---------------	---	---

E-3. Parameters for Operation Tomodachi

For this analysis, the portable survey meter was assumed to be a Thermo Scientific HP-210 probe (also known as a DT-304 probe) with an IM-265/PDR Multi-Function Control unit (Cassata et al., 2012). A linear fit of the beta efficiency of the HP-210 probe as a function of

maximum beta energy was made using manufacturer-provided data (Thermo Scientific, 2007), as shown in Figure E-1.

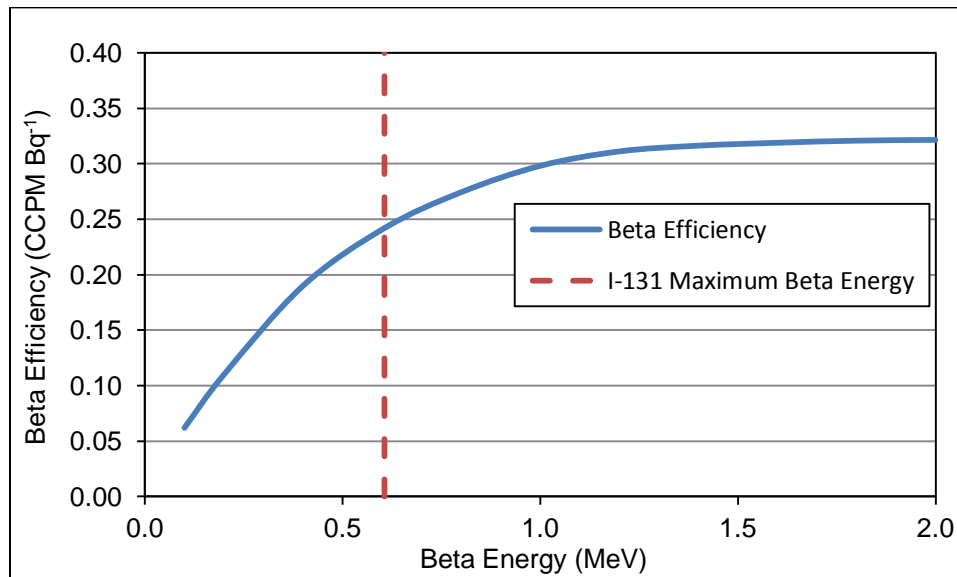


Figure E-1. Detection efficiency as a function of beta energy for an HP-210 probe

To accomplish this analysis, all of the detected activity was assumed to be from I-131. The efficiency for I-131's maximum beta energy (endpoint) of 0.606 MeV was used. The detector efficiency for swipes and LAWs was assumed to be the same as the beta efficiency of the HP-210 probe for I-131. The transfer from a contaminated surface to a swipe was assumed to be 0.3 (Floekher, 2013). The dose coefficients for ingestion used for this analysis were for adult members of the general population (ICRP, 2001). The palmar surface area used was for an adult male (Weitz and McKenzie-Carter, 2011). All calculations assumed that the transfer only occurred once for an individual and that both hands transferred radioactive contamination to the mouth. The parameter values used in this analysis are provided in Table E-1.

E-4. Results

The corrected counts per minute that would result in a committed equivalent dose to the thyroid of 10 μ Sv (1 mrem) are provided in Table E-2. The dose of 10 μ Sv (1 mrem) is the result from calculations for a hypothetical exposure scenario used only for discussion. The dose is approximately a factor of two lower than the lowest thyroid dose from internally-deposited radioactive materials in this report. The results represent the detectable radioactive contamination on a surface or a swipe/wipe or measured directly with a survey instrument.

In this example, the activity of the radioactive contamination transferred by hand to the mouth of an individual would be greater than the measured activity of a survey instrument or a swipe survey. This is because the area of the palmar surfaces of the hands modified by F_{SH} and F_{HM} (63 cm²) is greater than the surface area of the survey probe or a swipe modified by F_{Swipe} and Det_{Eff} (3.7 cm² and 7.2 cm², respectively). A LAW could contain more removable activity than an individual would incidentally ingest from hand-to-mouth transfer.

Table E-1. Parameter values used for example calculation of incidental ingestion of surface contamination

Parameter	Variable	Parameter Value
Committed equivalent dose to the thyroid from ingestion of I-131 (μSv)	D_i	10
Effective detector area or area swiped (cm^2)	Det_{Area}	15.5 for HP-210 100 for swipe 10,000 for LAW
Detector efficiency for HP-210 probe for I-131 maximum beta energy ($\text{count disintegration}^{-1}$)	Det_{Eff}	0.24
Transfer factor for surface to hand (unitless)	F_{SH}	0.3
Transfer factor for hand to mouth (unitless)	F_{HM}	0.5
Transfer factor for swipe or large area wipe (unitless)	F_{Swipe}	0.3 for swipe or LAW 1.0 for HP-210 probe
Area of the palmar surface of an adult male for both hands (cm^2)	S_{Palm}	420
Dose coefficient for iodine-131 (Sv Bq^{-1})	DC_i	4.3×10^{-7} (thyroid)

Table E-2. Count rate corresponding to a 10 μSv (1 mrem) dose to the thyroid from incidental ingestion of surface contamination

Type of Measurement	CCPM
HP-210 (surface)	83
Swipe (removable)	160
Large Area Wipe (removable)	16,000

Appendix F.

Dose from Skin Contamination

During OT, there were identified instances where skin contamination was detected on fleet-based individuals (highest reading was 4,000 CCPM). In all cases, the contamination was easily removed with soap and water. In addition, the relative amount of radioactivity detected was low, and length of time the skin was directly exposed was short. These factors supported the belief that skin doses were far below those associated with any health effects of the skin. However, a conservative assessment of skin dose was conducted to estimate the potential quantitative effect. The dose to live skin is measured at a depth of 7 milligrams (mg) per square centimeter (cm^2); at $1,000 \text{ mg cm}^{-3}$ density of skin, the quotient of depth and density results in a distance of 0.007 cm from the radioactive material (contamination) to the top layer of live skin.

Skin dose from direct skin contamination is primarily based on the time integral of the emitted beta particles associated with the isotopic activity in the contamination. Equation F-1, with input from empirical instrument skin survey data, provides a method for calculating skin dose (Delacroix et al., 2002):

$$H_{T(\text{skin})} = \frac{C_{\text{skin}} \cdot CF_{\text{Beta-skin}} \cdot t}{SF_{\text{Beta}}} \quad (\text{F-1})$$

where:

$H_{T(\text{skin})}$	=	equivalent dose to the skin (μSv);
C_{skin}	=	highest surface concentration of radionuclide on skin or clothing (Bq cm^{-2}); calculated by dividing the net counts per minute by the efficiency (counts/disintegrations), conversion from minutes to seconds, and area of the probe (15 cm^2);
$CF_{\text{Beta-skin}}$	=	conversion factor: beta dose rate to skin per unit activity density [$(\mu\text{Gy h}^{-1})/(\text{Bq cm}^{-2})$];
SF_{Beta}	=	shielding factor for beta radiation (= 1 for direct skin exposure); and
T	=	time of exposure (h). (Delacroix et al., 2002).

Due to the assumed reactor source term (isotopes available for release from containment), time since release of isotopes, mode of decay, and distance from FDNPS to individuals with detectable skin contamination, the isotopes of primary concern with potential to produce skin dose were I-131, Te-132, Cs-134, and Cs-137.

Table F-1 lists the dose conversion factors, associated maximum beta energies, and measurement efficiencies for these isotopes (Delacroix et al., 2002).

Table F-1. Radionuclide dose conversion factors for skin contamination

Radionuclide	Half-life (d)	$CF_{Beta-skin}$ ($\mu\text{Sv h}^{-1}/\text{Bq cm}^{-2}$)	Maximum Beta Energy* (MeV)	Efficiency (c d ⁻¹) [†]
I-131	8.02	1.6	0.606	0.21
Te-132	3.2	0.78	0.215	0.06
Cs-134	754	1.4	0.658	0.22
Cs-137	10,950	1.6	0.511	0.19

* Maximum energy is associated with the beta energy of the highest yield.

† The term c d⁻¹ refers to counts per disintegration.

The highest detected count rate using a Geiger-Mueller (G-M)-type pancake probe (with an associated 15 cm² area probe) during decontamination efforts was 4,000 CCPM. This net count rate can be converted into activity (disintegrations per second) by dividing by efficiency (counts per disintegrations) for that isotope. Although Te-132 has a significantly lower detection efficiency in the G-M pancake probe than the other isotopes, it would result in the highest calculated activity per detection when divided by the smallest of the efficiency values. A conservative calculation to account for an acute contamination event was made assuming:

- All activity was from Te-132;
- All contamination was distributed uniformly on the skin;
- No significant reduction of activity from radiological decay (over 24 hours, the expected activity rate reduction from radiological decay of Te-132 was approximately 20 percent);
- No contamination was removed from natural skin shedding; and

The total skin dose was calculated as approximately 1.4 mSv (0.14 rem) as follows:

$$H_{T(\text{skin})} = \left(\frac{4,000 \text{ c}}{\text{m}} \right) \left(\frac{\text{m}}{60 \text{ s}} \right) \left(\frac{\text{decay}}{0.06 \text{ c}} \right) \left(\frac{\text{Bq} \cdot \text{s}}{\text{decay}} \right) \left(\frac{0.78 \mu\text{Sv} \cdot \text{cm}^2}{\text{Bq} \cdot \text{h}} \right) (24 \text{ h}) \left(\frac{1}{15 \text{ cm}^2} \right) = 1,387 \mu\text{Sv}$$

This skin dose is far less than that associated with any deterministic or stochastic health effects and is less than one percent of the U.S. annual occupational skin extremity dose limit of 50 rem (0.5 Sv).

Although highly unlikely because of the emphasis on quickly identifying and restricting access to contaminated areas, a conservative calculation to account for chronic contamination exposure was also made. These calculations applied different assumptions compared to the acute exposure scenario. For example, because the half-life of Te-132 is very much less than the two-month chronic exposure period, over time a significant amount of Te-132 activity would have been reduced via radiological decay. Therefore, under chronic conditions over the two-month period, a conservative assessment of skin dose must assume Cs-137 as the source of contamination, because of its longer half-life and similar detection efficiency and dose conversion factor compared to Cs-134 (the other relatively longer-lived radionuclide). Therefore, the conservative assumptions for a chronic skin exposure included:

- All activity was from Cs-137 (700 CCPM, the approximate average detected contamination level);
- Contamination remained on the skin for 12 hours per day; and
- The same skin site was similarly re-contaminated each day for the two-month period.

The total skin dose from a chronic exposure over the two-month time period was calculated to be approximately 4.7 mSv (0.47 rem) as follows:

$$\begin{aligned}
 H_{T(\text{skin})} &= (60 \text{ d}) \left(\frac{700 \text{ c}}{\text{m}} \right) \left(\frac{\text{m}}{60 \text{ s}} \right) \left(\frac{\text{decay}}{0.06 \text{ c}} \right) \left(\frac{\text{Bq} \cdot \text{s}}{\text{decay}} \right) \left(\frac{1,6 \text{ } \mu\text{Sv} \cdot \text{cm}^2}{\text{Bq} \cdot \text{h}} \right) \frac{(12 \text{ h})}{d} \left(\frac{1}{15 \text{ cm}^2} \right) \\
 &= 4,716 \text{ } \mu\text{Sv}
 \end{aligned}$$

This skin dose is far less than that associated with any deterministic or stochastic health effects and less than one percent of the U.S. annual occupational skin extremity dose limit of 0.5 Sv (50 rem). Therefore, skin dose from potential contamination was not considered a significant source of dose to fleet-based individuals.

This page intentionally left blank.

Appendix G.

Shipboard Water Analysis

G-1. Potable Water Analysis

Based on surveys of 25 water systems from nine different vessels using high-purity germanium (HPGe) detector gamma spectroscopy systems (NSWC, 2012d), the Naval Surface Warfare Center, Dahlgren, VA, recommended that controls to reduce the likelihood of potable water contamination be discontinued. Although much of the analysis was performed several weeks after the accident, a positive result was reported for only one sample, with 1.34×10^{-8} microcurie per milliliter ($\mu\text{Ci mL}^{-1}$) of Cs-134 measured. This result is significantly less than the Environmental Protection Agency (EPA) Maximum Contaminant Level (MCL) of about $1.0 \times 10^{-7} \mu\text{Ci mL}^{-1}$ established in EPA regulations to implement the Safe Drinking Water Act for community water systems in the United States (EPA, 1998). Although trace levels of shorter-lived isotopes (such as I-131) could have been present and decayed away prior to sample analysis, the absence of longer-lived radionuclides known to be part of the releases from the FDNPS strongly suggests that there were no significant levels of radionuclides in the potable water systems. The half-life of Cs-134 (2.065 years) is sufficiently long that it would not have decayed to undetectable levels from the time of release from FDNPS until the sample was collected and analyzed. Although the system concentrators (reverse osmosis membranes) were not surveyed, those components were kept under strict radiological controls, and no routine access was possible (NSWC, 2012d).

An HPGe detector provides reasonably sensitive radiation detection capabilities with much improved energy resolution compared to scintillation-type detectors, such as those with sodium iodide-based crystals. The HPGe detector improved ability to identify specific radionuclides and to quantify their activities with greater sensitivity. Figure G-1 displays an example of a gamma-ray spectrum of a potable water sample acquired under the following conditions:

- A sample count date of April 1, 2011;
- A sample count time of two hours; and
- Channel setting spectrum set at 1 to 4096 (0.6 keV to 2044 keV).

Review of the HPGe energy spectrum in Figure G-1 indicates:

- The energy range was sufficient to identify all relevant radionuclides present in the sample;
- No significant, discernible peaks (no contamination above background radiation);
- Low energy peaks (less than 50 keV) are present and are typical artifacts resulting from backscattering photons, characteristic x-rays from shielding materials, and electronic noise. These peaks are not indicative of radioactive contamination;

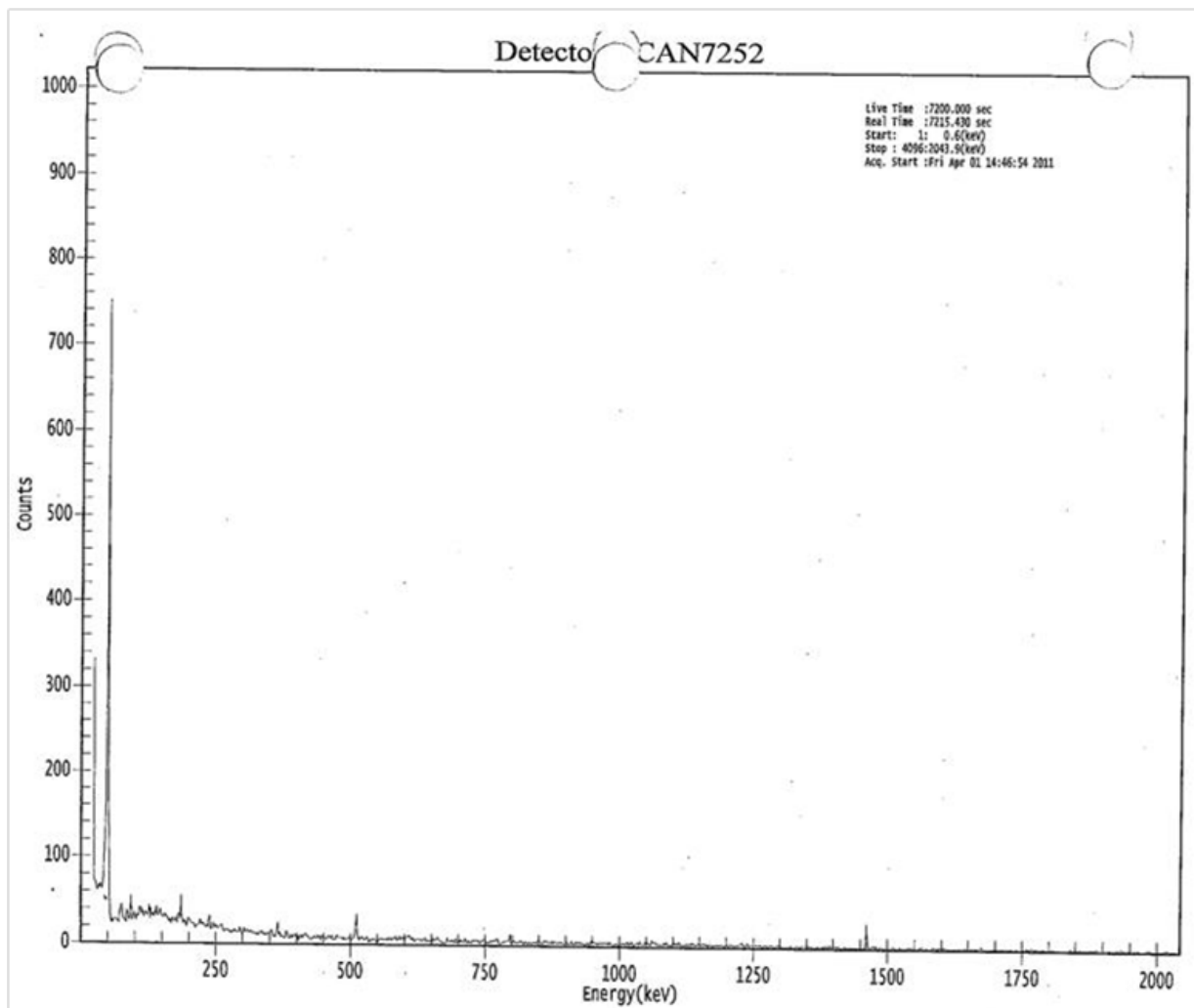


Figure G-1. Example of a potable water gamma ray energy spectrum

- The energy peak at approximately 510 keV is present and is a result of specific photon/electron interactions associated with the rest mass energy of the electron (511 keV). Identification of this peak is not indicative of radioactive contamination but demonstrates the counting system was working properly; and
- The energy peak at approximately 1,460 keV indicates the presence of naturally occurring K-40. In addition, the peak at about 190 keV is likely to originate in natural radium, which is normally present in building materials. The absence of any other spectral characteristics (such as obvious peaks associated with contamination in any significant amount) supports the assertion that no contamination is present in the sample.

Table G-1 (Cassata et al. 2012) provides additional measurement results for drinking water generated on ship and other water sources. These results further support the conclusion that individuals were not exposed to contaminated water.

Table G-1. Summary of U.S. Navy water analyses

Water Type	Sampling Dates (2011)	Number of Samples	Maximum Concentration (Bq kg ⁻¹)		
			I-131	Cs-134	Cs-137
Naval Ships (potable water)	Mar 29–Apr 24	46	3.0	<0.88	<0.93
Yokosuka NB (sea water)	Mar 27–Apr 24	41	2000	222	429
Yokosuka NB (fire pump water)	Mar 27–Mar 28	3	<0.84	<0.58	<0.67
Atsugi NAF (helicopter washdown)	Apr 9	2	29	7.3	8.2
Yokosuka NB (rain)	Mar 22–Apr 11	3	45	27	112
USS Ronald Reagan (sea water)*	Apr 15	6	0.56	0.59	0.69
Yokosuka NB (pure water)	Apr 21-23	5	0.50	29.5	0.68

*The source of this sea water was assumed to be a grab sample taken at the location of the USS Ronald Reagan at sea.

Although Table G-1 includes an I-131 result of 3.0 Bq kg⁻¹ for a sample of ship potable water, which is above the EPA MCL of 0.11 Bq kg⁻¹, this does not contradict the conclusion stated above because:

- The maximum result was for one sample among 46 samples with reported results that were lower concentrations that did not exceed the MCL;
- The MCL for I-131 is based on an annual dose limit to the thyroid organ of 4 mrem, which was scaled down from the 30 rem annual occupational limit to the thyroid from National Bureau of Standards Handbook 69. The Handbook followed the methodology of ICRP 2, which was produced in about 1959. Based on this model, an individual would have to drink 2 liters of water at the MCL concentration per day for 365 days to receive the 4 mrem thyroid dose;
- It was not possible for fleet-based individuals to have been exposed to this type of scenario because of the two-month exposure time period, fluctuating isotopic analysis results, and other factors; and
- The MCLs for Cs-134 and Cs-137 were not exceeded (approximately 5.0 and 7.4 Bq kg⁻¹) respectively.

It should be noted that the doses from application of ICRP 2 methodology may be more conservative than results obtained using more current radiation protection guidelines. For

example, the ICRP 2 model bases the Cs-134 and Cs-137 limits on the stochastic effects³¹ limit of 5 rem to the whole body. In contrast, the ICRP 2 thyroid organ limit was based on a deterministic effects³² limit, which was much more limiting compared to if the limit was applied to the whole body. If more appropriately derived from the total body, i.e., based on a stochastic limit, the MCL would be about 500-times higher. Nevertheless, the dose over an annual period of time is important because this is the basis for the EPA limit. These short-term, higher levels of I-131 observed in seawater become negligible on an annual basis.

G-2. MEXT Surveys of Water Activity Concentrations

MEXT conducted radiological surveys for water and air contamination at ten ocean locations northeast from the FDNPS to south-southeast of the FDNPS. Table G-2 lists the specific locations of each sampling point, and the map in Figure G-2 graphically illustrates the locations (MEXT, 2011). The samples were collected over several months from March 23, 2011, until June 29, 2011.

Table G-2. Location of MEXT ocean sampling points

Sampling Point	Latitude, Longitude
[1]	37° 39.3' N, 141° 24.0' E
[2]	37° 35.0' N, 141° 23.9' E
[3]	37° 30.2' N, 141° 23.9' E
[4]	37° 24.1' N, 141° 24.4' E
[5]	37° 16.1' N, 141° 23.8' E
[6]	37° 12.1' N, 141° 23.9' E
[7]	37° 05.7' N, 141° 24.0' E
[8]	36° 59.9' N, 141° 23.8' E
[9]	37° 00.0' N, 141° 24.0' E
[10]	37° 00.0' N, 141° 05.0' E

³¹ Health effects (e.g., cancer), which occur at random and for which the probability of occurrence is proportional to dose (Shleien, et al., 1998).

³² Health effects (e.g., cataracts), for which the severity of effect varies with dose and for which there is assumed to be a threshold. (Shleien, et al., 1998).

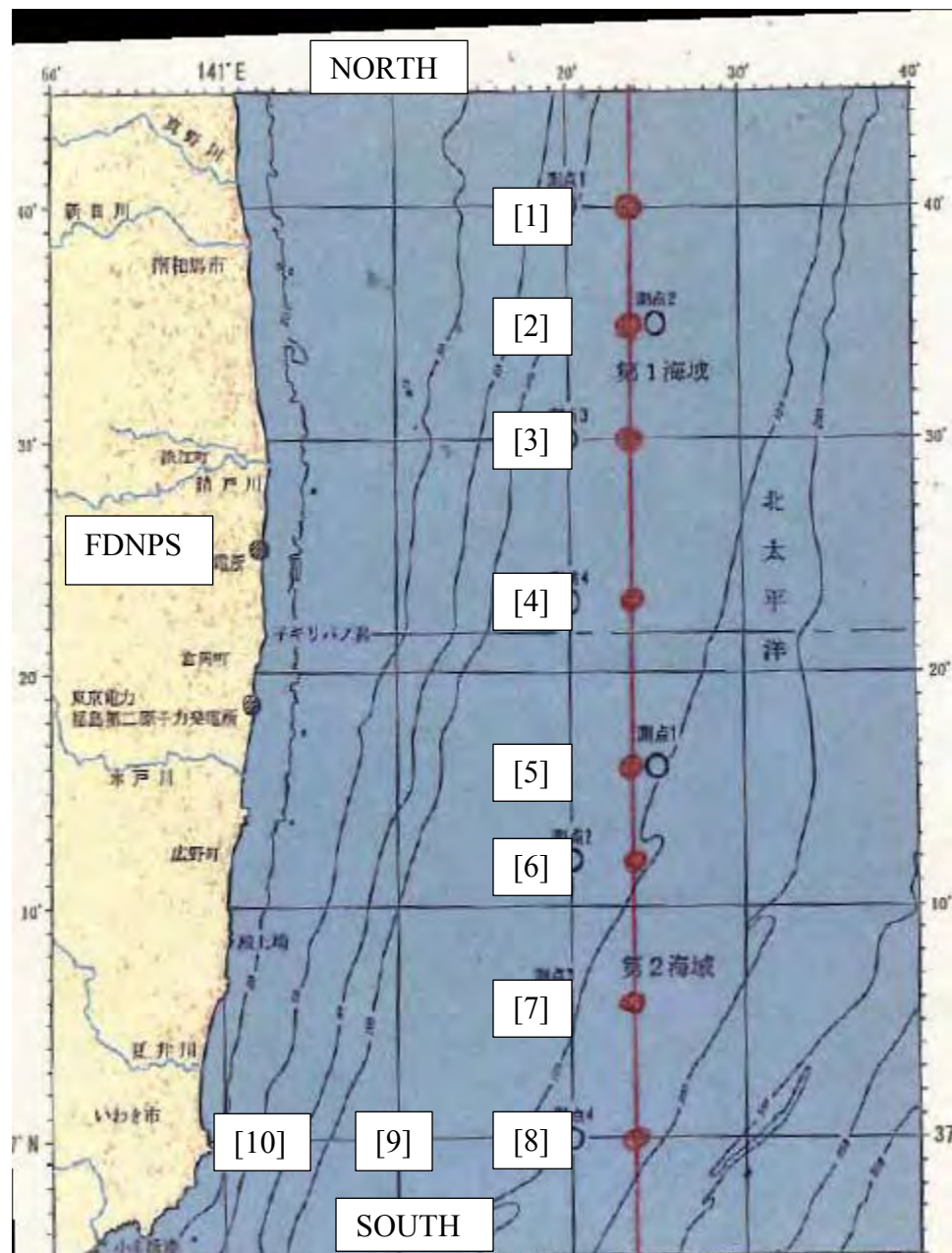


Figure G-2. Location of MEXT ocean sampling points

Table G-3 provides measured activity concentrations in sea water for the three predominant isotopes of concern, the type of sampling, and the corresponding sampling date and location (MEXT, 2011). All date/time entries are local time.

Table G-3. Sea water activity concentration

Sampling Date/Time (Japanese Standard Time) (2011)	Sampling Point*	Activity Concentration (Bq L ⁻¹)		
		I-131	Cs-134	Cs-137
March 23/0810	[3]	24.9	13.3	16.4
March 23/0900	[4]	30	10.7	11.2
March 23/0930	[5]	76.8	20.5	24.1
March 23/1015	[6]	37.3	15.4	18.2
March 23/1120	[7]	54.7	12.2	12.7
March 23/1200	[8]	42	11	12.8
March 23/1237	[1]	29	14.1	15.3
March 23/1332	[2]	39.4	14.5	15.2
March 24/0807	[3]	22.3	12.2	15.1
March 24/0909	[4]	16.9	7.4	8.3
March 24/1000	[5]	57.4	21.5 [†]	26.1 [†]
March 24/1100	[6]	59.1	14.6	16
March 24/1148	[7]	40.5	11.1	11.1
March 24/1235	[8]	36.2	15.4	16.9
March 24/1324	[1]	33.4	11.6	12.3
March 24/1418	[2]	37.5	12.8	13.4
March 25/0755	[3]	3.5	ND [‡]	ND [‡]
March 25/0842	[4]	3.3	0.74	0.7
March 25/0914	[5]	29	8.7	8.0
March 25/1000	[6]	30	5.4	5.9
March 25/1052	[7]	25	2.8	3.1
March 25/1117	[8]	18	2.0	2.6
March 25/1158	[1]	13	1.7	1.7
March 25/1232	[3]	12	2	2.7
March 26/0805	[1]	18.1	11.8	16.4
March 26/0912	[3]	15.3	1.74	ND [‡]
March 26/1030	[5]	14	15.9	5.90
March 26/1135	[7]	6.6	7.94	2.84
March 27/0815	[2]	5.4	1.3	1.5
March 27/0920	[4]	12	3.6	3.9
March 27/1030	[6]	15	2.8	2.3
March 27/1145	[8]	8.5	1.2	1.6
March 30/0748	[2]	3.3	ND [‡]	ND [‡]

* Seawater was collected at five different spots at location specified.

[†] Indicates highest value for that isotope.

[‡] ND means “not detectable”.

Table G-3. Sea water activity concentration (cont.)

Sampling Date/Time (Japanese Standard Time) (2011)	Sampling Point [*]	Activity Concentration (Bq L ⁻¹)		
		I-131	Cs-134	Cs-137
March 30/0924	[4]	ND [‡]	9.8	ND [‡]
March 30/1054	[6]	8.7	15.3	8.46
March 30/1248	[8]	2.58	ND [‡]	ND [‡]
March 30/1442	[10]	79.4 [†]	6.47	7.24
April 1/0807	[1]	11.0	1.88	4.06
April 1/0949	[3]	1.96	3.12	ND [‡]
April 1/1129	[5]	12.0	9.86	15.7
April 1/1314	[7]	8.17	3.66	11.7
April 1/1434	[9]	7.75	ND [‡]	2.03
April 3/0809	[2]	5.96	ND [‡]	ND [‡]
April 3/0940	[4]	11.6	ND [‡]	ND [‡]
April 3/1104	[6]	18.3	7.00	10.7
April 3/1253	[8]	5.55	3.80	1.16
April 3/1435	[10]	37.5	5.02	4.75
April 5/0948	[1]	ND [‡]	ND [‡]	ND [‡]
April 5/1100	[3]	10.9	ND [‡]	ND [‡]
April 5/1242	[5]	66.1	45.4	38.5
April 5/1400	[7]	ND [‡]	ND [‡]	ND [‡]
April 5/1518	[9]	ND [‡]	ND [‡]	ND [‡]

^{*} Seawater was collected at five different spots at location specified.

[†] Indicates highest value for that isotope.

[‡] ND means “not detectable”.

The results listed in Table G-3 support the conclusion that significant amounts of radioactive contamination, such as those associated with expected health effects, and which had the potential to enter shipboard systems, were not detected in the ocean. Also, any potential radioactivity uptake would have been reduced by the routine treatment using shipboard reverse osmosis or similar processes prior to general access to ship’s crew.

This page intentionally left blank.

Appendix H.

External and Internal Monitoring of Personnel

H-1. Dosimeter Data

Available dosimetry results were not directly used to calculate fleet doses because the monitoring periods typically started after the FDNPS accident or the sufficient numbers of dosimeters were not worn to provide representative cohort monitoring of ships' crew. The computer modeling results were compared with dosimeter results to assess whether the calculated doses were lower than any monitored individual's dose.

H-2. External Dosimetry

The DOD maintains nationally accredited dosimetry centers for processing personal dosimeters to accurately measure the radiation dose from external sources to a monitored individual.

- The USN and U.S. Air Force (USAF) used EPDs, which provided individual, accumulated, real-time radiation doses.
- The USN and USAF also provided TLDs, which were worn by an individual from a start to an end time (issue period) and subsequently collected for processing.
- The USA provided optically stimulated luminescent (OSL) dosimeters. The OSL-type dosimeters were issued and worn in the normal, passive device-mode and processed after the issue period because there was concern that contamination of OSL equipment could occur if the readers were taken into contaminated areas for dose checks.

The personal dosimeters (TLDs and OSLs) were authorized for issue during periods ranging from days to months based on operational circumstances. Categories of individuals issued dosimeters defined in USPACOM (2011a) included:

- Those individuals who entered warm and hot zones.
 - Warm Zone: Initially defined as the area between 25 and 125 nautical miles from FDNPS or an area in which general area radiation levels were between 0.1 and 10 mrem h⁻¹ (USFJ, 2011a); later revised to an area between 40 and 80 km from FDNPS or an area in which general area radiation levels were between 0.1 and 10 mrem h⁻¹ (USFJ, 2011b).
 - Hot Zone: Initially defined as the area within 25 nautical miles of FDNPS or an area in which general area radiation levels were in excess of 10 mrem h⁻¹ (USFJ, 2011a); later revised to an area within 40 km of FDNPS or an area in which general area radiation levels were in excess of 10 mrem h⁻¹ (USFJ, 2011b).
- Individuals who had significant potential to contact loose surface contamination (i.e., decontamination personnel).
- Individuals who were part of an aircrew that flew into an identified radioactive plume.

- Individuals likely to exceed a control level of 300 mrem, as predicted by exposure models and/or environmental measurements.”

Some individuals were assigned dosimetry based on occupational duties such as:

- Nuclear-trained personnel at Yokosuka Shipyard or on aircraft carriers.
- Medical personnel who routinely worked near radiation sources.
- Non-destructive inspection personnel that operated portable radiography equipment.

Individuals could have been monitored with more than one dosimeter, especially EPD in response to OT HADR efforts. Some dosimeter issue periods exceeded the two-month OT time period, Nevertheless their results provided usable information. Although doses for the OT period could not be isolated for the total reported dose, any result of zero would indicate that no dose was received in performing OT-related HADR activities. Analyses of the issue periods and associated duties for individuals with non-zero TLD results determined whether it was likely that the non-zero result was from OT-related efforts. The results of dosimetry monitoring are summarized in Table H-1.

Table H-1. External individual monitoring data

Service	No. of Dosimeters	Unique Individuals	Number of Dosimeters per Dose Range (mrem)					
			0	1–25	26–50	51–100	101–500	>501
USN	1,870	1,720	1560	310	0	0	0	0

Table H-1 results indicate that over 90 percent of those monitored received doses of 0 mrem and less than 10 percent received external doses between 1 and 25 mrem. The highest monitored TLD result was 25 mrem; this is less than the final reported calculated effective dose of 34 mrem. The data in Table H-2 and Figure H-3 are detailed summaries of dosimetry results specific to USS Ronald Reagan. The EPD data from the USS Ronald Reagan are summarized in Table H-4 and Table H-5. The TLD and EPD results support the conclusion that reported doses are conservative because the vast majority of monitored dosimetry results were zero; while the few readings above zero range from less than 1 to 21 mrem (these dose readings are consistent with the reported fleet external doses for this report). In addition, the TLD readings with reported doses greater than 0 rem include issue periods that began prior to the FDNPS accident and are almost certainly occupational doses (i.e., medical, industrial, etc.). This is supported by the fact that EPD readings were either zero or less than 1 mrem. For the U.S. Navy, the official occupational dose of record is provided by TLDs rather than EPDs, which are typically used as a secondary monitoring device so that exposures can be tracked in real time.

Table H-2. Summary of TLD results (USS Ronald Reagan)

Unit*	TLD Dates† (2011)	Number of TLDs			Collective Dose (mrem)	Non-Zero Doses (mrem)		
		Total	=0 mrem	>0 mrem		min	max	ave.
Vent Team‡	18Jan–25Apr	1	1	0	0	-	-	-
	5Feb–25Apr	1	1	0	0	-	-	-
	28/31Mar–27Apr	9	9	0	0	-	-	-
	7Apr–25Apr	1	1	0	0	-	-	-
	26Apr–7-22May	3	3	0	0	-	-	-
	26Apr–6-10Jun	3	3	0	0	-	-	-
	26Apr–16-22Jul	4	4	0	0	-	-	-
	All periods	22	22	0	0	-	-	-
CT‡	17Jan–26Apr	16	16	0	0	-	-	-
	5-15Feb–26Apr	7	7	0	0	-	-	-
	1-28Mar–26Apr	4	4	0	0	-	-	-
	7-11Apr–6May	28	28	0	0	-	-	-
	25Apr–5Sep	36	36	0	0	-	-	-
	All periods	91	91	0	0	-	-	-
Vent Team and CT‡	17Jan–26Apr	17	17	0	0	-	-	-
	5-15Feb–25Apr	7	7	0	0	-	-	-
	1-31Mar–27Apr	13	13	0	0	-	-	-
	7/11Apr–26Apr	27	27	0	0	-	-	-
	11Apr–6May	1	1	0	0	-	-	-
	25Apr–19/22Jun	2	2	0	0	-	-	-
	25Apr–21/28Jul	2	2	0	0	-	-	-
	All periods	69	69	0	0	-	-	-
ELT§, RHT††, RHO‡‡	17Jan–25Apr**	22	6	16	136	3	21	8.5
	26Jan–13Apr	1	0	1	3	3	3	3
	23Feb–13Apr	2	0	2	13	4	9	6.5
	7/12Mar–25Apr	3	3	0	0	-	-	-
	13Apr–25Apr	2	2	0	0	-	-	-
	13/18Apr–26Apr	2	2	0	0	-	-	-
	All periods	32	13	19	152	3	21	8.0
HS-4§§	15Mar–25Apr	118	110	8	25	3	4	3.1
	26Apr–29Jun	124	121	3	9	3	3	3.0
	6/17May–29Jun	4	4	0	0	-	-	-
	All periods	246	235	11	34	3	4	3.1
All units/All Periods***		539	497	42	244	3	21	5.8

* Military personnel only (three readings of 0 mrem for civilian personnel are not included).

† Single dates are approximate (typically ± 1 day); examples of other date listings: “6/17May” indicates start or end date is either 6May or 17May; “5-15Feb” indicates several start or end dates with range from 5Feb to 15Feb.

‡ Vent Team: Contamination Technician (CT) who performed surveys, cleaning, and replacement of filters throughout the ventilation system and who also performed decontamination duties.

§ ELT: Engineering Laboratory Technician; radiation workers who wear a TLD as part of their duties.

** Doses greater than zero, for this cohort who are considered radiation workers (exposed to radiation as part of their primary duties), correspond to a TLD issue period starting well before FDNPS releases and was most likely occupational in nature.

†† RHT: Radiation Health Technician; an individual specifically trained to assist the Radiation Health Officer.

‡‡ RHO: Radiation Health Officer; an individual specifically trained in health physics.

§§ Four HS-4 TLD readings were excluded from this summary because there was no name associated with the readings.

*** Values listed for All Units exclude duplicate TLDs.

Table H-3. USS Ronald Reagan TLD results grouped by dates with duplicates removed

Unit	TLD Dates* (2011)	Number of TLDs			Collective Dose (mrem)	Non-Zero Readings (mrem)		
		Total	=0 mrem	>0 mrem		min	max	ave
CVN-76 [†]	17Jan–25Apr	17	17	0	0	-	-	-
	5–15Feb–25Apr	7	7	0	0	-	-	-
	1–31Mar–26Apr	13	13	0	0	-	-	-
	7–11Apr–26Apr	28	28	0	0	-	-	-
	26Apr to 7–27May	5	5	0	0	-	-	-
	25Apr–5Sep	40	40	0	0	-	-	-
	All periods	110	110	0	0	-	-	-

*Includes TLDs for Vent Team, CT, Vent Team and CT, and USS Ronald Reagan.

Table H-4. Summary of issued EPD results from USS Ronald Reagan

EPD Statistics	Number
Total number of EPD entries	642
Entries with Date	642
Entries with EPD#	642
Entries with an Associated Name	438
Entries with an EPD Serial Number	208
Entries with a Flight Time	276
Blank entries	70
Entries marked “N/A”	2
Entries with 0 mrem	340
Total number of EPDs with dose > 0	230

Table H-5. Summary of EPD readings from USS Ronald Reagan

Range of EPD Readings (mrem):	
>0.0 – 0.1	168
0.1 – 0.2	34
0.2 – 0.3	20
0.3 – 0.4	1
0.4 – 0.5	1
0.5 – 0.6	3
0.6 – 0.7	1
0.7 – 0.8	1
0.8 – 0.9	0
0.9 – 1.0	1

H-3. Other Individual Dosimetry Data

Of the approximately 120 TLDs that DOE issued to its personnel, including those that supported the Aerial Monitoring System missions conducted throughout the OT time period, all received doses less than the Lower Limit of Detection (LLD) of 15 mrem. However, the dosimetry information was not directly comparable to DOD dosimetry results because the majority of TLDs issued to DOE personnel were for monitoring periods of three weeks or less. In contrast, the dosimeters issued to many DOD personnel were for periods exceeding three weeks, thereby providing an opportunity for total dose to exceed 15 mrem.

Although the dosimetry data were useful in monitoring radiation exposure associated with HADR efforts, many of the dosimeters were not issued until several days after the initial effluent releases from FDNPS. Therefore, that portion of potential radiation exposure before dosimeter issue was not monitored. However, dosimetry was capable of monitoring exposure to contamination deposited on the ground and other surfaces and if the initial effluent releases were significant, the subsequent TLD or EPD readings would be expected to be significantly higher than those recorded above. Internal monitoring (IM) was also conducted to measure radioactive contamination internalized via inhalation or ingestion. In contrast to external dosimeters issued after effluent releases from FDNPS, internal monitoring was effective in assessing radiation dose received from internally-deposited radioactive materials from the beginning of the accident.

H-4. Internal Monitoring

Internal monitoring measurements were made to assess whether individuals had intakes of radioactive material released from the FDNPS. Two types of equipment were used for IM to assess effective dose and thyroid dose: (1) fixed scanners designed specifically for IM, and (2) portable instruments configured for IM.

The use of portable instruments allowed for a large number of personnel to be monitored and also allowed for monitoring on ships and at remote locations. The portable instruments were initially operated to quickly identify individuals with measurable intakes of radioactive material. Whenever operationally possible, individuals with positive results from the portable systems were sent for confirmatory monitoring with the fixed scanner systems, which used spectrometric analysis to identify internally deposited radionuclides. If obtaining a fixed scanner measurement was not operationally possible for these individuals, a second portable instrument measurement was performed to confirm the initial measurement. Specific details about the equipment specifications and set-up design are provided in Cassata et al. (2013).

A total of 8,378 IM measurements were made during three phases of the OT IM program (Cassata et al., 2013):

1. Continental United States (CONUS): Personnel working in Yokosuka NB between March 11 and April 11, 2011. A total of 946 individual measurements were made from March 16 through April 11, 2011, using fixed scanners located in San Diego, CA and Bremerton, WA.
2. Outside CONUS, Operational phase: From April 14 through August 10, 2011, 7,277 IM measurements were made on DOD-affiliated individuals in the following categories.
 - a. Active duty personnel operating within the Sendai area.

- b. Aviators (i.e. helicopter pilots and aircrews) who flew through known plumes.
 - c. Personnel supporting aviation operations and aircraft/ship decontamination.
 - d. Supporting ship crew (including nuclear trained personnel).
 - e. Supporting shore activity personnel.
 - f. Naval Nuclear Propulsion personnel.
 - g. Ten percent selected randomly from other groups.
 - h. Additionally, each service component was asked to provide lists of personnel who had a higher potential for internal exposure who were then internally monitored.
3. Outside CONUS, Open Availability phase: From July 26 through August 31, 2011, IM was conducted on a voluntary basis for Service members, civilian employees, contractors, and family members, including infants and children. One hundred fifty-five (155) IM measurements were made on 97 family members (51 children and 46 adults), 38 DOD civilian employees/contractors, and 20 Service members. All results for this phase were below the minimum detectable activity (MDA).

A summary of IM results is shown in Table H-6. All IM results support the conclusion that no DOD-affiliated individuals were exposed to radioactive material at levels associated with the potential for adverse health effects.

Table H-6. Summary of OT internal monitoring results

Category	Number of Measurements	Percent of Total
Measurements less than MDA	8,140	97.2
Measurements at MDA or greater	238	2.8
Total Measurements	8,378	100
Mean Committed Effective Dose (mrem)	4.2*	-
Highest Committed Effective Dose (mrem)	25	-

* Mean dose for 238 measurements equal to or greater than the MDA

The assumptions made for the IM program (such as particle size, inhalation class, and concentrations of radioactive nuclides in the air) and literature values used (such as dose coefficients from ICRP Report 71 and intake retention fractions from ICRP Report 68) are described in Cassata et al. (2013). Table H-7 provides a summary of the IM results for fleet individuals.

Table H-7. Fleet internal monitoring summary

Ship	Work Location	Number of People Monitored	Number of Doses > 0	Maximum Dose (mSv)		Average Dose (mSv)	
				Effective	Thyroid	Effective	Thyroid
USS George Washington (CVN 73)	CCSG 5	1	1	0.08	1.34	0.08	1.34
	COM CVW 5	1	0				
	CVN 73	533	26	0.06	0.90	0.03	0.46
	HS 14	213	1	0.03	0.44	0.03	0.44
	VAQ 136	2	0				
	VAW 115	22	0				
	VFA 102	9	0				
	VFA 115	9	0				
	VFA 195	7	0				
	VFA 27	6	1	0.04	0.60	0.04	0.60
	VRC 30 DET 5	49	0				
	Ship Total	852	29	0.08	1.34		
USS Ronald Reagan (CVN 76)	CCSG 7	1	0				
	COM CVW 14	3	0				
	CVN 76	664	30	0.25	4.03	0.04	0.61
	HS 4	115	1	0.03	0.49	0.03	0.49
	VAQ 139	134	7	0.03	0.56	0.03	0.48
	VAW 113	109	1	0.03	0.53	0.03	0.53
	VFA 146	100	4	0.03	0.52	0.03	0.47
	VFA 147	112	0				
	VFA 154	122	0				
	Ship Total	1360	43	0.25	4.03		

Table H-7. Fleet internal monitoring summary (cont.)

Ship	Work Location	Number of People Monitored	Number of Doses > 0 mSv	Maximum Dose (mSv)		Average Dose (mSv)	
				Effective	Thyroid	Effective	Thyroid
USS Blue Ridge (LCC 19)	LCC 19	100	0				
	COMDESRON 15	40	0				
	COMSEVENTHFLT	36	0				
	Ship Total	176	0				
USS Chancellorsville (CG 62)	CG 62	29	0				
USS Cowpens (CG 63)	CG 63	168	0				
USS Shiloh (CG 67)	CG 67	42	0				
USS Curtis Wilbur (DDG 54)	DDG 54	33	0				
USS John S. McCain (DDG 56)	DDG 56	32	0				
USS Fitzgerald (DDG 62)	DDG 62	228	0				
USS Stethem (DDG63)	DDG 63	29	0				
USS Lassen (DDG 82)	DDG 82	37	0				
USS McCampbell (DDG 85)	DDG 85	33	0				
USS Preble (DDG 88)	DDG 88	24	0				
USS Mustin (DDG 89)	DDG 89	33	0				
USS Essex (LHD 2)	LHD 2	731	1	0.03	0.42	0.03	0.42
USS Germantown (LSD 42)	LSD 42	5	0				
USS Tortuga (LSD 46)	LSD 46	175	1	0.02	0.40	0.02	0.40
USS Harpers Ferry (LSD 49)	LSD 49	26	0				
	All Ships	4013	74	0.25	4.03		
HSL 51 LAMPS (Assigned to Misawa AB)	HSL 51 LAMPS	174	2			0.11	1.84
	Total	4187	76	0.25	4.03		

The average effective dose was 0.03 mSv (0.003 rem) and the average thyroid dose was 0.57 mSv (0.057 rem) for doses greater than zero.

- No IM results are available for seven USNS ships (Richard E Byrd, Carl Brashear, Matthew Perry, Pecos, Rappahannock, Bridge, and Safeguard).

H-5. USS Ronald Reagan Air Monitoring Data

Data obtained from the USS Ronald Reagan air monitoring were used in the calibration of HPAC models. This ship (and assigned aircraft) was one of the first to encounter the FDNPS effluent releases based on survey results, ship location data, and personal accounts.

Table H-8 provides a copy of available environmental monitoring data and location information (latitude and longitude) from the USS Ronald Reagan for the time period March 12–16, 2011. The monitoring included sampling of airborne aerosols with portable air samplers (PAS) and air particle detectors (APDs).). U.S. Navy PAS units include the HD-732 model powered by 115 volts AC, and the HD-1150 and HD-1151 models that are battery powered (DTRA, 2005). The U.S. Navy fixed APD located on nuclear powered ships, is the IM-239, powered by 115 volts AC (DTRA, 2005).

PAS filters were analyzed with portable pancake G-M detectors. A typical air sample result on the ship would be less than $1 \times 10^{-9} \mu\text{Ci mL}^{-1}$. In addition, assessment of surface-borne contamination was made with a portable pancake G-M detector/meter combination. Because measurements were made without precise knowledge of the isotopic mixture of the radioactive material collected on air sample filters or that adhered to the surfaces being assessed, the measurements were semi-quantitative in nature and provide a general sense of the magnitude of radioactive material in air and on surfaces. Table H-9 provides a list of the locations associated with the PAS and APD sample results. Note: in Table H-8, the term “sec” means secured, or not in use. The wind coordinates are displayed as direction associated with the 360 degrees in a full circle (0 degrees equals north), and speed, recorded in knots. The units for all activity values is $\mu\text{Ci mL}^{-1}$ unless otherwise listed.

Table H-8. USS Ronald Reagan air monitoring results

Radiation Monitoring

March 12, 2011										
Time	APD 1-1	APD 1-2	APD 1-3	APD 1-4	APD 2-1	APD 2-2	APD 2-3	APD 2-4	Flight Deck PAS	
0:00	3.8x10-11	sec	6.0x10-11	1.2x10-10	2.8x10-11	8.5x10-11	8.6x10-11	sec	1900	<5x10-10
0:00	3.7x10-11	sec	6.2x10-11	1.2x10-10	3.1x10-11	8.7x10-11	7.9x10-11	sec	2130	<5x10-10

March 13, 2011										
Time	APD 1-1	APD1-2	APD 1-3	APD 1-4	APD 2-1	APD 2-2	APD 2-3	APD 2-4	Flight Deck PAS	
2400	3.3x10-11	sec		1.1x10-1	2.8x10-11	9.6x10-11	6.7x10-11	sec	2330	<5x10-10
0100	3.1x10-11	sec	5.6x10-11	9.4x10-11	2.7x10-11	8.0x10-11	6.8x10-11	sec	1300	<5x10-10
0100	3.0x10-11	sec	4.7x10-11	9.3x10-11	2.5x10-11	7.6x10-11	6.3x10-11	sec	1150	<5x10-10
0200	3.0x10-11	sec	5.0x10-11	9.6x10-11	2.5x10-11	7.4x10-11	6.6x10-11	sec	2000	<5x10-10
0300	3.4x10-11	sec	5.3x10-11	9.9x10-11	2.6x10-11	7.8x10-11	6.7x10-11	sec	0300	<5x10-10
0400	3.3x10-11	sec	5.4x10-11	1.0x10-10	2.5x10-11	7.6x10-11	6.7x10-11	sec	0350	<5x10-10
0500	3.4x10-11	sec	5.5x10-11	1.0x10-10	2.4x10-11	8.2x10-11	7.1x10-11	sec	0445	<5x10-10
0600	3.3x10-11	sec	5.2x 10-11	1.0x10-10	2.5x10-11	8.3x10-11	7.1x10-11	sec	0520	<5x10-10
0700	3.2x10-11	sec	5.5x10-11	9.7x10-11	2.5x10-11	7.6x10-11	6.9x10-11	sec	0600	<5x10-10
0800	3.3x10-11	sec	5.5x10-11	9.9x10-11	2.5x10-11	7. 5x10-11	6.6x10-11	sec	0800	<5x10-10
0900	3.4x10-11	sec	6.0x10-11	1.0x10-10	2.7x10-11	8.2x10-11	7.5x10-11	sec	1110	<5x10-10
1000	4.0x10-11	sec	7.0x10-11	1.2x10-10	3.0x10-11	8.7x10-11	9.1x10-11	sec		
1100	4.4x10-11	sec	4.5x10-11	1.3x10-10	3.3X10-11	9.3X10-11	9.2X10-11	sec		
1200	4.8X10-11	sec	2.7x10-11	1.5x10-10	3.6x10-11	8.9x10-11	9.2x10-11	sec		
1300	1.4x10-10	sec	2.5x10-10	6.7x10-10	1.3x10-10	2.5x10-10	5.5x10-10	sec	1300	7.5x10-9
1400	7.1x10-10	sec	1.1x10-9	2.7x10-9	4.9x10-10	7.2x10-10	1.6x10-9	sec	1430	3.0x10-9
1500	3.6x10-10	sec	5.5x10-10	1.1x10-9	3.2x10-10	5.2X-10	9.3X10-10	sec	1630	1.25x10-8
1600	1.1x10-10	sec	1.7x10-10	3.7x10-10	1.0x10-10	1.9x10-10	2.8x10-10	sec		
1700	1.1X10-9	sec	1.3x10-9	3.2x10-9	5.6x10-10	8.9x10-10	2.3x10-9	sec		
1800	1.5x10-9	sec	2.4-10-9	5.0x10-9	1.1x10-9	1.6x10-9	3.5x10-9	sec	1830	2x10-9
1900	1.1x10-9	sec	1.7x10-9	3.4x10-9	1.0x10-9	1. 3x10-9	3.4x10-9	sec		
2000	2.1x10-9	sec	3.3x10-9	7.2x10-9	1.3x10-9	1.8x10-9	4.2x10-9	sec	2130	1x10-8
2100	1.5x10-9	sec	1.9x10-9	4.1x10-9	2.1x10-9	1.7x10-10	3.2x10-9	sec		
2200	2. 3x10-10	sec	2.2x10-10	3.8x10-10	9.7x10-11	1.4x10-10	1.6x10-10	sec	2230	2.4x10-9
2300	1.0x10-10	sec	1.0x10-10	2.2x10-10	9.7x10-11	1.4x10-10	1.6x10-10	sec		
2400	7.8x10-11	sec	9.5x10-11	2.1x10-10	6.4x10-10	1.2x10-10	1.5x10-10	sec		

1630 APD 2-3 1x10-9

1638 APD 1-4 1x10-9

*1635 all friskers reading 1.2K CPM as background throughout ship

*1830 all fliskers reading 300 CPM as background throughout ship.

*1915 all fliskers reading 1.9K CPM as background throughout the ship

*0530 all fliskers reading 40-100 CPM as background throughout the ship

Table H-8. USS Ronald Reagan air monitoring results (cont.)

March 14, 2011																
Time	APD 1-1	APD 1-2	APD1-3	APD 1-4	APD 2-1	APD 2-2	APD 2-3	APD 2-4	Flight Deck PAS		Rad level (mrem h ⁻¹)	Bkgrd		Wind	Lat	Long
2400	7.8x10-11	sec	9.5x10-11	2.9x10-11	6.4x10-11	1.2x10-10	1.5x10-10	sec	Time	Reading						
0100	1.1x10-10	sec	1.5x10-10	3.0x10-10	7.6x10-11	1.5x10-10	2.1x10-10	sec								
0200	7.2x10-11	sec	9.9x10-11	2.1x10-10	5.8x10-11	1.2x10-10	1.4x10-10	sec	0200	5x10-10	0.01	200cpm		202 @ 31 Kts	40 12.9' N	143 25.6' E
0300	7.6x10-11	sec	1.0x10-10	2.3x10-10	5.6x10-11	1.1x10-10	1.4x10-10	sec	0240	<5x10-10	0.01	200cpm		197 @ 30	40 19.9' N	143 09.7' E
0400	7.1x10-11	sec	9.6x10-11	2.0x10-10	6.7x10-11	1.2x10-10	1.5x10-10	sec	0340	<5x10-10	0.01	200cpm		201 @ 25	40 26' N	143 05' E
0500	7.3x10-11	sec	9.5x10-11	1.8x10-10	5.9x10-11	1.2x10-10	1.4x10-10	sec	0515	<5x10-10	0.01	AftSS900cpm		196 @ 23	40 19.6' N	143 04' E
0600	5.6x10-11	sec	1.3x10-10	1.7x10-10	5.6x10-11	1.3x10-10	1.7x10-10	sec						197 @ 26	40 17.9' N	142 56.8' E
0700	9.5x10-11	sec	1.3x10-10	2.8x10-10	6.9x10-11	1.4x10-10	1.9x10-10	sec	0702	<5x10-10	Max: 2000 cpm on BOW; Ave.: 400cpm			193 @ 30	40 17.2' N	142 56.8' E
0800	9.5x10-11	sec	1.2x10-10	2.8x10-10	6.9x10-11	1.3x10-10	1.8x10-10	sec	0815	<5x10-10	0.01			194 @ 34	40 35N	142 39 E
0900	6.7x10-11	sec	9.8x10-11	1.4x10-10	5.9x10-11	1.2x10-10	1.4x10-10	sec	0930	<5x10-10				194 @ 34	40 35N	142 39 E
1000	6.5x10-11	sec	9.9x10-11	1.9x10-10	4.5x10-11	1.0x10-10	1.8x10-10	sec	1030	<5x10-10				200 @ 25	40 39 N	142 31 E
1100	6.5x10-11	sec	9.9x10-11	1.9x10-10	5.1x10-11	1.1x10-10	1.4x10-10	sec	1130	<5x10-10				204 @ 10	40 39 N	142 26 E
1200	6.9x10-11	sec	1.0x10-10	1.9x10-10	5.1x10-11	1.1x10-10	1.4x10-10	sec	1230	<5x10-10				255 @ 30	40 479 N	14217.110 E
1300	6.3x10-11	sec	8.2x10-11	1.7x10-10	5.0x10-11	1.0x10-10	3.1x10-10	sec	1330	<5x10-10				310 @ 17	40 39' N	142 10' E
1400	6.4x10-11	sec	9.2x10-11	1.8x10-10	4.7x10-11	1.0x10-10	1.2x10-10	sec	* shifted to 4hr PAS					278 @ 24	40 39.2 N	142 2.060' E
1500	7.3x10-11	sec	1.1x10-10	2.7x10-10	5.1x10-11	1.2x10-10	1.6x10-10	sec	* next PAS due 1730					280 @ 28	40 36.874 N	141 52 242 E
1600	7.6x10-11	sec	1.1x10-10	1.2x10-10	5.5x10-11	1.2x10-10	1.5x10-10	sec	1710	<5x10-10				280 @ 32	40 33.485 N	141 55. 327 E
1700	6.9x10-11	sec	1.0x10-10	2. 0x10-10	5.5x10-11	1.1x10-10	1.6x10-10	sec						300 @ 30	40 31.866 N	142 05.167 E
1800	9.2x10-10	sec	1.5x10-10	2.6x10-10	8.0x10-10	1.4x10-10	2.2x10-10	sec						310 @ 37	40 32.652 N	142 07.945 E
1900	9.6x10-11	sec	1.6x10-10	3.0x10-10	8.4x10-11	1.4x10-10	2.2x10-10	sec						310 @ 34	40 35.247 N	142 04.630 E
2000	9.6x10-11	sec	1.6x10-10	3.0x10-10	7.0x10-11	1.4x10-10	2.0x10-10	sec						305 @ 29	40 35.738 N	142 7.668 E
2100	8.3x10-11	sec	1.2x10-10	2.3x10-10	6.3x10-11	1.3x10-10	1.6x10-10	sec	2100	<5x10-10				310 @ 26	40 55N	142 23E
2200	6.9x10-11	sec	9.3x10-11	1.9x10-10	5.4x10-11	1.2x10-10	1.3x10-10	sec						331 @ 18	40 28.630 N	142 20.228 E
2300	6.1x10-11	sec	9.1x10-11	1.8x10-10	4.5x10-11	1.1x10-10	1.3x10-10	sec						340 @ 21.6	40 24.408 N	142 24.891 E

Table H-8. USS Ronald Reagan air monitoring results (cont.)

March 15, 2011																
Time	APD 1-1	APD 1-2	APD 1-3	APD 1-4	APD 2-1	APD 2-2	APD 2-3	APD 2-4	Flight Deck PAS					Wind	Lat	Long
2400	5.5x10-11	sec	8.7x10-11	1.7x10-10	4.3x10-11	1.0x10-10	1.3x10-10	sec	Time	Reading				334 @ 17.7	4016.578 N	142 27.125 E
0100	5.7x10-11	sec	8.8x10-11	1.8x10-11	4.4x10-11	9.7x10-11	1.2x10-10	sec	0100	<5x10-10				348 @ 18.8	4010.377 N	142 32.775 E
0200	6.1x10-11	sec	3.0x10-11	1.7x10-10	4.8x10-11	1.2x10-10	1.1x10-10	sec						323 @ 19	40 11.520 N	14238.151 E
0300	6.6x10-11	sec	8. 8x10-11	1.7x10-10	4.6x10-11	1.0x10-10	1.3x10-10	sec						346 @ 16.2	40 13.187 N	142 39.137 E
0400	6.9x10-11	sec	8.6x10-11	1.8x10-10	5.0x10-11	1.1x10-10	1.3x10-10	sec						346 @ 16.2	40 13.187 N	142 39.137 E
0500	6.7x10-11	sec	9.2x10-11	1.7x10-10	5.1x10-11	1.1x10-10	1.2x10-10	sec	0500	<5x10-10				346 @ 16.2	40 13.187 N	142 39.137 E
0600	6.5x10-11	sec	9. 6x10-11	1.6x10-10	4.9x10-11	1.1x10-10	1.2x10-10	sec						216 @ 11.7	40 08.490 N	142 33.631 E
0700	6.4x10-11	sec	8. 8x10-11	1.7x10-10	4.8x10-11	1.0x10-10	1.2x10-10	sec						15 @ 13	40 05.3 N	142.30E
0800	5.8x10-11	sec	8.1x10-11	1.7x10-10	4.6x10-11	1.0x10-10	1.2x10-10	sec						37 @ 8	40 8 N	142.28 E
0900	5.6x10-11	sec	8.3x10-11	1.7x10-10	4.0x10-11	1.1x10-10	1.1x10-10	sec	0900	<5x10-10				40 @ 7.5	4012.670	142 29.320
1000	6.2x10-11	sec	3.7x10-11	1.4x10-10	4.5x10-11	1.0x10-10	1.1x10-10	sec						050@ 6	40 12N	142 35E
1100	6.1x10-11	sec	9.1x10-11	1.7x10-10	4. 5x10-11	9.4x10-11	1.2x10-10	sec						060@ 6	39.58N	142 39E
1200	6.0x10-11	sec	8.7x10-11	1.8x10-10	4.8x10 -11	1.0x10-10	1.1x10-10	sec	1230	<5x10-10				049@ 4	39 47.362 N	142 43.325E
1300	5.6x10-11	sec	9.2x10-11	1.7x10-10	4.7x10-11	1.0x10-10	1.1x10-10	sec	1300					030@ 4 5	39.38N	142.41E
1400	5.5x10-11	sec	9.3x10-11	1.5x10-10	4.8x10-11	1.1x10-10	1.0x10-10	sec						014 @ 6	39.38N	142.43E
1500	4.7x10-11	sec	1.0x10-10	1.2x10-10	5.4x10-11	7.9x10-11	1.5x10-10	sec						060@ 5	40.3N	142.37E
1600	6.0x10-11	sec	8.7x10-11	1.8x10-10	4.5x10-11	1.0x10-10	1.1x10-10	sec	1600	<5x10-10				340 @ 6	40.6N	142.59E
1700	6.1x10-11	sec	8.7x10-11	1.7x10-10	4.7x10-11	1.0x10-10	1.1x10-10	sec						320@ 3	40 12.100N	143 2.300E
1800	5.9x10-11	sec	7.8x10-11	1.4x10-10	4.2x10-11	9.8x10-11	1.0x10-10	sec						302@ 1.9	40 12.788N	143 5.400E
1900	4.6x10-11	sec	7. 1x10-11	1.3x10-10	3.9x10-11	9.5x10-11	9.5x10-11	sec						060@ 5.2	40 13.122N	143 2. 300E
2000	4.2x10-11	sec	6.8x10-11	1.3x10-11	3.5x10-11	9.2x10-11	9.2x10-11	sec	2000	<5x10-10				119@7.9	40 13.882N	142 52.025E
2100	4.4x10-11	sec	6.7x10-11	1.4x10-10	3.5x10-11	9.7x10-11	1.0x10-10	sec						114@ 3.7	40 19.196N	142 49.723E
2200	5.2x10-11	sec	6.6x10-11	1.4x10-10	3.5x10-11	9.5x10-11	9.8x10-11	sec						117 @ 2.7	40 25.775N	142 48.046E
2300	4.3x10-11	sec	7.0x10-11	1.4x10-10	3.7x10-11	9.2x10-11	9.7x10-11	sec						330@ 4.9	40 25.06N	142 47.85E

Table H-8. USS Ronald Reagan air monitoring results (cont.)

March 16, 2011																
Time	APD 1-1	APD1-2	APD 1-3	APD 1-4	APD 2-1	APD 2-2	APD 2-3	APD 2-4	Flight Deck PAS		Continuous PAS		Wind	Lat	Long	
									Time	Reading	Time	Reading				
0:00	4.6x10-11	sec	7.0E-11	0.00	3.6x10-11	9.5x10-11	0.00	sec	2400	<5x10-10			046@ 6.6	40 18.802N	142 46.476E	
0100	4.6x10-11	sec	6.9E-11	0.00	3.4x10-11	8.9x10-11	0.00	sec			1915	<5x10-10	194 @5	40 13.472N	142 45.575E	
0200	4.6x10-11	sec	6.7E-11	1.30E-10	3.4x10-11	8.8x10-11	9.1E-11	sec			1936	<5x10-10	194@ 8	40 4.9N	142 43 09E	
0300	4.0x10-11	sec	6.4E-11	1.30E-10	3.2x10-11	8.7x10-11	8.5E-11	sec			1945	<5x10-10	035@ 9.6	39 56.0N	142 40.2E	
0400	4.1x10-11	sec	6.5E-11	1.20E-10	2.9x10-11	9.1x10-11	9.1E-11	sec	0400	<5x10-10	1955	<5x10-10	026 @ 18	39 49.8N	142 38.4E	
0500	3.9x10-11	sec	5.8E-11	1.20E-10	3.0x10-11	8.5x10-11	7.8E-11	sec			2007	<5x10-10	000 @ 15	3941N	142 35E	
0600	4.5x10-11	sec	5.8E-11	1.30E-10	3.2x10-11	8.8x10-11	8.3E-11	sec			2017	<5x10-10	003 @ 18	39 55N	142 56E	
0700	3.8x10-11	sec	5.8E-11	1.30E-10	3.0x10-11	9.0x10-11	7.8E-11	sec			2027	<5x10-10	010 @23	39 40N	142 51E	
0800	3.0x10-11	sec	8.7E-11	8.20E-11	3.0x10-11	8.7x10-11	8.2E-11	sec	0800	<5x10-10	2036	<5x10-10	060 @ 24	39 36N	142 48E	
0900	4.3x10-11	sec	5.3E-11	1.10E-11	3.1x10-11	8.5x10-11	8.2E-11	sec			2046	<5x10-10	060 @24	39 41N	142 49E	
1000	3.9x10-11	sec	5.4E-11	1.30E-10	3.0x10-11	8.8x10-11	7.9E-11	sec			2057	<5x10-10	355@ 18	39 22N	142 26E	
1100	4.4x10-11	sec	5.9E-11	1.1E-10	3.2x10-11	9.0x10-11	8.1E-11	sec			2106	<5x10-10	005@ 16.6	39 20N	142 21E	
1200	4.0x10-11	sec	5.6E-11	1.1E-10	3.0x10-11	8.7x10-11	7.9E-11	sec	1200	<5x10-10	2117	<5x10-10	010 @ 15	39 35N	142 40E	
1300	4.1x10-11	sec	5.6E-11	1.1x10-11	3.0x10-11	8.4x10-11	7.2E-11	sec			2127	<5x10-10	340 @ 15	39 25N	142 52E	
1400	1.8x10-11	sec	5.3E-11	1.1x10-10	2.9x10-11	8.2x10-11	8.2E-11	sec			2137	<5x10-10	003 @ 243	3919.020E	142 31.095E	
1500	3.7x10-11	sec	5.4E-11	1.1x10-10	2.9x10-11	8.6x10-11	7.0E-11	sec			2145	<5x10-10	011 @ 23.4	39 23.292N	142 31.457E	
1600	3.9x10-11	sec	5.8E-11	1.1E-10	3.0x10-11	8.7x10-11	8.2E-11	sec	1600	<5x10-10			349 @25	39 22.690N	142 47.455E	
1615	6.3x10-11	sec	6.3E-11	1.2E-10	3.1x10-11	8.6x10-11	9.1E-11	sec								
1630	6.3x10-11	sec	6.3E-11	1.2E-10	3.1x10-11	8.6x10-11	9.1E-11	sec								
1645	4.5x10-11	sec	6.1E-11	1.2E-10	3.3x10-11	8.7x10-11	8.2E-11	sec								
1700	4.5x10-11	sec	6.1E-11	1.2E-10	3.3x10-11	8.7x10-11	8.2E-11	sec	1700	<5x10-10			003@ 20	3919.047N	14319.67E	
1715	4.6x10-11	sec	6.0E-11	1.2E-10	3.2x10-11	8.9x10-11	8.7E-11	sec								
1730	4.4x10-11	sec	5.8E-11	1.2E-10	3.2x10-11	8.6x10-11	8.2E-11	sec								
1745	4.5x10-11	sec	5.2E-11	1.2E-10	3.2x10-11	8.6x10-11	8.9E-11	sec								
1800	4.2x10-11	sec	5.7E-11	1.1E-10	3.2x10-11	8.1x10-11	7.8E-11	sec	1800	<5x10-10			432@ 19	39 14.04N	143 50.59E	
1815	4.1x10-11	sec	5.0E-11	1.1E-10	3.0x10-11	8.2x10-11	7.8E-11	sec								
1830	4.4x10-11	sec	5.1E-11	1.1E-11	2.6x10-11	7.9x10-11	7.1E-11	sec								
1845	3.7x10-11	sec	5.2E-11	1.2E-10	2.9x10-11	7.9x10-11	7.2E-11	sec								
1900	3.9x10-11	sec	4.7E-11	1.1E-10	2.9x10-11	7. 8x10-11	7.0E-11	sec	1900	<5x10-10			340@ 12	3921 N	142 96 E	
1915	4.1x10-11	sec	5.0E-11	1.1E-10	2.5x10-11	8.4x10-11	7.3E-11	sec								
1930	4.1x10-11	sec	5.2E-11	1.1E-10	2.7x10-11	8.3x10-11	6.9E-11	sec								
1945	3.5x10-11	sec	4.6E-11	1.2E-10	2.7x10-11	8.0x10-11	7.6E-11	sec								
2000	3.5x10-11	sec	4.6E-11	1.2E-10	2.7x10-11	7.9x10-11	6.7E-11	sec					310@ 22	3907N	144 05E	
2015	3.3x10-11	sec	4.9E-11	1. 0E-10	2.7x10-11	8.4x10-11	6.7E-11	sec								
2030	sec	sec	4.6E-11	1.0E-10	2.8x10-11	7.7x10-11	6.3E-11	sec								

Table H-8. USS Ronald Reagan air monitoring results (cont.)

March 16, 2011																	
Time	APD 1-1	APD1-2	APD 1-3	APD 1-4	APD 2-1	APD 2-2	APD 2-3	APD 2-4	Flight Deck PAS				Winds	Lat	Lonq	Continuous PAS	
2045	sec	sec	4.2E-11	1.0E-10	sec	sec	6.1E-11	sec								Time	Reading
2100	sec	sec	4. 5E-11	1.0E-10	sec	sec	6.2E-11	sec					320@23	3879N	144 05E	2145	<5x10-10
2115	sec	sec	3.9E-11	1.0E-10	sec	sec	6.3E-11	sec									
2130	sec	sec	4. 6E-11	1.2E-10	sec	sec		sec									
2145	sec	sec	4.8E-11	1.2E-10	sec	sec	7.0E-11	sec									
2200	sec	sec						sec									
2215	sec	sec						sec									
2230	sec	sec						sec									
2245	sec	sec						sec									
2300	sec	sec						sec									
2315	sec	sec						sec									
2330	sec	sec						sec									
2345	sec	sec						sec									

Table H-9. Locations of USS Ronald Reagan air monitoring equipment

Equipment	Location
APD	Main Machinery Rooms
Flight Deck PAS	Flight Deck (topside)
Continuous PAS	Various

The USS Ronald Reagan’s air monitoring results included survey data beginning soon after the FDNPS effluent releases until several days later. Much of the data was collected from the topside or flight deck of the ship and indicated low levels of airborne radioactivity and external radiation levels. The data in Table H-8 indicate a slight increase in airborne activity concentrations on March 13, 2011, lasting for only a few hours, and then returning to previous levels. The topside PAS data were the most relevant for direct comparison to air concentrations predicted by HPAC for the ship’s location and time when the PAS data were observed. However, because the PAS filters were not assessed for isotopic composition, a direct comparison cannot be made with HPAC predictions could not be made. Although early airborne releases from the FDNPS were known to be dominated by radioactive noble gases³³, PAS filters were designed to collect only radioactive aerosols. Due to the stable or long-lived progeny of noble gases released in the accident, the radioactive aerosols detected on the filters was most likely dominated by aerosols released from the reactor or by a condensate of a gaseous release. Therefore, the detected contamination topside on the USS Ronald Reagan almost certainly was a result of non-noble gas or deposition-type contamination. Directly comparing the PAS result to the HPAC output concentrations required additional analysis because:

- The recorded PAS airborne concentration was determined using a conversion from corrected counts per minute³⁴ (CCPM) rate to activity concentration ($100 \text{ CCPM} / 4.5 \times 10^{-10} \text{ Ci m}^{-3}$) based on a Co-60 equivalent, which assumes all detectable activity is from Co-60 (Benevides, 2012); and
- The actual isotopic contributors to the detectable counts may have included iodine, cesium, and other isotopes that had the potential to be collected and counted in the PAS analysis procedure.

Therefore, it was necessary to convert the predicted HPAC isotopic air activity concentration to a total air activity concentration that would be reported using standard Navy PAS collection and reporting procedures as were used by the USS Ronald Reagan. This was accomplished by using an estimated filter count rate that would be observed after sampling the HPAC calculated isotopic air concentrations for the USS Ronald Reagan at the times and locations the PAS samples were actually taken, together with the same ccpm-to-total air activity concentration conversion factor as the one used for the PAS filters. This calculation is performed using Equation H-1.

³³ Noble gases are helium, neon, argon, krypton, xenon, and radon.

³⁴ The term “corrected” refers to net count, determined by subtracting the background from gross counts.

$$< A > = < C > k_1 \quad (\text{H-1})$$

where:

- $< A >$ = expected PAS measurement of air activity concentration for HPAC-predicted isotopic air activity concentrations (Ci m^{-3});
- $< C >$ = estimated PAS filter count rate from sampling HPAC-predicted air activity concentrations (CCPM); and
- k_1 = air activity concentration to cpm conversion factor ($4.5 \times 10^{-12} \text{ Ci m}^{-3} \text{ CCPM}^{-1}$).

The estimated filter count rate after sampling HPAC-predicted air activity concentrations was determined by assuming that a 1 cubic meter air sample was collected and radionuclides in particulate form were collected on a filter paper and counted with a G-M type instrument. Equation H-2 provides the model used to estimate the observed filter count rate, as displayed in Figure H-2.

$$< C > = V k_2 \varepsilon \sum_i A_i E_i \quad (\text{H-2})$$

where:

- V = volume of air sampled (1 m^3);
- k_2 = disintegration per minute (dpm) to Ci conversion factor ($2.22 \times 10^{12} \text{ dpm Ci}^{-1}$);
- ε = filter paper particulate collection efficiency (0.9, unitless);
- A_i = HPAC predicted air activity concentration for isotope i (Ci m^{-3}); and
- E_i = detection efficiency for emitted radiations for isotope i (CCPM dpm^{-1}).

The detection efficiency E_i for individual isotopes was determined by using the beta particle detection efficiency of a pancake G-M, with an industry standard 15.5 cm^2 entrance window according to Figure H-1 adapted from the G-M beta response information and discussion in Steinmeyer (2005). The beta efficiencies in Table H-10.10 were obtained from Figure H-1. For radionuclides with gamma-ray emissions, it was assumed that the G-M had a photon detection efficiency of 1 percent. In general, the beta-particle detection efficiency among G-M detectors of this type is consistent for medium-to-high-energy beta particles. A greater difference in efficiencies exist for low-energy beta particles, dependent on the density thickness of the entrance window and existence or absence of protective wire mesh covering the entrance window. The efficiency values displayed in Figure H-1 were based on absolute efficiency

(4π geometry) which accounted for all emission of radiation, and provided values of CCCM dpm⁻¹.

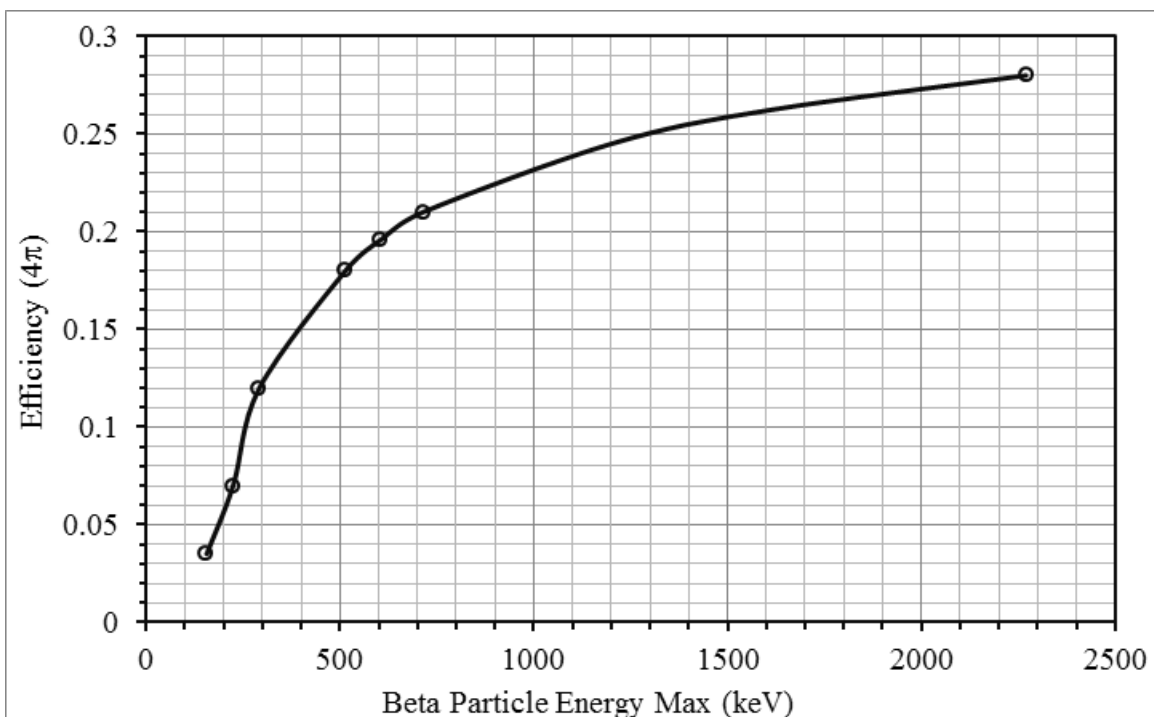


Figure H-1. Beta particle energy and associated detection efficiency

Table H-10 provides beta G-M detection efficiencies determined from Figure H-1 and gamma efficiencies assuming 1 percent efficiency for all gamma ray energies. The table also shows the frequency-weighted efficiencies for both beta particles and gamma rays and the overall detection efficiency (E_i) for each isotope based on isotopic emitted radiation. The values listed below include those principal, isotopes in particulate form that have significant potential for collection on a filter paper in the PAS, and no noble gases.

Table H-10. List of isotopes and associated efficiencies for PAS analysis

Isotope	Beta Particles				Gamma Weighted Efficiency [‡] (cpm dpm ⁻¹)	Overall Detection Efficiency, ^{**} E_i (cpm dpm ⁻¹)
	E_{\max} (MeV)	Frequency [*]	G-M Efficiency (cpm dpm ⁻¹)	Weighted efficiency [†] (cpm dpm ⁻¹)		
Cs-134	0.622	1.0	0.20	0.20	0.020	0.22
Cs-136	0.341	0.93	0.14	0.14	0.030	0.17
	0.657	0.070	0.20			
Cs-137	0.541	0.93	0.18	0.18	0.010	0.19
	1.18	0.070	0.24			
I-131	0.606	1.0	0.20	0.20	0.010	0.21
I-132	2.12	1.0	0.28	0.28	0.030	0.31
I-133	1.27	1.0	0.25	0.25	0.010	0.26
Te-129	1.45	1.0	0.26	0.26	0.004	0.26
Te-129m	1.60	0.36	0.26	0.094	0.0006	0.095
Te-132	0.220	1.0	0.060	0.060	0.011	0.070

* Frequency is emissions per disintegration (dis).

† Weighted efficiency for beta particles is the sum of the products of frequency and G-M efficiency for all beta particles.

‡ Weighted efficiency for gamma rays is the product of gamma frequency and an efficiency of 1% (0.01).

** Overall detection efficiency is the sum of weighted efficiency for beta particles and the gamma weighted efficiency.

The overall efficiencies from Table H-10 were used in Equation H-2 to determine the expected count rate from HPAC-predicted air activity concentrations. This expected count rate was then used in Equation H-1 to estimate the associated total air activity concentration that would be reported from sampling air containing the HPAC-predicted air activity concentrations. This allowed for comparison to the USS Ronald Reagan PAS count rate results to assess how well the HPAC-predicted results compared to the PAS measurements at the same sampling time and location. The results are shown in Figure H-2.

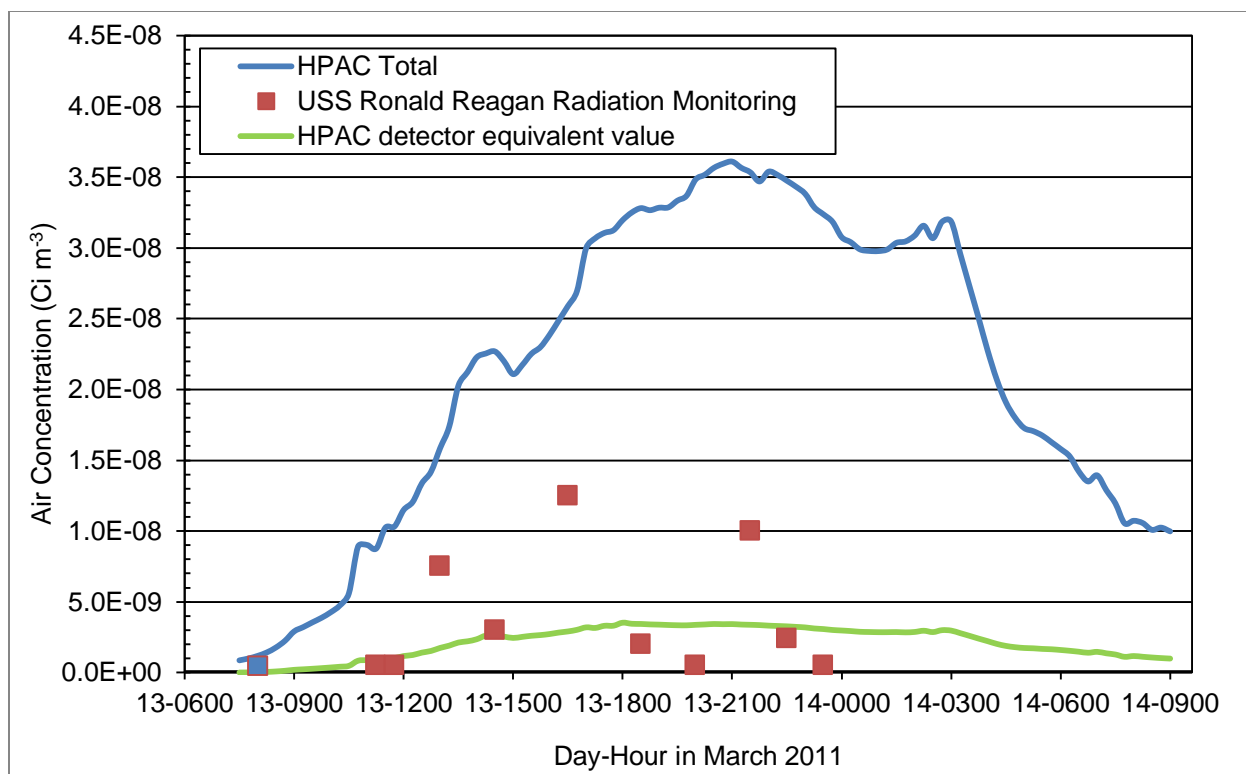


Figure H-2. Comparison of HPAC-predicted results to USS Ronald Reagan PAS data

The blue “HPAC Total” points are significantly higher than the other data points because these are the total HPAC air activity concentrations, which include contributions from the noble gases. These results were utilized in the dose calculations including contribution from external radiation from noble gases as described previously in the discussions of the semi-infinite cloud model. The green “HPAC detector equivalent value” points consist of the estimated air activity concentrations that would be reported from PAS collection/measurement procedures using predicted air concentrations for the isotopes listed in Table H-10, which represents only those elements that have potential to be collected on the filter paper and subsequently counted. Therefore, only the comparison of the “HPAC detector equivalent value” with the “USS Ronald Reagan Radiation Monitoring” data is valid because they represent the same isotope cohort (no noble gases). Comparative analysis of the reported USS Ronald Reagan PAS data and the estimated reported values based on HPAC-predicted air concentrations indicated:

- HPAC-predicted results are consistent with PAS measurements; given their respective uncertainties;
- For the March 13, 2011 measurements, the HPAC-predicted results are within the range of the PAS measurements; and
- The HPAC-predicted results showed a gradual build-up of air concentrations until about 1800, followed by a slight decrease, and then to a steady state after 2100.

The above comparison indicated correspondence between HPAC-predicted results and measured air concentration data, which supported the conclusion that HPAC could accurately

model the fleet radiological environment and calculate associated radiation dose. Differences in the HPAC and PAS measured data could be attributed, at least in part, to:

- The granularity of the ship's location data (every six hours versus continuous location data);
- Variations in individual observations of the G-M measurements themselves;
- Variations in the G-M instruments' responses, which were calibrated to $\pm 20\%$ (Johnson, 2011); and
- Wind speed and direction, source term, etc.).

H-6. USS Ronald Reagan Contamination Data

During flight operations aircraft encountered radioactive contamination present in the effluent clouds from FDNPS or on the ground when landing. Because of this, aircrew had a potential to inadvertently transfer contamination from the ground or other surfaces onto their clothes or skin. To identify individuals who may have been contaminated, a total of 1,844 whole-body frisk surveys³⁵ were performed from March 14 to April 6, 2011, on flight crew members to detect radiation emitted from whole body (skin or clothing). The results are presented in Figure H-3.

The terms "positive" and "negative" refer to the presence or not of detectable contamination (pre-set action level of 100 CCPM; activity at or above this level would result in decontamination of the detectable contamination). The results from Figure H-3 indicated:

- Approximately 10 percent (187) of flight crew surveyed had detectable contamination levels ranging from 100 to 4,000 CCPM;
- The frequency of positive results were heavily weighted towards the time period soon after the initial FDNPS effluent releases; and
- The dates associated with higher frequencies or percentage of positive versus negative surveys appears to coincide with known dates of FDNPS effluent releases.

³⁵ Whole body surveys were conducted with G-M type pancake probe detector.

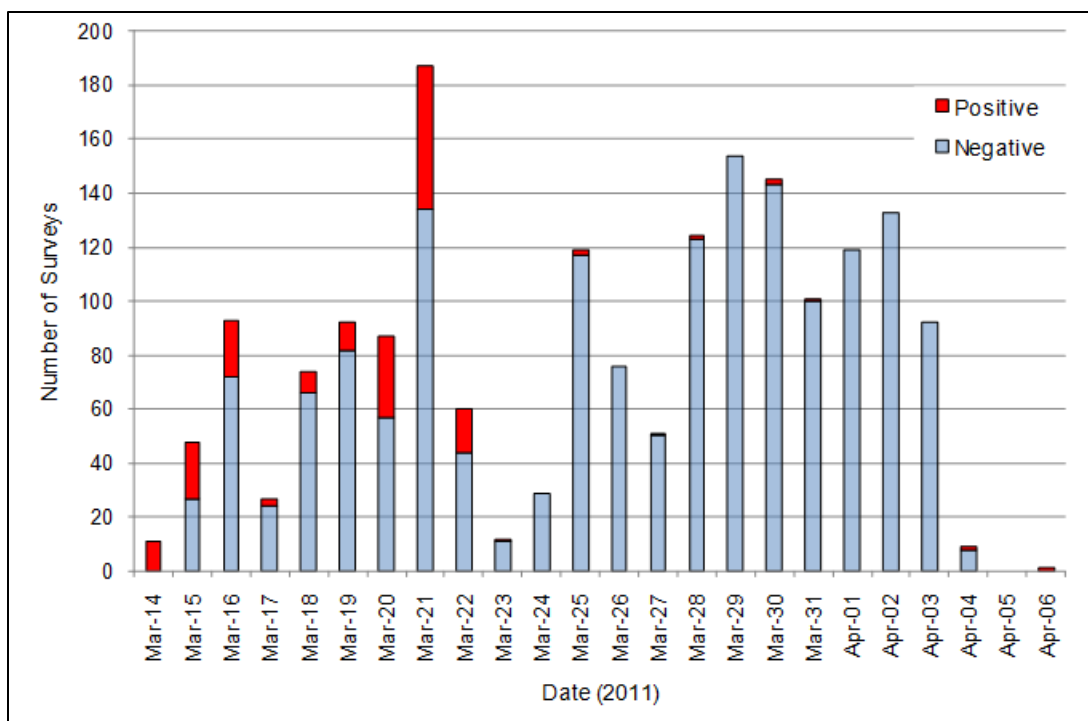


Figure H-3. USS Ronald Reagan aircrew survey results

All of the detectable contamination was low level, and virtually all of it was on clothing and easily removed. IM results conducted to assess detectable levels of internal contamination from inhalation or ingestion of radioactive material, as discussed previously, indicated no significant internal dose associated with the detected contamination.

In addition to individual contamination surveys, a total of 3,335 aircraft contamination surveys³⁶ were performed on USS Ronald Reagan helicopters that conducted HADR operations as part of OT from March 13 to April 11, 2011. Figure H-4 provides a summary of the contamination data.

³⁶ Surveys consisted of either direct instrument frisk (G-M type pancake detector) or area wipe.

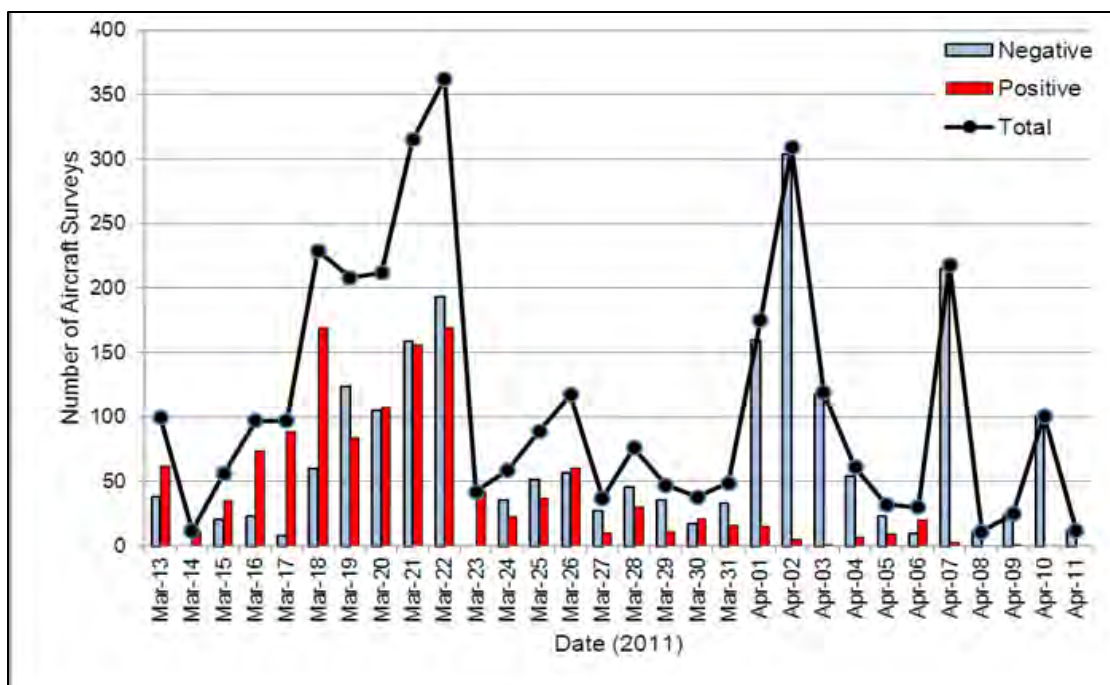


Figure H-4. USS Ronald Reagan aircraft contamination survey results

Of the 1,248 surveys that were distinguishable from background (greater than or equal to 100 CCPM), the observed results averaged 880 CCPM and ranged from 100 to 114,000³⁷. The median value for these contamination surveys was 200 CCPM. As was the case for aircrew data, positive and negative peaks occurred at or near known times of effluent releases and times well after the releases, respectively. In addition, a relatively equal number of positive and negative results were observed during the time between March 23 to March 31, 2011, which could be considered a “transition” period between the peak in positive results and the peak in negative results. These results were generally consistent with the results for aircraft operating in a radiological environment and with a reduction in contamination levels because of decay, dispersion, and weather effects.

³⁷ This value was observed on one survey, the vast majority of results were well below this activity.

Appendix I.

HPAC Modeling and Uncertainties

I-1. HPAC Modeling Process

The Hazard Prediction & Assessment Capability (HPAC) is a Defense Threat Reduction Agency (DTRA) software application. The HPAC application is an integrated package of models that cover the various aspects of the physical processes involved in predicting the consequences of hazardous events. Those elements of HPAC that were used in preparing this report are addressed in this appendix.

The process began with the combination of modeling the reactors and subsequent effluent releases from the primary containment to the external environment; this resulted in defining the source term. The next step was acquiring the weather data needed for computing the transport and dispersion (T&D) of radioactive material as it was released from FDNPS. Finally, the output of results, including the element of modeling radioactive material decay, was generated. Uncertainties were associated with the following elements of the modeling process:

- Source term;
 - NFAC (nuclear facility) material was modeled as a vapor with a single parameter deposition velocity
 - Very complex sequence of events and releases of radioactive material
- Weather;
- T&D process; and
- Ship location.

The uncertainties associated with each of the four elements are discussed in the following sections. Data were available for comparison with HPAC results which minimized some of the uncertainty.

I-2. Source Term

HPAC's Nuclear Facility module, designated NFAC, was used to model the source term for this event. This model has a number of different modes ranging from a simple choice between a moderate or severe incident each with a set of default specifications. This simple choice is often used in operational situations when there is very little information available. In contrast, a more complex model ("percent inventory model") was used in which the percentage from each set of 12 different groups of elements was specified. The actual percentages used in this report are discussed in detail in Sections I-2.2 to I-2.5. Each percentage was based upon the isotopic inventory at the time of reactor shutdown. Those isotopes were all decayed in time to the start of each of the specified periods. The mixture of the release was constructed based on the fraction of the initial inventory specified. This mixture was released over the time period specified. There were several sources of uncertainty in each of these pieces. In the decay process it was possible for certain isotopes to decay into elements that were in other groups. These

transmutations could also occur in the radioactive decay during the release period. Typically these were small in comparison with the uncertainties in the dispersion computation and in the specification of the release rate itself.

I-2.1. Physical Form of Released Material

The physical form of the material released was a factor in the uncertainty. The NFAC source model in HPAC models a vapor release. The form of this release limited the characterization of the material deposition rate to a single parameter, the vapor deposition velocity, with a value fixed 3 mm per second. Physically, this is actually more representative of a material composed of uniformly sized, very small (sub-micron) particles than a true vapor, which would typically have a deposition velocity about an order of magnitude higher than 3 mm per second. If the physical release was actually composed of an aerosol, the droplets might be large enough to have a settling velocity, which is the velocity that droplets move downward with the force of gravity. The liquid in the droplets would evaporate over time, potentially leaving dry particles. HPAC is capable of transporting aerosols or particles, but because of the origins of the NFAC model in early regulatory practices, a more realistic transport model for these materials has not been implemented.

It is difficult to quantify the uncertainty in the final result that might be incurred due to the simplicity of this assumption. Since the vapor material would not fall with gravity, if the real release was composed of droplets that were larger than 10 microns for any substantial period of time, HPAC would under-predict the deposition rate due to this factor. However, in comparing HPAC and deposition field measurements, there was no evidence that HPAC under-predicted the deposition. In fact, the reverse appeared to be the case because where data were available for the comparison, the HPAC model, in dry conditions, resulted in a deposition rate higher than the data. Depending on the actual size of any particulates when they were being deposited, evidence suggested that locally the deposition rate varied from as low as 1 mm per second to as high as 30 mm per second. The possibility existed that an overly high deposition rate could have depleted the cloud of material. This possibility was tested by doing the reverse (i.e., increasing the deposition rate by increasing the material deposition rate). This task proved difficult to do because the HPAC user interface did not provide such an option. Instead, this task was performed by manually editing the project file and increasing the default values stored in the material property prior to the run. Following the run, there was no appreciable reduction in the air concentration, so it was concluded that any potential difference in the air concentration due to an overly high deposition rate of the default value of 3 mm per second, was negligible. Therefore, the default value for the deposition rate in the NFAC model was retained without modification.

I-2.2. Isotopic Fractions in Releases

The source term described by the isotopic release rates, the height above the ground and the initial size of the release was determined via an iterative process that started simply and evolved by including progressively more detail and fidelity. Initially a very simple source model was used that modeled all three reactors as a single reactor with all inventories combined. This resulted in simple release fractions based on total reported activity releases that yielded 2.6 percent iodine (halogens), 2.0 percent cesium (alkali metals), and 100 percent of the noble gases (Cassata et al., 2012) when scaled to reactor inventories at shutdown.

The next step refined the methodology to account for different events that occurred, including releases from each reactor including core uncover times, controlled vents, and hydrogen gas explosions. These refinements resulted in more complex release fractions, which more closely described the actual release fractions. One indicator of reactor core conditions was the radiation detector readings at the FDNPS Main Gate 1, which were strongly affected by the wind direction. The weather station that provided the wind direction and intensity at the Main Gate 1 did not always work properly because of power outages, and there were periods when no wind data were available. However, although many of the on-site radiation detectors also lost power, TEPCO improvised by using car-mounted G-M survey instruments to collect dose rate readings at those locations. The modeling during these periods assumed that the wind was constant and at a value of the last available data point. The effect of this assumption is shown in Figure I-9 for short periods of time when the HPAC results were approximately constant while the Main Gate 1 exposure rate measurements varied during the same time period. However, this did not significantly affect the results because the variances during these time periods were noted in the HPAC iterative calibration process.

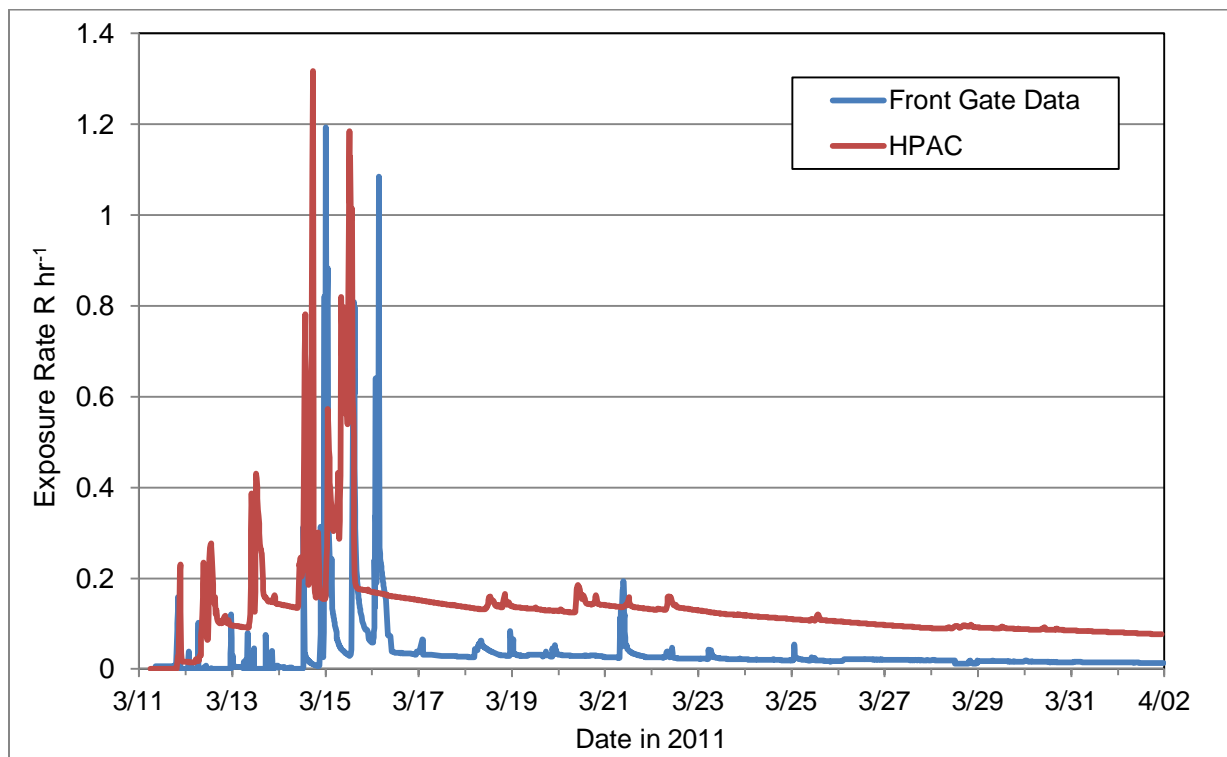


Figure I-1. Comparison of HPAC results with measured exposure rates at the FDNPS main gate

Releases from each reactor were divided into multiple time segments to reflect the time that each core melted down. This was then modeled and resulting exposure rates associated with the radiological releases were compared to the FDNPS Main Gate 1 exposure rate data. That comparison resulted in further refinements of the time periods and release rates to more approximately reflect the measured data. This created a reasonable qualitative matching of the

gate data in terms of plant characteristics prior to core meltdown as well as the days following reactor meltdowns. The height above ground of the release was a significant factor in the prediction of the FDNPS Main Gate 1 results. This parameter was varied to the degree that the source might have actually varied given the height of the exhaust stacks, and a height of 20 meters (m) was selected.

The source term was progressively calibrated through approximately 30 iterations. Analysis of the iterations was conducted to determine use of other sources of data or additional data points in any particular data set, or a parametric variation in the input parameters, and this resulted in a better match. For example, the Yokota AB air sampler data peak air concentration occurred on March 14, 2011. The releases from the reactors during this period were adjusted in a way that was consistent with their meltdown and response scenarios and released approximately the right amount of material from each chemical group (see Section I-2.4) so that the daily average air concentration of the measured isotopes was approximately matched. The precise ratios of the isotope activities within each group (i.e., the ratio of I-132 to I-131) were not reproducible. The group's release was adjusted to the point that some of the isotopes in the group might be high, but others might be low, but in general they were about right, typically within 50 percent. Data from Yokota AB was also available for other days, and while adjustment was possible to match relatively closely data collected on March 14, 2011, this resulted in under and over predicting data from March 13 and March 15, 2011, respectively. This was the status at version 26 in the iterative process. Version 26 was a potential candidate for use in the next phase of the analysis so it was analyzed thoroughly. Comparisons of HPAC results with shipboard measurements were a critical part of this analysis.

I-2.3. Comparison of HPAC-generated Results with Measured Data

Because the isotopic air concentration measured on the USS Ronald Reagan could not be directly compared to the total isotopic air concentration output from HPAC, the application of detector efficiency for each isotope was required, as discussed in Appendix H. The principal reason for this was that noble gases were not being collected and measured with the USS Ronald Reagan methods, which were designed for particulate monitoring. The Yokota AB data clearly indicated there was a small release of both the halogen and alkali metal groups that were captured in the March 13, 2011, USS Ronald Reagan sample, so a release with characteristics of the isotopic mixture measured at Yokota AB was used corresponding to the peak measurement on the USS Ronald Reagan. This iteration also improved comparison to the Yokota AB data of March 13, 2011. It did not substantially impact the air concentration result obtained on March 14, 2011.

The next iteration was performed because of two factors. The first factor was based on what has been called the "Northwest plume" (an obvious effluent cloud emanating in the northwest direction from FDNPS). This plume was the primary reason for the magnitude of the release rate on March 15, 2011. To obtain a dry radioactive material deposition similar to that which was measured, it was necessary to increase the release rate during the period that the wind was blowing to the northwest; however, when this plume continued to drift south to Yokota AB, comparison with the measured isotopic air concentrations on March 15, 2011, the HPAC result was high by a factor of about 50. This showed that there was a problem with this assumption.

The second factor was the realization that the source of the northwest plume was not dry deposition, but wet deposition or rain out, the process by which the rain falling through the cloud

of radioactive material collected the material in the cloud and deposited it on the ground. The precipitation record showed relatively intense rain showers in the area to the northwest of FDNPS at this time. The dry deposition rate was much less than the wet deposition or rain out rate. When the northwest plume was modeled only with dry deposition, the required release rate was much too high. Replication of the northwest plume's deposition field without modeling rain out effects required release rates during that time period that were considered much too high, and if used, would result in unrealistic over predictions of isotopic air concentrations and air submersion exposure rates. Instead, the release rates were adjusted so that the Yokota AB data on March 15, 2011, were approximately matched. This was used for the final results in this report. Note that there were parametric variations in the weather data set used in this iterative progression.

Keeping the modeled air concentrations as accurate as possible was important. The computed ground deposition was useful at locations for purposes of validation if that deposition occurred during periods when it was not raining. Since this report did not use the deposition calculated by HPAC for computing the fleet doses, but rather used only the isotopic air concentrations and air submersion exposure rates, the lack of wet deposition model capability was only a factor regarding use of the HPAC results in that it reduced the amount of validation or calibration data that were available for comparison.

HPAC has the capability to model wet deposition, but the capability is limited to switching the conditions in the entire domain to a rain condition for the period of rainfall. Because of the large domain used for this model and the limited extent and dynamic nature of the rain events, it was determined to be impractical and not helpful to implement this capability purely to replicate the fallout associated with the "Northwest plume". The capability also had limited utility since the primary purpose of the modeled output was to compute radiation doses to fleet-based individuals while at sea.

I-2.4. Iodine Gas Fraction

The HPAC model did not differentiate between the aerosol and gaseous forms of iodine. The model used the assumption in NUREG-1465 (NRC, 1995) that almost all of the iodine was in aerosol form in the FDNPS primary containment, and further, that when this iodine aerosol was released into the environment, it remained in the aerosol form. The calibration process used the Yokota AB data that consisted predominantly of measurements of accumulated aerosols on filters. The USS Ronald Reagan PAS data were also from measurements of accumulated aerosols on filters. Gaseous iodine would not be collected on filters with the same efficiency as aerosols, and if not measured, would not be accounted for in the HPAC model calibration. Contrary to these assumptions, low-volume sampling conducted by DOE and documented in the shore-based report indicated that not only was there gaseous iodine present, but that it was present at levels that were on average over two times higher than the aerosol fraction. Because iodine is just one component of the halogen group, the NFAC percent inventory model used for this analysis could not be adjusted to only increase the iodine upward to account for the gaseous fraction; however, it was simple to account for this gaseous fraction while at sea by using the in-port dose calculation procedure. This procedure assumed that the average aerosol to gaseous iodine ratio was representative over time. This assumption did incur a substantial uncertainty as both the DOE data and the various circumstances and physics driving the release of the gaseous iodine, were in fact highly variable.

Some of the factors that could have affected whether iodine was released in gaseous or aerosol form from the FDNPS included deliberate venting through a filter system before release to the environment, acidification of the containment water, and boron injection³⁸. Filtering tends to increase the vapor fraction relative to the particulate fraction. Acidification increases the vapor fraction in the air. Boron injection increases the acidity of the containment water that in turn increases the vapor fraction in air. In addition to these factors, if the release consisted of water droplets, then evaporation from droplets during T&D could have increased the droplets' acidity with a corresponding increase in gaseous iodine.

I-2.5. Calibration of the Isotopic Mix

The isotopic air concentrations measured at Yokota AB were also used to refine the precision of the source releases. When these data were compared to the modeling results, it became apparent some of the other groups of isotopes were missing from the release. The HPAC specification of the NFAC percent inventory release allowed the user to specify the percentage of the available isotope inventory whose elements fell into one of 12 different groups based on their general physical and chemical behavior. Any isotopes measured at Yokota AB that were not previously accounted for were identified as belonging to their corresponding element's group. The percent release of that group was added to the overall release term so that these isotopes were included in the analysis. However, the isotopes in these groups did not significantly contribute to the total dose compared to iodine and cesium. The actual percentage releases added to the model were adjusted to approximate the isotopes measured at Yokota AB on March 14, 2011. The HPAC-predicted isotopic air concentrations at Yokota AB increased during the next 24-hour period while measured air concentrations actually decreased. This was likely an effect of the intense plume that initially moved northwest but then drifted due south.

The precision of the HPAC-interpolated wind field was very important in computing the intensity of the concentration at Yokota AB. If the winds actually blew this radioactive material farther west than was predicted by HPAC, this would not have been a discrepancy. This difference demonstrates how the precise temporal match between data measured on the ground can be different than the HPAC predictions at any particular time. For fixed locations, this weather uncertainty was usually the greatest contributor to the final uncertainty. Because of the random nature of the weather, this high uncertainty was often averaged away over time. After going through the process described above, which more precisely determined the sequence of releases from the FDNPS, the final source term was complex. Figure I-2 and Figure I-3 show the final releases and their complexity.

³⁸ Boron was used as a neutron absorber to prevent re-criticality.

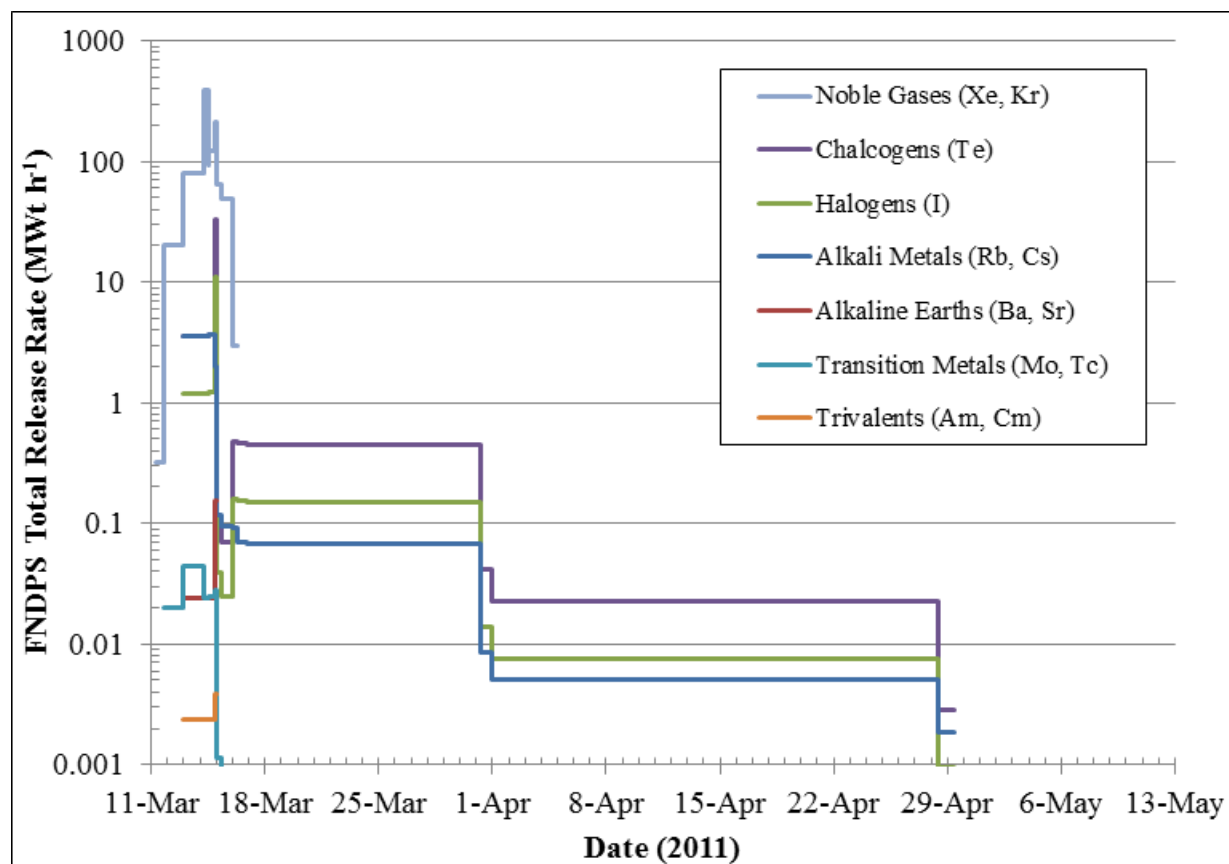


Figure I-2. Release rate groups in version 26

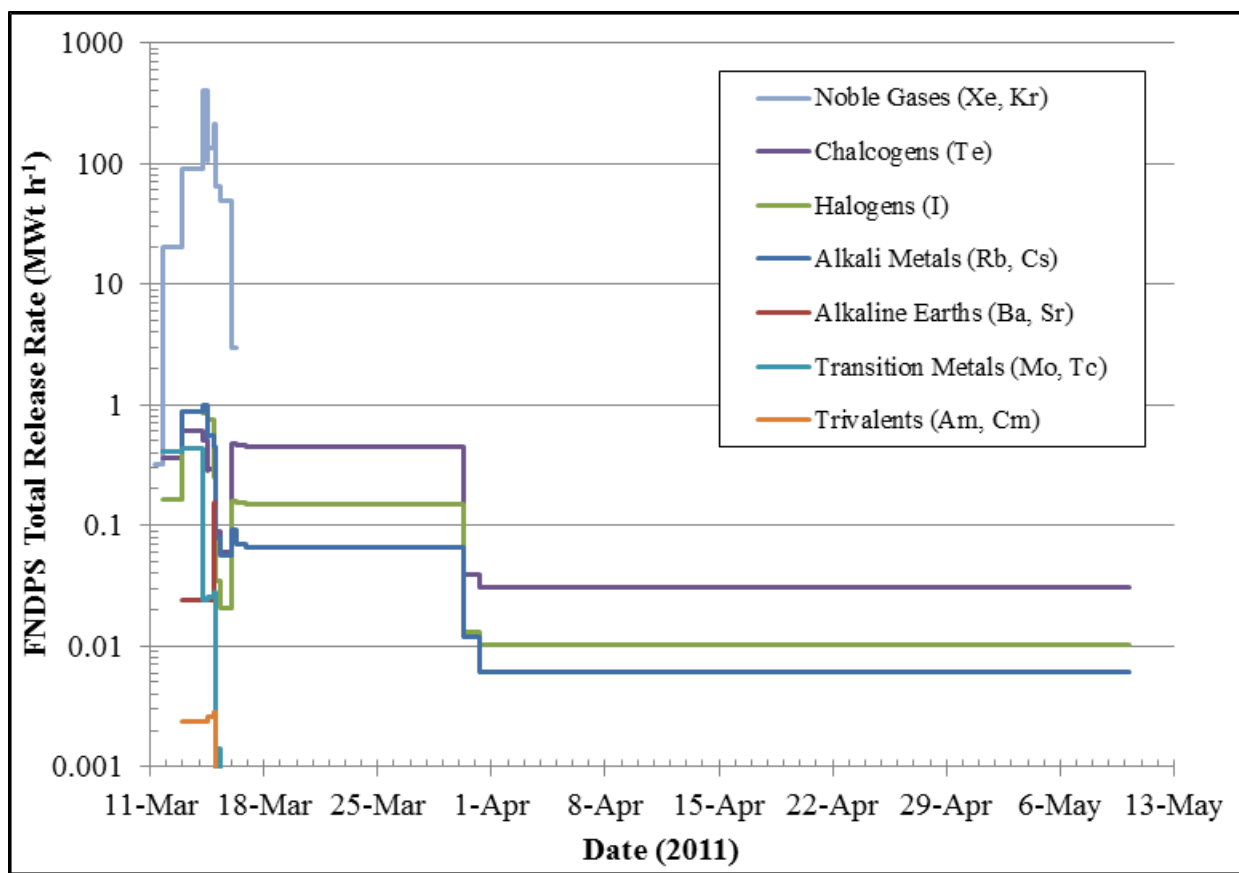


Figure I-3. Release rate groups in version 31

Although HPAC accounted for radioactive decay, these simplified graphs only illustrate the magnitude and extent of the releases and do not show the radioactive decay factor. The units on the y-axis of these graphs represent the reactor operating power per hour of the release. For example, if all of the material in all three of the reactors was released in one hour, that release rate would be the sum of the operating power of all three reactors. Unit One had an operating power of 1,317 megawatts thermal (MWt), and Units Two and Three each had an operating power of 2,280 MWt, so for this example the one-hour total release operating power would be $1,317 + 2,280 + 2,280 = 5,877$ MWt per hour total for each of the groups. Since almost all of the noble gases were released, the time integrated value for the line shown in Figure I-3 would approach 5,877 MWt. That value is the time integral of the release rates. From Figure I-3, the peak release rate is about 400 MWt per hour. When this line was integrated over time by multiplying the height of the line by the time at that height and then adding all of these areas together, the sum approached this time-integrated value. Figure I-3 shows that the release rates for the alkali metals, alkaline earths, halogens, chalcogens, early transition elements, and trivalents were all much smaller. The elements included in each of these seven groups were:

- Noble Gases: xenon, helium, neon, argon, krypton, radon, hydrogen, nitrogen;
- Alkali Metals: cesium, lithium, sodium, potassium, rubidium, francium, copper;

- Alkali Earths: barium, beryllium, magnesium, calcium, strontium, radium, einsteinium, fermium;
- Halogens: iodine, fluorine, chloride, bromine, astatine;
- Chalcogens: tellurium, oxygen, sulfur, selenium, polonium;
- Early Transition Elements: molybdenum, vanadium, chromium, iron, cobalt, manganese, niobium, technetium, tantalum, tungsten; and
- Trivalents: lanthanum, aluminum, scandium, yttrium, actinium, praseodymium, neodymium, promethium, samarium, europium, gadolinium, terbium, dysprosium, holmium, erbium, thulium, ytterbium, lutetium, americium, curium, berkelium, californium.

The HPAC model did not account for release of any elements other than those in the groups above. The initial isotope inventory for each reactor was input into the HPAC model and contained all of the 1052 different isotopes in the reactor with their activities at shutdown in proportion to the operating power of the reactor in curies per MWt. These three reactor inventories were computed by the ORNL using the ORIGEN code. The initial isotope inventory was processed for each release to compute the actual inventory composition as a function of time considering the radioactive decay of the isotopes in the inventory. This inventory was then split into the element groups above in the proportions specified (and shown in Figure I-2 and Figure I-3) and the two composite materials were released and the T&D computed for each. One of the materials was categorized as a non-depositor and included the elements (such as the noble gases) that will not deposit and remain on the ground. The other material, called the depositor, contained all of the other isotopes that will deposit. The depositor material had the fixed deposition velocity of 3 mm per second.

I-3. Weather

I-3.1. HPAC Weather Input Source Types

HPAC has the capability to incorporate many different sources of weather (meteorological) data. The wind field data, primarily the horizontal direction of the winds relatively near the ground, was often the most significant source of uncertainty in the entire modeling process. For this analysis it was possible to numerically reconstruct the 3-D wind field using any number of standard modeling tools. A team from Pennsylvania State University spent a substantial amount of time using the MM5 model to produce a weather input for HPAC. A team of meteorologists from the DTRA Reachback group ran HPAC using this weather input, but they were not satisfied with the results. Alternatively HPAC can also use measured weather data as the input source. The DTRA Reachback team then tested HPAC using measured weather data and concluded that use of the measured weather data was a better option.

I-3.2. HPAC-predicted Deposition Field and the “Northwest plume”

The next data input set used was the deposition field measured around the FDNPS within 80 km. However, this resulted in a misleading branch in the calibration process. The diversion centered on the fact that HPAC only models the dry deposition and not wet dispersion or rain out. Although HPAC can model rain out, this capability is very basic and must be applied to the

entire domain, which was impractical for the situation considered in this report. There were two major rain events on March 15 and March 21, 2011, that coincided with significant releases of radioactive material from the FDNPS. The rain out on March 15, 2011, resulted in the areas of higher contamination to the northwest as shown in Figure I-4.



Figure I-4. “Northwest Plume” Data

The quest for a more comprehensive answer occurred because initially it was not known that this plume was created by the rain event. The HPAC model was consistently unable to produce a deposition field that approximately replicated this result with the full set of winds as shown in Figure I-7. at 1200 on March 15, 2011. Note: The wind barbs indicate wind direction and speed. For example, the wind barb is shaped somewhat like a hockey stick attached to a circle. The wind direction is therefore defined as coming “from” the direction of the stick and “to” the direction of the circle. The wind speed is listed in knots and represented by the shape of the wind barb.

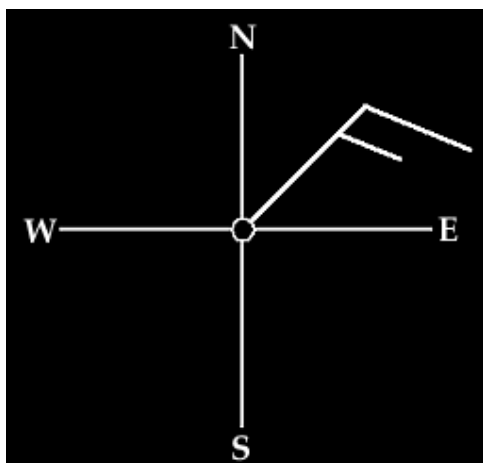


Figure I-5. Demonstration regarding how a wind barb indicates wind direction

The wind barb in Figure I-5 indicates the wind is coming from the northeast and heading towards the southwest; Figure I-6 demonstrates how a wind barb indicates wind speed.

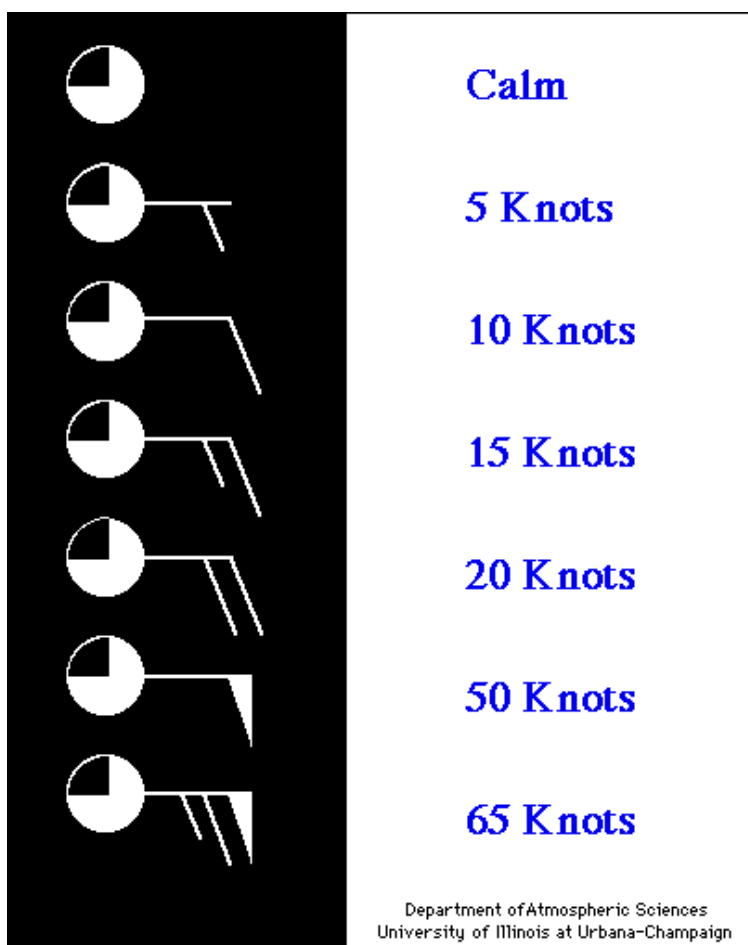


Figure I-6. Demonstration showing how a wind barb indicates wind speed

The map displays the Baltic Sea region, with the Ignalina Nuclear Power Plant (INPP) located on the Lithuanian coast. Various monitoring stations are marked with numbers and symbols, indicating different types of measurements or data points. The stations are distributed across the region, with some located near the coast and others further inland. A scale bar for 100 km and a north arrow are also present.

162

Because it was possible that the wind data were inaccurate, the weather data set was reduced to several smaller sets in an attempt to establish whether any particular measurements were unduly affecting the results. One of the obvious candidates was the point to the northwest where the wind direction was due south with a temperature of 5°C and a dew point of -2°C, displayed as (5, -2). This weather station is in the Yamagata prefecture. One hypothesis was that the weather data at this location was strongly influenced by the local topography and possibly changed the larger wind field in a manner that was not consistent with the actual winds. One weather file was run with the data from this location removed. Another alternative was to limit the wind data to those closest to the FDNPS—the closest point straight north (6, 2) and the closest point to the southwest (5, 2) for the time period prior to March 16, 2011. The full set of weather data also included data from all locations in the entire region rather than just the computational domain. This large set of weather data should not have weighed heavily in the result but could have had a corrupting effect. To eliminate this possibility, the set of weather locations was also filtered to include only those within the computational domain. This set of weather data was then extended to include the weather data measured by the ships located outside and east of the domain. HPAC included weather data from outside the computational domain (the domain where the dispersion was computed) in the computation of the resolved wind field inside the computational domain. This resulted in a very intense release during the period that the winds were blowing towards the northwest. Figure I-8 shows the result using the weather dataset with only the two points prior to March 16, 2011. This data set produced the most northerly plume. The final computation of results in this report used the weather data set that had all of the data from all of the locations in the computational domain, plus those from the ships to the east of the domain.

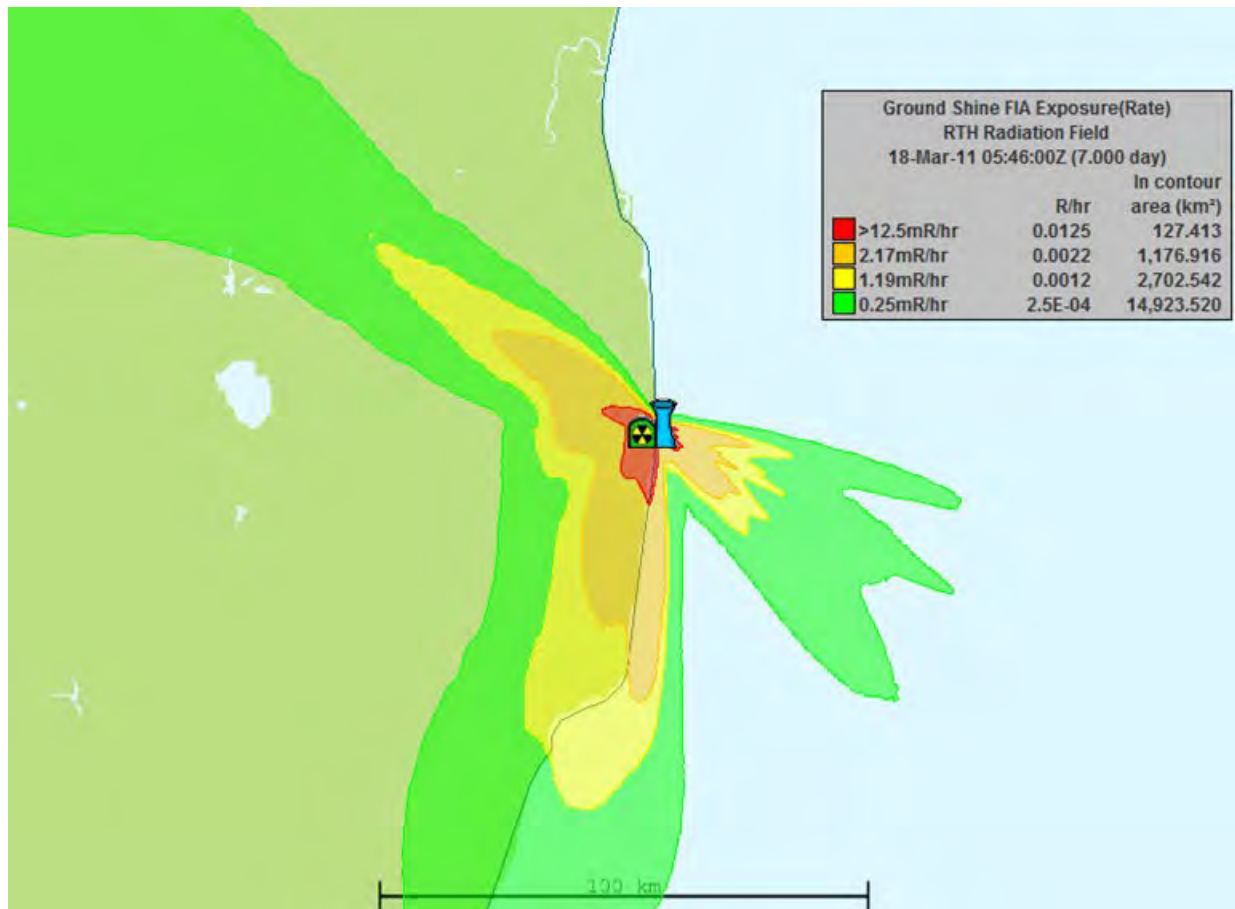


Figure I-8. HPAC Northwest plume result for version 26

A review of Figure I-8 indicates that although the model results started to approximate the intensity of the northwest plume, the deposition to the south was much too high, and manipulation of the HPAC input was unable to get the plume to be quite as far north as the measured data indicated. HPAC results were also almost a factor of 50 too high when compared to the Yokota AB data. Rain data indicated that this plume was the result of rain out. Reduction in the number of wind locations and the high-intensity plume were counterproductive when the goal was to produce a consistent prediction of the doses to the fleet-based individuals. Note that HPAC computes ground shine in the ocean in the same manner as on land, which explains the continuous plot from the land to the ocean.

These results explain why the HPAC deposition outputs were not used in the calculation of ship doses. Instead, the measured results at Yokosuka NB were used to account for surface deposition and subsequent radiation exposure. The ratio of air submersion dose to the total dose at this location was used to scale all of the individual ship results. The details of the approach used are explained in Section 3.3.3.

I-3.3. Terrain and Land Cover Impact on the Wind Field

In the final analysis, the HPAC model was run without activating terrain or land cover (forest, farmland, urban, etc.) input parameters.. In many cases, especially if the result was small

scale and there was significant terrain variation, HPAC would typically be run with terrain and land cover turned on. When this switch was activated, the weather module changed from being computed by SCIPUFF to being computed by another model. While it was presumed that results would be more accurate with this switch activated, one consequence was that the computation took longer to run because not only did the resolved wind field need to be computed in a more strenuous manner, but the resultant complexities in the wind field required reduction in the size of the time steps in the dispersion computation. In tests of the model, the time required for the computation went up an order of magnitude. Calculations that included full-terrain capability for the entire two-month run could take several months to complete. But more importantly, for the computation that was performed out to March 16, 2011 at 1131, the results were a poor comparison to the data. A possible reason for this was the model was calibrated for cases where the terrain was turned off. However, it appeared likely that the alternate, resolved wind field computation was incorrect. All of the prior validation of SCIPUFF, at the domain scales that were computed in this report, was done with the terrain and land cover switch set to “off”. This indicated there was a problem using this software with terrain and land cover on over such a large spatial domain.. Since the goal of this computation was not to duplicate the results to the north and west of the FDNPS, but rather to obtain reliable results out to sea where the ships were located and terrain affects were not an issue, switching “off” the terrain and land cover was deemed the appropriate option. This may in part explain the difficulty in duplicating the measured data to the north and west using HPAC-predicted results.

I-4. Ship Location

HPAC was used to predict isotopic air concentrations and external dose rates to which individuals may have been exposed while the ships were at sea. To accomplish this, the HPAC model required the creation of moving virtual sampler locations using time and latitude and longitude information at each subsequent location during a ship’s travels. The HPAC model linearly interpolated between locations documented in ship’s logs by assuming the ship sailed in a straight path from one point to the next. Ideally these locations would be at a temporal resolution at least as fine as the HPAC output time intervals of 15 minutes; however, the ship locations were typically provided at 6-hour intervals. This raised the possibility that if a ship actually moved in a slightly different path, its movement could have exposed the ship and crew to a different exposure rate than predicted by HPAC modeling. For example, Figure I-9 shows the reported locations of the USS John S. McCain at two subsequent times of 0900 and 1500 on March 13, 2011. These locations appear on top of an overlay of the total activity air concentration computed at 1200; midway between the two times. These two points are a straight line distance of approximately 250 km apart. In addition, Figure I-9 illustrates an alternative course, connected by lines, with the same initial and final location points, but is about 15 km longer. The ship encounters a higher radiation area compared to that associated with a direct straight course between the two points. This route could result in an increased dose compared to the assumed straight line course. To evaluate the uncertainty and subsequent effect on the reported doses, an HPAC calculation was performed using the hypothetical alternate course. The air submersion exposure computed during this 6-hour period was 2.5 times higher for the alternate course than for the straight line course. The corresponding increased dose was still small and far below that associated with any adverse health effects; however, this illustrates the complexity of and precision required by the computations where both the clouds and ships were moving as well as the potential uncertainty associated with ship locations reported every 6 hours.

In addition, ships were provided direction to avoid potential radioactive plumes, so the calculated activity concentrations are likely conservative when accounting for the differences in ship positions.

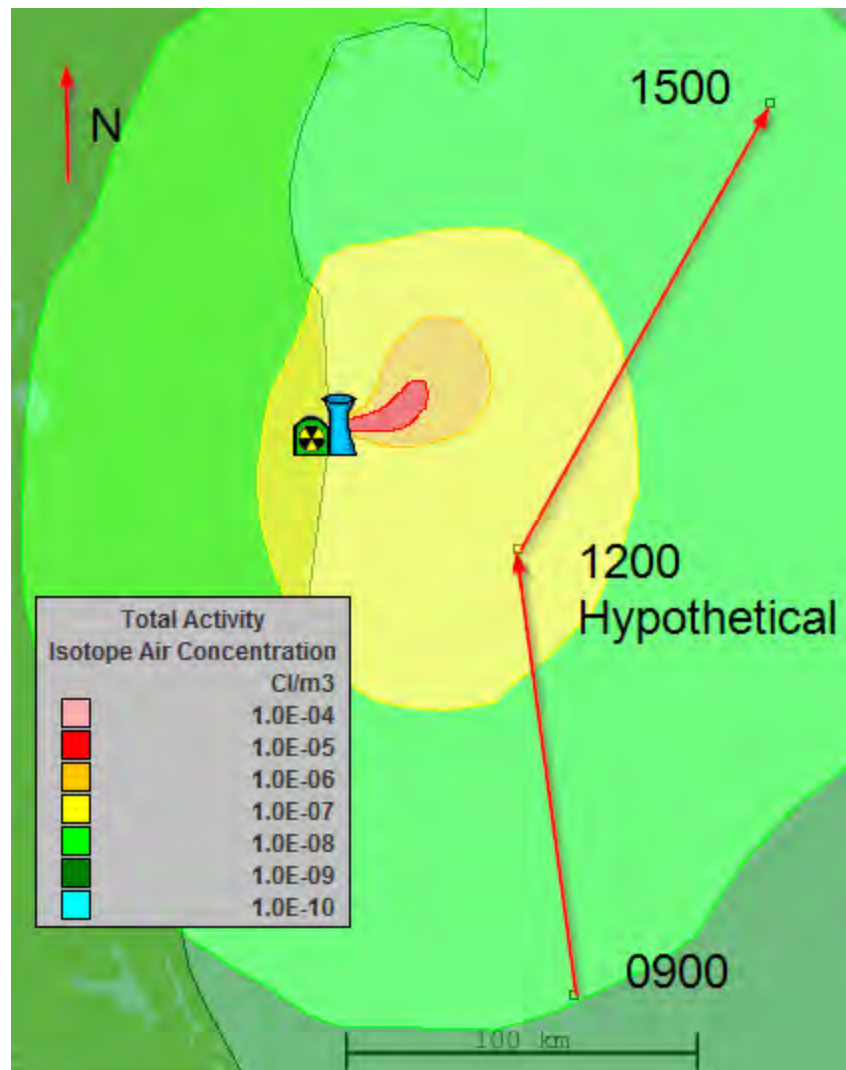


Figure I-9. Hypothetical route for the USS John S. McCain

I-5. HPAC Software Component Validation and Maturity

HPAC is an export-controlled DOD software product that is used operationally to provide hazard area predictions. Use of HPAC during the Fukushima accident enabled ships at sea to avoid subsequent effluent clouds. There were a number of software issues that were referred to the HPAC development branch. The final computation was conducted using development build 195 of HPAC version 5.2.

I-5.1. NFAC Incident Model

The NFAC source incident model is used to model a nuclear reactor accident. This model was based on a U.S. nuclear regulatory model, but operationally it had not been widely used with recent versions of HPAC before the FDNPS accident event. The modeling conducted during the event identified several challenges that limited model fidelity. Many of these were addressed prior to the start of the modeling process described in this report, but there was another major challenge that was identified in this work, which, when addressed, increased the average dose by a factor of three. This challenge that presented itself was that the modeled ground deposition was determined to be significantly inaccurate because the dry deposition rate was too high, and the HPAC wet deposition capability was too limited. Coincidentally, the average external doses computed at the Main Gate using the exposure rates from HPAC-generated deposition were three times higher than the measurements. This raised the possibility that there were low-level calibration choices associated with NFAC that were predicated on the results before the issue was identified and corrected. For this reason, the ground shine output from HPAC was not used for any of the doses to individuals in this report. Rather, the total external dose from air submersion and ship shine was estimated as a ratio of the integrated air submersion dose predicted by HPAC scaled to the measured external dose at Yokosuka NB.

I-5.2. SCIPUFF Transport and Dispersion Model

The dispersion component of HPAC, SCIPUFF, is a mature, robust model that has been validated repeatedly using a variety of source models, weather sources, and domain scales. SCIPUFF reports an uncertainty for the dispersion computation. Software validation tests (standard software development process tests of SCIPUFF compared to data) were consistent with both the temporal and spatial domains in this report. SCIPUFF also has the capability to compute the resolved wind field (the wind field actually used to compute the dispersion) given the measured values in the weather file; however, there was no validation of the uncertainty estimate due to the spatial distribution of the weather stations. The level of uncertainty was a rough estimate based on the assumption that the uncertainty was small when close to the observation in time and space but that it approached the variance in the climatology at that location (HPAC contains a worldwide climatology database) as time and distance increased between the measured weather locations and the resolved weather locations. Because of the relative sparseness of the observed weather data used in this analysis, especially near FDNPS, the dispersion uncertainty was relatively large. However, the overall quality of the validation and the maturity of the SCIPUFF component for this application was high.

I-6. Estimated Uncertainties

I-6.1. Uncertainties Computed and Propagated in the T&D Process

The SCIPUFF T&D computation computes uncertainty in time and space and reported this as a variance in requested outputs. This reported variance did not include the uncertainties in the source term or ship locations, nor did it account for explicit uncertainties in the wind data. Most other sources of uncertainty were accounted for, especially those incurred due to the assumptions in the turbulent averaging of the wind fields. A review of the output data revealed that in most cases the standard deviation (the square root of this variance) in either the exposure or the concentration was about the size of the value itself. All of the parameters in the T&D portion of the computation were essentially best-estimate predictions. There was no particularly

high or low bias to the result. However, since the standard deviation was the same size as the result, it was expected that many individuals at these locations might not be exposed at all, or at levels many times lower than the mean. This was consistent with the fact that many of the dosimeters had zero doses reported. On the high side, the probabilities associated with a random sample and a standard deviation could be applied. For example, if the HPAC model predicted an integrated external dose of 10 mrem, with a standard deviation of 10 mrem, it would be expected that approximately 2 percent of the individuals at this location would be exposed to more than 30 mrem.

I-6.2. Combining Sources of Uncertainty

There were assumptions in the final step of this process, the selection of the outputs, which were biased toward a high-sided result. For example, modelers used a simple exposure assumption that the point of measurement was outside (on the weather deck of the ship) for the two-month duration of the computation. Modelers also assumed that any deposition on the deck was not washed off but continued to provide a ship shine dose. Additionally, no reduction was assumed for obstructions or alterations in the semi-infinite plume model. All of these assumptions supported the characterization that reported doses were high-sided.

The temporal scope of any uncertainty was also a significant issue. Although the HPAC sampler produced output at a 15-minute average, the comparative data were usually averaged over 1 hour, but in some cases the comparative data were only random measurements during that 1-hour period. There were also daily averages, or 24-hour period averages that did not correspond to a particular day in either Z or local time as was the case for the Yokota AB data.

The last factor in the uncertainty was the uncertainty associated with the reporting of a single, maximum dose for the two-month period for every ship in the fleet. This maximum dose was determined as the sum of the maximum at-sea dose for any ship and the maximum in-port dose for any ship.

Sources of uncertainty in doses to fleet-based individuals are:

(1) Source Term

- a. Source term intensity during the period of any release
- b. Period of any reactor release at a continuous level
- c. Height of the release from the reactor building

(2) Weather

- a. Source
 - i. MM5 synthesized weather
 - ii. Measurements
- b. Selected subset (see section H-2.3.3)
 - i. Entire set
 - ii. Computational domain limits set
 - iii. Limited to robust 1-hour reported values

- iv. Removal of Yamagata data point
 - v. Use of only two closest points to the FDNPS prior to 16 Mar
- (3) Dispersion
- (4) Ship location

Some of these uncertainties were uncorrelated and random and could be combined in quadrature. Others were systematic and non-random. The systematic uncertainties were explicitly accounted for with high-sided inputs when possible (e.g., use of the factor of 3.49 to adjust exposure rates as explained in Section 4.2.3, and use of the factor 3 to account for the uncertainties in dose coefficients for internal doses as described in Section 4.2.2).

Uncertainties in the dispersion computations were characterized by the standard deviations in the isotope air concentrations and the air submersion exposures rates. These outputs of the dispersion computations provided measures of uncertainty for that portion of the computation, which considered and propagated many of the random uncertainties within its scope. The dispersion results showed that the standard deviations were about equal to the values of the corresponding isotope air concentrations and the air submersion exposure rate values themselves. Use of the adjustment factor of 3.49 discussed above results in external dose output values that are 2.49 standard deviations above the mean. This result contributed to a high degree of confidence that an actual dose received by any member of the POI would be less than the reported dose.

The HPAC inputs associated with source releases were refined during the calibration process for episodic and uneven releases that occurred in the first five days of the event. Over the next 15 days, relatively constant releases occurred that approximated long-term average releases. However, there were also releases during this period that resulted in small measured radiation peaks, as can be seen from the measured FDNPS front gate data (blue line) in Figure I-1. The most significant example of such peaks occurred on or about March 21, 2011. Initial HPAC modeling did not accurately predict this peak, and no attempt was made to calibrate and refine the model to more accurately capture it. One reason a calibration attempt was not made to reflect the March 21 peak is because a very high rainfall occurred over most of the computational domain on that day. This event resulted in wet deposition that could have dominated the radiation reading for that day. A potential complicating factor is that this peak could also have been caused in part by a specific release event at the plant. Because of these issues, a short-term, high-level release may not always be easily disambiguated. Overall, after the initial 5-day period there were no significant releases with sufficient, available supporting data that warranted further calibrating and refining of HPAC inputs.

Modeling releases of short duration was also difficult in using HPAC due to combined uncertainties. It is possible that plumes of high concentration but relatively short duration were released from the FDNPS, but given the HPAC model, the data available for calibration, and the calibration and refinement process, model output would be unable to accurately reflect a very short-duration, high-concentration release. In these situations, the calibrated and refined results would instead reflect modeling in a more time-averaged manner. At very short distances from the reactors (e.g., at the front gate), this could explain the mismatched peaks in Figure I-1, but at much greater distances from FDNPS, such as the locations of affected ships when they

encountered radioactive plumes, atmospheric dispersion modeling tended to average out high-concentration, short-duration releases. This resulted in a plume that was reasonably well-modeled from a long-term perspective.

The combination of the many uncertainties discussed above makes it difficult to have a high degree of confidence that the estimated doses for any particular ship accurately reflect actual doses received by any fleet individuals. This is especially true given the low reported doses for most ships. The most influential uncertainties and sensitivities include those associated with factors such as the wind field, the spatial and temporal intersection of the modeled plumes with the precise location of each ship, and the fact that the calculated doses for most ships were often dominated by one period of interaction with a radioactive cloud. However, because systematic, high-sided assumptions were used and because the highest internal doses were combined with the highest external dose from among all the participating ships, there is a high measure of confidence that the reported dose values do not underestimate the actual doses received by any member of the fleet.

I-7. Outputs during the FDNPS Accident

During the FDNPS accident, DTRA provided the fleet with predictive effluent T&D information every six hours for the first 31 days, beginning on March 12, 2011, and then every 24 hours for the next 11 days. These analyses enabled ships and aircraft to avoid the radioactive clouds produced by effluent releases of radioactive material from FDNPS, which resulted in reduced exposures to fleet-based individuals. Best estimates of core status in each of the three units, integrity of primary containments, FDNPS venting status, and isotope effluent releases were also provided.

Appendix J.

Calculated Doses for Crews of All Ships

The doses estimated for the crews of all ships included in this report using the methods described in Section 4 are listed in Table J-1 (effective doses) and Table J-2 (thyroid equivalent doses). Each table lists for each ship the external and internal committed components of the at-sea doses calculated using the HPAC-generated air activity concentrations, the in-port doses calculated using the methods the shore-based report, as well as the total effective doses and the total thyroid equivalent doses.

As discussed in Section 4, doses for ship-based individuals while in port (mainland Japan) were estimated using the data and methods described in the shore-based report. Because actual in-port arrival times and departure times were not available, it was assumed that a ship was in-port for the entire 24 hours for any arrival or departure day. It was also assumed that an individual was on shore for all of the in-port period. While on shore, ship personnel were assumed to have activities similar to a humanitarian relief worker as described in the shore-based report.

Doses for ship-based individuals during at-sea periods were estimated using HPAC-generated air activity concentrations and human behavior assumptions described in Section 4. External doses were calculated for air-submersion and ship-shine components. Contributions to internal doses consisted of doses from inhalation intakes of the modeled air activity concentrations. The human behavior parameter values for humanitarian relief individuals from the shore-based report were used for the internal dose calculations, which were also consistent with the external dose calculations.

Table J-1. Effective doses for crews of all OT ships while at sea, in port, and totals

Ship	External Dose [mSv (rem)]			Internal Committed Effective Dose [mSv (rem)]			Total Effective Dose* [mSv (rem)]
	HPAC two-month	In-port (shore)	Total External	At-sea (HPAC)	In-port (shore)	Total Internal	
USS Blue Ridge (LCC 19)	†,‡	0.05 (0.005)	0.05 (0.005)	†,‡	‡	0.00† (0.000)	0.05 (0.005)
USS George Washington (CVN 73)	0.11 (0.011)	0.04 (0.004)	0.15 (0.015)	‡	0.16 (0.016)	0.16 (0.016)	0.31 (0.031)
USS Cowpens (CG 63)	0.06 (0.006)	0.06 (0.006)	0.12 (0.012)	0.05 (0.005)	‡	0.06 (0.006)	0.18 (0.018)
USS Shiloh (CG 67)	0.11 (0.011)	0.06 (0.006)	0.17 (0.017)	0.01 (0.001)	0.15 (0.015)	0.16 (0.016)	0.33 (0.033)
USS Curtis Wilbur (DDG 54)	0.01† (0.001)	0.07 (0.007)	0.08 (0.008)	0.06† (0.006)	0.01 (0.001)	0.07 (0.007)	0.15 (0.015)
USS John S. McCain (DDG 56)	0.03 (0.003)	0.06 (0.006)	0.08 (0.008)	0.11 (0.011)	0.02 (0.002)	0.13 (0.013)	0.21 (0.021)
USS Fitzgerald (DDG 62)	0.02 (0.002)	0.08 (0.008)	0.10 (0.010)	0.11 (0.011)	0.02 (0.002)	0.13 (0.013)	0.23 (0.023)
USS Stethem (DDG 63)	‡	0.05 (0.005)	0.05 (0.005)	‡	‡	‡	0.05 (0.005)
USS Lassen (DDG 82)	0.11 (0.011)	0.02 (0.002)	0.13 (0.013)	‡	0.17 (0.017)	0.18 (0.018)	0.30 (0.030)
USS McCampbell (DDG 85)	0.01 (0.001)	0.03 (0.003)	0.04 (0.004)	0.06 (0.006)	‡	0.07 (0.007)	0.11 (0.011)
USS Mustin (DDG 89)	0.01 (0.001)	0.02 (0.002)	0.03 (0.003)	0.04 (0.004)	0.01 (0.001)	0.06 (0.006)	0.09 (0.009)
USS Ronald Reagan (CVN 76)	0.01 (0.001)	‡	0.02 (0.002)	0.06 (0.006)	‡	0.06 (0.006)	0.08 (0.008)
USS Chancellorsville (CG 62)	0.01 (0.001)	‡	0.01 (0.001)	0.04 (0.004)	‡	0.04 (0.004)	0.05 (0.005)

Table J-1. Effective doses for crews of all OT ships while at sea, in port, and totals (cont.)

Ship	External Dose [mSv (rem)]			Internal Committed Effective Dose [mSv (rem)]			Total Effective Dose* [mSv (rem)]
	HPAC two-month	In-port (shore)	Total External	At-sea (HPAC)	In-port (shore)	Total Internal	
USS Preble (DDG 88)	0.01 (0.001)	‡	0.01 (0.001)	0.04 (0.004)	‡	0.04 (0.004)	0.05 (0.005)
USS Essex (LHD 2)	‡	‡	‡	‡	‡	0.01 (0.001)	0.02 (0.002)
USS Germantown (LSD 42)	‡	‡	‡	‡	‡	0.01 (0.001)	0.02 (0.002)
USS Tortuga (LSD 46)	‡	‡	‡	‡	‡	0.01 (0.001)	0.02 (0.002)
USS Harpers Ferry (LSD 49)	‡	‡	‡	‡	0.01 (0.001)	0.01 (0.001)	0.02 (0.002)
USNS Richard E. Byrd (T-AKE 4)	‡	‡	‡	‡	‡	‡	0.01 (0.001)
USNS Carl Brashear (T-AKE 7)	‡	0.01 (0.001)	0.01 (0.001)	‡	‡	‡	0.02 (0.002)
USNS Matthew Perry (T-AKE 9)	‡	‡	‡	‡	‡	‡	‡
USNS Pecos (T-AO 197)	‡	0.01 (0.001)	0.01 (0.001)	‡	0.01 (0.001)	0.01 (0.001)	0.02 (0.002)
USNS Rappahannock (T-AO 204)	‡	0.01 (0.001)	0.01 (0.001)	‡	0.02 (0.002)	0.02 (0.002)	0.03 (0.003)
USNS Bridge (T-AOE 10)	‡	‡	0.01 (0.001)	0.03 (0.003)	0.01 (0.001)	0.04 (0.004)	0.05 (0.005)
USNS Safeguard (T-ARS 50)	0.08 (0.008)	0.02 (0.002)	0.10 (0.010)	0.03 (0.003)	0.04 (0.004)	0.07 (0.007)	0.17 (0.017)

* Total Effective Dose is the (rounded) sum of the Total External Dose and the Total Internal Committed Effective Dose for each ship.

† At sea (HPAC) doses for these ships are based on qualitative knowledge of ship locations, and/or surrogate ship data.

‡ Dose is less than 0.01 mSv (0.001 rem).

Table J-2. Thyroid doses for crews of all OT ships while at sea, in port, and totals

Ship	External Dose [mSv (rem)]			Internal Committed Thyroid Dose [mSv (rem)]			Total Thyroid Dose* [mSv (rem)]
	HPAC two-month	In-port (shore)	Total External	At-sea (HPAC)	In-port (shore)	Total Internal	
USS Blue Ridge (LCC 19)	†,‡	0.05 (0.005)	0.05 (0.005)	†,‡	0.02 (0.002)	0.02 (0.002)	0.07 (0.007)
USS George Washington (CVN 73)	0.11 (0.011)	0.04 (0.004)	0.15 (0.015)	0.02 (0.002)	2.9 (0.29)	3.0 (0.30)	3.1 (0.31)
USS Cowpens (CG 63)	0.06 (0.006)	0.06 (0.006)	0.12 (0.012)	0.92 (0.092)	0.12 (0.012)	1.0 (0.10)	1.2 (0.12)
USS Shiloh (CG 67)	0.11 (0.011)	0.06 (0.006)	0.17 (0.017)	0.24 (0.024)	2.7 (0.27)	2.9 (0.29)	3.1 (0.31)
USS Curtis Wilbur (DDG 54)	0.01 [†] (0.001)	0.07 (0.007)	0.08 (0.008)	1.0 [†] (0.10)	0.23 (0.023)	1.2 (0.12)	1.3 (0.13)
USS John S. McCain (DDG 56)	0.03 (0.003)	0.06 (0.006)	0.08 (0.008)	1.8 (0.18)	0.30 (0.030)	2.1 (0.21)	2.2 (0.22)
USS Fitzgerald (DDG 62)	0.02 (0.002)	0.08 (0.008)	0.10 (0.010)	1.8 (0.18)	0.46 (0.046)	2.3 (0.23)	2.4 (0.24)
USS Stethem (DDG 63)	‡	0.05 (0.005)	0.05 (0.005)	‡	0.05 (0.005)	0.05 (0.005)	0.10 (0.010)
USS Lassen (DDG 82)	0.11 (0.011)	0.02 (0.002)	0.13 (0.013)	0.04 (0.004)	3.2 (0.32)	3.2 (0.32)	3.3 (0.33)
USS McCampbell (DDG 85)	0.01 (0.001)	0.03 (0.003)	0.04 (0.004)	1.0 (0.10)	0.14 (0.014)	1.2 (0.12)	1.2 (0.12)
USS Mustin (DDG 89)	0.01 (0.001)	0.02 (0.002)	0.03 (0.003)	0.75 (0.075)	0.21 (0.021)	0.96 (0.096)	1.0 (0.10)
USS Ronald Reagan (CVN 76)	0.01 (0.001)	‡	0.02 (0.002)	1.0 (0.10)	0.03 (0.003)	1.1 (0.11)	1.1 (0.11)
USS Chancellorsville (CG 62)	0.01 (0.001)	‡	0.01 (0.001)	0.73 (0.073)	0.03 (0.003)	0.76 (0.076)	0.77 (0.077)

Table J-2. Thyroid doses for crews of all OT ships while at sea, in port, and totals (cont.)

Ship	External Dose [mSv (rem)]			Internal Committed Thyroid Dose [mSv (rem)]			Total Thyroid Dose* [mSv (rem)]
	HPAC two-month	In-port (shore)	Total External	At-sea (HPAC)	In-port (shore)	Total Internal	
USS Preble (DDG 88)	0.02 (0.002)	‡	0.01 (0.001)	0.67 (0.067)	0.03 (0.003)	0.70 (0.070)	0.71 (0.071)
USS Essex (LHD 2)	‡	‡	‡	0.08 (0.008)	0.15 (0.015)	0.23 (0.023)	0.24 (0.024)
USS Germantown (LSD 42)	‡	‡	‡	0.09 (0.009)	0.16 (0.016)	0.25 (0.025)	0.25 (0.025)
USS Tortuga (LSD 46)	‡	‡	‡	0.14 (0.014)	0.09 (0.009)	0.23 (0.023)	0.24 (0.024)
USS Harpers Ferry (LSD 49)	‡	‡	‡	0.09 (0.009)	0.18 (0.018)	0.27 (0.027)	0.28 (0.028)
USNS Richard E. Byrd (T-AKE 4)	‡	‡	‡	0.08 (0.008)	0.05 (0.005)	0.13 (0.013)	0.13 (0.013)
USNS Carl Brashear (T-AKE 7)	‡	0.01 (0.001)	0.01 (0.001)	‡	0.09 (0.009)	0.09 (0.009)	0.10 (0.010)
USNS Matthew Perry (T-AKE 9)	‡	‡	‡	0.02 (0.002)	0.05 (0.005)	0.07 (0.007)	0.07 (0.007)
USNS Pecos (T-AO 197)	‡	0.01 (0.001)	0.01 (0.001)	‡	0.26 (0.026)	0.27 (0.027)	0.28 (0.028)
USNS Rappahannock (T-AO 204)	‡	0.01 (0.001)	0.01 (0.001)	0.02 (0.002)	0.29 (0.029)	0.32 (0.032)	0.33 (0.033)
USNS Bridge (T-AOE 10)	‡	‡	0.01 (0.001)	0.52 (0.052)	0.18 (0.018)	0.70 (0.070)	0.72 (0.072)
USNS Safeguard (T-ARS 50)	0.08 (0.008)	0.02 (0.002)	0.10 (0.010)	0.53 (0.053)	0.70 (0.070)	1.2 (0.12)	1.3 (0.13)

* Total thyroid dose is the (rounded) sum of the total external dose and the total internal committed thyroid dose for each ship.

† At sea (HPAC) doses for these ships, are based on qualitative knowledge of ship locations, and/or surrogate ship data.

‡ Dose is less than 0.01 mSv (0.001 rem).

This page intentionally left blank.

Abbreviations, Acronyms, and Symbols

AAW	anti-air warfare
AB	Air base
AEW	Airborne early warning
AC	Alternating current
AFB	Air Force Base
AFSOG	Air Force Special Operations Group
AMAD	activity median aerodynamic diameter
AOR	area of responsibility
ARG	amphibious readiness group
ASW	anti-submarine warfare
ASUW	anti-surface warfare
AW	anti-warfare
BMD	ballistic missile defense
Bq	becquerel
BUMED	U.S. Navy Bureau of Medicine and Surgery
Buno	bureau number
C	Celsius
CBR	chemical, biological, and radiological
CCPM	Corrected counts per minute
CD-ROM	compact disc-read only memory
CFR	Code of Federal Regulations
CHSCWL	Commander, Helicopter Sea Combat Wing, Atlantic Fleet
Ci	curie
CJTF	Commander Joint Task Force
CLF	Combat Logistics Force
cm	centimeter
COD	carrier onboard delivery
COMNAVSURFPAC	Commander, Naval Surface Force United States Pacific Fleet
CONUS	Continental United States
CPRW	Patrol and Reconnaissance Wing
CPS	Collective Protection System
CSAR	Combat Search and Rescue
CSG	carrier strike group
CT	contamination technician
d	day
DARWG	Dose Assessment and Recording Working Group
DC	dose coefficient
DET	detachment
DOD	Department of Defense
DOE	Department of Energy
dpm	disintegrations per minute
DTRA	Defense Threat Reduction Agency

E	effective dose
ECMO	Electronic Countermeasures Officer
EDE	effective dose equivalent
ELT	Engineering Laboratory Technician
EODMU	explosive ordinance disposal mobile unit
EPA	Environmental Protection Agency
EPD	Electronic Personal Dosimeter
ESG	Expeditionary Strike Group
FARP	Forward Area Refueling Points
FDNPS	Fukushima Daiichi Nuclear Power Station
FISC	Fleet Industrial Supply Center
G-M	Geiger-Mueller
GOJ	Government of Japan
GSD	geometric standard deviation
Gy	gray
H	equivalent dose
h	hour
HADR	Humanitarian Aid and Disaster Relief
HMM	Marine Medium Helicopter Squadron
HPAC	Hazard Prediction and Assessment Capability
ICRP	International Commission on Radiological Protection
ICRU	International Commission on Radiation Units and Measurements
IM	internal monitoring
IMS	International Monitoring Station
IRF	Intake Retention Factor
J	joule
JASDF	Japanese Air Self Defense Force
JFSOCC	Joint Force Special Operations Component Commander
kg	kilogram
λ	physical (radiological) decay constant
L	liter
LCAC	Landing Craft Air Cushion
LCU	Landing Craft Utility
LEX	leading edge extensions
LLD	Lower Limit of Detection
m	meter
MAG	Marine Aircraft Group
MAGTF	Marine Air-Ground Task Force
MAW	Marine Aircraft Wing
MCL	Maximum Contaminant Level
MDA	minimum detectable activity
MEB	Marine Expeditionary Battalion
MEDEVAC	aeromedical evacuation
MeV	Mega electron volt
μ Sv	microsievert

MEU	Marine Expeditionary Unit
MEXT	Japanese Ministry of Education, Culture, Sports, Science and Technology
mg	milligram
mL	milliliter
mm	millimeter
MOFA	Ministry of Foreign Affairs
mrem	millirem
NAS	National Academy of Sciences
NASA	National Aeronautics and Space Administration
NAVSEA	Naval Sea Systems Command
NB	naval base
NCRP	National Council on Radiation Protection and Measurements
NFAC	nuclear facility module in HPAC
nmi	nautical miles
NSWU	Naval Special Warfare Unit
NSFS	Naval Surface Fire Support
NWP	numerical weather predictions
OPNAVINST	Naval Operations Instruction
ORIGEN	Oak Ridge Isotope Generation
OSL	optically stimulated luminescence
OT	Operation Tomodachi
OTR	Operation Tomodachi Registry
PAG	Protective Action Guide
PAS	portable air sampler
pCi	picocurie
PEP	potentially exposed population
POI	population of interest
PPE	Personal Protective Equipment
R	roentgen
rem	roentgen equivalent man
RHIB	Rigid Hull Inflatable Boat
RHO	Radiation Health Officer
RHT	Radiation Health Technician
ROK	Republic of Korea
RW	rotary wing
SAR	Search and Rescue
SCIPUFF	second-order closure, integrated puff
SEAD	suppression of enemy air defenses
SI	International System of Units (from the French <i>Système International d'Unités</i>)
SOG	Special Operations Group
STRW	strike warfare
Sv	sievert
T&D	transport and dispersion
TACC	Tanker Airlift Control Center

TAKAMO	take off and maneuver
TED	Total Effective Dose
TEPCO	Tokyo Electric Power Company
TLD	thermoluminescent dosimeter
TR	technical report
TRAP	tactical recovery of aircraft and personnel
UCT	underwater construction team
UNREP	underway replenishment
U.S.	United States
USA	United States Army
USAF	United States Air Force
USFJ	United States Forces Japan
USMC	United States Marine Corps
USN	United States Navy
USNS	United States Naval Ship
USPACOM	United States Pacific Command
USS	United States Ship
USW	undersea warfare
UF	uncertainty factor
VERTREP	vertical replenishment
VLS	vertical launch system
VMFA	Marine Fighter Attack Squadron
VMGR	Marine Aerial Refueler Transport Squadron
VTOL	Vertical Take-off and Landing
WHO	World Health Organization
y	year

**DISTRIBUTION LIST
DTRA-TR-12-41**

DEPARTMENT OF DEFENSE

DEFENSE THREAT REDUCTION
AGENCY
8725 JOHN J. KINGMAN ROAD
STOP 6201
FORT BELVOIR ,VA 22060
ATTN: P. BLAKE

DEFENSE TECHNICAL
INFORMATION CENTER
8725 JOHN J. KINGMAN ROAD,
SUITE 0944
FT. BELVOIR, VA 22060-6201
ATTN: DTIC/OCA

**DEPARTMENT OF DEFENSE
CONTRACTORS**

EXELIS, INC.
1680 TEXAS STREET, SE
KIRTLAND AFB, NM 87117-5669
ATTN: DTRIAC